MICROCOPY RESOLUTION TEST CHART

NATIONAL BUREAU OF STANDARDS-1963-A

AD-A172 716

AFOSR-TR- 86-0905

DTIC
ELECTE
OCT 0 8 1986
S D
D

Optimization of Closed Loop Eigenvalues: Maneuvering, Vibration Control, and Structure/Control Design Iteration for Flexible Spacecraft

John L. Junkins
Texas A&M University
May 1986

FINAL REPORT
VPI&SU SUB-CONTRACT NO. 4174-352142-1

DTIC FILE COPY

86 10 8 086

AD-A172 716

REPORT DOCUMENTATION PAGE

1a. REPORT SECURITY CLASSIFICATION unclassified	1b. RESTRICTIVE MARKINGS
2a. SECURITY CLASSIFICATION AUTHORITY	3. DISTRIBUTION/AVAILABILITY OF REPORT
2b. DECLASSIFICATION/DOWNGRADING SCHEDULE	Approved for public release, unclassified/unlimited distribution unlimited
4. PERFORMING ORGANIZATION REPORT NUMBER(S)	5. MONITORING ORGANIZATION REPORT NUMBER(S) AFOSR-TR- 86-0905

6a. NAME OF PERFORMING ORGANIZATION Virginia Polytechnic Institute & State University	6b. OFFICE SYMBOL (If applicable) ESM	7a. NAME OF MONITORING ORGANIZATION AFOSR
6c. ADDRESS (City, State and ZIP Code) Dept. of Engineering Science & Mechanics VPI&SU Blacksburg, VA 24061		7b. ADDRESS (City, State and ZIP Code) Bolling AFB 20332-6448

8a. NAME OF FUNDING/SPONSORING ORGANIZATION AFOSR	8b. OFFICE SYMBOL (If applicable) na	9. PROCUREMENT INSTRUMENT IDENTIFICATION NUMBER F49620-83-K-0032

8c. ADDRESS (City, State and ZIP Code) Bolling AFB, DC 20332-6648	10. SOURCE OF FUNDING NOS.			
	PROGRAM ELEMENT NO. 61102F	PROJECT NO. 2302	TASK NO. B1	WORK UNIT NO.

11. TITLE (Include Security Classification) Optimization of Closed Loop Eigenvalues for Flexible Spacecraft Secturn

12. PERSONAL AUTHOR(S)
John L. Junkins

13a. TYPE OF REPORT Final Report	13b. TIME COVERED FROM 6/85 TO 5/86	14. DATE OF REPORT (Yr., Mo., Day) May 31, 1986	15. PAGE COUNT 150

16. SUPPLEMENTARY NOTATION

17.	COSATI CODES		18. SUBJECT TERMS (Continue on reverse if necessary and identify by block number)
FIELD	GROUP	SUB. GR.	active control, structural analysis, optimization integrated design, spacecraft dynamics

19. ABSTRACT (Continue on reverse if necessary and identify by block number)

This report summarizes new results on spacecraft dynamics and control. Perturbation methods are presented for computing nonlinear open- and closed-loop optimal maneuver control. Homotopy optimization algorithms are presented for tuning linear regulators vis-a-vis eigenvalue placement and robustness. A simultaneous structure/controller design optimization algorithm is developed.

20. DISTRIBUTION/AVAILABILITY OF ABSTRACT UNCLASSIFIED/UNLIMITED ☒ SAME AS RPT. ☐ DTIC USERS ☐	21. ABSTRACT SECURITY CLASSIFICATION UNCLASSIFIED	
22a. NAME OF RESPONSIBLE INDIVIDUAL Dr. Anthony Amos	22b. TELEPHONE NUMBER (Include Area Code) 202-767-4937	22c. OFFICE SYMBOL AFOSR/NA

DD FORM 1473, 83 APR EDITION OF 1 JAN 73 IS OBSOLETE.

SUMMARY

This document represents the final report under Contract No. F49620-83-K-0032-P00001 from the Air Force Office of Scientific Research to Virginia Polytechnic Institute and State University. To accommodate the fact that the Principal Investigator (J.L. Junkins) accepted a position at Texas A&M University, effective September 1, 1985, the effort was performed at Texas A&M under Sub-Contract No. 4174-352142-1 from Virginia Polytechnic Institute.

Significant progress is reported on methodology to optimize open and closed loop control laws for flexible vehicles. Also a new method for simutaneous structure/controller design optimization is reported.

DISCUSSION OF RESULTS

Since the effort in this contract resulted in ten manuscripts which document the results in detail, we append here to these manuscripts and provide below a brief statement of the main results contained in these papers.

Nonlinear Feedback Control

In Attachment 1, we present a generalization of classical linear-quadratic regulator theory to accommodate polynominal nonlinearities in dynamical models of the form

$$\dot{x}_i = a_{ij}x_j + c_{ijk}x_jx_k + \cdots + b_{ij}u_j \qquad (i=1,2,\ldots,n) \qquad (1)$$

where x_i are state variables, u_i are control variables, and summation over repeated indices is implied. We consider polynomial nonlinear feedback of the form

2

$$u_i = -(d_{ij}x_j + e_{ijk}x_jx_k + f_{ijkl}x_jx_kx_l + \cdots) \qquad (i=1,\ldots,m) \qquad (2)$$

For the case of a quadratic performance index, we show in Attachment No. 1 that the gains satisfy a <u>sequence</u> of differential equations. The linear gains (d_{ij}) are determined by solving the usual Riccati equation, whereas the quadratic gains (e_{ijk}), cubic gains (f_{ijkl}) and all higher order gains satisfy <u>linear</u> differential equations. Numerical implementations have been carried out and the validity of the formulation has been established. Several applications are described in Attachment 1 which shows that the nonlinear feedback terms are significant and constructive in designing optimal nonlinear controls. In all cases studied, except one, convergence has been reliably achieved. This convergence failure was found to depend upon the weights selected in the performance index and was easily eliminated. More generally, conditions which guarantee convergence remain a difficult unresolved issue which requires further research. The most significant practical difficulty associated with this approach lies in the system specific algebra required to derive the differential equations satisfied by the higher order gains. We are investigating the use of algebraic manipulators (MACSYMA and SMP) to automate the derivation and coding of these equations.

In Attachment 2, we extend these ideas by using canonical state variables (the euler parameters and the corresponding conjugate momentum variables). This formulation is very elegant for spacecraft attitude maneuvers. While we clearly establish the validity of the formulations (through analytical and numerical comparisons to the results in Attachment 1), the advantages of this canonical variable approach have not been established. Also, we consider in Attachment 2 a Liapunov approach to design of nonlinear feedback control; these results look very promising, especially for systems of moderate dimensions.

3

Nonlinear Open Loop Control

In Attachments 3,4,5, we present a novel method for computing nonlinear open loop spacecraft maneuvers by a perturbation method. As with the problems addressed in Attachments 1 and 2, we consider only polynomial nonlinearities. We establish a quasi-analytical, non-iterative method (based upon asymptotic expansions) which we demonstrate to work well on several problems. The method presented is attractive because it appears suitable for semi-automation and also because it has worked well on most examples tried to date.

Structural Identification

In Attachment 6, we present a time-domain method for structural identification which combines both free and forced response measurements to determine system mass and stiffness estimates. The method is shown to work well for "academic" structures of moderate dimensionality. However difficulties associated with lack of uniqueness, rank deficiency and data requirements are noted which limit the practical utility of this approach. Recent research has established a new frequency domain approach which promises to circumvent many (if not most) of these difficulties. The method is based upon parameterization of the frequency response function in terms of physical system parameters and recovering estimates of these parameters to fit the frequency response in a least square sense. Rank deficiencies are addressed using a singular value decomposition algorithm. The details of this method will be presented in N.G. Creamer's forthcoming dissertation, including applications to structures with linear viscoelastic models.

Structure/Controller Optimization

In Attachments 7 and 8, we present homotopy methods for simultaneous optimization of structural design parameters, sensor/actuator locations, and the feedback gains in an output feedback control law. The algorithm of Attachment 7 is based upon a "minimum modification" strategy which is shown convergent with as many as 60 design variables. The algorithm of Attachment 8 is based upon sequential linear programming. This approach is especially well-suited to high dimensioned problems involving a large number of inequality constraints. In Attachment 8, we consider a simple example with eigenvalue placement constraints and two alternative optimization criteria (minimum mass, minimum closed-loop eigenvalue sensitivity); both structure and control parameters are simultaneously iterated. Several variations in problem statement and starting iterative support the validity and usefulness of both the minimum correction and sequential linear programming homotopy algorithms.

In Attachments 9 and 10, we extend the methodology of Attachments 7 and 8 to consider tuning of optimal quadratic regulators. In Attachment 10, we establish that the weight matrices selected for the usual quadratic performance index have a strong impact upon eigenvalue placement and other stability/performance robustness measures. We also establish an algorithm which we have found useful for "optimal tuning" of the weight matrices; we have successfully iterated as many as 150 weight elements to optimize eigenvalue placement and robustness indices.

The most significant unifying feature of the methods in attachments 7-10 is the use of homotopy methods. This approach is most important in practical situations for which the initially stated contraints have no feasible solution. The homotopy method gradually imposes constraints, and as a consequence, convergence failures are informative. Conflicting and active

5

constraints can be easily identified, leading to "least compromised" revisions of the problem statement. This feature appears to be a key ingredient in developing practical optimization strategies for high-dimensioned systems.

Student Support

The four students supported by this contract are nearing completion of their Ph.D. dissertations. They are as follows:

(1) R.C. Thompson, (2) K.B. Lim, (3) D.W. Rew, and (4) N.G. Creamer.

These four students, the principal investigator, and the two academic institutions have certainly benefited significantly from this research project. The fruits of the research are most significant and we trust will be the basis for many future developments.

ATTACHMENT INDEX

Optimal Nonlinear Feedack Control for Spacecraft Attitude Maneuvers

C.K. Carrington* and J.L. Junkins†

Virginia Polytechnic Institute and State University, Blacksburg, Virginia

Polynomial feedback controls for large-angle, nonlinear spacecraft attitude maneuvers are developed. A five-body configuration consisting of an asymmetric spacecraft and four reaction wheels is considered. Attention is restricted to the momentum transfer class of internal control torques; this, in conjunction with the choice of Euler parameters as attitude coordinates, permits several important order reduction simplifications. Three numerical examples are included to illustrate applications of the concepts presented.

Introduction

RAPID large-angle attitude maneuvers have become increasingly important to the success of many current and future spacecraft missions. These maneuvers are characterized by nonlinear behavior, however, resulting in a control problem that is likewise nonlinear. One approach to feedback control of nonlinear motion is "gain scheduling" in which the control history is divided into segments, each determined by its own set of linear gains. A more attractive approach is control of the entire nonlinear maneuver by a single set of gains.

For the latter approach, a method is presented whereby the optimal nonlinear control problem is solved in polynomial feedback form and a suboptimal control law is determined by truncation. Currently there are two approaches used to determine the polynomial coefficients for the control. One is to expand the coast-to-go functional as a polynomial in the states and then recursively solve the Hamilton-Jacobi-Bellman equation, as discussed by Willenstein,[1] Dabbous and Ahmed,[2] and Dwyer and Sena.[3] In the method used here,[4] the control itself is expanded as a polynomial and the coefficients determined recursively from the costate equations.

General Formulation

Polynomial state equations may be written in indicial notation as

$$\dot{x}_i = a_{ij}x_j + c_{ijk}x_jx_k + \ldots + b_{ij}u_j \qquad (i=1,2,\ldots,n) \qquad (1)$$

where x_i are the states and u_i the controls to be determined. Consider the optimal control problem of finding a feedback control law that brings the states to zero while minimizing a quadratic performance index

$$J = \frac{1}{2}\int_{t_0}^{t_f} \{q_{ij}x_ix_j + r_{ij}u_iu_j\}dt \qquad (2)$$

The Hamiltonian for this system is

$$\mathcal{H} = \tfrac{1}{2}\{q_{ij}x_ix_j + r_{ij}u_iu_j\} + \lambda_i\dot{x}_i \qquad (3)$$

where it is understood that $\dot{x}_i$ is symbolic for the right-hand side of Eq. (1). The necessary conditions for a minimum provide the state equation, Eq. (1),

$$\dot{x}_i = \frac{\partial\mathcal{H}}{\partial\lambda_i} \qquad (4)$$

and the costate equation

$$\dot{\lambda}_i = -\frac{\partial\mathcal{H}}{\partial x_i} \qquad (5)$$

For unbounded control

$$\frac{\partial\mathcal{H}}{\partial u_i} = 0 \qquad (6)$$

which implies

$$u_i = -r_{ij}^{-1}b_{kj}\lambda_k \qquad (7)$$

where r_{ij}^{-1} represents the elements of the matrix inverse of r_{ij}. By assuming the costates can be expressed as a polynomial in the states, as in Ref. 4,

$$\lambda_i = k_{ij}x_j + d_{ijk}x_jx_k + \ldots \qquad (8)$$

a nonlinear feedback control law is determined in which $k_{ij}(t)$ and $d_{ijk}(t)$ are the control gains sought. By substituting Eq. (8) into Eq. (5) and carrying out the ensuing algebra, we are led to n homogeneous polynomial equations of the form

$$[\alpha]x_j + [\beta]x_jx_k + \ldots = 0 \qquad (9)$$

where

$$[\alpha] = \text{function }(A,B,Q,R,\dot{K},K)$$

$$[\beta] = \text{function }(A,B,C,R,K,\dot{D},D)$$

and K and D are arrays whose elements are the gains k_{ij} and d_{ijk}. Since Eq. (9) must hold at every point in the state space, it is concluded that the functions in brackets must vanish in-

dependently, so we obtain

$$[\alpha(A,B,Q,R,\dot{K},K)] = 0 \tag{10}$$

$$[\beta(A,B,C,R,K,\dot{D},D)] = 0 \tag{11}$$

Equation (10) is a matrix differential equation determining the linear feedback gains; upon carrying through the details, we find that the scalar equations of Eq. (10) are precisely the elements of the matrix Riccati equation which generates the optimal feedback control if all nonlinear terms in the state equation are absent. The solution for the matrix Riccati equation can be determined by Potter[5] or Turner's[6] method, in which an associated eigenvalue problem is solved and matrix exponentials are used.

The quadratic feedback gains are determined by Eq. (11), which can be rearranged into a set of linear differential equations of the form

$$\dot{d}_{ijk} = [\eta]d_{bmr} + [\gamma] \tag{12}$$

where

$$[\eta] = \text{function } (A,B,C,R,K)$$
$$[\gamma] = \text{function } (A,B,C,R,K) \tag{13}$$

Upon solving the Riccati eqaution for the linear gains $k_{bm}(t)$, Eq. (12) provides nonautonomous, nonhomogeneous, but linear equations that determine the quadratic gains $d_{ijk}(t)$. For the steady-state case, Eqs. (10) and (11) can be solved algebraically for the constant feedback gains subject to

$$\dot{k}_{bm} = \dot{d}_{bmk} = 0 \tag{14}$$

The k_{bm} are solutions of the algebraic Riccati equation, and the d_{bmr} are obtained by setting $\dot{d}_{ijk} = 0$ in Eq. (12) and inverting the linear algebraic system. In the numerical examples considered herein, attention is restricted to the constant gain case.

Since for n states there are $n^2(n+1)/2$ equations in Eq. (12), we do not include the algebra of the system considered here. The emphasis of this discussion is the following generalization: After solving the Riccati equation for the linear gains, one is led to sets of linear differential equations, of the functional form shown in Eq. (12), that can be solved sequentially to obtain the quadratic gains, the cubic gains, and so on, up to any desired order. The differential equations for the gains of each order depend upon the lower order gains.

Scalar Example

Consider the optimal control problem of minimizing the following performance index:

$$J = \frac{1}{2}\int_{t_0}^{t_f} \{x^2 + u^2\}\,dt \tag{15}$$

subject ot the state equation

$$\dot{x} = -x + \epsilon x^2 + u \tag{16}$$

The costate equation is

$$\dot{\lambda} = -x + \lambda - 2\epsilon\lambda x \tag{17}$$

and the control is

$$u = -\lambda \tag{18}$$

Table 1 Scalar example performance indices

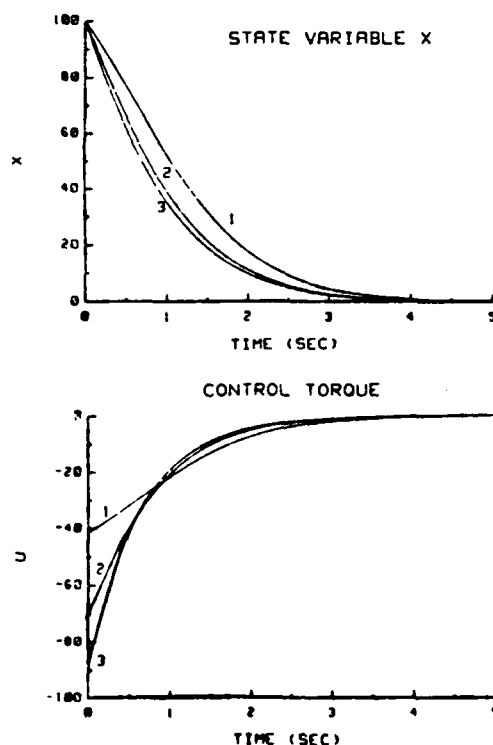| Feedback order	Performance index
1	4314.8
2	3796.4
3	3725.5
4	3717.2
5	3716.8

Fig. 1 Scalar example: 1, linear feedback; 2, linear plus quadratic feedback; 3, linear through cubic feedback.
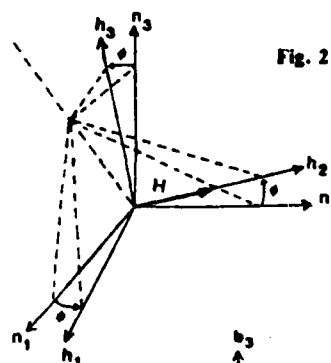

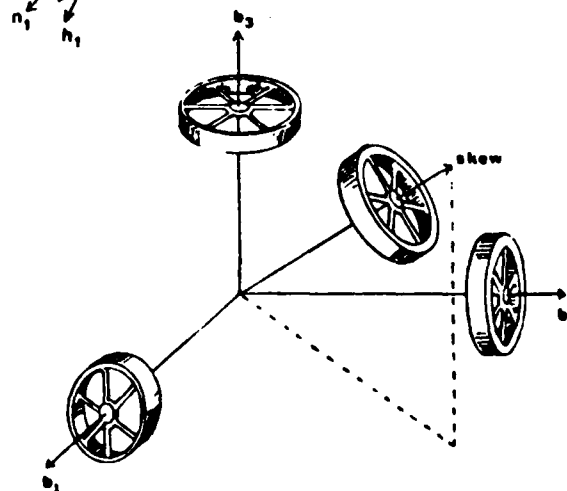Fig. 2 Momentum reference frame.

Fig. 3 NASA standard four reaction wheel attitude control system.

Assuming the costate as a polynomial in state x,

$$\lambda = k_1 x + k_2 x^2 + k_3 x^3 + \dots \qquad (19)$$

then the coefficient differential equations corresponding to Eqs. (10) and (11) and higher order terms are

$$\dot{k}_1 - 2k_1 + 1 - k_1^2 = 0$$

$$\dot{k}_2 - 3(k_1 + 1)k_2 = -3k_1\epsilon$$

$$\dot{k}_3 - 4(k_1 + 1)k_3 = 2k_2^2 - 4k_2\epsilon$$

$$\dot{k}_4 - 5(k_1 + 1)k_4 = 5k_2 k_3 - 5k_3\epsilon$$

$$\dot{k}_5 - 6(k_1 + 1)k_5 = 6k_2 k_4 + 3k_3^2 - 6k_4\epsilon$$

$$\vdots$$

$$\dot{k}_n - (n+1)(k_1 + 1)k_n = (n+1)\{k_2 k_{n-1} + k_3 k_{n-2} + \dots$$

$$+ k_{n/2} k_{n/2+1} - k_{n-1}\epsilon\} \text{ for } n \text{ even}$$

$$\dot{k}_n - (n+1)(k_1 + 1)k_n = (n+1)\{k_2 k_{n-1} + k_3 k_{n-2} + \dots$$

$$+ k_{(n-1)/2} k_{(n+3)/2} + \tfrac{1}{2}k_{(n+1)/2}^2 - k_{n-1}\epsilon\} \text{ for } n \text{ odd} \qquad (20)$$

Making the change of variable from time t to time-to-go $\tau = t_f - t$ and assuming a solution of the form

$$k_1 = k_{1SS} + z_1^{-1}$$

$$k_2 = z_1^{-3} z_2$$

$$k_3 = z_1^{-4} z_3$$

$$\vdots$$

$$k_n = z_1^{-(n+1)} z_n \qquad (21)$$

where k_{1SS} is the steady-state solution for k_1, we obtain the following equations:

$$\frac{dz_1}{d\tau} - 2(1 + k_{1SS})z_1 - 1 = 0$$

$$\frac{dz_2}{d\tau} - 3(1 + k_{1SS})z_2 = 3(k_{1SS}z_1^3 + z_1^2)\epsilon$$

$$\frac{dz_3}{d\tau} - 4(1 + k_{1SS})z_3 = 4z_1 z_2 \epsilon - 2z_1^{-2} z_2^2$$

$$\vdots$$

$$\frac{dz_n}{d\tau} - (n+1)(1 + k_{1SS})z_n = (n+1)\{z_1 z_{n-1}\epsilon - z_1^{-2}(z_2 z_{n-1}$$

$$+ z_3 z_{n-2} + \dots + z_{(n/2+1)})\} \text{ for } n \text{ even}$$

$$\frac{dz_n}{d\tau} - (n+1)(1 + k_{1SS})z_n = (n+1)\{z_1 z_{n-1}\epsilon - z_1^{-2}(z_2 z_{n-1}$$

$$+ z_3 z_{n-2} + \dots + z_{(n-1)/2} z_{(n+3)/2} + \tfrac{1}{2}z_{(n+1)/2}^2)\} \text{ for } n \text{ odd} \qquad (22)$$

The variable changes of Eqs. (21) are generalizations of and were motivated by Refs. 6 and 7.

Equations (22) are easily solved, subject to specification of the boundary conditions; e.g., $k_1(\tau) = \dots = k_2(\tau) = 0$ at $\tau = 0$.

Substitution of the solution for $z_1(\tau)$ into Eqs. (21) and then Eq. (19) yields a polynomial feedback control law with time-dependent coefficients.

A numerical example for the scalar case is included, using $\epsilon = 0.01$ and $t_f = 5$ s. The performance indices are given in Table 1, and the state variable and control histories are given in Fig. 1. Curves corresponding to fourth- and fifth-order feedback are coincident with third order and, hence, are not plotted. Fifth-order polynomial feedback essentially has converged to the optimal control for this scalar problem.

A system for attitude control of a spacecraft with four reaction wheels is now examined.

Spacecraft Orientation

Euler Parameters

A spacecraft body-fixed reference frame $\{\hat{b}\}$ is related to an inertial frame $\{\hat{n}\}$ by the direction cosine matrix $[C(\beta)]$,

$$\{\hat{b}\} = [C(\beta)]\{\hat{n}\} \qquad (23)$$

where $[C(\beta)]$ is defined in terms of the four Euler parameters $(\beta_0, \beta_1, \beta_2, \beta_3)$.[8] These attitude variables are related to the body-frame components of the spacecraft angular velocity ω by the following kinematic differential equations:

$$\dot{\beta}_0 = -\tfrac{1}{2}(\beta_1\omega_1 + \beta_2\omega_2 + \beta_3\omega_3), \quad \dot{\beta}_1 = \tfrac{1}{2}(\beta_0\omega_1 - \beta_3\omega_2 + \beta_2\omega_3)$$

$$\dot{\beta}_2 = \tfrac{1}{2}(\beta_3\omega_1 + \beta_0\omega_2 - \beta_1\omega_3), \quad \dot{\beta}_3 = -\tfrac{1}{2}(\beta_2\omega_1 - \beta_1\omega_2 - \beta_0\omega_3) \qquad (24)$$

with

$$(\cdot) \equiv \frac{d}{dt}(\ )$$

Momentum Reference Frame

In addition to using an arbitrary, general inertial frame $\{\hat{n}\}$, a special inertial angular momentum frame $\{\hat{h}\}$ is introduced where $\hat{h}_2$ is aligned with the system angular momentum H, as discussed by Vadali and Junkins[9] and Kraige and Junkins.[10] The other two unit vectors can be defined by the directions $\hat{n}_1$ and $\hat{n}_3$ assume after $\hat{n}_2$ is rotated to coincide with H (see Fig. 2). This reference frame can be considered inertial if the external torques are negligible during the maneuver and only internal torques are present. As is shown below, introducing this frame allows a use of the angular momentum integral to reduce the number of state variables.

The orientation of $\{\hat{b}\}$ with respect to the momentum frame $\{\hat{h}\}$ is given by the projection

$$\{\hat{b}\} = [C(\delta)]\{\hat{h}\} \qquad (25)$$

where the 3×3 direction cosine matrix $[C]$ is a function of four variable Euler parameters $(\delta_0, \delta_1, \delta_2, \delta_3)$. The inertial frame $\{\hat{n}\}$ is projected onto $\{\hat{h}\}$ by

$$\{\hat{n}\} = [C(\alpha)]\{\hat{h}\} \qquad (26)$$

where $(\alpha_0, \alpha_1, \alpha_2, \alpha_3)$ are constant Euler parameters since both $\{\hat{n}\}$ and $\{\hat{h}\}$ are inertial. Using the inertial frame $\{\hat{n}\}$ components of the system angular momentum

$$H = H_{n1}\hat{n}_1 + H_{n2}\hat{n}_2 + H_{n3}\hat{n}_3 \qquad (27)$$

the constant α_i Euler parameters can be defined as

$$\alpha_0 = \left[\frac{H + H_{n2}}{2H}\right]^{1/2}$$

$$\alpha_1 = -H_{n1}\left[\frac{H - H_{n2}}{2H(H_{n1}^2 + H_{n3}^2)}\right]^{1/2}$$

$$\alpha_2 = 0$$

$$\alpha_3 = H_{n1}\left[\frac{H - H_{n2}}{2H(H_{n1}^2 + H_{n3}^2)}\right]^{1/2} \quad (28)$$

The δ_i Euler parameters are then related to the α_i parameters by the bilinear, orthogonal equation

$$\begin{Bmatrix} \delta_0 \\ \delta_1 \\ \delta_2 \\ \delta_3 \end{Bmatrix} = \begin{bmatrix} \alpha_0 & -\alpha_1 & -\alpha_2 & -\alpha_3 \\ \alpha_1 & \alpha_0 & -\alpha_3 & \alpha_2 \\ \alpha_2 & \alpha_3 & \alpha_0 & -\alpha_1 \\ \alpha_3 & -\alpha_2 & \alpha_1 & \alpha_0 \end{bmatrix} \begin{Bmatrix} \beta_0 \\ \beta_1 \\ \beta_2 \\ \beta_3 \end{Bmatrix} \quad (29)$$

and are related to the body-frame components of ω by the differential equations

$$\dot{\delta}_0 = -\tfrac{1}{2}(\delta_1\omega_1 + \delta_2\omega_2 + \delta_3\omega_3)$$

$$\dot{\delta}_1 = \tfrac{1}{2}(\delta_0\omega_1 - \delta_3\omega_2 + \delta_2\omega_3)$$

$$\dot{\delta}_2 = \tfrac{1}{2}(\delta_3\omega_1 + \delta_0\omega_2 - \delta_1\omega_3)$$

$$\dot{\delta}_3 = -\tfrac{1}{2}(\delta_2\omega_1 - \delta_1\omega_2 - \delta_0\omega_3) \quad (30)$$

It can be shown from Eq. (25) and using the algebraic expressions for $[c(\delta)]$ from Ref. 8 or 10 that

$$\hat{h}_2 = 2(\delta_1\delta_2 + \delta_0\delta_3)\hat{b}_1 + (\delta_0^2 - \delta_1^2 + \delta_2^2 - \delta_3^2)\hat{b}_2$$

$$+ 2(\delta_2\delta_3 - \delta_0\delta_1)\hat{b}_3 \quad (31)$$

so the body-frame components of the system angular momentum can now be written from $H = H\hat{h}_2$ as

$$H_1 = 2(\delta_1\delta_2 + \delta_0\delta_3)H$$

$$H_2 = (\delta_0^2 - \delta_1^2 + \delta_2^2 - \delta_3^2)H$$

$$H_3 = 2(\delta_2\delta_3 - \delta_0\delta_1)H \quad (32)$$

Thus we have an explicit relationship to eliminate H_i in terms of δ_i.

Spacecraft and Reaction Wheel Dynamics

An arbitrary asymmetric spacecraft with four reaction wheels in NASA standard configuration is considered (see Fig. 3). The system angular momentum H is the sum of the spacecraft and wheel angular momenta; the body components of H and ω are related by

$$H = [I^\bullet]\omega + [\tilde{C}]^T[J]\Omega \quad (33)$$

where $[I^\bullet]$ is the system inertia matrix with respect to the body frame $\{\hat{b}\}$, Ω a vector of the four-wheel angular velocities, and $[J]$ the wheel axial moment of inertia matrix defined by $[J] = \text{diag}\{J_{ai}\}$, $i = 1,2,3,4$. $[\tilde{C}]$ is a 4×3 matrix whose rows are the three orthogonal body-frame components of four unit vectors along the wheel spin axes.

Assuming negligible external torques, the time rate of change of the angular momentum is zero, and thus the Eulerian equation of motion is obtained

$$\dot{H} = [I^\bullet]\dot{\omega} + [\tilde{C}]^T[J]\dot{\Omega} + [\tilde{\omega}]H = 0 \quad (34)$$

where

$$[\tilde{\omega}] = \begin{bmatrix} 0 & -\omega_3 & \omega_2 \\ \omega_3 & 0 & -\omega_1 \\ -\omega_2 & \omega_1 & 0 \end{bmatrix} \quad (35)$$

The reaction wheel equations of motion are

$$[J]\dot{\Omega} + [J][\tilde{C}]\dot{\omega} = u \quad (36)$$

where the four components of the control vector u are the axial torques applied to their respective wheels by the motors. To eliminate the wheel angular velocities Ω from the spacecraft equations of motion, Eq. (36) is multiplied by $[\tilde{C}]^T$ and then substituted into Eq. (34) to obtain

$$\dot{\omega} = -[G]\{[\tilde{\omega}]H + [\tilde{C}]^T u\} \quad (37)$$

where $[G] = [I^\bullet - \tilde{C}^T J\tilde{C}]^{-1}$, a constant matrix. Implicit in Eq. (37) is the substitution of Eqs. (32); thus, $\dot{\omega} = f(\omega, \delta, u)$. Notice the pleasing truth that rest-to-rest maneuvers (characterized by $H = 0$) remove all of the gyroscopic terms in Eq. (37). It is evident that, for this class of maneuvers, angular velocity control is near trivial and attitude control is nonlinear only because of kinematic nonlinearities.

The three equations of motion in Eq. (37) and the four attitude equations in Eq. (30) will be used to determine the state equations.

Optimal Feedback Control Formulation

State Equations

To obtain state equations of the form

$$\dot{x} = Ax + F(x) + Bu \quad (38)$$

in which A is a constant coefficient matrix and $F(x)$ a vector function containing the nonlinear terms, let the state variables be the spacecraft angular velocities ω_i and Euler parameter differences δ_i; thus, the seven-element state vector is

$$x = \{\omega_1 \ \omega_2 \ \omega_3 \ \bar{\delta}_0 \ \bar{\delta}_1 \ \bar{\delta}_2 \ \bar{\delta}_3\}^T \quad (39)$$

where

$$\bar{\delta}_i = \delta_i - \delta_i(t_f) \quad (i = 0,1,2,3) \quad (40)$$

These new state variables introduce linear terms into the dynamic and kinematic equations, Eqs. (37) and (30), respectively.

The elements of the A matrix for the linear part of the state equations are found to be

$$a_{11} = g_{12}H_3^0 - g_{13}H_2^0 \qquad a_{12} = g_{13}H_1^0 - g_{11}H_3^0$$

$$a_{13} = g_{11}H_2^0 - g_{12}H_1^0 \qquad a_{21} = g_{22}H_3^0 - g_{23}H_2^0$$

$$a_{22} = g_{23}H_3^0 - g_{21}H_3^0 \qquad a_{23} = g_{21}H_2^0 - g_{22}H_1^0$$

$$a_{31} = g_{32}H_3^0 - g_{33}H_2^0 \qquad a_{32} = g_{23}H_1^0 - g_{31}H_3^0$$

$$a_{33} = g_{31}H_2^0 - g_{32}H_1^0 \qquad a_{41} = -\delta_1(t_f)/2$$

$$a_{42} = -\delta_2(t_f)/2 \qquad a_{43} = -\delta_3(t_f)/2$$

$$a_{51} = \delta_0(t_f)/2 \qquad a_{52} = -\delta_3(t_f)/2$$

$$a_{53} = \delta_2(t_f)/2 \qquad a_{61} = \delta_3(t_f)/2$$

$$a_{62} = \delta_0(t_f)/2 \qquad a_{63} = -\delta_1(t_f)/2$$

$$a_{71} = -\delta_2(t_f)/2 \qquad a_{72} = \delta_1(t_f)/2$$

$$a_{73} = \delta_0(t_f)/2$$

$$a_{ij} = 0 \ (i = 1,\dots,7; \qquad j = 4,\dots,7) \quad (41)$$

where H^0 is Eq. (32) evaluated at $\delta_i(t_f)$ and g_{ij} are the elements of matrix $[G]$ defined after Eq. (37). Notice that a_{ij}
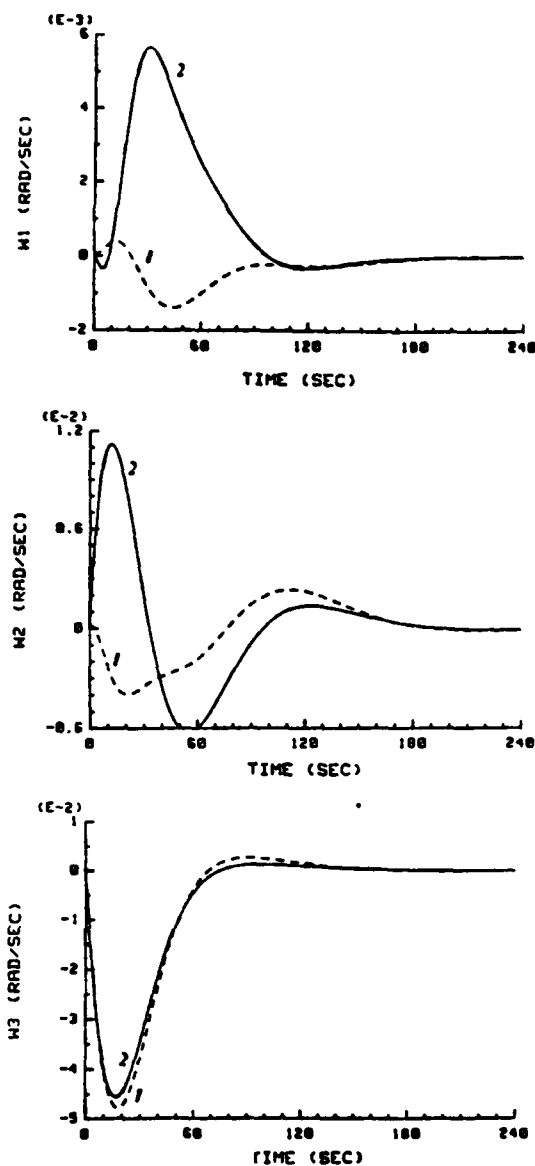
11

Fig. 4   Case 1: Spacecraft angular velocities.

Fig. 5   Case 1: Wheel angular velocities: 1, linear feedback; 2, linear plus quadratic feedback.

are explicit functions of the specific terminal state $\delta_i(t_f)$ and the magnitude of the system angular momentum H. B is a 7×4 matrix

$$B = \left[\begin{array}{c} -[G][\check{C}]^T \\ \hline 0 \end{array} \right] \tag{42}$$

and the vector $F(x)$ contains quadratic and cubic terms in x_i.

Performance Index

Two quadratic performance indices are considered

$$J_1 = \frac{1}{2} \int_{t_0}^{t_f} \{x^T Q x + u^T R u\} dt \tag{43}$$

and

$$J_2 = \frac{1}{2} \int_{t_0}^{t_f} \{x^T Q x + m^T W m\} dt \tag{44}$$

where

$$m = [\check{C}]^T u \tag{45}$$

is a 3×1 vector containing the orthogonal components of the vector sum of the motor torques. J_1 penalizes the four motor torques and J_2 penalizes their projections on the principal axes.

In the numerical examples, performance index J_1 is used for maneuvers involving all four wheels. Performance index J_2 may also be used with four wheels, but the wheel torques are not unique, as shown below. All examples utilizing three wheels use J_2, in which the 4×3 matrix $[\check{C}]$ in Eq. (45) is replaced by its 3×3 nonzero submatrix. Q is a positive semidefinite weighting matrix, and R and W are identity matrices for the examples considered.

Feedback Control

For the performance index in Eq. (43), the optimal control is

$$u = -R^{-1} B_1^T \lambda \tag{46}$$

where B_1 is the B matrix of Eq. (42). The analogous development for the performance index of Eq. (44) uses the state equations in the form

$$\dot{x} = A x + F(x) + B_2 m \tag{47}$$

12

Fig. 6 Case 1: Control torques.

Table 3 Inertia and wheel geometry matrices

$$[I^o] = \begin{bmatrix} 87.212 & -0.2237 & -0.2237 \\ -0.2237 & 86.067 & -0.2237 \\ -0.2237 & -0.2237 & 114.562 \end{bmatrix}$$
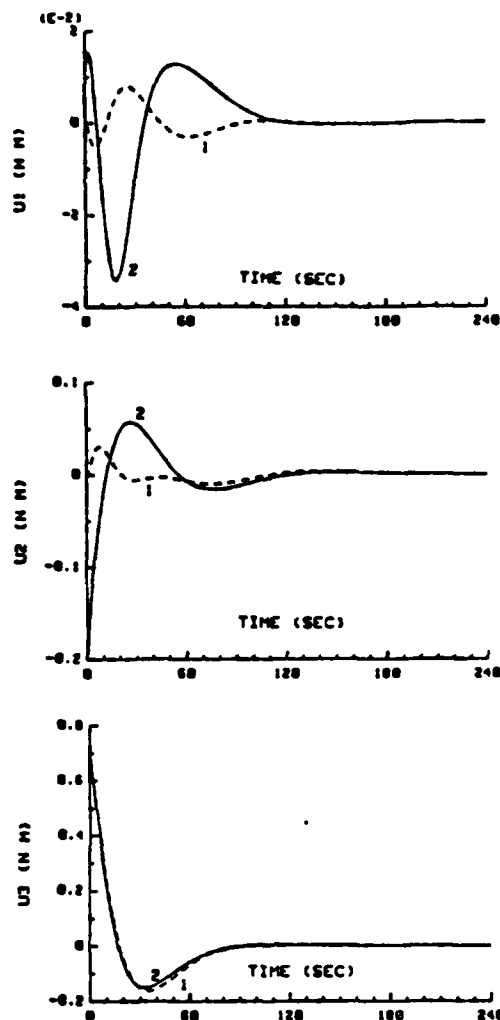
$$[\bar{C}] = \begin{bmatrix} 1 & 0 & 0 \\ 0 & 1 & 0 \\ 0 & 0 & 1 \\ \sqrt{3}/3 & \sqrt{3}/3 & \sqrt{3}/3 \end{bmatrix}$$

Table 4 Case 1: Boundary conditions

	Initial states	Final states
ω_1	0.0001	0.0
ω_2	0.0001	0.0
ω_3	0.0001	0.0
ϕ	$-\pi/2$	$\pi/2$
θ	$-\pi/3$	$\pi/3$
φ	$-\pi/4$	$\pi/4$
δ_0	-0.54611	-0.30257
δ_1	0.47921	-0.13976
δ_2	0.67687	0.81747
δ_3	0.11820	046974
β_0	-0.33141	0.33141
β_1	0.46194	0.46194
β_2	-0.19134	0.19134
β_3	0.80010	0.80010
Ω_1	0.0	$-$[a]
Ω_2	0.0	$-$[a]
Ω_3	0.0	$-$[a]
Ω_4	0.0	$-$[a]

[a]Specific final boundary conditions for $\Omega_i(t_f)$ need not be formally enforced; these are determined implicitly because angular momentum is conserved; i.e., for H = const and $\omega(t_f)$ specified, $\Omega(t_f)$ is implicitly constrained by Eq. (33).

where B_2 is a 7×3 matrix

$$B_2 = \begin{bmatrix} -[G] \\ \hline 0 \end{bmatrix} \qquad (48)$$

The optimal control m for J_2 is

$$m = -W^{-1}B_2^T\lambda \qquad (49)$$

and the wheel torques u are obtained by inverting Eq. (45). This solution for u is not unique unless $[\bar{C}]$ is a square matrix.

Numerical Examples

Several examples are considered for an asymmetric spacecraft with four reaction wheels, as shown in Fig. 3. The moments of inertia of the spacecraft without the wheels and the wheel axial moment of inertia are given in Table 2; the inertia matrix $[I^o]$ and the wheel geometry matrix $[\bar{C}]$ are given in Table 3. All examples were performed using linear and quadratic steady-state gains with free final time t_f. The examples start with zero initial conditions for wheel and spacecraft velocities and end with large initial conditions.

Case 1

A four-wheel maneuver using J_1 and several three-wheel maneuvers using J_2 are executed, all with zero initial wheel speeds. Boundary conditions are given in Table 4 using the 3-1-3 Euler angles. Table 5 contains the performance indices,

Table 5 Case 1: Performance indices

	Linear feedback	Linear plus quadratic feedback
Four wheels, J_1		
Q_1	6.15126	6.13691
Q_2	5.76886	5.62314
Skew wheel off, J_2		
Q_1	6.48600	6.47143
Q_2	5.92983	5.73828
Third wheel off, J_2		
Q_2	5.93077	5.76176
Second wheel off, J_2		
Q_2	5.92980	5.76077
First wheel off, J_2		
Q_2	5.92962	5.76071

13
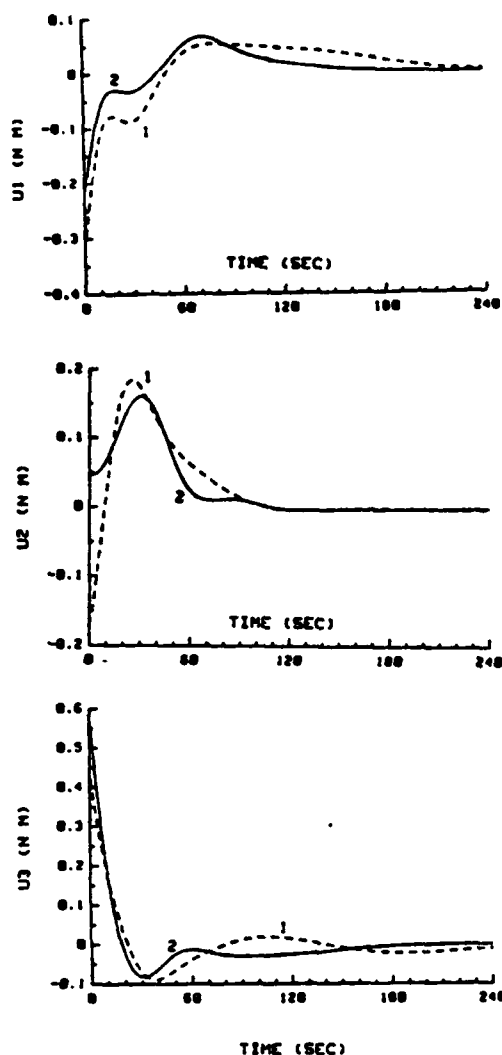
Fig. 7 Case 2: Control torques: 1, linear feedback; 2, linear plus quadratic feedback.

Fig. 8 Case 2: Spacecraft angular velocities.

which are evaluated at $t_f = 120$ s for the four-wheel maneuver and $t_f = 240$ s for the three-wheel maneuvers.

A comparison of performance indices with full and partial weighting on the Euler parameters is made. Q_1 indicates full state penalties in the performance index, and Q_2 implies that no penalties are put on δ_0. Figures 4 and 5 show the spacecraft and wheel angular velocities for the case of three orthogonal wheels (skew wheel off) and Q_2 in performance index J_2, which produced the lowest three-wheel performance index. The control torques are shown in Fig. 6.

Case 2

A rest-to-rest maneuver with nonzero initial wheel speeds is performed with three orthogonal wheels (skew wheel off) and no penalty on δ_0 in performance index J_2. This weighting produced the lowest performance index in cases 1 and 2. The boundary conditions are given in Table 6 and the performance indices evaluated at $t_f = 240$ s are given in Table 7. Since the initial and final Euler angles are the same as in case 1, the Euler parameters β_i are the same, but the system angular momentum is larger and, hence, the Euler parameters δ_i are different. Figures 7-9 plot the spacecraft and wheel angular velocities and control torques. Note that the final wheel speeds are 75, 50, and 100 rad/s for Ω_1, Ω_2, and Ω_3, respectively.

Case 3

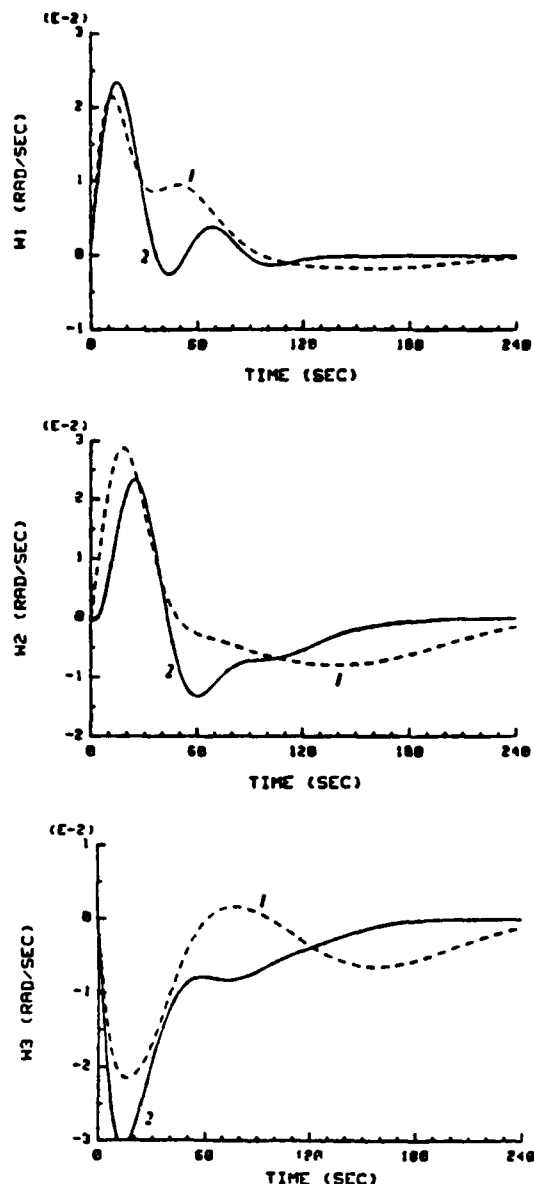A three-dimensional maneuver is demonstrated for the three-wheel configuration with large initial spacecraft angular

velocities and the initial wheel speeds of case 2. The boundary conditions for this maneuver are given in Table 8. Performance index J_2 was used, once with equal weights on all Euler parameters δ_i and once with no weight on δ_0. Only linear feedback was used for both performance indices to demonstrate the differences between full and partial weighting, although quadratic feedback improves control performance when stable linear control is obtained. Figures 10 and 11 give the time histories of the Euler parameters, spacecraft angular velocities, and wheel speeds for these two cases.

Discussion

The performance indices in Tables 5 and 7 were reduced when quadratic feedback was added to the linear control. In both cases quadratic feedback produced Euler parameters that reached their final states earlier and resulted in a lower performance index. This also occurred with the spacecraft angular velocities in case 2.

A comparison was made between full and partial Euler parameter weighting in the performance index, since specifying values for three Euler parameters automatically produces a value for the fourth when the nonlinear state equations are used. No stability problems were encountered using partial
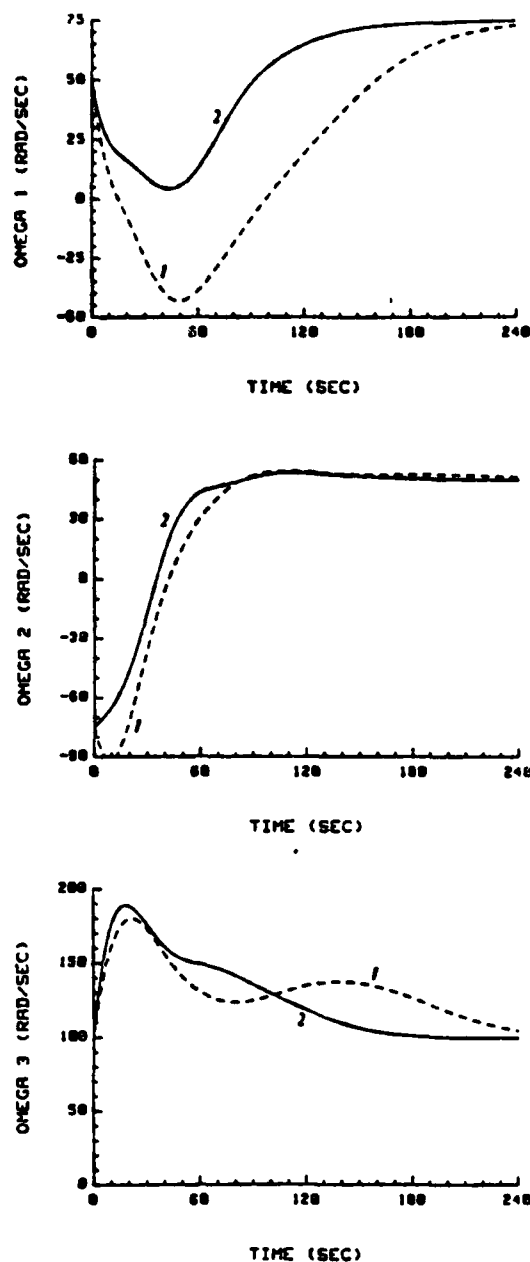
14

Fig. 10 Case 3: Unstable control.

Fig. 9 Case 2: Wheel angular velocities: 1, linear feedback; 2, linear plus quadratic feedback.

Table 7 Case 2: Performance indices

Linear feedback	4.81211
Linear plus quadratic feedback	4.29420

Table 6 Case 2: Boundary conditions

	Initial states	Final states
ω_1	0.0	0.0
ω_2	0.0	0.0
ω_3	0.0	0.0
ϕ	$-\pi/2$	$\pi/2$
θ	$-\pi/3$	$\pi/3$
φ	$-\pi/4$	$\pi/4$
δ_0	-0.12815	0.37037
δ_1	0.59459	0.10026
δ_2	0.45281	0.74062
δ_3	0.65192	0.55159
Ω_1	50.0	$-$[a]
Ω_2	-75.0	$-$[a]
Ω_3	100.0	$-$[a]
Ω_4	0.0	$-$[a]

[a]See Table 4 footnote.

Table 8 Case 3: Boundary conditions

	Initial states	Final states
ω_1	0.0	0.0
ω_2	0.0	0.0
ω_3	-0.01	0.0
ϕ	$-\pi/2$	$\pi/2$
θ	$-\pi/3$	$\pi/3$
φ	$-\pi/4$	$\pi/4$
δ_0	-0.22769	-0.07728
δ_1	0.47213	-0.25249
δ_2	0.84335	0.93018
δ_3	0.11840	0.24472
Ω_1	50.0	$-$[a]
Ω_2	-75.0	$-$[a]
Ω_3	100.0	$-$[a]
Ω_4	0.0	$-$[a]

[a]See Table 4 footnote.

15

EULER PARAMETERS DELTA
LINEAR FEEDBACK

SPACECRAFT ANGULAR VELOCITIES
LINEAR FEEDBACK

WHEEL ANGULAR VELOCITIES
LINEAR FEEDBACK

Fig. 11 Case 3: Stable control.

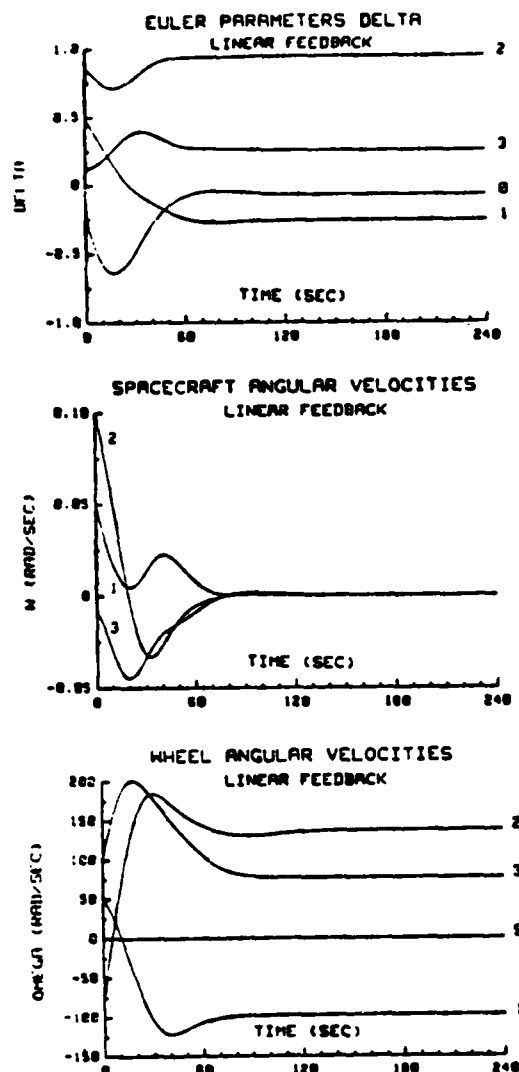weighting as long as spacecraft velocities were small, but in case 3 partial weighting produced the tumbling behavior in Fig. 10. This unstable behavior occurs because the linear feedback gains are determined by only the linear parts of the state equations. Although the nonzero eigenvalues of $A - BR^{-1}B^T K$ have negative real parts, so that the linear closed-loop system is stable, the nonlinear terms in the state equations are large and produce unstable behavior in the simulation. Similar behavior is seen in cases 1 and 2, except that the quadratic terms in the state equations change δ_0 by a smaller perturbation that is not destabilizing.

When the departure motion of all four Euler parameters is penalized in the performance index, linear gains are determined that will keep δ_0 close to its desired final state. The quadratic terms in the state equations then do not produce

destabilizing corrections to the linear closed-loop equations, since bounds have been placed on the states through the performance index. As is evident in comparing Figs. 10 and 11, introducing the penalty on δ_0 departure motion eliminates the tumbling motion and yields an attractive optimal maneuver.

Conclusions

Polynomial feedback on angular velocities and Euler parameters have been used for nonlinear control of a spacecraft with four reaction wheels. A comparison of linear and quadratic control was made, with a reduction in the performance index for quadratic feedback. When using redundant attitude variables, care must be taken so that the linear gains (based upon linearized departure motion state equations) result in modest violations of the implicit constraints. This may be enforced by penalizing all states in the performance index weight matrix.

References

[1]Willenstein, A.P., "Optimal Regulation of Nonlinear Dynamical Systems on a Finite Interval," *SIAM Journal of Control and Optimization*, Vol. 15, Nov. 1977, pp. 1050-1069.

[2]Dabbous, T.E. and Ahmed, N.U., "Nonlinear Optimal Feedback Regulation of Satellite Angular Momenta," *IEEE Transactions on Aerospace and Electronic Systems*, Vol. AES-18, Jan. 1982, pp. 2-10.

[3]Dwyer, T.A.W. III and Sena, R.P., "Control of Spacecraft Slewing Maneuvers," *IEEE 21st Conference on Decision and Control*, Orlando, FL, Dec. 1982.

[4]Carrington, C.K. and Junkins, J.L., "Nonlinear Feedback Control of Spacecraft Slew Maneuvers," *Journal of the Astronautical Sciences*, Vol. 32, Jan.-March 1984, pp. 29-45.

[5]Potter, J.E., "Matrix Quadratic Solutions," *SIAM Journal of Applied Mathematics*, Vol. 14, May 1966, pp 496-501.

[6]Turner, J.D. and Chun, H.M., "Optimal Feedback Control of a Flexible Spacecraft During a Large-Angle Rotations Maneuver," AIAA Paper 82-1589, Aug. 1982.

[7]Juang, J.-N., Turner, J.D., and Chun, H.M., "Large-Angle Maneuvers of Flexible Spacecraft Using a Closed Form Solution for the Terminal Tracking Problem," AAS/AIAA Paper 83-375, Aug. 1983.

[8]Whittaker, E.T., "A Treatise on the Analytical Dynamics of Particles and Rigid Bodies," Dover Publications, New York, 1944, pp. 10-11.

[9]Vadali, S.R. and Junkins, J.L., "Spacecraft Large Angle Rotational Maneuvers with Optimal Momentum Transfer," *Journal of the Astronautical Sciences*, Vol. XXXI, April-June 1983, pp. 217-235.

[10]Kraige, L.G. and Junkins, J.L., "Perturbation Formulations for Satellite Attitude Dynamics," *Celestial Mechanics*, Vol. 13, 1976, pp. 39-64.

[11]Lee, E.B. and Markus, L., *Foundations of Optimal Control Theory*, John Wiley & Sons, New York, 1967.

[12]Kirk, D.E., *Optimal Control Theory*, Prentice-Hall, 1970.

[13]Hoffman, H.C., Donohue, J.H., and Datley, T.W., "SMM Attitude Control Recovery," AIAA Paper 81-1760, Aug. 1981.

AAS 85-361

Spacecraft Attitude Control Using Generalized Angular Momentum

C. K. Carrington and J. L. Junkins

SPACECRAFT ATTITUDE CONTROL USING
GENERALIZED ANGULAR MOMENTA

Connie K. Carrington *
John L. Junkins +

Suboptimal nonlinear state feedback control laws are developed for space-craft attitude control using the Euler parameters and conjugate angular momenta. Time-dependent gains are determined in closed form for polynomial feedback laws, and stable nonlinear state feedback laws are developed from Lyapunov functions. The Lyapunov laws are made optimal by adjusting constants to minimize a quadratic performance index. Numerical simulations for single and three-axis large-angle slew maneuvers are presented.

INTRODUCTION

Many current and future spacecraft missions require rapid large-angle reorientation maneuvers. Traditional feedback controls may not be adequate for the accuracy and speed required for on-board, real-time implementation, prompting investigation of control laws using alternate state variables. Recently, feedback control laws using the four Euler parameters or quaternions[1,2] and the spacecraft angular velocities have been developed for attitude control (see Refs. 3-8).

Morton[9] has presented a new formulation of rigid body rotational dynamics in terms of four generalized angular momenta that are conjugate to the Euler parameters. Rotational motion is determined by eight state equations that are cubic polynomials in the states. The development includes applied torques, which will be used in this paper for spacecraft attitude control.

Suboptimal polynomial state feedback control laws [8,10] that minimize a quadratic performance index are developed for rapid large-angle spacecraft maneuvers. The costates are written as polynomials in the states, producing sets of differential equations for the gains. These equations are solved recursively, since the linear and zeroth-order gains determine coefficients in the equations for the quadratic gains. Each set of equations are solved in closed form, producing gains that are polynomials in time. A suboptimal control law is generated by truncation of the polynomial expansion in the states. A numerical example using this control law is presented for a single-axis, large-angle, spin-down maneuver.

Nonlinear state feedback control laws utilizing Lyapunov functions[11] are also investigated for single and three-axis maneuvers, as in Refs. 3 and 4. Unlike the time-dependent polynomial control laws examined earlier, these feedback controls

---

* Assistant Professor of Mechanical Engineering, College of Engineering, University of South Carolina, Columbia, South Carolina 29208.

+ Professor of Engineering Science and Mechanics, Virginia Polytechnic Institute and State University (VPI & SU), Blacksburg, Virginia 24061.

are guaranteed to produce a closed-loop system that is asymptotically stable in the large. Constants in the Lyapunov laws may also be adjusted to minimize the quadratic performance index of an optimal control formulation. The system response for the optimal Lyapunov control law demonstrates the moderate rise-time, short settling time, and low overshoot associated with optimally damped ($\varsigma = 0.707$) second-order systems.

EQUATIONS OF MOTION

The attitude control problem for a rigid spacecraft is governed by a set of kinematic equations defining orientation of the body with respect to an inertial frame, and a set of dynamic equations representing rotational motion. The orientation of a body-fixed reference frame $\{\hat{b}\}$ to an inertial frame $\{\hat{n}\}$ is given by the projection

$$\{\hat{b}\} = [C]\{\hat{n}\} \tag{1}$$

where $[C]$ is the direction cosine matrix. Instead of three Euler angles. the four Euler parameters[1,2] will be used to parameterize the elements of $[C]$. The Euler parameters are defined as

$$\begin{aligned} \beta_0 &= \cos(\Phi/2) \\ \beta_i &= l_i \sin(\Phi/2) \end{aligned} \tag{2}$$

where l_i are components of a unit vector along the principal axis of rotation when rotating from $\{\hat{n}\}$ to $\{\hat{b}\}$, and Φ is the rotation angle for that reorientation. Since rotational motion has three degrees of freedom, the four Euler parameters are once redundant and satisfy the constraint

$$\sum_{i=0}^{3} \beta_i^2 = 1 \tag{3}$$

The time derivatives of the Euler parameters are functions of the spacecraft angular velocity components ω_i and the Euler parameters.

Rotational motion is governed by Euler's equations, which are generally written in terms of the angular velocity components ω_i. Consistant with the development of Hamilton's canonical equations[12], Euler's equations are reformulated in terms of generalized angular momenta p_i that are conjugate to the Euler parameters. They are defined from the rotational kinetic energy T as follows

$$p_i = \frac{\partial T}{\partial \dot{\beta}_i} \quad i = 0, 1, 2, 3 \tag{4}$$

The equations governing the time derivatives of the Euler parameters are also reformulated in terms of the generalized angular momenta, producing the following eight equations of motion[9]

19

$$\{\dot{p}\} = -\frac{1}{4}[Q(p)][I^{-1}]_4[Q(p)]^T\{\beta\} + 2[Q(\beta)]\{u\}_4$$
$$\{\dot{\beta}\} = \frac{1}{4}[Q(\beta)][I^{-1}]_4[Q(\beta)]^T\{p\}$$

(5)

where $[Q(\beta)]$ and $[I^{-1}]_4$ are 4x4 matrices defined as follows

$$[Q(\beta)] = \begin{bmatrix} \beta_0 & -\beta_1 & -\beta_2 & -\beta_3 \\ \beta_1 & \beta_0 & -\beta_3 & \beta_2 \\ \beta_2 & \beta_3 & \beta_0 & -\beta_1 \\ \beta_3 & -\beta_2 & \beta_1 & \beta_0 \end{bmatrix}$$

(6)

and

$$[I^{-1}]_4 = diag\ \{0,\ 1/I_1,\ 1/I_2,\ 1/I_3\}$$

(7)

I_1, I_2, and I_3 are the spacecraft moments of inertia in a body-fixed, principal-axis reference frame. The nonzero elements of $\{u\}_4$ are the control torques about the principal axes

$$\{u\}_4 = \{\ 0\ u_1\ u_2\ u_3\ \}^T$$

(8)

Eqs. (5) are Hamilton's canonical equations in which $\{p,\ \beta\}$ are the eight state variables. These variables are twice redundant, with the β_i satisfying Eq. (3) and the p_i satisfying the following constraint

$$\sum_{i=0}^{3} p_i^2 = 4H^2$$

(9)

where H is the magnitude of the system angular momentum vector. These constraints are both integral properties of the system equations, however, and hence they do not need to be explicitly enforced when defining the optimal control problem.

OPTIMAL CONTROL PROBLEM

Formulation

The state equations are cubic polynomials, so that polynomial feedback control laws may be developed using an optimal control formulation[8,10]. No linear terms are present in Eqs. (5), however, and there are fewer control variables than states, so that the algebraic gain equations are in many instances degenerate. In these cases no solution can be found for constant gains.[13] Two remedies can be considered for this situation. The first is to introduce linear terms into the system equations by using the system errors as new state variables. The new state vector is $z(t) = r(t) - r(t_f)$, where $r(t)$ is the old state vector and $r(t_f)$ is the desired final state. Linear terms with constant coefficients $r(t_f)$ appear in the new state equations. The optimal control problem is formulated using the error vector z, and the costates are written as polynomials in z. Sets of equations for the gains are determined by equating

20

coefficients of like powers of $\underline{z}$ in the costate equations. Constant linear gains can be determined from the algebraic Riccati equations if at most one zero pole occurs in the linear part of the state equations, and higher order gains can be calculated recursively from the subsequent linear algebraic equations. Unfortunately, the system represented by Eqs. (5) contain two zero poles, corresponding to β_0 and p_0. The eigenvectors for these poles cannot be determined accurately enough to produce a reasonable solution to the Riccati equation using Schur's method [14], so the constant gain solution will not be used.

The other solution technique for state equations containing no linear terms is to determine time-dependent gains using the original cubic state equations. The tracking problem can be formulated using a performance index that minimizes the difference between the state and the target, and a final state penalty can be posed. The costates are written as polynomials in the original states $\underline{x}$, and the gain equations are defined as before from the costate equations. The differential equations defining the gains are simple, so that closed-form solutions may be found by integration. The terminal boundary conditions for the costates, which are determined by the performance index, specify constants of integration in the expressions for the gains.

Given the state equations in Eqs. (5), the performance index to be minimized is

$$J = \frac{1}{2}\underline{z}^T(t_f)H\underline{z}(t_f) + \frac{1}{2}\int_{t_0}^{t_f}\{\underline{z}^TQ\underline{z} + \underline{u}_4^TR\underline{u}_4\}dt \tag{10}$$

where $\underline{z}$ is the difference between the state $\underline{x}$ and the target state $\underline{r}$

$$\underline{z}(t) = \underline{x}(t) - \underline{r}(t_f)$$
$$\underline{x}(t) = \{\ p_0\ p_1\ p_2\ p_3\ \beta_0\ \beta_1\ \beta_2\ \beta_3\ \} \tag{11}$$

The necessary conditions for optimality produce the following costate equations

$$\dot{\lambda}_i = \frac{1}{4}\left[\frac{\partial C_{jk}(p)}{\partial p_i}\right]\lambda_j\beta_k - \frac{1}{4}C_{ji}(\beta)\gamma_j - q_{il}z_l$$

$$\dot{\gamma}_i = \frac{1}{4}C_{ji}\lambda_j - \frac{1}{4}\left[\frac{\partial C_{jk}(\beta)}{\partial\beta_i}\right]\gamma_jp_k - 2\left[\frac{\partial Q_{jk}(\beta)}{\partial\beta_i}\right]\lambda_ju_k - q_{il}z_l \tag{12}$$

$$i,j,k = 0,...,3$$
$$l = 1,...,8$$

where λ_i and γ_i are the costates corresponding to p_i and β_i respectively; the 4x4 matrix C is

$$C(p) = [Q(p)][I^{-1}]_4[Q(p)]^T \tag{13}$$

and the terms in brackets are Jacobians. The control is

$$\underline{u}_4 = -2R^{-1}Q^T(\beta)\underline{\lambda} \tag{14}$$

and the terminal boundary conditions on the costates are

$$\left\{\begin{array}{c}\lambda_i(t_f)\\\gamma_i(t_f)\end{array}\right\} = H\underline{z}(t_f) \tag{15}$$

Assuming the costates are polynomials in the states,

$$\left\{ \begin{array}{c} \lambda_i(t) \\ \gamma_i(t) \end{array} \right\} = s_i(t) + k_{ij}(t)x_j + d_{ijk}(t)x_j x_k + \ldots \tag{16}$$

then the boundary conditions of Eq. (15) produce the following conditions for the time-dependent coefficients in the polynomial expansion

$$\begin{aligned} \underline{s}(t_f) &= -H\underline{r}(t_f) \\ K(t_f) &= H \end{aligned} \tag{17}$$

with all higher-order coefficients going to zero at $t = t_f$.

By substituting Eq. (16) into the costate equations and equating coefficients of like powers of x, we obtain the following sets of equations

$$\begin{aligned} \dot{s}_i &= q_{ij}r_j \\ \dot{k}_{ij} &= -q_{ij} + f_1(s_i) \\ \dot{d}_{ijk} &= f_2(s_i, k_{ij}) \\ &\ \ \vdots \end{aligned} \tag{18}$$

where f_1 and f_2 are functions of lower order coefficients. Eqs. (18) can be integrated in closed-form, and the constants of integration determined by Eqs. (17). The feedback gains produced in this method are polynomials in time, which are substituted back into Eqs. (16) and (14). A suboptimal control law is determined by taking a finite number of terms in Eq. (16).

Single Axis Maneuvers

For single-axis maneuvers about the first principal axis, Eqs. (5) reduce to the following equations

$$\begin{aligned} \dot{x}_1 &= \frac{1}{4J}(x_1 x_2 x_4 - x_2^2 x_3) - 2x_4 u \\ \dot{x}_2 &= \frac{1}{4J}(x_1 x_2 x_3 - x_1^2 x_4) + 2x_3 u \\ \dot{x}_3 &= \frac{1}{4J}(x_1 x_4^2 - x_2 x_3 x_4) \\ \dot{x}_4 &= \frac{1}{4J}(x_2 x_3^2 - x_1 x_3 x_4) \end{aligned} \tag{19}$$

where $\underline{x} = \{ \begin{array}{cccc} p_0 & p_1 & \beta_0 & \beta_1 \end{array} \}^T$ and u is the control torque to be determined. For the following performance index

$$J = \frac{1}{2}\underline{z}^T(t_f)H\underline{z}(t_f) + \frac{1}{2}\int_{t_0}^{t_f}\{\underline{z}^T Q\underline{z} + u^2\}dt \tag{20}$$

where $\underline{z}(t) = \underline{x}(t) - \underline{r}(t_f)$ and $\underline{r}(t_f)$ is the desired final state, then the costate equations are

$$\dot{\lambda}_1 = -q_{1j}z_j - \frac{1}{4I}(\lambda_1 x_2 x_4 + \lambda_2(x_2 x_3 - 2x_1 x_4) + \lambda_3 x_4^2 - \lambda_4 x_3 x_4)$$

$$\dot{\lambda}_2 = -q_{2j}z_j + \frac{1}{4I}(\lambda_1(2x_2 x_3 - x_1 x_4) - \lambda_2 x_1 x_3 + \lambda_3 x_3 x_4 - \lambda_4 x_3^2)$$

$$\dot{\lambda}_3 = -q_{3j}z_j + \frac{1}{4I}(\lambda_1 x_2^2 - \lambda_2 x_1 x_2 + \lambda_3 x_2 x_4 + \lambda_4(x_1 x_4 - 2x_2 x_3)) - 2\lambda_2 u \tag{21}$$

$$\dot{\lambda}_4 = -q_{4j}z_j - \frac{1}{4I}(\lambda_1 x_1 x_2 - \lambda_2 x_1^2 + \lambda_3(2x_1 x_4 - x_2 x_3) - \lambda_4 x_1 x_3) + 2\lambda_1 u$$

and the control is

$$u = 2(x_4\lambda_1 - x_3\lambda_2). \tag{22}$$

λ_1 and λ_2 are the costates corresponding to the conjugate angular momenta p_0 and p_1, and λ_3 and λ_4 correspond to Euler parameters β_0 and β_1.

For this example, the weighting matrices Q and H are

$$Q = diag\{\ q_1\ q_2\ q_3\ q_4\ \}$$
$$H = diag\{\ h_1\ h_2\ h_3\ h_4\ \} \tag{23}$$

The zeroth-order equations are

$$\dot{s}_i = q_i r_i(t_f) \tag{24}$$

which, with the boundary conditions in Eq. (17), have the solution

$$s_i(t) = -q_i r_i(t_f)(t_f - t) - h_i r_i(t_f) \tag{25}$$

The linear equations are

$$\dot{k}_{ii} = -q_i \qquad\qquad i = 1,2$$
$$\dot{k}_{33} = -q_3 + 4s_2^2$$
$$\dot{k}_{44} = -q_4 + 4s_1^2 \tag{26}$$
$$\dot{k}_{ij} = 0 \qquad\qquad i \neq j$$

These equations have the solution

$$k_{ii}(t) = q_i(t_f - t) + h_i \qquad\qquad i = 1,2$$
$$k_{33}(t) = q_3(t_f - t) + h_3 - 4r_2^2(t_f)\{q_2^2\tau + q_2 h_2(t_f - t)^2 + h_2^2(t_f - t)\} \tag{27}$$
$$k_{44}(t) = q_4(t_f - t) + h_4 - 4r_1^2(t_f)\{q_1^2\tau + q_1 h_1(t_f - t)^2 + h_2(t_f - t)\}$$

where
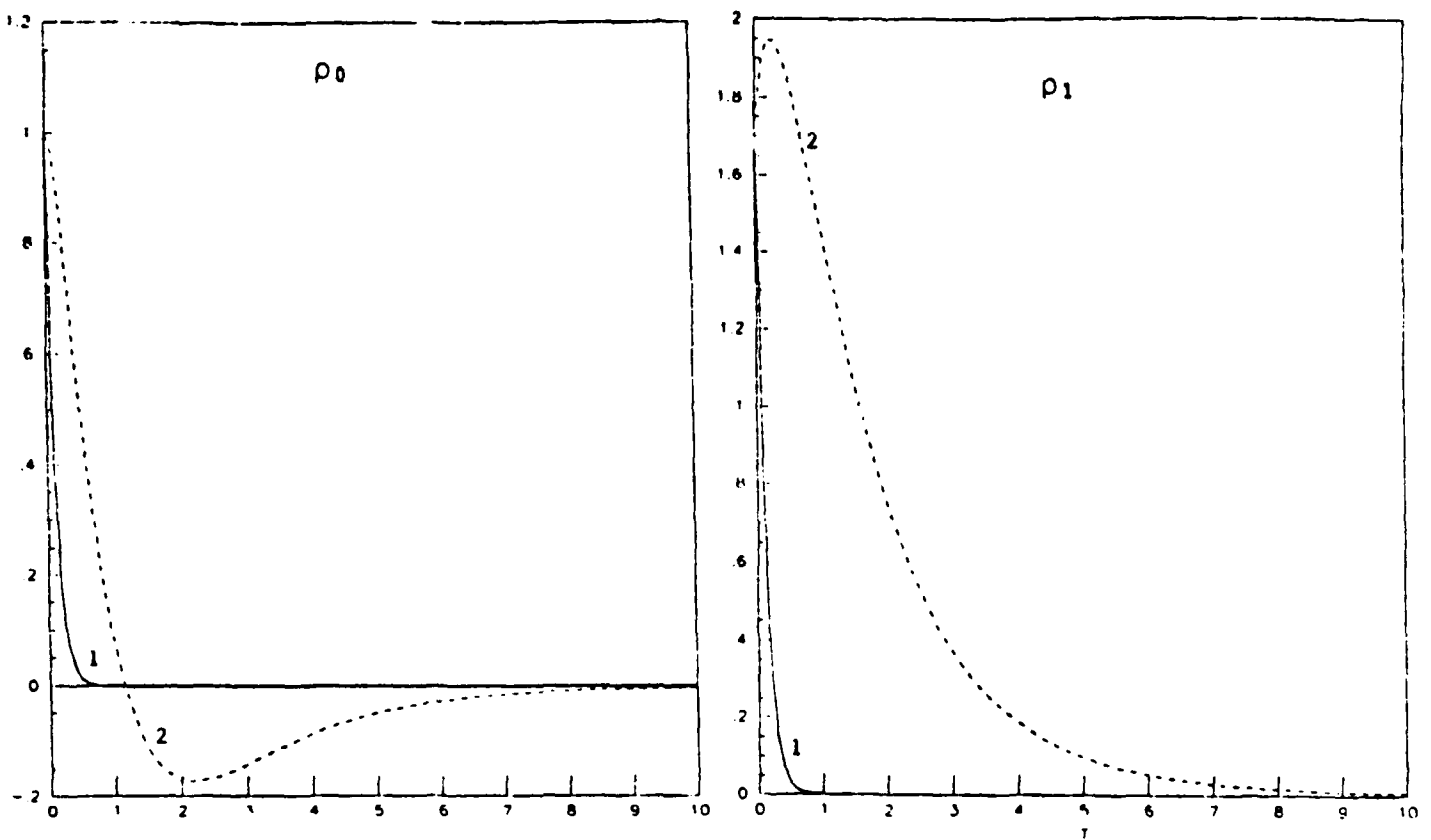
$$\tau = (t_f^3 - t^3)/3 + t_f t^2 - t_f^2 t \tag{28}$$

23

Fig. 1 Single-Axis Conjugate Angular Momenta

1     $s_i + k_{ij}x_j$
2     $s_i + k_{ij}x_j + d_{ijk}x_jx_k$

The quadratic equations are

$$\dot{d}_{114} = s_2/2I$$

$$\dot{d}_{123} = -s_2/4I$$

$$\dot{d}_{124} = -s_1/4I$$

$$\dot{d}_{134} = -4k_{11}s_2 + s_4/4I$$

$$\dot{d}_{144} = 4k_{11}s_1 - s_3/4I$$

$$\dot{d}_{213} = -s_2/4I$$

$$\dot{d}_{214} = -s_1/4I$$

$$\dot{d}_{223} = s_1/2I$$

$$\dot{d}_{233} = 4k_{22}s_2 - s_4/4I$$

$$\dot{d}_{234} = -4k_{22}s_1 + s_3/4I$$

(29)

and $\dot{d}_{ijk} = 0$ where not otherwise specified. The terminal boundary conditions for these equations are $d_{ijk}(t_f) = 0$, and the solutions contain linear through cubic powers in time. Similar polynomials in time are found for higher order gains.
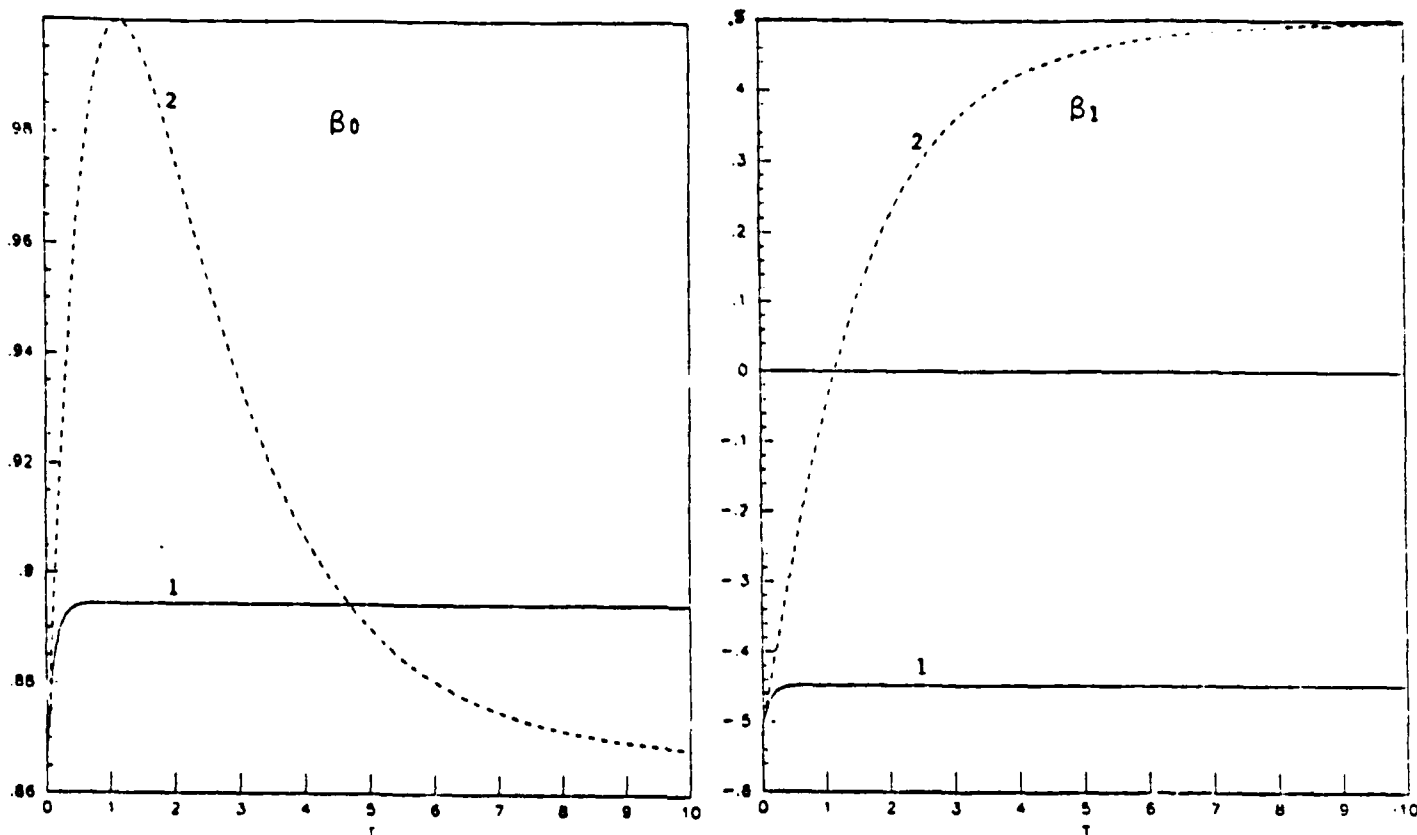
Fig. 2 Single-Axis Euler Parameters

1    $s_i + k_{ij}x_j$

2    $s_i + k_{ij}x_j + d_{ijk}x_jx_k$.

Numerical Example

A rapid large-angle, spin-down maneuver was simulated with $I = 1.00$ kg m^2 and $t_f = 20$ sec. The boundary conditions for the maneuver are listed in Table 1, and the performance indices in Table 2. The performance index weights were

$$H = Q = diag\{\, 0.1 \quad 0.1 \quad 0.1 \quad 0.1 \,\} \tag{30}$$

The conjugate angular momenta and Euler parameters are plotted in Figs. 1 and 2. Fig. 3 contains the maneuver angle and control torque histories.

Table 1

SINGLE-AXIS BOUNDARY CONDITIONS

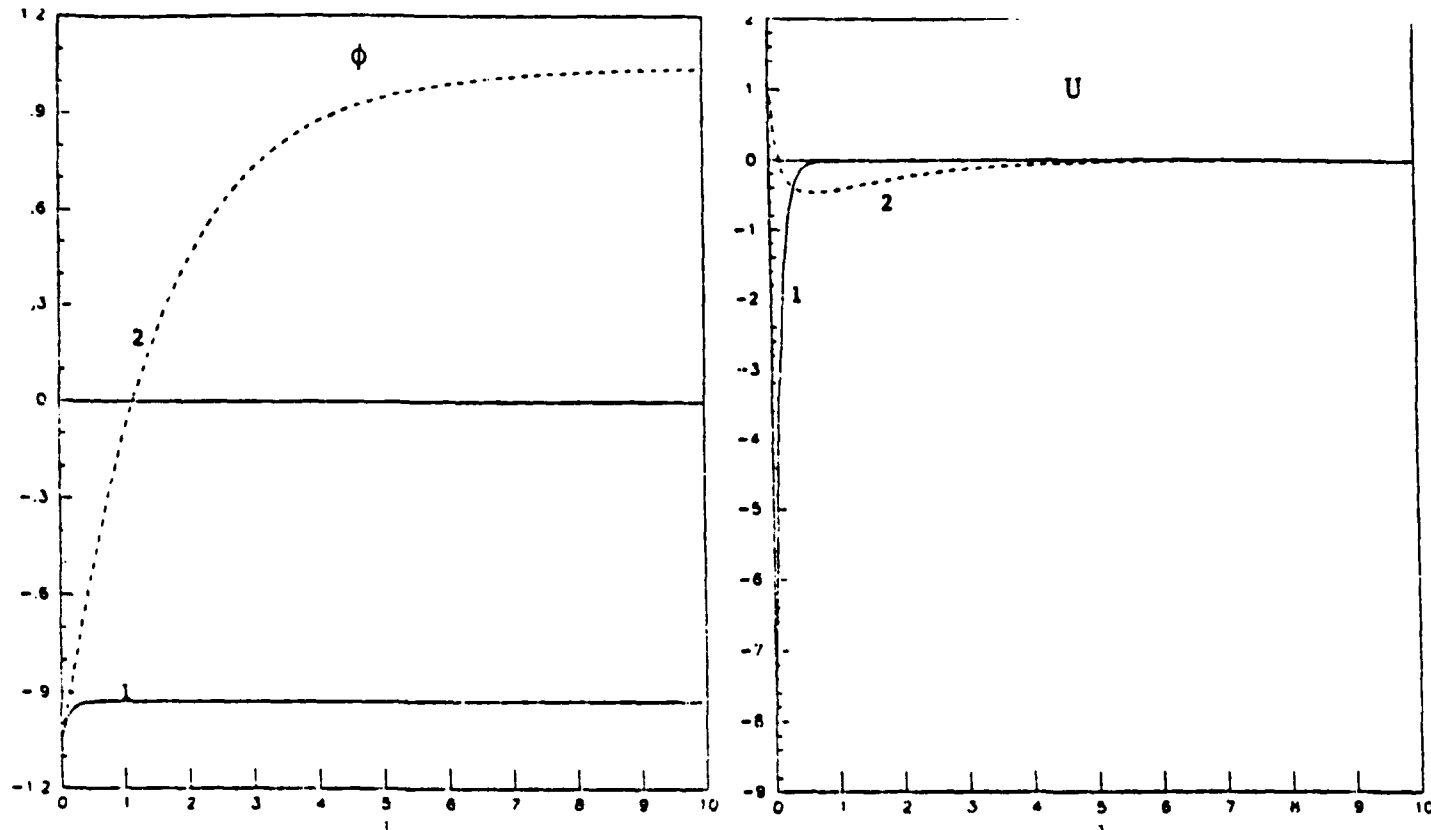| State	Initial State	Final State
ϕ (rad)	$-\pi/3$	$\pi/3$
ω (rad/sec)	1.000	0.000
β_0	0.866	0.866
β_1	-0.500	0.500
p_0 (kg m^2 rad/sec)	1.000	0.000
p_1 (kg m^2 rad/sec)	1.732	0.000

Fig. 3 Single-Axis Maneuver Angle and Control Torque

1    $s_i + k_{ij}x_j$

2    $s_i + k_{ij}x_j + d_{ijk}x_jx_k$

Table 2

SINGLE-AXIS PERFORMANCE INDICES
POLYNOMIAL FEEDBACK CONTROL

λ	Performance Index
$s_i + k_{ij}x_j$	3.13
$s_i + k_{ij}x_j + d_{ijk}x_jx_k$	0.49

Note that $\lambda_i = s_i + k_{ij}x_j$ only controls angular momentum, and the addition of quadratic terms are required for attitude control. Since the control influence matrix contains the Euler parameters, $\lambda_i = s_i + k_{ij}x_j + d_{ijk}x_jx_k$ results in cubic control terms in the state equations. This cubic feedback law provides a significant reduction in the performance index by reducing the Euler parameters errors, even though larger angular momentum values are incurred.

LYAPUNOV CONTROL LAWS

Formulation

Stable feedback control laws may be determined for autonomous systems from Lyapunov's second method[11]. To apply this method, the state equations are trans-

26

formed so that the target state is the origin. This is accomplished by defining new states $\underline{z}(t) = \underline{x}(t) - r(t_f)$ as discussed in the previous section. A scalar positive definite function $V(\underline{z})$ is defined, and a control law is found that makes the total time derivative of $V(\underline{z})$ negative definite. This control law will then be asymptotically stable and drive the system to the origin.

Consider the positive definite function

$$V = 2 \sum_{i=1}^{8} z_i^2 \tag{31}$$

where

$$z_i(t) = x_i(t) - r_i(t_f)$$
$$\underline{x} = \{ \ p_0 \ p_1 \ p_2 \ p_3 \ \beta_0 \ \beta_1 \ \beta_2 \ \beta_3 \ \}^T \tag{32}$$

Then

$$\dot{V} = 4 \sum_{i=1}^{8} z_i \dot{z}_i \tag{33}$$

where $\dot{z}_i = \dot{x}_i$. Eqs. (5) are substituted into Eq. (33) to give $\dot{V}$ the following form

$$\dot{V} = f_1(\underline{z})u_1 + f_2(\underline{z})u_2 + f_3(\underline{z})u_3 + f_4(\underline{x}) + f_5(\underline{x}) + f_6(\underline{x}) \tag{34}$$

where u_1, u_2, u_3 are the control torques to be determined. For asymptotically stable control, $\dot{V}$ must be negative definite. A suitable expression for $\dot{V}$ is

$$\dot{V} = -\{ C_1 f_1^2(\underline{z}) + C_2 f_2^2(\underline{z}) + C_3 f_3^2(\underline{z}) \} \tag{35}$$

where C_1, C_2, C_3 are constants to be defined later. By equating Eqs. (34) and (35), a solution for the control torques is found

$$u_1 = - \left[\frac{f_4(\underline{x})}{f_1(\underline{z})} \right] - C_1 f_1(\underline{z})$$
$$u_2 = - \left[\frac{f_5(\underline{x})}{f_2(\underline{z})} \right] - C_2 f_2(\underline{z}) \tag{36}$$
$$u_3 = - \left[\frac{f_6(\underline{x})}{f_3(\underline{z})} \right] - C_3 f_3(\underline{z})$$

The functions f_1, f_2, f_3 are quadratic polynomials in $\underline{z}$ and f_4, f_5, f_6 are cubic polynomials in $\underline{z}$, so that the quotients in Eqs. (36) are well-behaved as $\underline{z} \to 0$. The control laws are made optimal by adjusting the constants C_1, C_2, and C_3 to minimize the quadratic performance index in Eq. (10).

Single Axis Maneuvers

The large-angle, spin-down maneuver that was demonstrated with polynomial feedback control is repeated with Lyapunov control. The boundary conditions are those listed in Table 2. The Lyapunov function is

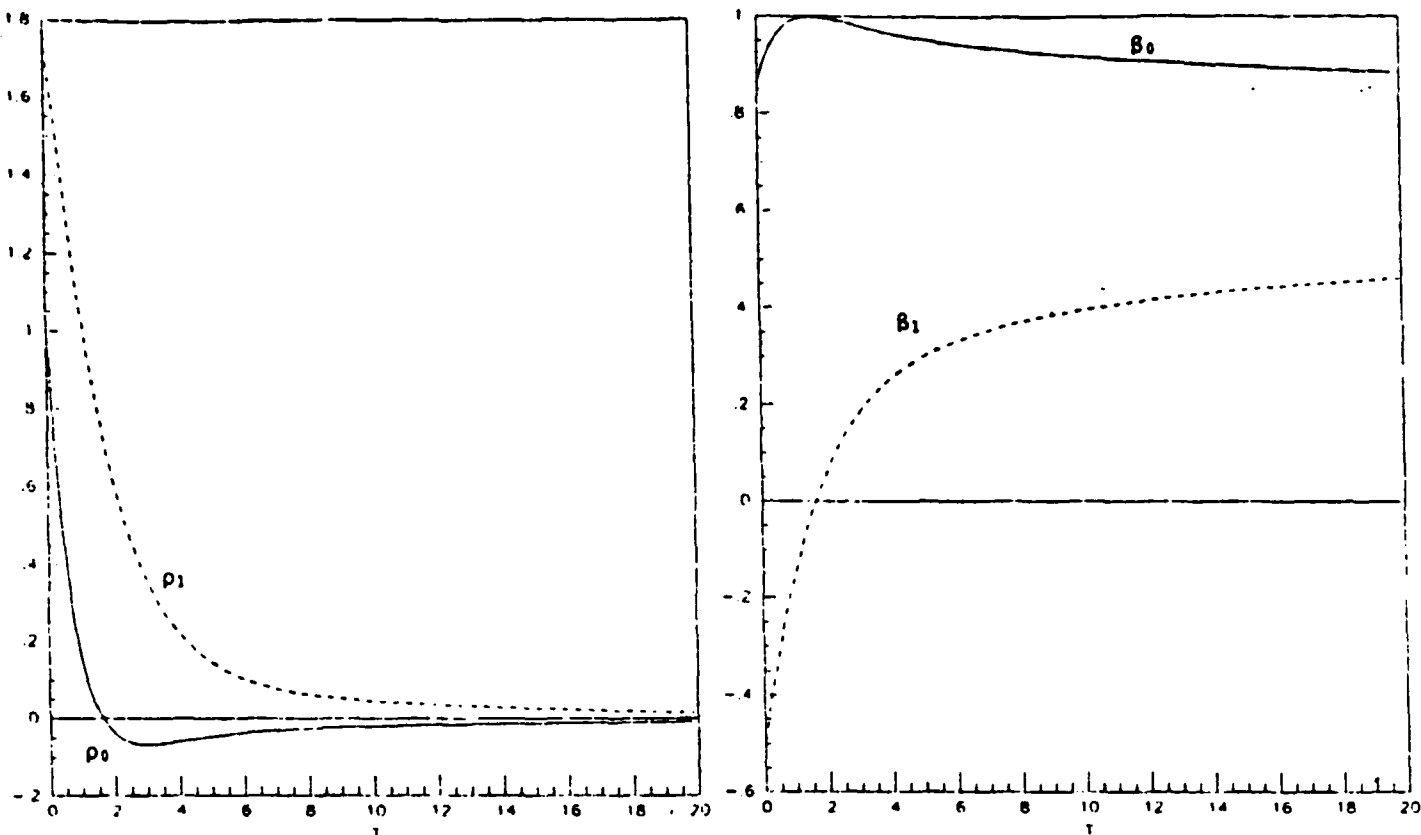$$V = 2 \sum_{i=1}^{4} z_i^2 \tag{37}$$

27

Fig. 4 Single-Axis Conjugate Angular Momenta and
Euler Parameters Using Lyapunov Control

and

$$\dot{V} = 8\{x_3 z_2 - x_4 z_1\}u - r_1 g_1(\underline{x}) - r_2(t_f)g_2(\underline{x}) - r_3(t_f)g_3(\underline{x}) - r_4(t_f)g_4(\underline{x}) \quad (38)$$

where

$$g_1(\underline{x}) = (x_1 x_2 x_4 - x_2^2 x_3)/I$$
$$g_2(\underline{x}) = (x_1 x_2 x_3 - x_1^2 x_4)/I$$
$$g_3(\underline{x}) = (x_1 x_4^2 - x_2 x_3 x_4)/I \quad (39)$$
$$g_4(\underline{x}) = (x_2 x_3^2 - x_1 x_3 x_4)/I$$

To obtain

$$\dot{V} = -C(x_3 z_2 - x_4 z_1)^2 \quad (40)$$

let

$$u = \frac{\sum_{i=1}^{4} r_i(t_f)g_i(\underline{x})}{8(x_3 z_2 - x_4 z_1)} - \frac{C}{8}(x_3 z_2 - x_4 z_1) \quad (41)$$

This control law produced the performance indices in Table 3 for various values
of C. These performance indices were evaluated at $t_f = 30$ sec. The minimum
performance index occurred for $C = 2.9$, and the corresponding system response is
plotted in Figs. 4 and 5. The conjugate angular momenta and Euler parameters are
shown in Fig. 4, and the maneuver angle ϕ and control torque u are plotted in Fig.
5. The weighting matrices Q and H in this example are the identity matrix.

28
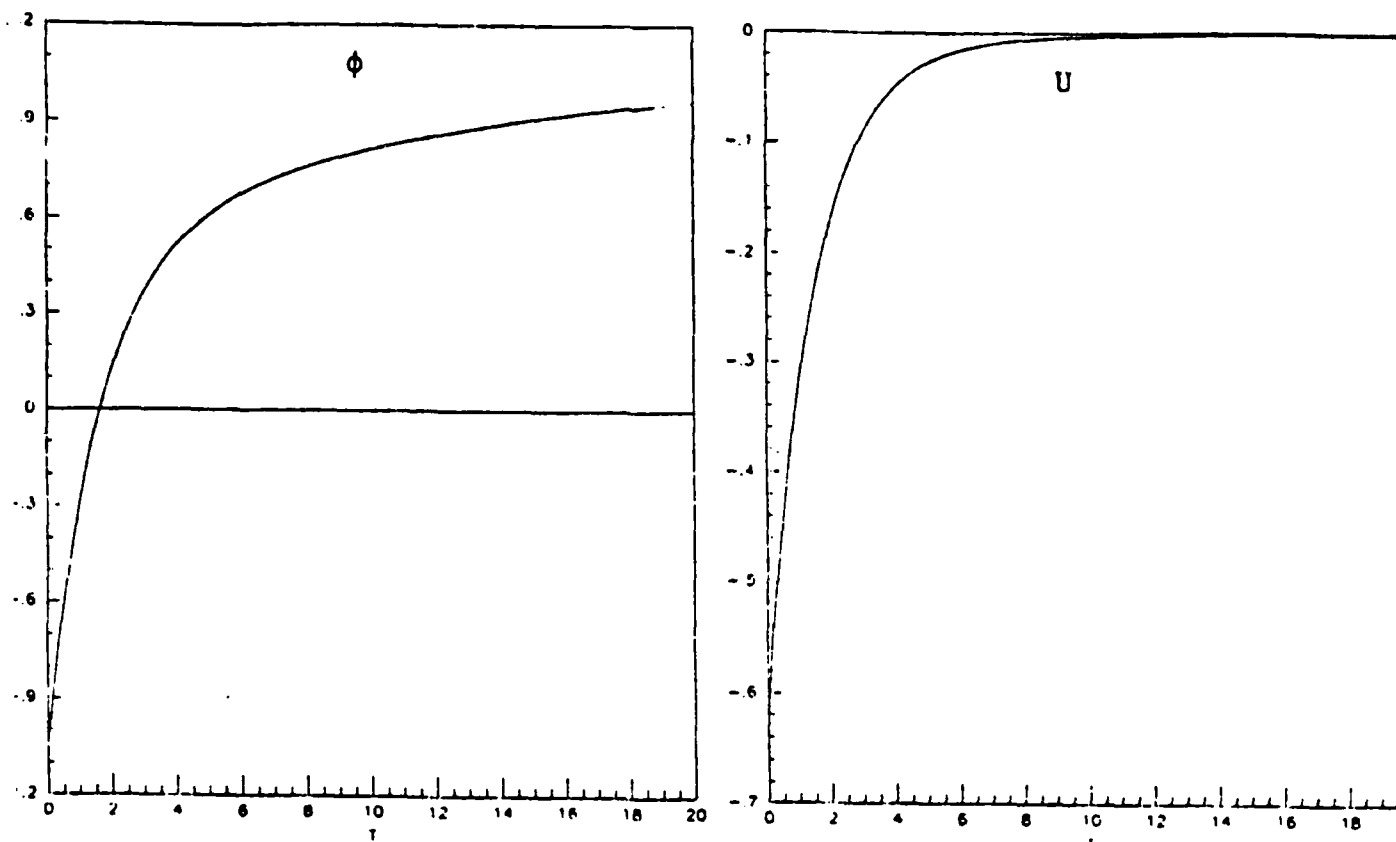
Fig. 5 Single-Axis Maneuver Angle and
Control Torque Using Lyapunov Control

Table 3

SINGLE-AXIS PERFORMANCE INDICES
LYAPUNOV CONTROL

C	Performance Index
1.0	7.05
2.0	3.13
2.9	2.61
3.5	2.71

To demonstrate the variations in response for changes in C, a 90° maneuver was
executed. Fig. 6 shows this maneuver angle for several values of C. When C is
smaller than its optimal value, the response is similar to an underdamped second-
order system, and for large values of C the response is overdamped. For $C = 1.5$, the
maneuver angle responds like an optimally damped ($\varsigma = 0.707$) second-order system,
and the quadratic performance index is minimized. Table 4 lists the performance
indices corresponding to the curves plotted in Fig. 6.

29
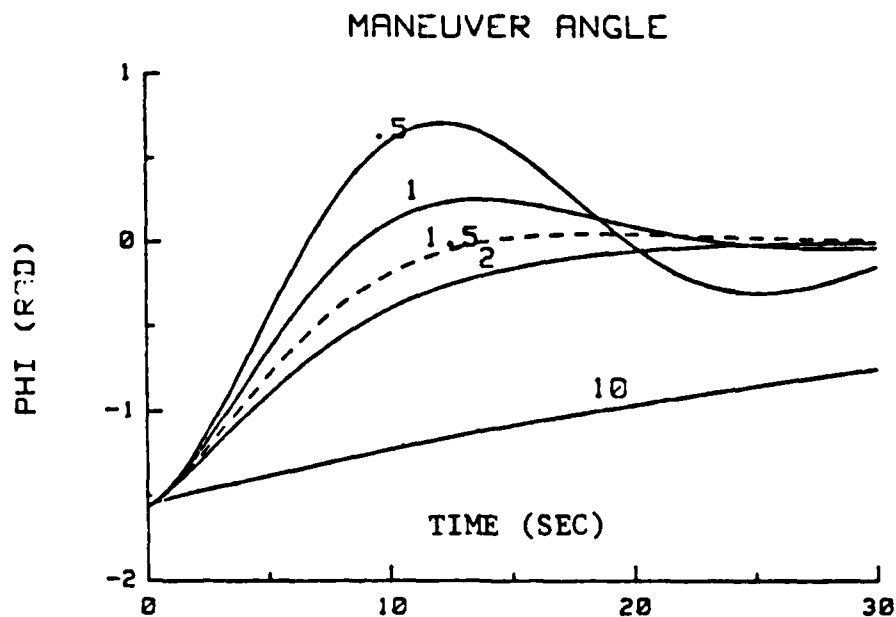
MANEUVER ANGLE

Fig. 6 Single-Axis Maneuver Angle Responses
for Several Values of C

Table 4

SINGLE-AXIS PERFORMANCE INDICES
LYAPUNOV CONTROL

C	Performance Index
0.5	2.49
1.0	1.59
1.5	1.48
2.0	1.58
10.0	4.70

Three Axis Maneuvers

By substituting Eqs. (5) into the Lyapunov function of Eq. (31), $\dot{V}$ becomes

$$
\begin{aligned}
\dot{V} = 8\{ & (-x_6 z_1 + x_5 z_2 + x_8 z_3 - x_7 z_4)u_1 \; + \\
& (-x_7 z_1 - x_8 z_2 + x_5 z_3 + x_6 z_4)u_2 \; + \\
& (-x_8 z_1 + x_7 z_2 - x_6 z_3 + x_5 z_4)u_3 \; + \\
& \underline{p}(t_f)^T [Q(p)][I^{-1}]_4 [Q(p)]^T \underline{\beta} \; - \\
& \underline{\beta}(t_f)^T [Q(\beta)][I^{-1}]_4 [Q(\beta)]^T \underline{p} \}
\end{aligned}
\tag{42}
$$

Fig. 7 Three-Axis Conjugate Angular Momenta and
Euler Parameters Using Lyapunov Control

A negative definite form for $\dot{V}$ is

$$\dot{V} = -\{C_1(-x_6 z_1 + x_5 z_2 + x_8 z_3 - x_7 z_4)^2 \;\; + $$
$$C_2(-x_7 z_1 - x_8 z_2 + x_5 z_3 + x_6 z_4)^2 \;\; + \tag{43}$$
$$C_3(-x_8 z_1 + x_7 z_2 - x_6 z_3 + x_5 z_4)^2\}$$
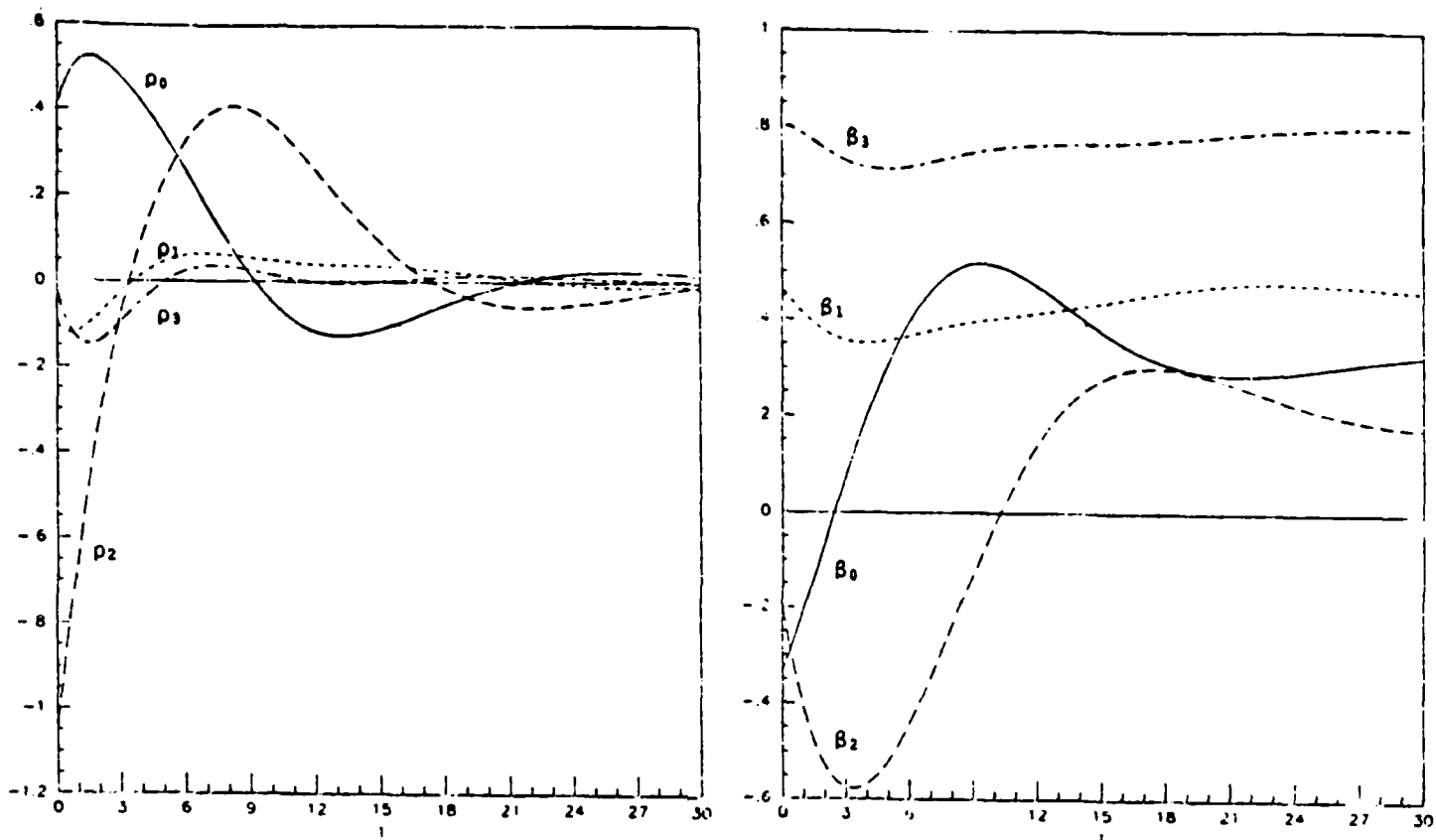
By equating Eqs. (42) and (43), and assigning all terms containing I_1 to $f_4(\underline{x})$, all terms containing I_2 to $f_5(\underline{x})$, and those containing I_3 to $f_6(\underline{x})$, then the control torques are defined by Eqs. (36). The functions $f_1(\underline{z})$, $f_2(\underline{z})$, and $f_3(\underline{z})$ are identified by comparing Eqs. (35) and (43).

A large-angle three-axis spin-down maneuver was executed using the boundary conditions listed in Table 5. The 3-1-3 Euler angles ϕ, θ, ψ correspond to the given Euler parameters. Table 6 contains the mass properties of the spacecraft, and the final time is $t_f = 50$ sec. As in the single-axis maneuvers, varying the constants C_1, C_2, and C_3 produce responses that exhibit the characteristics of damped second-order systems. Several values of these constants with their corresponding performance indices are listed in Table 7. The minimum performance index occurs for

$$C_1 = 1/I_1$$
$$C_2 = 1/I_2 \tag{44}$$
$$C_3 = 1/I_3$$

and Figs. 7 and 8 plot the state variables, angular velocities, and control torques for this case.

31
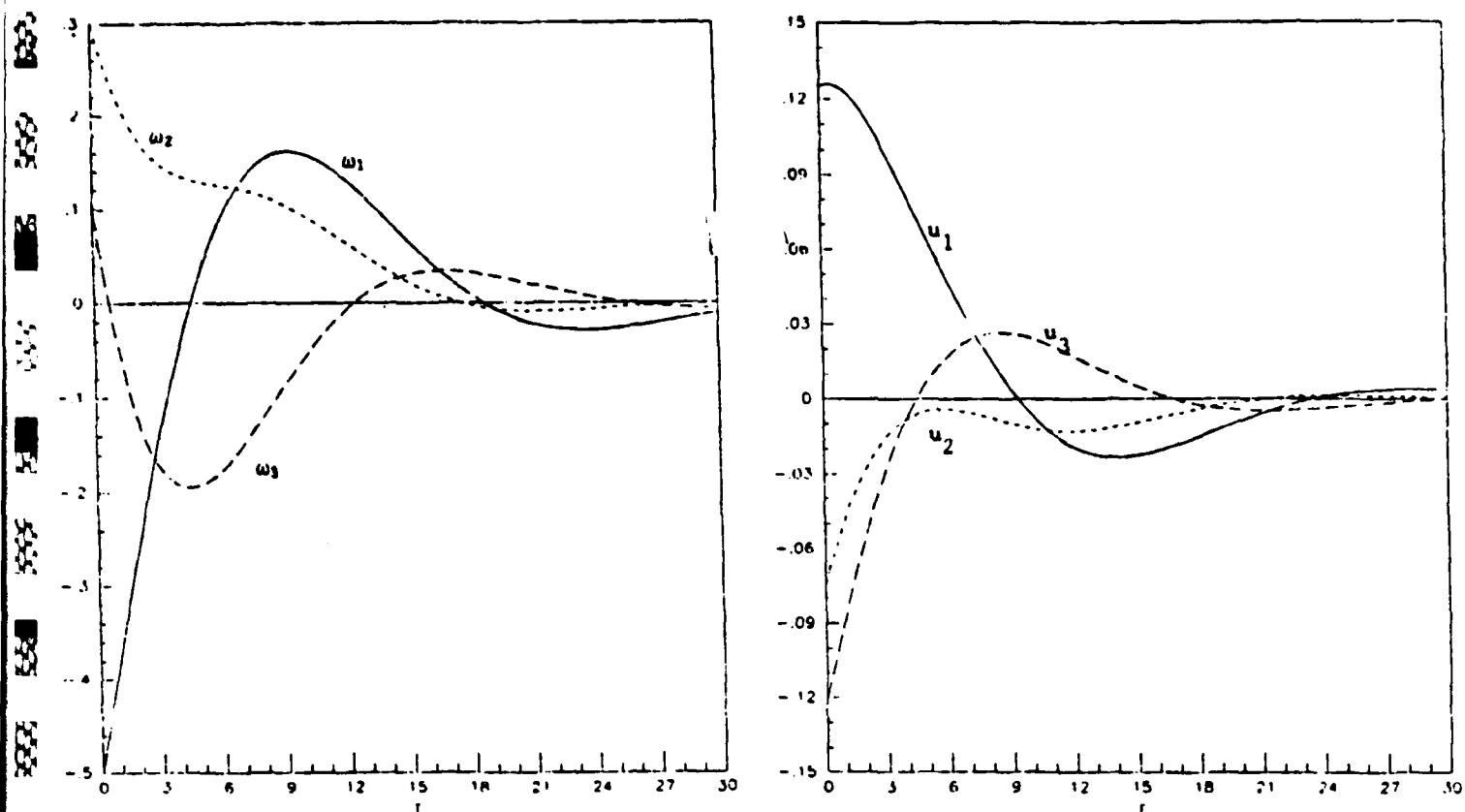
Fig. 8 Three-Axis Angular Velocities and Control
Torques Using Lyapunov Control

Table 5

THREE-AXIS BOUNDARY CONDITIONS

State	Initial State	Final State
ϕ (rad)	$-\pi/2$	$\pi/2$
θ (rad)	$-\pi/3$	$\pi/3$
ψ (rad)	$-\pi/4$	$\pi/4$
ω_1 (rad/sec)	$-.5$	0.0
ω_2 (rad/sec)	0.3	0.0
ω_3 (rad/sec)	0.1	0.0
β_0	-0.331	0.331
β_1	0.462	0.462
β_2	-0.191	0.191
β_3	0.800	0.800
p_0 (kg m^2 rad/sec)	0.410	0.000
p_1 (kg m^2 rad/sec)	-0.102	0.000
p_2 (kg m^2 rad/sec)	-1.050	0.000
p_3 (kg m^2 rad/sec)	-0.022	0.000

Table 6
SPACECRAFT INERTIA

Axis	Moment of Inertia (kg m^2)
1	1.00
2	0.83
3	0.92

Table 7
THREE-AXIS PERFORMANCE INDICES

C_1	C_2	C_3	Performance Index
1.00	1.00	5.00	4.893
1.00	0.83	0.92	4.543
1.00	1.00	1.00	4.368
1.00	1.20	1.09	4.225
1.00	0.60	0.20	6.710

CONCLUSIONS

State feedback control laws have been formulated for a new set of state equations representing rigid-body rotational motion. The polynomial state equations allow development of polynomial feedback controls using optimal control theory. The absence of linear terms in the state equations and the double redundancy of the state variables preclude the use of constant gains, but time-dependent gains are determined in closed form. A single-axis example demonstrates that quadratic terms in the costates are required for complete attitude control.

A second group of control laws is developed using Lyapunov functions. Although nonoptimal, these laws produce asymptotically stable closed-loop systems, and constants may be adjusted to minimize the quadratic performance index of an optimal control formulation. The system response for both single- and three-axis maneuvers exhibit characteristics of a damped second-order system; the combination of constants that minimizes the performance index produces a response associated with an optimally damped ($\varsigma = 0.707$) system.

A comparision of polynomial feedback laws and Lyapunov laws shows that Lyapunov control is easier to formulate. For systems involving more than a modest number of states, the algebra required by polynomial control becomes prohibitive and an algebraic manipulator should be used. There are several advantages in using the conjugate angular momenta for state variables instead of the three angular velocities. Polynomial feedback control using angular velocities was examined in Refs. 8 and 10, and those state equations produced coefficients in the gain equations that are dependent on the final states. Although the equations do not need to be reformulated each time the target states were changed, a system of simultaneous equations must be resolved to find new gains. In this paper, the time-dependent

gains using the conjugate angular momenta are found in closed-form and are quickly calculated f·· changes in the target state. The cubic form of the angular momenta equations also produce Lyapunov control laws that are well behaved as the errors go to zero.

ACKNOWLEDGEMENTS

REFERENCES

1. E. T. Whittaker, *A Treatise on the Analytical Dynamics of Particles and Rigid Bodies*, Dover Publications, New York, 1944.

2. T. R. Kane. P. W. Likins, and D. A. Levinsion, *Spacecraft Dynamics*, McGraw-Hill Book Co., New York, 1983.

3. Bong Wie and Peter M. Barba, "Quaternion Feedback for Spacecraft Large Angle Maneuvers," AIAA *J. of Guidance, Control, and Dynamics*, Vol. 8, No. 3, May-June 1985, pp. 360-365.

4. S. R. Vadali and J. L. Junkins, "Optimal Open Loop and Stable Feedback Control of Rigid Spacecraft Attitude Maneuvers," AAS/AIAA Astrodynamics Specialist Conference, Lake Placid, New York, Aug. 1983, AAS Paper No. 83-373.

5. T. A. W. Dwyer, III, "Exact Nonlinear Control of Large Angle Rotational Maneuvers," IEEE *Transactions on Automatic Control*, Vol. AC-29, No. 9, pp. 769-774, Sept. 1984.

6. S. V. Salehi and E. P. Ryan, "A Nonlinear Feedback Attitude Regulator," *International Journal of Control*, Vol. 41, No. 1, pp. 281-287, Jan. 1985.

7. L. R. Dickey, "A Spacecraft Control System for Large Attitude Maneuvers," *IEEE Proceedings of 16th Southeastern Symposium on System Theory*, Mar. 1984, pp. 65-68.

8. C. K. Carrington and J. L. Junkins, "Optimal Nonlinear Feedback Control for Spacecraft Attitude Maneuvers," to appear in AIAA *J. of Guidance, Control, and Dynamics*, (AIAA Paper No. 83-2230-CP, Gatlinburg, Tenn.)

9. Harold S. Morton, Jr., "A Formulation of Rigid-Body Rotational Dynamics Based on Generalized Angular Momentum Variables Corresponding to the Euler Parameters," AIAA/AAS Astrodynamics Conference, Seattle, WA, Aug. 1984, Paper No. 84-2023.

10. C. K. Carrington and J. L. Junkins, "Nonlinear Feedback Control of Spacecraft Slew Maneuvers," *J. of Astronautical Sciences*, Vol. 32, No. 1, Jan-Mar. 1984, pp. 29-45.

11. Fred Brauer and John A. Nohel. *Qualitative Theory of Ordinary Differential Equations*, W. A. Benjamin, Inc., 1969.

12. Leonard Meirovitch, *Methods of Analytical Dynamics*, McGraw-Hill Book Co., 1970.

13. C. K. Carrington, *Optimal Nonlinear Feedback Control of Spacecraft Attitude Maneuvers*, Ph. d. dissertation, VPI&SU, Dec 1983.

14. Alan J. Laub, "A Schur Method for Solving Algebraic Riccati Equations," IEEE *Transactions on Automatic Control*, Vol. AC-24, No. 6, Dec. 1979, pp. 913-921.
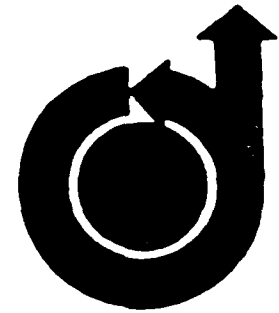
AN ASYMPTOTIC PERTURBATION METHOD FOR NONLINEAR OPTIMAL CONTROL PROBLEMS

John L. Junkins
Texas A&M University
College Station, Texas

R. C. Thompson
Virginia Polytechnic Institute and State University
Blacksburg, Virginia

AAS/AIAA Astrodynamics Specialist Conference

36

AN ASYMPTOTIC PERTURBATION METHOD
FOR NONLINEAR OPTIMAL CONTROL PROBLEMS

J. L. Junkins[*]
Texas A&M University
College Station, Texas 77843
R. C. Thompson[**]
Virginia Polytechnic Institute and State University
Blacksburg, Virginia 24061

ABSTRACT

A quasi-analytical method is presented for solving nonlinear, open-loop, optimal control problems. The approach combines a simple analytical, straightforward expansion from perturbation methods with powerful numerical algorithms (due to Ward and Van Loan) to solve a series of nonhomogeneous, linear, optimal control problems. In the past, the only recourse for solving such nonlinear problems relied almost exclusively on iterative numerical methods whereas the asymptotic perturbation approach may produce accurate solutions to nonlinear problems without iteration. The nonlinear state and costate equations are derived from the optimal control formulation and expanded in a power series in terms of a small parameter contained either explicitly in the equations or implicitly in the boundary conditions. Each order of the expansion is shown to be governed by a nonhomogeneous, ordinary differential equation. Representing the generally non-integrable, nonhomogeneous terms by a finite Fouries series, efficient matrix exponential algorithms are then used to solve the system at each order, where the order of the expansion is extended to achieve the appropriate precision. The asymptotic perturbation method is broadly applicable to weakly nonlinear optimal control problems, including higher order systems frequently encountered in

---

[*] Professor of Aerospace Engineering, AIAA Fellow.

[**]Graduate Research Assistant, Engineering Science and Mechanics, AIAA Member.

aerospace vehicle dynamics and control. A number of numerical examples demonstrating the perturbation approach are included.

OPTIMAL CONTROL FORMULATION

Consider a nonlinear system of the form

$$\ddot{\underline{x}} + \Gamma\dot{\underline{x}} + \Lambda\underline{x} = B\underline{u} + \underline{f}(\underline{x},\dot{\underline{x}},\underline{u},\dot{\underline{u}},t) \tag{1}$$

where $\underline{x}$ is an nx1 vector of system coordinates, Γ is a diagonal matrix of damping factors, Λ is a diagonal matrix of stiffness factors, B is the control influence matrix, $\underline{u}$ is an mx1 vector of controls, and $\underline{f}$ is a vector containing all nonlinear terms. The form of Eq. (1) is based upon the assumption that the linear part of the equations of motion have been rendered independent via a linear transformation to reduce the complexity of the optimal control formulation. If all of the n system coordinates are to be controlled, this procedure is entirely arbitrary although it will often prove useful (with regard to the validity of the methods herein). However, for a control problem in which a subset of the system linear modal coordinates are to be controlled, the decoupling procedure is necessary. Furthermore, it is recommended that the equations be nondimensionalized to reduce the number of parameters involved and to isolate the dimensionless parameters critical to the behavior of the system. We shall proceed with the development of the perturbation approach in configuration coordinates, based upon the assumption that the linear part of the equations of motion have been decoupled while recognizing that the use of dimensionless coordinates would merely scale the coefficient matrices.

Forming the state vector of the system coordinates, controls, and their first derivatives, the state equation is

$$\underline{\dot{z}} = F\underline{z} + D\underline{U} + \underline{\rho} \tag{2}$$

where

$$\underline{z} = [\underline{x}^T \ \underline{\dot{x}}^T \ \underline{u}^T \ \underline{\dot{u}}^T]^T \qquad (2n+2m) \times 1$$

$$F = \begin{bmatrix} 0 & I & 0 & 0 \\ -\Lambda & -\Gamma & B & 0 \\ 0 & 0 & 0 & I \\ \rho & 0 & 0 & 0 \end{bmatrix} \qquad (2n+2m) \times (2n+2m)$$

$$D = \begin{bmatrix} 0 \\ 0 \\ 0 \\ I \end{bmatrix}. \qquad (2n+2m) \times m$$

$$\underline{U} = \underline{\dot{u}} \qquad m \times 1$$

$$\underline{\rho} = [\underline{0}^T \ \underline{f}^T \ \underline{0}^T \ \underline{0}^T]^T \qquad (2n+2m) \times 1$$

Including the controls and control rates in the state vector $\underline{z}$ allows us to penalize large control accelerations in the optimal control problem. This will insure that the control trajectories generated will be smooth and continuous, with prescribed (usually zero) magnitudes at the initiation and completion of the maneuver (Ref. 1,2). We seek the optimal control trajectory that minimizes the quadratic performance index

$$J = \frac{1}{2} \underline{z}^T S\underline{z} \Big|_{t=t_f} + \frac{1}{2} \int_{t_o}^{t_f} (\underline{z}^T Q\underline{z} + \underline{u}^T R\underline{u}) dt \tag{3}$$

where R and S are positive definite, diagonal weight matrices, and Q is a symmetric, positive semi-definite weight matrix, where $Q = 0$ is not excluded. It is clear that the matrix Q may be used to weight not only the position and velocities of the system coordinates, but the controls and

39

control rates as well due to the inclusion of these variables in the state vector $\underline{z}$.

The Hamiltonian, formed from the system given by Eq. (2) and the integrand of Eq. (3), is defined to be

$$H = \frac{1}{2}(\underline{z}^T Q \underline{z} + \underline{U}^T R \underline{U}) + \underline{\lambda}^T (F\underline{z} + D\underline{U} + \underline{\rho}) \qquad (4)$$

where the costates $\underline{\lambda}$ are a set of undetermined Lagrange multipliers. Pontryagin's necessary conditions for determining the optimal control, operating on the Hamiltonian, yield the equations

$$\underline{\dot{z}} = \frac{\partial H}{\partial \underline{\lambda}} = F\underline{z} + D\underline{U} + \underline{\rho} \qquad (5)$$

$$\underline{\dot{\lambda}} = -\frac{\partial H}{\partial \underline{z}} = -Q\underline{z} - F^T\underline{\lambda} - [\frac{\partial \underline{\rho}}{\partial \underline{z}}]^T \underline{\lambda} \qquad (6)$$

$$\underline{0} = \frac{\partial H}{\partial \underline{U}} = R\underline{U} + D^T\underline{\lambda} \qquad (7)$$

with the boundary condition $\underline{\lambda}(t_f) = S\underline{z}(t_f)$.

Solving Eq. (7) for $\underline{U}$ and substituting into Eq. (5) reduces the optimal control problem to two coupled first-order, nonlinear, ordinary differential equations. Combining the unknowns, $\underline{z}$ and $\underline{\lambda}$, into a single augmented state/costate vector $\underline{X}$, the optimal control problem may be restated as

$$\underline{\dot{X}} = A\underline{X} + \epsilon\{NLT\} \qquad (8)$$

where

$$\underline{X} = [\underline{z}^T \; \underline{\lambda}^T]^T \qquad \qquad 2(2n+2m) \times 1$$

$$A = \begin{bmatrix} F & -DR^{-1}D^T \\ -Q & -F^T \end{bmatrix} \qquad \qquad 2(2n+2m) \times 2(2n+2m)$$

$$\{NLT\} = \left\{ \begin{array}{c} \underline{\rho} \\[2mm] -[\frac{\partial \underline{\rho}}{\partial \underline{z}}]^T \underline{\lambda} \end{array} \right\} \qquad 2(2n+2m) \times 1$$

and where the dimensionless parameter ϵ is a "bookkeeping" term indicating the numerical order of the nonlinear terms.

Upon solving the Two-Point Boundary-Value Problem given by Eq. (8), the state trajectory, which includes the optimal controls, may be generated at any point within the time interval $t_0 \le t \le t_f$. However, as a consequence of the presence of the nonlinear terms, the system governed by Eq. (8) is analytically intractable. Although there are many iterative methods available for solving such nonlinear systems, we wish to construct an approach, using the most basic of the perturbation methods, that circumvents the iterative techniques in favor of a quasi-analytical solution to the optimal control problem.

AN ASYMPTOTIC PERTURBATION METHOD: THE PEDESTRIAN EXPANSION

For any given weakly nonlinear, differential equation, it is often constructive to employ a straightforward expansion from perturbation methods to produce an approximate solution to the problem (Ref. 3). We assume the solution to Eq. (8) may be represented by a power series in terms of a small dimensionless parameter ϵ

$$\underline{X}(t) = \underline{X}_0(t) + \epsilon \underline{X}_1(t) + \epsilon^2 \underline{X}_2(t) + \ldots \qquad (9)$$

For small nonlinearities (small ϵ), the series is expected to produce accurate results where the accuracy will improve as the nonlinearities, and consequently the parameter ϵ approach zero. Indeed, in the limit, as the number of terms in the series approaches infinity, the solution given by Eq. (9) will be exact if the expansion is convergent.

41

Substituting Eq. (9) into Eq. (8) the optimal control problem may be expressed as

$$\underline{\dot{X}}_0 + \epsilon \underline{\dot{X}}_1 + \epsilon^2 \underline{\dot{X}}_2 + O(\epsilon^3) = A\underline{X}_0 + \epsilon A\underline{X}_1 + \epsilon^2 A\underline{X}_2 + \epsilon\{NLT_1(\underline{X}_0)\}$$
$$+ \epsilon^2\{NLT_2(\underline{X}_0,\underline{X}_1)\} + O(\epsilon^3) \qquad (10)$$

where the nonlinear terms have been expanded in a similar power series and the dependence of each term upon the expansion variables $(\underline{X}_i)$ at each order is indicated. Equating terms with equivalent powers of ϵ yields the series of equations

$$\underline{\dot{X}}_0 = A\underline{X}_0 \qquad (11)$$

$$\underline{\dot{X}}_1 = A\underline{X}_1 + \{NLT_1(\underline{X}_0)\} \qquad (12)$$

$$\underline{\dot{X}}_2 = A\underline{X}_2 + \{NLT_2(\underline{X}_0,\underline{X}_1)\} \qquad (13)$$

where for illustrative purposes we have included only the equations through order ϵ^2. However, we note that the order may be extended to achieve the degree of precision required for a specific problem. The boundary conditions of the expansion variables are

$$\underline{X}_0(t_0) = \left\{ \begin{array}{c} \underline{z}(t_0) \\ \underline{\lambda}_0(t_0) \end{array} \right\} \qquad \underline{X}_0(t_f) = \left\{ \begin{array}{c} \underline{z}(t_f) \\ \underline{\lambda}_0(t_f) \end{array} \right\} \qquad (14a)$$

$$\underline{X}_i(t_0) = \left\{ \begin{array}{c} \underline{0} \\ \underline{\lambda}_i(t_0) \end{array} \right\} \qquad \underline{X}_i(t_f) = \left\{ \begin{array}{c} \underline{0} \\ \underline{0} \end{array} \right\} \qquad i = 1,2,3,\ldots \quad (14b)$$

where we recall that the final conditions of the states and costates are related at each order through the boundary condition $\underline{\lambda}_i(t_f) = S\underline{z}_i(t_f)$. The straightforward expansion produces a strictly linear problem as the first approximation (zero order) of the nonlinear problem and then provides a series

42

of "small corrections" (higher-order terms) to account for the effects of the nonlinearities. Furthermore, the nonhomogeneous term in the ith equation of higher order ($i = 1,2,...$) is independent of the expansion variable $\underline{X}_i$ for that particular equation. Upon solving Eqs. (11-13) sequentially, the significance of this observation becomes clear; the nonhomogeneous terms constitute known functions of time. By employing the perturbation method, we have, as usual, replaced an intractable nonlinear problem with a series of nonhomogeneous, linear, first-order, ordinary differential equations.

SOLUTION OF THE NONHOMOGENEOUS EQUATIONS

The solution of a system of the form given by Eqs. (11-13) can be shown to be

$$\underline{X}_i(t) = e^{At}[\underline{X}_i(0) + \int_0^t e^{-A\tau}\underline{d}_i(\tau)d\tau] \quad , \quad i = 0,1,2,... \quad (15)$$

where

$$\underline{d}_0(\tau) = \underline{0}$$

$$\underline{d}_i(\tau) = \{NLT_i\} \quad , \quad i = 1,2,...$$

and where $t_0 = 0$ has been assumed without loss of generality. Although Eq. (15) provides the solution for each expansion variable, evaluating the integral for an arbitrary function $\underline{d}_i$ presents a formidable task and may require numerical integration. On the other hand, if the nonhomogeneous term may be represented accurately by a continuous function of time, in exponential form, the entire solution given by Eq. (15) may be evaluated using a matrix exponential.

Since we have no closed form expressions for the nonhomogeneous terms, at best we can generate a large set (k) of data points which are the "sampled" trajectories of the forcing terms. A finite Fourier series of the form

$$f(t) = b_0 + \sum_{i=1}^{r} a_i \sin i\omega_0 t + b_i \cos i\omega_0 t \quad (16)$$

43

may then be used to represent the nonhomogeneous terms as a continuous function of time. To calculate the coefficients of the series, we use a least squares fit of the series to the data points describing the nonhomogeneous function. It can be shown that the Fourier series of the jth element of the ith forcing term may be put into the form

$$A\underline{c}_j = \underline{\tilde{d}}_j \qquad (17)$$

where

$$A = \begin{bmatrix} 1 & 0 & 1 & 0 & 1 & \cdots & 0 & 1 \\ 1 & s(\tau_1) & c(\tau_1) & s(2\tau_1) & c(2\tau_1) & \cdots & s(r\tau_1) & c(r\tau_1) \\ 1 & s(\tau_2) & c(\tau_2) & s(2\tau_2) & c(2\tau_2) & \cdots & s(r\tau_2) & c(r\tau_2) \\ \vdots & & \vdots & & \vdots & & & \\ 1 & s(\tau_k) & c(\tau_k) & s(2\tau_k) & c(2\tau_k) & \cdots & s(r\tau_k) & c(r\tau_k) \end{bmatrix}$$

$$\underline{c}_j = [b_{oj} \ a_{1j} \ b_{1j} \ a_{2j} \ b_{2j} \ \cdots \ a_{rj} \ b_{rj}]^T$$

$$\underline{\tilde{d}}_j = [\underline{d}_i^j(0) \ \underline{d}_i^j(\Delta t) \ \underline{d}_i^j(2\Delta t) \ \cdots \ \underline{d}_i^j(k\Delta t)]^T$$

$$\tau_\ell = \ell \omega_o \Delta t \ , \qquad \ell = 1,2,3,\ldots,k$$

$$\Delta t = t_f/k \qquad \omega_o = 2\pi/t_f$$

$$c(\ ) = \cos(\ ) \qquad s(\ ) = \sin(\ )$$

and the notation $\underline{d}_i^j(k\Delta t)$ indicates the jth element of $\underline{d}_i(t)$ evaluated at t = kΔt. The unknown coefficients may then be found from the least squares approximation

$$\underline{c}_j = (A^T A)^{-1} A^T \underline{\tilde{d}}_j \qquad (18)$$

Note that with appropriate sample points (symmetric about $\tau = \pi$), $A^T A$ is diagonal and the inverse is trivial. Alternatively, we can develop these coefficients from a discrete Fourier transform. Proceeding element by element through the ith forcing term, we can then represent each element by a finite Fourier series. It can also be shown that the forcing term may then be given

44

by the matrix exponential equation

$$\underline{d}_i(t) = G_i e^{\Omega t} \underline{q}_0 \tag{19}$$

where

$$G_i = [\underline{g}_1 \quad \underline{g}_2 \quad \underline{g}_3 \quad \cdots \quad \underline{g}_s]^T \quad , \quad s = 2(2n+2m)$$

$$\underline{g}_j = [b_{oj} \quad \omega_0 a_{1j} \quad b_{1j} \quad 2\omega_0 a_{2j} \quad b_{2j} \quad \cdots \quad r\omega_0 a_{rj} \quad b_{rj}]^T$$
$$j = 1,2,3,\ldots,s$$

$$\underline{q}_0 = [1 \quad 0 \quad 1 \quad 0 \quad 1 \quad \cdots \quad 1]^T \qquad (2r+1) \times 1$$

$$\Omega = \text{Block Diag } [0,\Omega_1,\Omega_2,\ldots,\Omega_r] \qquad (2r+1) \times (2r+1)$$

$$\Omega_\ell = \begin{bmatrix} 0 & 1 \\ -(\ell\omega_0)^2 & 0 \end{bmatrix} \quad , \qquad \ell = 1,2,3,\ldots,r$$

We now have the nonhomogeneous term represented by a continuous function of time given in exponential form. Consequently, we may use "Van Loan's identity" (Ref. 4) to produce the solution given by Eq. (15) using any available matrix exponential algorithms[5]. To accomplish this, we define

$$Y_i = \begin{bmatrix} A & G_i \\ 0 & \Omega \end{bmatrix} \tag{20}$$

and Van Loan proves that

$$e^{Y_i t} = \begin{bmatrix} \Phi_1(t) & \Phi_{2i}(t) \\ 0 & \Phi_3(t) \end{bmatrix} \tag{21}$$

where the state transition sub-matrices satisfy the identities

$$\Phi_1(t) = e^{At} \tag{22a}$$

$$\Phi_{2i}(t) = e^{At} \int_0^t e^{-A\tau} G_i e^{\Omega\tau} d\tau \tag{22b}$$

$$\Phi_3(t) = e^{\Omega t} \tag{22c}$$

Clearly, Eqs. (22a, 22b) may be substituted into Eq. (15) yielding

$$\underline{X}_i(t) = \phi_1(t)\underline{X}_i(0) + \phi_{2i}(t)\underline{q}_o \qquad (23)$$

where we note that $\phi_{2i}(t)$ is numerically different for each expansion variable $\underline{X}_i$, as indicated by the subscript (i) in Eqs. (21-23).

SOLVING FOR THE INITIAL COSTATES

Equation (23) is the form of the solution for each unknown variable $(\underline{X}_i)$, however recalling the boundary conditions on the unknowns, Eq. (14), we realize that the initial costates, $\underline{\lambda}_i(0)$, and hence $\underline{X}_i(0)$ are as yet undetermined. The initial costates must be found in order for Eq. (23) to provide the numerical solution of the optimal control problem. Evaluating Eq. (23) at $t = t_f$ and recalling the boundary conditions from Eq. (14), we get

$$\underline{X}_i(t_f) = \begin{Bmatrix} \underline{z}_i(t_f) \\ S\underline{z}_i(t_f) \end{Bmatrix} = \phi_1(t_f) \begin{Bmatrix} \underline{z}_i(0) \\ \underline{\lambda}_i(0) \end{Bmatrix} + \phi_{2i}(t_f)\underline{q}_o \qquad (24)$$

It will prove useful to write the state transition matrix $\phi_1(t_f)$ in partitioned form and to partition the last term in Eq. (24). Therefore, we define

$$\phi_1(t_f) = \begin{bmatrix} \phi_1^{11}(t_f) & \phi_1^{12}(t_f) \\ \phi_1^{21}(t_f) & \phi_1^{22}(t_f) \end{bmatrix} \qquad (25a)$$

$$\phi_{2i}(t_f)\underline{q}_o = \begin{Bmatrix} \psi_{1i}(t_f) \\ \psi_{2i}(t_f) \end{Bmatrix} \qquad (25b)$$

Substituting Eq. (25) into Eq. (24) yields the two coupled algebraic equations

$$\underline{z}_i(t_f) = \phi_1^{11}(t_f)\underline{z}_i(0) + \phi_1^{12}(t_f)\underline{\lambda}_i(0) + \underline{\psi}_{1i}(t_f) \qquad (26)$$

$$S\underline{z}_i(t_f) = \phi_1^{21}(t_f)\underline{z}_i(0) + \phi_1^{22}(t_f)\underline{\lambda}_i(0) + \underline{\psi}_{2i}(t_f) \qquad (27)$$

in which $\underline{\lambda}_i(0)$ is the only unknown.

46

Multiplying Eq. (26) by the positive definite matrix S, combining this with Eq. (27), and collecting terms yields

$$[\phi_1^{22}(t_f) - S\phi_1^{12}(t_f)]\underline{\lambda}_i(0) = [S\phi_1^{11}(t_f) - \phi_1^{21}(t_f)]\underline{z}_i(0)$$

$$+ S\underline{\psi}_{1i}(t_f) - \underline{\psi}_{2i}(t_f) \tag{28}$$

which can easily be solved for the initial costates using any appropriate algorithm. Now that all of the initial conditions of $\underline{X}_i$ are known, Eq. (23) can be used to produce the optimal control at any time in the interval $0 \le t \le t_f$.

RECURSIVE SOLUTION OF THE STATE TRAJECTORIES

Once the solution for a given expansion variable is found, we then proceed to the next higher order. However, to produce the Fourier Series approximation of the nonhomogeneous term in the next higher order requires that we sample the trajectory of the current order at fixed intervals of time (Δt) throughout the maneuver. Evaluating the matrix exponential indicated in Eq. (21) at each time interval would prove computationally costly and time consuming. An alternative procedure is to develop a recursive formula for calculating the state trajectories whereby the matrix exponential is evaluated only once at $t = \Delta t$. We make use of the exponential matrix recursion

$$e^{A(k+1)\Delta t} = e^{A\Delta t}e^{Ak\Delta t} \tag{29}$$

to modify Eq. (23). Applying the identity in Eq. (29) to the definitions in Eq. (21) produces

$$\begin{bmatrix} \phi_1[(k+1)\Delta t] & \phi_{2i}[(k+1)\Delta t] \\ 0 & \phi_3[(k+1)\Delta t] \end{bmatrix} = \begin{bmatrix} \phi_1(\Delta t) & \phi_{2i}(\Delta t) \\ 0 & \phi_3(\Delta t) \end{bmatrix} \begin{bmatrix} \phi_1(k\Delta t) & \phi_{2i}(k\Delta t) \\ 0 & \phi_3(k\Delta t) \end{bmatrix} \tag{30}$$

47

Carrying out the partitioned products indicated yields the three recursive equations for the sub-matrices

$$\phi_1[(k+1)\Delta t] = \phi_1(\Delta t)\phi_1(k\Delta t) \tag{31a}$$

$$\phi_{2i}[(k+1)\Delta t] = \phi_1(\Delta t)\phi_{2i}(k\Delta t) + \phi_{2i}(\Delta t)\phi_3(k\Delta t) \tag{31b}$$

$$\phi_3[(k+1)\Delta t] = \phi_3(\Delta t)\phi_3(k\Delta t) \tag{31c}$$

where $\phi_1(0) = I$, $\phi_{2i}(0) = 0$, and $\phi_3(0) = I$.

Similarly, evaluating Eq. (23) at $t = (k+1)\Delta t$ gives

$$\underline{X}_i[(k+1)\Delta t] = \phi_1[(k+1)\Delta t]\underline{X}_i(0) + \phi_{2i}[(k+1)\Delta t]\underline{q}_o \tag{32}$$

We can then simplify Eq. (32) by defining the vectors $\underline{v}_{ji}$, $j = 1,2,3$ to be

$$\underline{v}_{1i}[(k+1)\Delta t] = \phi_1[(k+1)\Delta t]\underline{X}_i(0)$$

$$\underline{v}_{2i}[(k+1)\Delta t] = \phi_{2i}[(k+1)\Delta t]\underline{q}_o$$

$$\underline{v}_{3i}[(k+1)\Delta t] = \phi_3[(k+1)\Delta t]\underline{q}_o \tag{33}$$

Substituting Eq. (31) into Eq. (33) and substituting this result into Eq. (32) yields the recursive formula

$$\underline{X}_i[(k+1)\Delta t] = \underline{v}_{1i}[(k+1)\Delta t] + \underline{v}_{2i}[(k+1)\Delta t] \tag{34}$$

and

$$\underline{v}_{1i}[(k+1)\Delta t] = \phi_{1i}(\Delta t)\underline{v}_{1i}(k\Delta t), \qquad \underline{v}_{1i}(0) = \underline{X}_i(0)$$

$$\underline{v}_{2i}[(k+1)\Delta t] = \phi_1(\Delta t)\underline{v}_{2i}(k\Delta t) + \phi_{2i}(\Delta t)\underline{v}_{3i}(k\Delta t), \quad \underline{v}_{2i}(0) = \underline{0}$$

$$\underline{v}_{3i}[(k+1)\Delta t] = \phi_3(\Delta t)\underline{v}_{3i}(k\Delta t), \qquad \underline{v}_{3i}(0) = \underline{q}_o$$

48

As a result of Eq. (34), the matrix exponential must be calculated only twice for each $\underline{X}_i$; once at $t = t_f$ for solving the initial costates, and once at $t = \Delta t$ for the recursive formula. After completing the solutions of each $\underline{X}_i$ in the series, the optimal control trajectory is produced by combining the trajectories from each expansion variable in the series given by Eq. (9). We again stress the fact that the solution to the nonlinear optimal control problem has been produced by solving a series of strictly linear, constant coefficient subproblems without the need for iterative techniques. We shall illustrate the effectiveness of the perturbation method with numerical examples of low order systems.

NUMERICAL EXAMPLES

Case 1:

To demonstrate the perturbation method, the first example of a nonlinear system is a scalar problem with both quadratic and cubic nonlinear terms. The system, in configuration space, is given by

$$\ddot{x} + c\dot{x} + kx = u + \epsilon(\beta u x - \alpha x^3) \qquad (35)$$

where $c = 0.1$ $\beta = 1.0$ $\epsilon = 0.1$

$k = 1.0$ $\alpha = 0.5$

$x(0) = 1.0$ $\dot{x}(0) = 0$ $t_f = 2$

The objective is to determine the optimal controls that will drive the variable (x) to zero (with a final velocity of zero) in a two second time interval. To verify that the system is weakly nonlinear, the nondimensional form of Eq. (35) can be shown to be

$$\ddot{\eta} + \delta_1\dot{\eta} + \eta = \tilde{u} + \delta_2\tilde{u}\eta - \delta_3\eta^3 \qquad (36)$$

with $\delta_1 = 0.1$ $\delta_2 = 0.1$ $\delta_3 = 0.05$

where η is the dimensionless position coordinate and $\tilde{u}$ is the dimensionless control force. Clearly, from Eq. (36), the system is lightly damped with weak

49

nonlinearities. We shall choose to penalize only the control accelerations and the final state in the performance measure, Eq. (3), and as such we let R = 1, Q = 0, and S = $10^{20}[I]$. The effect of the large weight matrix (S) is to rigidly enforce the final conditions in the optimal control problem. In the vernacular of optimal control theory this example is a fixed time, fixed final state optimal control problem (Ref. 6). Numerically, we shall solve this problem in configuration space, and as such the matrix, F, is given by

$$F = \begin{bmatrix} 0 & 1 & 0 & 0 \\ -1 & -0.1 & 1 & 0 \\ 0 & 0 & 0 & 1 \\ 0 & 0 & 0 & 0 \end{bmatrix}$$

Similarly, the vector of nonlinear terms in Eq. (8) can be shown to be

$$\{NLT\} = \begin{Bmatrix} 0 \\ \beta ux - \alpha x^3 \\ 0 \\ 0 \\ (3\alpha x^2 - \beta u)\lambda_2 \\ 0 \\ -\beta x \lambda_2 \\ 0 \end{Bmatrix}$$

where λ_2 is the second element of the costate vector $\underline{\lambda}$. We evaluate the effectiveness of the optimal control approximations by integrating Eq. (35), numerically, using a 4-cycle Runge-Kutta routine and examining the final boundary condition errors of the numerically integrated solution.

A second order expansion in the power series yields a final condition $x(t_f) = -0.000322$ from the integrated equation of motion. While not exactly zero, the error is less than 0.04%. By comparison, the linearized optimal control, obtained by dropping the nonlinear terms (note that this is also the zeroth order expansion variable) produces $x(t_f) = -0.0402$ or an error of over 4%. The perturbation approach reduced the error by two orders of magnitude

50

for a second-order exansion, demonstrating the effectiveness of the method. The trajectories of the position and control are shown in Fig. 1, where each profile exhibits the smooth, continuous behavior expected of an optimal solution of this problem.

Case 2:

For the second example, the perturbation method is applied to the second-order system

$$\ddot{x}_1 + c_1\dot{x}_1 + k_1 x_1 = u_1 + \epsilon\alpha_1 x_1 x_2$$

$$\ddot{x}_2 + c_2\dot{x}_2 + k_2 x_2 = u_2 + \epsilon\alpha_2 x_1 x_2 \qquad (37)$$

where

$$c_1 = 0.1 \qquad k_1 = 1.0 \qquad \alpha_1 = 1.0$$

$$c_2 = 0.1 \qquad k_2 = 0.5 \qquad \alpha_2 = 0.5$$

$$x_1(0) = 1.0 \qquad \dot{x}_1(0) = 0 \qquad \epsilon = 0.1$$

$$x_2(0) = 2.0 \qquad \dot{x}_2(0) = 0$$

In nondimensional, matrix format, the equations of motion are

$$\ddot{\underline{n}} + \begin{bmatrix} 0.1 & 0 \\ 0 & 0.1 \end{bmatrix} \dot{\underline{n}} + \begin{bmatrix} 1 & 0 \\ 0 & 0.5 \end{bmatrix} \underline{n} = \underline{\tilde{u}} + \begin{Bmatrix} (0.1)n_1 n_2 \\ (0.05)n_1 n_2 \end{Bmatrix} \qquad (38)$$

where again we see that Eq. (38) is a lightly damped, weakly nonlinear system. We shall choose to penalize the final states and the second derivatives of the controls in the performance index. Mathematically, we state this by setting $R = I$, $Q = 0$, and $S = 10^{20}[I]$. Proceeding as with Case 1, the results of a second order expansion are compared to the linearized optimal control problem as shown.

	$x_1(t_f)$	$x_2(t_f)$
Linearized optimal control approximation:	0.135	0.0868
Second order control approximation:	0.0000166	0.00000945

The final position errors for the zeroth order control approximation are 13.5%

and 4.3% respectively for the state variables x_1 and x_2. The control determined from the second order perturbation expansion reduces the errors by approximately four orders of magnitude. Such explosive convergence is not typical but it does demonstrate how well the perturbation method may solve open loop optimal control problems.

Case 3:

As a final example, we wish to test the method with a system containing larger nonlinearities. To accomplish this, we shall use the same system as used in Case 2 with the following parameter changes:

$$\alpha_1 = 2 \qquad x_1(0) = 3 \qquad \varepsilon = 0.4 \qquad \alpha_2 = 3 \qquad x_2(0) = 2$$

In dimensionless form, the system is given by

$$\ddot{\underline{n}} + \begin{bmatrix} 0.1 & 0 \\ 0 & 0.1 \end{bmatrix} \dot{\underline{n}} + \begin{bmatrix} 1 & 0 \\ 0 & 0.5 \end{bmatrix} \underline{n} = \tilde{\underline{u}} + \begin{Bmatrix} (2.4)n_1 n_2 \\ (3.6)n_1 n_2 \end{Bmatrix} \tag{39}$$

We notice immediately that this system is strongly nonlinear, and would not expect controls from the zeroth order solution to accurately approximate the actual optimal control. However, we shall proceed with the perturbation approach while recognizing that this is a significant test of the method. The final conditions are shown in Table 1 for controls computed from expansions of zero (linearized system) through sixth order.

TABLE 1 FINAL STATE ERRORS

Approximation Order	$x_1(t_f)$	$x_2(t_f)$
0	110.00	168.86
1	4.164	6.859
2	0.3654	0.6124
3	-0.01957	-0.03416
4	-0.01001	-0.01677
5	0.0006371	0.001106
6	0.0002444	0.0003835

The controls from the sixth-order expansion produces very accurate results with errors substantially less than 0.04% for both coordinates. The position and control profiles are shown in Figs. 2 and 3 respectively; each trajectory is a smooth and continuous path to the origin. The excellent convergence is achieved for this problem in which the nonlinear terms are of a significant magnitude. In Ref. 7, we document analogous results for maneuvers of a flexible spacecraft; we have achieved reliable convergence for a system having order 42.

CONCLUSIONS

A procedure for solving nonlinear, open loop, optimal control problems has been presented. In this approach, an asymptotic perturbation method is applied, thereby obtaining a solution process without the traditional dependence on iterative numerical methods. The nonlinear system is "separated" into a set of nonhomogeneous, linear, optimal control problems that may be solved sequentially. Upon combining the solutions of the subproblems in a straightforward power series, an optimal control for the nonlinear system is generated. This novel process for solving nonlinear optimal control problems is a result of the marriage of a simple analytical technique (the perturbation method) and a powerful numerical algorithm (the matrix exponential).

Although the asymptotic perturbation method was conceived as a solution process for weakly nonlinear problems, the method has demonstrated extraordinary effectiveness when applied to many strongly nonlinear problems such as the system presented in Case 3. Certainly, the perturbation method will not produce accurate results for all nonlinear systems. However, the family of nonlinear problems to which the method is effective is considerably larger than we initially expected. We therefore anticipate that this

asymptotic perturbation method will be found to be broadly applicable to a large family of generally nonlinear problems, including higher dimensioned systems.

ACKNOWLEDGEMENTS

REFERENCES

1. Junkins, J. L., "Comment on Optimal Feedback Slewing of Flexible Spacecraft," Journal of Guidance, Control and Dynamics, Vol. 5, No. 3, May-June, 1982, p. 318.

2. Turner, J. D., Chun, H. M., and Juang, Jer-Nan, "Optimal Slewing Maneuvers for Flexible Spacecraft Using a Closed Form Solution for the Linear Tracking Problem," Paper No. 83-374, presented at the AAS/AIAA Astrodynamics Conference, Lake Placid, New York, August 22-25, 1983.

3. Nayfeh, Ali Hasan, and Mook, Dean T., Nonlinear Oscillations, John Wiley and Sons, New York, 1979.

4. Van Loan, C. F., "Computing Integrals Involving the Matrix Exponential," IEEE Transactions on Auto Control, Vol. AC-23, No. 3, June, 1978, pp. 395-404.

5. Ward, R. C., "Numerical Computation of the Matrix Exponential with Accuracy Estimate," SIAM Journal of Numerical Analysis, Vol. 14, No. 4, September, 1977, pp. 600-610.
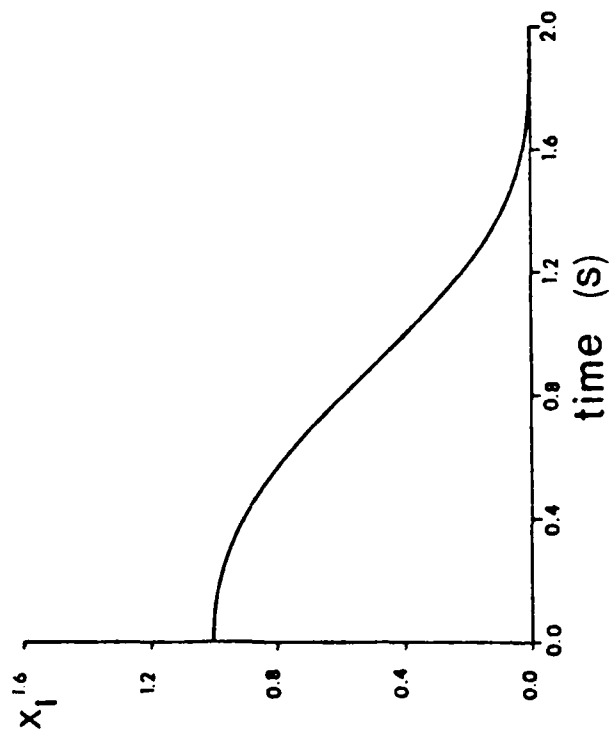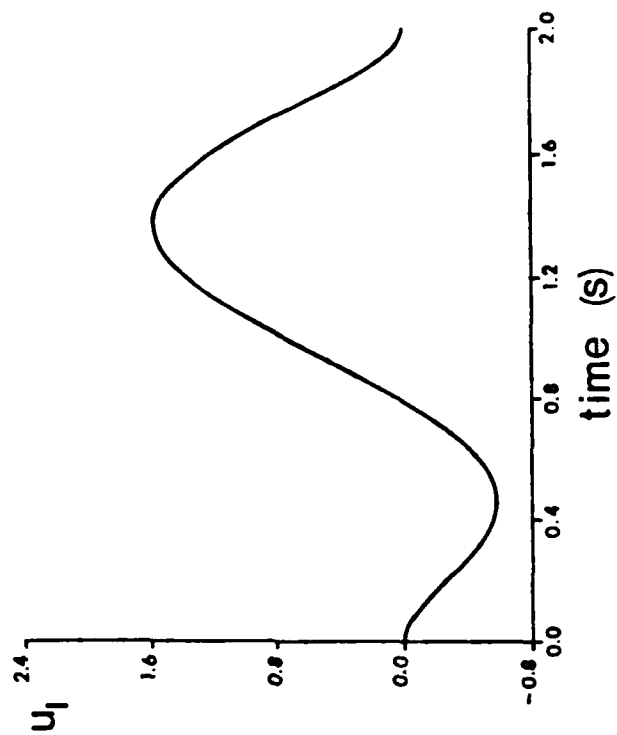
6. Kirk, Donald E., _Optimal Control Theory - An Introduction_, Prentice
    Hall, Inc., Englewood Cliffs, NJ, 1970.

7. Thompson, R. C., _A Perturbation Approach to Control of Rota-
    tional/Translational Maneuvers of Flexible Space Vehicles_, M. S.
    Thesis, Engineering Mechanics, VPI&SU, Blacksburg, VA, 1985.

LIST OF FIGURES

AMERICAN *ASTRONAUTICAL* SOCIETY
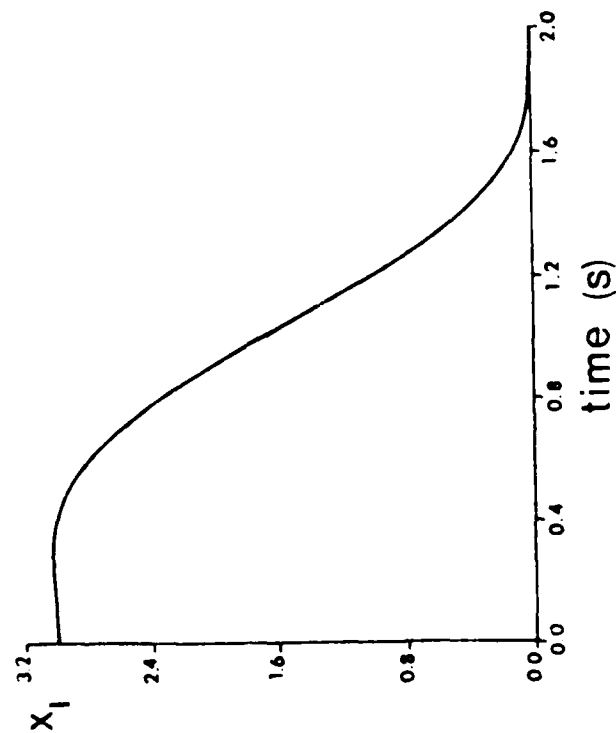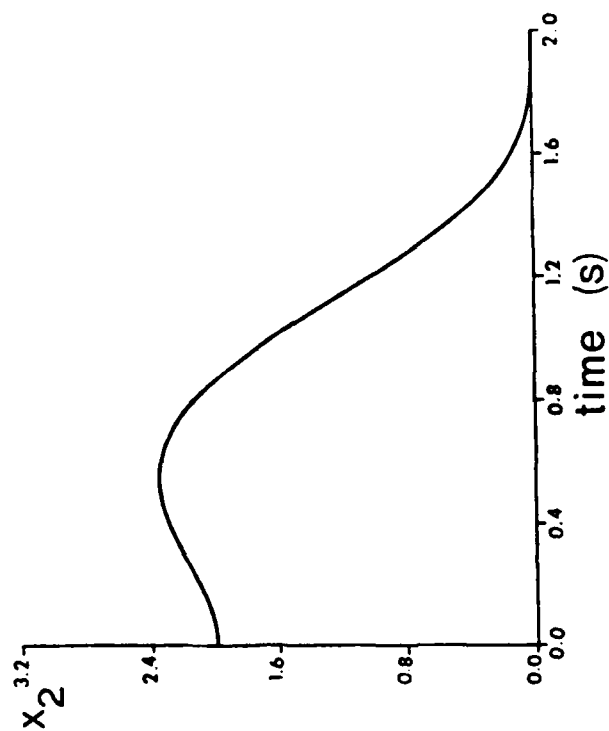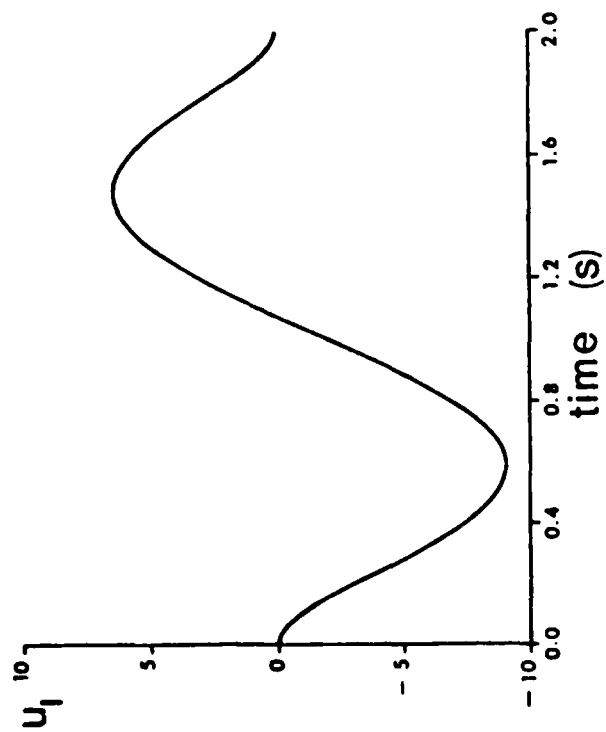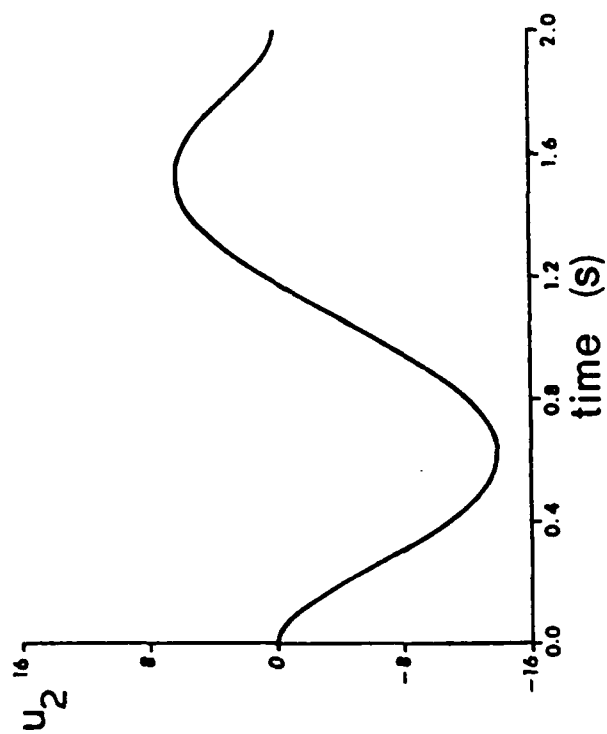
A QUASI-ANALYTICAL METHOD FOR COMPUTING NONLINEAR ATTITUDE MANEUVER CONTROLS

R.C. Thompson
Texas A&M University
College Station, Texas

Dr. J.L. Junkins
Texas A&M University
College Station, Texas

Dr. J.D. Turner
Cambridge Research
Cambridge, Massachusetts

ANNUAL ROCKY MOUNTAIN GUIDANCE AND CONTROL CONFERENCE

February 1 through February 5, 1986
Keystone, Colorado

A QUASI-ANALYTICAL METHOD FOR COMPUTING NONLINEAR ATTITUDE MANEUVER CONTROLS

R.C. Thompson[1], J.L. Junkins[2], and J.D. Turner[3]

A quasi-analytical method is presented for solving nonlinear, open loop, optimal control problems. Upon applying the most basic of the asymptotic expansions from perturbation methods (the pedestrian or power series expansion), the nonlinear control problem is replaced by a sequence of linear, non-homogeneous problems. In contrast to the usual emphasis (in perturbation methods) upon analytical solutions of the sequence of linear systems, we show that this sequence of problems can be solved sequentially using efficient numerical methods. The nonhomogeneous terms are represented by a finite Fourier series, allowing the use of matrix exponential algorithms due to Ward and Van Loan to be used to solve the system at each order. In principle, the order of the expansion may be extended indefinitely, however numerical difficulties will arise at some point. Historically, solutions to nonlinear control problems have relied almost exclusively on iteration methods (using one of several available algorithms); however, the perturbation method presented here often produces very accurate solutions to nonlinear problems without iteration. The perturbation method is broadly applicable to a variety of optimal control problems including large degree of freedom systems. Numerical examples of multi-axis attitude maneuvers of a rigid spacecraft are presented.

---

[1] Research Associate, Texas A&M University, College Station, Texas, 77843

[2] TEES Professor of Aerospace Engineering, AAS Fellow, Texas A&M University, College Station, 77843

[3] Cambridge Research, Cambridge, Massachusetts, 02138

-1-

OPTIMAL CONTROL FORMULATION

Consider a system governed by a nonlinear, vector equation with initial and terminal boundary conditions of the form

$$\dot{\underline{z}} = F\underline{z} + D\underline{U} + \varepsilon\underline{\rho}$$

$$\underline{z}(t_o) = \underline{\alpha} \qquad \underline{z}(t_f) = 0$$
(1)

where $\underline{z}$ is an nx1 state vector, $\underline{U}$ is an mx1 vector of controls, $\varepsilon\underline{\rho}$ is an nx1 vector containing all nonlinear terms and ε is a small dimensionless parameter. We note that many systems require some algebraic manipulations in order to represent the system in the form of Eq. (1). For example, the system may require a transformation to modal coordinates in order to produce an independent set of equations. Furthermore, the state vector may be augmented to contain "pseudo-state" variables such as the control magnitude and control rate in order to determine more realistic or desirable control profiles and (in the case of flexible bodies) reduce spillover into the higher frequency modes. (Ref. 1) If such an approach is taken, then the vector $\underline{U}$ may not be the applied control but instead will contain higher derivatives of the control variables. Because the perturbation method that we present depends upon a power series expansion, it is important to expand any transcendental functions into a truncated Taylor's series. Therefore, if a given system contains transcendental functions, we must start with an approximation of that system as a consequence of this procedure, where of course the accuracy of the approximation will depend upon the number of terms included in the formulation.

We seek the control trajectory that minimizes the functional

$$J = \frac{1}{2}\underline{z}^T S \underline{z}\Big|_{t=t_f} + \frac{1}{2}\int_{t_o}^{t_f}(\underline{z}^T Q \underline{z} + \underline{U}^T R \underline{U})\,dt$$
(2)

subject to the condition that Eq. (1) is satisfied; where R and S are positive definite, diagonal weight matrices, and Q is a symmetric, positive semi-definite weight matrix. The Hamiltonian, formed from the integrand of Eq. (2) and the system equations is given by

$$H = \frac{1}{2}(\underline{z}^T Q \underline{z} + \underline{U}^T R \underline{U}) + \underline{\lambda}^T(F\underline{z} + D\underline{U} + \varepsilon\underline{\rho})$$
(3)

where the costates, designated as $\underline{\lambda}$, are a set of n undetermined Lagrange multipliers. Pontryagin's necessary conditions for determining the optimal control yield the three equations

$$\underline{\dot{z}} = \frac{\partial H}{\partial \underline{\lambda}} = F\underline{z} + D\underline{U} + \varepsilon\underline{\rho} \tag{4}$$

$$\underline{\dot{\lambda}} = -\frac{\partial H}{\partial \underline{z}} = -Q\underline{z} - F^T\underline{\lambda} - \varepsilon[\frac{\partial\underline{\rho}}{\partial\underline{z}}]^T\underline{\lambda} \tag{5}$$

$$\underline{0} = \frac{\partial H}{\partial \underline{U}} = R\underline{U} + D^T\underline{\lambda} \tag{6}$$

and the boundary condition $\underline{\lambda}(t_f) = S\underline{z}(t_f)$.

Solving Eq. (6) for $\underline{U}$ and substituting into Eq. (4) reduces the problem of determining the optimal control to solving two coupled, nonlinear, first-order ordinary differential equations. The two equations may then be combined by defining the augmented state/costate vector, $\underline{X}$, such that

$$\underline{\dot{X}} = A\underline{X} + \varepsilon\{NLT\} \tag{7}$$

where

$$\underline{X} = [\underline{z}^T \quad \underline{\lambda}^T]^T \qquad\qquad 2n \times 1$$

$$A = \begin{bmatrix} F & -DR^{-1}D^T \\ -Q & -F^T \end{bmatrix} \qquad\qquad 2n \times 2n$$

$$\{NLT\} = \left\{ \begin{array}{c} \underline{\rho} \\ -[\frac{\partial\underline{\rho}}{\partial\underline{z}}]^T\underline{\lambda} \end{array} \right\} \qquad\qquad 2n \times 1$$

We have now reduced the optimal control problem to a Two-Point Boundary Value Problem with split boundary conditions on $\underline{z}$ and the condition that $\underline{\lambda}(t_f) = S\underline{z}(t_f)$. As a consequence of the existence of the vector of nonlinear terms, designated $\{NLT\}$, the problem given by Eq. (7) is analytically intractable, and we would ordinarily rely upon iterative methods to

63

complete the solution. However, we wish to construct a
quasi-analytical approach that eliminates the reliance upon
iteration.

THE PEDESTRIAN EXPANSION

For a weakly nonlinear system, as indicated by the
"bookkeeping" term ϵ, it is constructive to apply a straight-
fo ard power series expansion to produce an approximate
solution to the problem. (Ref. 3) Let the solution to
Eq. (7) be given by

$$\underline{X}(t) = \underline{X}_o(t) + \epsilon\underline{X}_1(t) + \epsilon^2\underline{X}_2(t) + \ldots \tag{8}$$

For small nonlinearities, and consequently small ϵ, the
series will produce accurate results and the accuracy will
improve as the nonlinearities approach zero. Substituting
Eq. (8) into Eq. (7) gives

$$\dot{\underline{X}}_0 + \epsilon\dot{\underline{X}}_1 + \epsilon^2\dot{\underline{X}}_2 + 0(\epsilon^3) = A\underline{X}_0 + \epsilon A\underline{X}_1 + \epsilon^2 A\underline{X}_2 + \epsilon\{NLT_1(\underline{X}_0)\}$$

$$+ \epsilon^2\{NLT_2(\underline{X}_0,\underline{X}_1)\} + 0(\epsilon^3) \tag{9}$$

where the nonlinear terms, $\{NLT_i\}$, have been expanded in a
similar power series and the functional dependence of each
term on the expansion variables $(\underline{X}_i)$ is indicated in each
term. Equating like powers of ϵ yields the series of equa-
tions

$$\dot{\underline{X}}_0 = A\underline{X}_0 \tag{10}$$

$$\dot{\underline{X}}_1 = A\underline{X}_1 + \{NLT_1(\underline{X}_0)\} \tag{11}$$

$$\dot{\underline{X}}_2 = A\underline{X}_2 + \{NLT_2(\underline{X}_0,\underline{X}_1)\} \tag{12}$$

For illustrative purposes, we have included only the terms
through second order; however the series could be continued
to higher orders if necessary to achieve the precision appro-
priate for a specific problem. In Ref [8], we show several
examples wherein 5th and 6th order expansions were routinely
computed; analytical perturbation solutions above third order
are very rare. The same procedure, when applied to the
boundary conditions yields

64

$$\underline{X}_0(t_0) = \left\{ \begin{matrix} \underline{z}(t_0) \\ \underline{\lambda}_0(t_0) \end{matrix} \right\} \qquad \underline{X}_0(t_f) = \left\{ \begin{matrix} \underline{z}(t_f) \\ \underline{\lambda}_0(t_f) \end{matrix} \right\} \qquad (13)$$

$$\underline{X}_i(t_0) = \left\{ \begin{matrix} \underline{0} \\ \underline{\lambda}_i(t_0) \end{matrix} \right\} \qquad \underline{X}_i(t_f) = \left\{ \begin{matrix} \underline{0} \\ \underline{\lambda}_i(t_f) \end{matrix} \right\} \quad i=1,2,3,\dots \qquad (14)$$

and we recall that the final conditions of the states and costates are related at each order by $\underline{\lambda}_i(t_f) = S\underline{z}_i(t_f)$. Note that the nonhomogeneous terms in the ith equation of Eqs. (10-12) are dependent only upon the preceeding i-1 expansion variables. Therefore, the nonhomogeneous term in each equation constitutes a known function of time and Eqs. (10-12) can be solved sequentially. The perturbation method has, as usual, replaced the original nonlinear problem with a series of linear, nonhomogeneous problems.

The solution of Eqs. (10-12) can be shown to be

$$\underline{X}_i(t) = e^{At}[\underline{X}_i(0) + \int_0^t e^{-A\tau}\underline{d}_i(\tau)d\tau] \quad i=0,1,2,\dots \qquad (15)$$

where

$$\underline{d}_0(\tau) = \underline{0}$$

$$\underline{d}_i(\tau) = \{NLT_i\} \quad i=1,2,\dots \qquad (16)$$

and where we have assumed $t_0=0$ without loss of generality. Evaluating the integral in Eq. (15) may be accomplished in any number of ways. Direct numerical integration could be used but a more attractive method would be to use a finite Fourier series approximation of the integrand (or some other orthogonal series) and then integrate the series term by term. The latter method will provide us with a model of the integral as a continuous function of time, an advantage when calculating the trajectories of the expansion variables. Another alternative, and perhaps the most elegant, is to use a matrix exponential to calculate the entire integral shown in Eq. (15).

The matrix exponential method requires the nonlinear terms, $\underline{d}_i(\tau)$, to be represented by a continuous function of time in exponential form. Since we have no closed form expression for the nonlinear terms, we can at best generate

a large set (k) of data points which are sampled values of the nonhomogeneous terms. A finite Fourier series, which can always be put in exponential form, is used as the continuous time representation, and is given by

$$d(t) = b_0 + \sum_{i=1}^{r} a_i \sin i\omega_0 t + b_i \cos i\omega_0 t \qquad (16)$$

To calculate the series coefficients, we use a least squares fit of the series to the sampled data sets. It can be shown that the Fourier series of the jth element of the ith non-linear term may be given by

$$\beta \underline{c}_j = \underline{\tilde{d}}_j \qquad (17)$$

where the matrix β contains the trigonometric functions evaluated at the sample times, $\underline{c}_j$ contains the unknown series coefficients, and $\underline{d}_j$ contains the sampled data of the jth element of $\underline{d}_i(t)$, as given by

$$\underline{\tilde{d}}_j = [\underline{d}_i^j(0) \ \underline{d}_i^j(\Delta t) \ \underline{d}_i^j(2\Delta t) \ \dots \ \underline{d}_i^j(k\Delta t)]^T \qquad (18)$$

where $\Delta t = t_f/k$. The unknown coefficients are then determined from the least squares approximation.

$$\underline{c}_j = (\beta^T \beta)^{-1} \beta^T \underline{\tilde{d}}_j \qquad (19)$$

Note that with appropriate sample points (symmetric about $\omega_0 \Delta t = \pi$) $\beta^T \beta$ is diagonal and the inverse is trivial. Alternatively, we can develop these coefficients from a discrete Fourier transform. Proceeding element by element (j=1,2,3,...,2n) through the vector of nonlinear terms, each element is represented by a finite Fourier series. The collection of series representations may then be put into the form

$$\underline{d}_i(t) = G_i e^{\Omega t} \underline{g}_0 \qquad (20)$$

where the jth row of G_i contains the series coefficients for the jth element of the nonlinear term, and the matrix, Ω, is defined to be

$$\Omega = \text{Block Diag} [0 \ \Omega_1 \ \Omega_2 \dots \Omega_r]$$

66

where

$$\Omega_\ell = \begin{bmatrix} 0 & 1 \\ -(\ell\omega_0)^2 & 0 \end{bmatrix} \qquad \ell = 1,2,3,\dots r$$

and $\underline{g}_0$ is a constant vector used to "separate" the trigonometric functions calculated in Eq. (20).

At this point, we have a continuous time representation of the nonlinear term in the form of a matrix exponential. We now employ Van Loan's identity (Ref. 4) which will produce the integral in Eq. (15) from a matrix exponential. We shall define

$$Y_i = \begin{bmatrix} A & G_i \\ 0 & \Omega \end{bmatrix} \tag{21a}$$

$$e^{Y_i t} = \begin{bmatrix} \Phi_1(t) & \Phi_{2i}(t) \\ 0 & \Phi_3(t) \end{bmatrix} \tag{21b}$$

where we note that $\Phi_{2i}(t)$ is different for each $\underline{X}_i$. The definitions of the state transition matrices $(\Phi_i)^i$ are (from Van Loan)

$$\Phi_1(t) = e^{At} \tag{22a}$$

$$\Phi_{2i}(t) = e^{At} \int_0^t e^{-A\tau} G_i e^{\Omega\tau} d\tau \tag{22b}$$

$$\Phi_3(t) = e^{\Omega t} \tag{22c}$$

We may then rewrite Eq. (15) using the definitions from Eq. (22) to get

$$\underline{X}_i(t) = \Phi_1(t)\underline{X}_i(0) + \Phi_{2i}(t)\underline{g}_0 \tag{23}$$

In order to use Eq. (23) to produce the trajectory of $\underline{X}_i$, we must first determine the n unknown initial conditions of $\underline{X}_i$ (i.e. the initial costates $\underline{\lambda}_i$).

67

SOLVING THE INITIAL COSTATES

We have noted that the costate boundary condition resulting from Pontryagin's principle is $\underline{\lambda}_i(t_f) = S\underline{z}_i(t_f)$. Until now, this boundary condition has not been used, however, it will be instrumental in completing the immediate task of solving for the initial costates. Evaluating Eq. (23) at $t=t_f$ and substituting the boundary condition into the result gives

$$\underline{X}_i(t_f) = \begin{Bmatrix} \underline{z}(t_f) \\ S\underline{z}_i(t_f) \end{Bmatrix} = \phi_1(t_f) \begin{Bmatrix} \underline{z}_i(0) \\ \underline{\lambda}_i(0) \end{Bmatrix} + \phi_{2i}(t_f)\underline{g}_0 \quad (24)$$

To simplify the notation, let us partition the components of Eq. (24) as

$$\phi_1(t_f) = \begin{bmatrix} \phi_1^{11}(t_f) & \phi_1^{12}(t_f) \\ \phi_1^{21}(t_f) & \phi_1^{22}(t_f) \end{bmatrix} \quad (25a)$$

$$\phi_{2i}(t_f)\underline{g}_0 = \begin{Bmatrix} \underline{\psi}_{1i}(t_f) \\ \underline{\psi}_{2i}(t_f) \end{Bmatrix} \quad (25b)$$

Substituting Eq. (25) into Eq. (24) leads to the two coupled algebraic equations

$$\underline{z}_i(t_f) = \phi_1^{11}(t_f)\underline{z}_i(0) + \phi_1^{12}(t_f)\underline{\lambda}_i(0) + \underline{\psi}_{1i}(t_f) \quad (26)$$

$$S\underline{z}_i(t_f) = \phi_1^{21}(t_f)\underline{z}_i(0) + \phi_1^{22}(t_f)\underline{\lambda}_i(0) + \underline{\psi}_{2i}(t_f) \quad (27)$$

where $\underline{\lambda}_i(0)$ is the only unknown term. Finally, multiplying Eq. (26) by S, substituting into Eq. (27), and collecting the terms produces

$$[\phi_1^{22}(t_f) - S\phi_1^{12}(t_f)]\underline{\lambda}_i(0) = [S\phi_1^{11}(t_f) - \phi_1^{21}(t_f)]\underline{z}_i(0)$$

$$+ S\underline{\psi}_{1i}(t_f) - \underline{\psi}_{2i}(t_f) \quad (28)$$

By using any appropriate algorithm, we can solve the linear, algebraic system given by Eq. (28). Substituting this solution into Eq. (23), we now have the solution for $\underline{X}_i(t)$.

RECURSIVE SOLUTION OF THE STATE TRAJECTORIES

We have found, in Eq. (23), the solution for a given perturbation expansion $\underline{X}_i(t)$. In order to proceed to the next order (i+1), we need a sampled data set of the trajectories of $\underline{X}_i(t)$. This will permit efficient calculation of the Fourier series representation of the inhomogeneous terms. To duplicate the procedure outlined above for each value of t would of course be far too costly in terms of time and computational efficiency. However, an alternative exists as a result of the particular exponential property

$$ e^{A(k+1)\Delta t} = e^{A\Delta t}e^{Ak\Delta t} \tag{29} $$

By making extensive use of the property given by Eq. (29), we can produce a recursive solution of Eq. (23) in which each data point (for a small, fixed time interval Δt) is found by simple matrix multiplication and addition.

It can be shown that applying the property in Eq. (29) to the definitions in Eq. (21b) gives

$$ \phi_1[(k+1)\Delta t] = \phi_1(\Delta t)\phi_1(k\Delta t) \tag{30a} $$

$$ \phi_{2i}[(k+1)\Delta t] = \phi_1(\Delta t)\phi_{2i}(k\Delta t) + \phi_{2i}(\Delta t)\phi_3(k\Delta t) \tag{30b} $$

$$ \phi_3[(k+1)\Delta t] = \phi_3(\Delta t)\phi_3(k\Delta t) \tag{30c} $$

where $\phi_1(0)=I$, $\phi_{2i}(0)=0$, and $\phi_3(0),=I$. Now let us define the three vectors $\underline{v}_{ji}$ to be

$$ \underline{v}_{1i}[(k+1)\Delta t] = \phi_1[(k+1)\Delta t]\underline{X}_i(0) \tag{31a} $$

$$ \underline{v}_{2i}[(k+1)\Delta t] = \phi_{2i}[(k+1)\Delta t]\underline{g}_0 \tag{31b} $$

$$ \underline{v}_{3i}[(k+1)\Delta t] = \phi_3[(k+1)\Delta t]\underline{g}_0 \tag{31c} $$

Evaluating Eq. (23) at $t=[(k+1)\Delta t]$, substituting Eq. (31) into the result, and by substituting Eq. (31) into Eq. (30) we get

69

$$\underline{X}_i[(k+1)\Delta t] = \underline{v}_{1i}[(k+1)\Delta t] + \underline{v}_{2i}[(k+1)\Delta t] \qquad (32a)$$

$$\underline{v}_{1i}[(k+1)\Delta t] = \Phi_{1i}(\Delta t)\underline{v}_{1i}(k\Delta t), \qquad \underline{v}_{1i}(0) = \underline{X}_i(0) \qquad (32b)$$

$$\underline{v}_{2i}[(k+1)\Delta t] = \Phi_1(\Delta t)\underline{v}_{2i}(k\Delta t)$$

$$+ \Phi_{2i}(\Delta t)\underline{v}_{3i}(k\Delta t) \qquad \underline{v}_{2i}(0) = \underline{0} \qquad (32c)$$

$$\underline{v}_{3i}[(k+1)\Delta t] = \Phi_3(\Delta t)\underline{v}_{3i}(k\Delta t), \qquad \underline{v}_{3i}(0) = \underline{g}_o \qquad (32d)$$

We can see by Eq. (32) that we need only to calculate the matrix exponential given by Eq. (21) once in order to implement this recursive solution. Clearly then, the solution of each order requires the calculation of the matrix exponential twice; once at $t=t_f$ to solve for the initial costates and once at $t=\Delta t$ to set up the recursive procedure. When the solution of each order is completed, the variables are combined according to Eq. (8) to produce the open loop optimal trajectories. We again stress the fact that the solution to the nonlinear optimal control problem has been produced by solving a sequence of strictly linear, constant coefficient subproblems without resorting to any iterative techniques. We shall illustrate the effectiveness of the perturbation method with numerical examples of a multi-axial attitude control of a rigid spacecraft.

SPACECRAFT EQUATIONS OF MOTION

The spacecraft configuration for a multi-axial rigid body is immaterial, but we shall assume that we have selected a body fixed set of axes, $\{\underline{b}_i\}$, located a the mass center of the body and aligned with the principal axes of the spacecraft. Describing the orientation of the body fixed frame relative to the inertial frame, $\{\underline{N}_i\}$, by a set of 1-2-3 Euler angles (ϕ, θ, ψ), we can show that the angular velocity of the spacecraft in body fixed axes is given by

$$\underline{\omega} = \omega_1 \hat{\underline{b}}_1 + \omega_2 \hat{\underline{b}}_2 + \omega_3 \hat{\underline{b}}_3 \qquad (33)$$

where

$$\omega_1 = \dot{\phi}c\theta c\psi + \dot{\theta}s\psi \qquad c(\ ) = \cos(\ )$$

$$\omega_2 = \dot{\theta}c\psi - \dot{\phi}c\theta s\psi \qquad s(\ ) = \sin(\ )$$

$$\omega_3 = \dot{\phi}s\theta + \dot{\psi}$$

Inverting these kinematic equations, we obtain the Euler
angle rates as

$$\dot{\phi} = \omega_1 c\psi/c\theta - \omega_2 s\psi/c\theta \tag{34a}$$

$$\dot{\theta} = \omega_1 s\psi + \omega_2 c\psi \tag{34b}$$

$$\dot{\psi} = -\omega_1 c\psi s\theta/c\theta + \omega_2 s\psi s\theta/c\theta + \omega_3 \tag{34c}$$

As indicated previously, we must expand the trigonometric
functions in a Taylor's series. In doing so, we shall
neglect all quartic and higher powers of the variables,
resulting in the approximate nonlinear equations

$$\dot{\phi} = \omega_1 + \omega_1(\theta^2/2 - \psi^2/2) - \omega_2\psi \tag{35}$$

$$\dot{\theta} = \omega_2 + \omega_1\psi - \omega_2\psi^2/2 \tag{36}$$

$$\dot{\psi} = \omega_3 - \omega_1\theta + \omega_2\theta\psi \tag{37}$$

We can show that these equations are adequate to describe
maneuvers of $<20°$ in any/all axes. The spacecraft is to
be controlled by three external control torques (u_i, i=1,2,3)
applied about the respective principal axes. Therefore
the dynamics of the multi-axial motion is defined by Euler's
equations as

$$\dot{\omega}_1 = u_1/I_1 + (I_2-I_3)\omega_2\omega_3/I_1 \tag{38}$$

$$\dot{\omega}_2 = u_2/I_2 + (I_3-I_1)\omega_1\omega_3/I_2 \tag{39}$$

$$\dot{\omega}_3 = u_3/I_3 + (I_1-I_2)\omega_1\omega_2/I_3 \tag{40}$$

where I_i is the ith principal inertia. The motion of the
spacecraft is governed by Eqs. (35-40) and our task is to
find the control torques required to drive the spacecraft
to a final state of zero attitude and zero angular velocity
from reasonable arbitrary initial conditions (defining the
fixed target orientation to be the inertial frame).

71

In the optimal control formulation, we shall include the control torques and their first derivatives in the state vector. By doing so, we define our pseudo-control $\underline{U} = \underline{\dot{u}}$ and as such, we shall be penalizing, in the performance functional, the integral norm of the "control accelerations". The resulting control profiles will then have prescribed (usually zero) magnitude and slope at the initiation and completion of the maneuver. Therefore, the augmented state and control vectors are defined to be

$$\underline{z} = [\phi\ \theta\ \psi\ \omega_1\ \omega_2\ \omega_3\ u_1\ u_2\ u_3\ \dot{u}_1\ \dot{u}_2\ \dot{u}_3]^T \qquad (41)$$

$$\underline{U} = [\ddot{u}_1\ \ddot{u}_2\ \ddot{u}_3]^T$$

We can then put Eqs. (35-40) into the matrix form indicated by Eq. (1), and follow the procedure outlined in the development of the perturbation method.

NUMERICAL EXAMPLES

We demonstrate how well the perturbation method performed in the following numerical examples by summarizing results from integrations of the exact equations of motion (Eq. (34) and Eqs. (38-40)), using the optimal controls generated by the perturbation method, and comparing the final conditions of the integrated equations with the desired final conditions. Repeating this procedure for solutions of different orders in the expansion given by Eq. (8) demonstrates how the accuracy is improved with each order.

CASE 1

For the first example, a small angle, rest-to-rest maneuver in 2 seconds is performed with the perturbation expansion carried to second order. The initial conditions are

$$\phi = 0.1\ \text{rad} \qquad \omega_1 = 0$$

$$\theta = 0.05\ \text{rad} \qquad \omega_2 = 0$$

$$\psi = 0.15\ \text{rad} \qquad \omega_3 = 0$$

We select the weight matrices $Q=0$, $R=I$, and $S=1.E20 \times [I]$. The large value of the matrix S serves as a requirement that the final conditions be rigidly enforced. In this problem, we are penalizing only the "control accelerations"

and the final state errors. Since this is a small angle
maneuver, we would expect the solution to be accurate, since
the Taylor's series approximation made in deriving Eqs. (35-37)
will be very accurate. The results of the integration of the
equations of motion are shown in Table 1 for each order. We
can see that the zero order solution alone is quite precise,
as we suspected, and that by the second order solution, we
have obtained nearly two orders of magnitude improvement
toward the final conditions. This level of precision is
probably all one would require for open loop maneuver controls,
since (i) modeling errors and implementation errors are always
present, (ii) if high precision is required, we would always
employ a terminal feedback control for precise target acqui-
sition. Clearly, the perturbation method is providing an
acceptable degree of accuracy for this open loop problem.

TABLE 1   FINAL STATE ERRORS

	Order Approximation		
	0	1	2
ϕ	-1.11E-3	-8.97E-5	-3.17E-4
θ	3.53E-3	2.87E-4	-7.11E-6
ψ	1.54E-3	-5.72E-5	-1.08E-5
ω_1	-4.48E-3	7.22E-4	.4.30E-5
ω_2	1.12E-2	5.78E-4	-4.48E-5
ω_3	-5.61E-4	7.72E-5	9.77E-6

CASE 2

In this example we shall challenge the perturbation
method by increasing the initial attitude to larger angles
and by letting the spacecraft be tumbling initially. As
in the previous example, we seek the optimal controls that
will drive the system to a zero attitude at rest with a
maneuver time of 2 sec. The initial conditions for this
case are

$$\phi = 0.25 \text{ rad} \qquad \omega_1 = 0.4 \text{ rad/sec}$$

$$\theta = 0.10 \text{ rad} \qquad \omega_2 = 0.2 \text{ rad/sec}$$

$$\psi = 0.40 \text{ rad} \qquad \omega_3 = 1.0 \text{ rad/sec}$$

The weight matrices are given the same values as in Case 1.
In like manner, the results of the perturbation solution to
order 2 are summarized in Table 2. We note immediately that
the zero order solution is ineffective at performing the
detumbling maneuver and may actually aggravate the motion of
the spacecraft. However, the first and second order approxi-
mations converge quickly to produce acceptable final state
errors and demonstrate the effectiveness of the perturbation
method. We would conclude that the control trajectories
produced by the first or second order approximations are
indeed adequate approximations of the open loop optimal
controls which we wished to determine. The trajectories
of the Euler angles, angular velocity, and controls for
the second order solution are shown in Figs. (1-3) respec-
tively.

TABLE 2   FINAL STATE ERRORS

	Order Approximation		
	0	1	2
ϕ	-0.218	-0.430E-1	-0.184E-1
θ	0.315	-0.138E-1	-0.435E-3
ψ	0.679E-1	-0.123E-2	0.142E-2
ω_1	-0.104E-1	0.157E-1	0.740E-2
ω_2	0.434	0.218E-1	-0.152E-1
ω_3	0.224E-2	0.147E-2	0.161E-2

CONCLUSIONS

A procedure for solving nonlinear, open loop, optimal
control problems has been presented. In this approach,
an asymptotic perturbation method is applied to the problem
thereby eliminating the traditional dependence on iterative
numerical methods. The nonlinear system is "separated"
into a set of nonhomogeneous, linear, optimal control prob-
lems that may be solved sequentially as "independent"
systems. Upon combining the solutions of the subproblems
in a straightforward power series, an optimal control for
the nonlinear system is generated. This novel process for
solving nonlinear optimal control problems is a result of
the marriage of a simple analytical technique (the pertur-
bation method) and a powerful numerical algorithm (the
matrix exponential).

We have applied the perturbation method to several classes of problems (Ref. 7,8) and have found it to be most effective for a large family of nonlinear problems, including large degree of freedom systems. The material presented in this paper is a further evaluation of the method in its present format regarding nonlinear three dimension spacecraft control. We are continuing to improve the method in an effort to achieve greater numerical efficiency while simultaneously applying the approach to a greater number and wider variety of nonlinear problems. Higher order solutions to common problems can be completed quickly and with minimal programming effort in a manner that cannot be matched by purely analytical methods, yet with an accuracy that is consistent with other numerical methods. We anticipate that the quasi-analytical perturbation method will prove the most useful approach for solving many nonlinear problems.
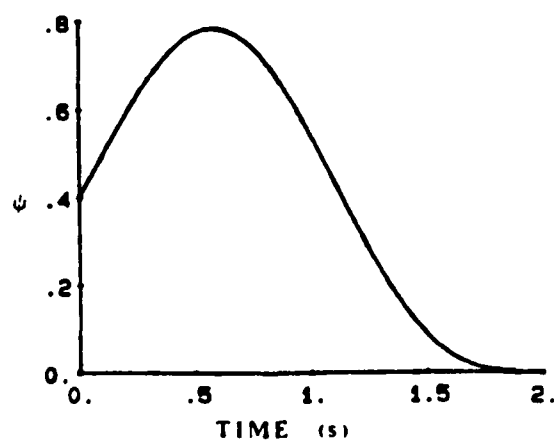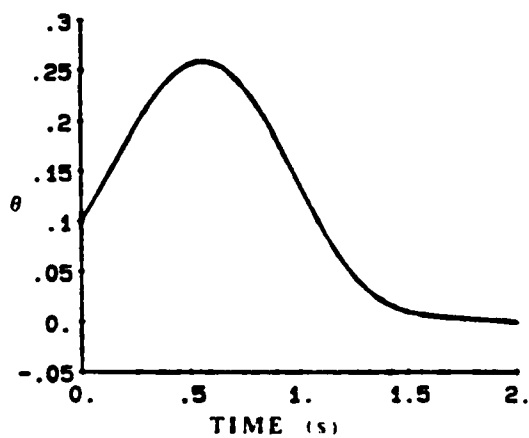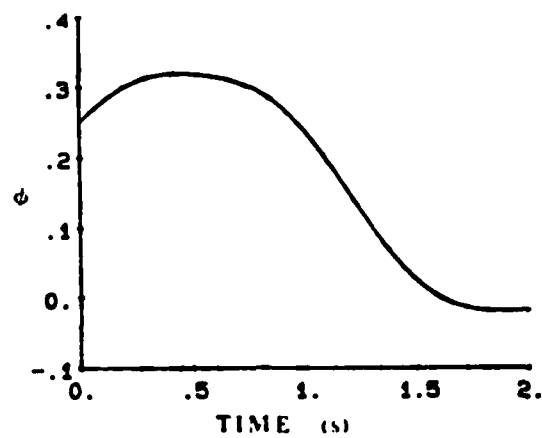
Figure 1   Euler Angle Histories For Case 2
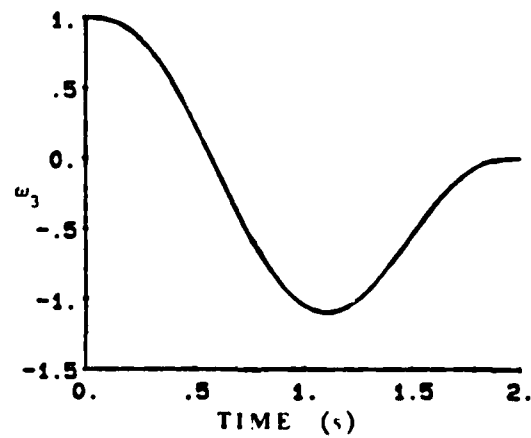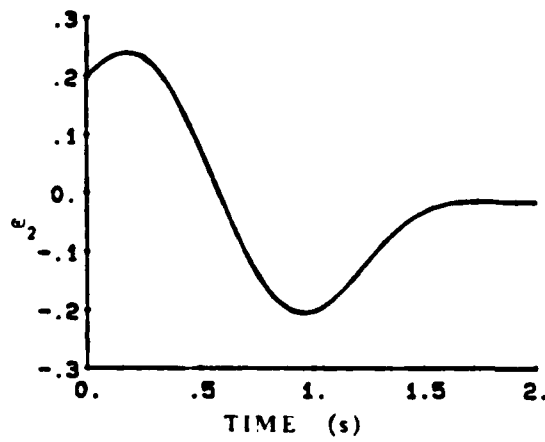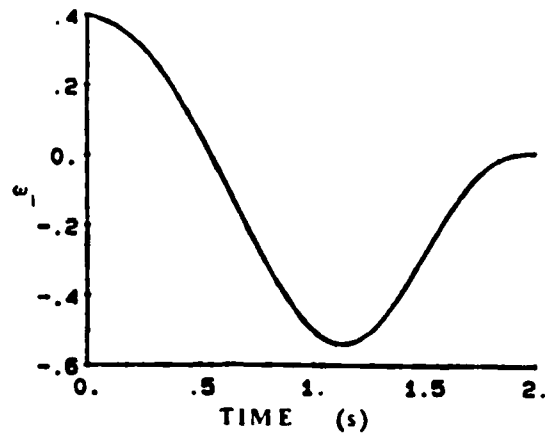Second Order Expansion

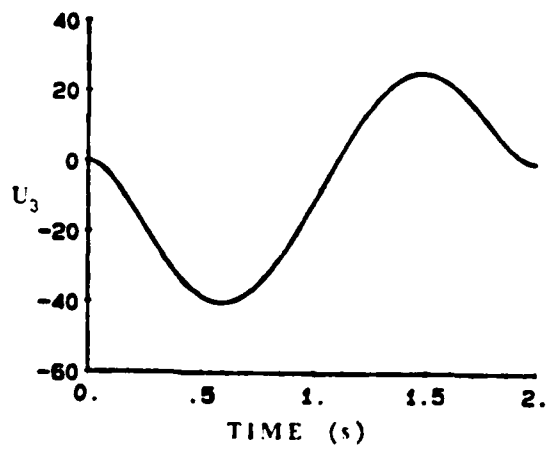Figure 2   Angular Velocity Components For Case 2
Second Order Expansion
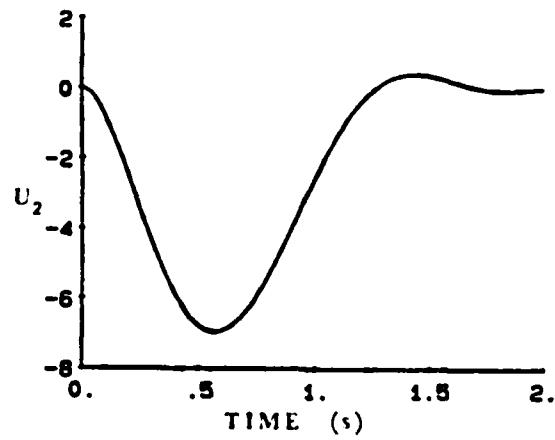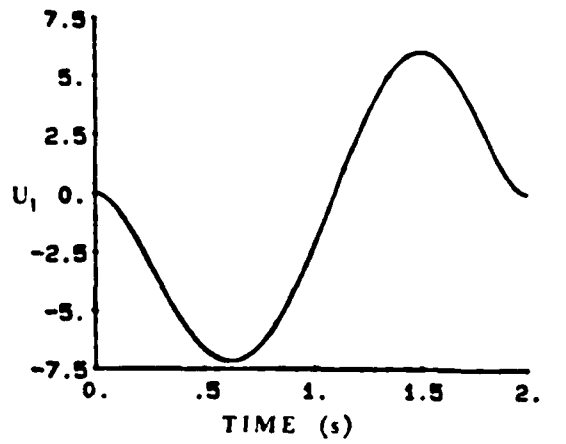
77

Figure 3   Optimal Control Torques for Case 2
                Second Order Expansion

78

REFERENCES

1. Junkins, J.L., "Comment on Optimal Feedback Slewing of Flexible Spacecraft," AIAA 82-4131, <u>Journal of Guidance and Control</u>, Vol. 5, No. 3, May-June, 1982, p. 318.

2. Turner, J.D., Chun, H.M., and Juang, Jer-Nan, "Optimal Slewing Maneuvers of Flexible Spacecraft Using a Closed Form Solution for the Linear Tracking Problem," Paper No. 83-374, presented at the AAS/AIAA Astrodynamics Conference, Lake Placid, New York, August 22-25, 1983.

3. Nayfeh, Ali Hasen, and Mook, Dean T., "<u>Nonlinear Oscillations</u>", John Wiley and Sons, New York, 1979.

4. Van Loan, C.F., "Computing Integrals Involving the Matrix Exponential," <u>IEEE Transactions on Auto Control</u>, Vol. AC-23, No. 3, June, 1978, pp. 395-404.

5. Ward, R.C., "Numerical Computation of the Matrix Exponential with Accuracy Estimate," <u>SIAM Journal of Numerical Analysis</u>, Vol. 14, No. 4, September, 1977. pp. 600-610.

6. Kirk, Donald E., <u>Optimal Control Theory - An Introduction</u>, Prentice Hall, Inc., Englewood Cliffs, NJ, 1970.

7. Thompson, R.C., <u>A Perturbation Approach to Control of Rotational/ Translational Maneuvers of Flexible Space Vehicles</u>, M.S. Thesis, Engineering Mechanics, VPI&SU, Blacksburg, VA, 1985.

8. Junkins, J.L., and Thompson, R.C., "An Asymptotic Perturbation Method for Nonlinear Optimal Control Problems," Paper No. AAS-85-364, presented at the AAS/AIAA Astrodynamics Specialists Conference, Vail, CO, August 12-15, 1985.

9. Junkins, J.L., and Turner, J.D., <u>Optimal Spacecraft Rotational Maneuvers</u>, Elsevier, Amsterdam, 1986.

A Quasi-Analytical Method for Non-iterative Computation of Nonlinear Controls

J. L. Junkins and R. C. Thompson
Texas A&M University
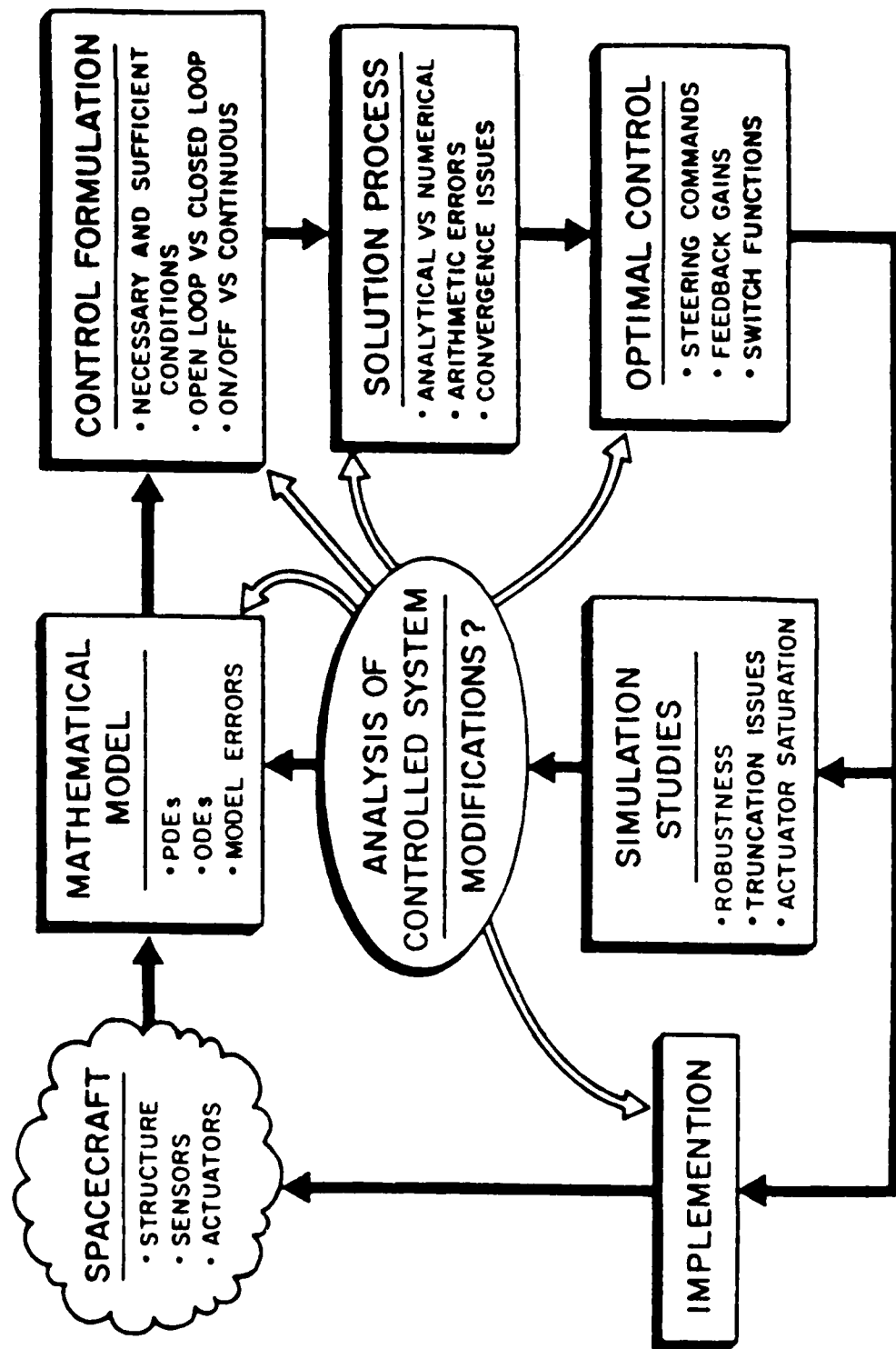
and

J. D. Turner
Cambridge Research Associates

presented to
WORKSHOP ON STRUCTURAL DYNAMICS AND CONTROL
INTERACTION FOR FLEXIBLE STRUCTURES
National Aeronautics and Space Administration
George C. Marshall Space Flight Center
Huntsville, Alabama

April 22-24, 1986

Coupling of Spacecraft Structural Modeling with Dynamics/Controls Analysis, Design, and Implementation*

PRELIMINARIES

Consider a dynamical system described by

$$\dot{z} = Fz + Du + \epsilon \, g(z,u,t) \qquad (1)$$

where

   z is an n×1 state vector

   u is an m×1 control vector

   F & D are constant matrices

   z, u, and the nonlinear terms g(z,u,t) are continuous & differentiable

We seek an optimal control u*(t) and corresponding optimal trajectory z*(t) which minimize the quadratic performance measure

$$J = 1/2 \, [z^T S z]_{t_f} + 1/2 \int_{0}^{t_f} (z^T Q z + u^T R u) \, dt \qquad (2)$$

The necessary conditions involve the Hamiltonian H(z , u , p , t)

$$H = 1/2 \, (z^T Q z + u^T R u) + p^T (Fz + Du + \epsilon g); \qquad (3)$$

These are:
$$\frac{\partial H}{\partial u} = 0, \qquad \frac{\partial H}{\partial p} = \dot{z}, \qquad -\frac{\partial H}{\partial z} = \dot{p}$$

plus boundary conditions: $z(0) = z_o, \quad p(t_f) = S z(t_f) \quad or \quad z(t_f) = z_f.$

PRELIMINARIES

Consider a dynamical system described by

$$\dot{z} = Fz + Du + \epsilon g(z,u,t) \qquad (1)$$

where

z is an nx1 state vector

u is an mx1 control vector

F & D are constant matrices

z, u, and the nonlinear terms g(z,u,t) are continuous & differentiable

We seek an optimal control u*(t) and corresponding optimal trajectory z*(t) which minimize the quadratic performance measure

$$J = 1/2 \, [z^T S z]_{t_f} + 1/2 \int_{0}^{t_f} (z^T Q z + u^T R u) dt \qquad (2)$$

The necessary conditions involve the Hamiltonian H(z, u, P, t)

$$H = 1/2 \, (z^T Q z + u^T R u) + p^T (Fz + Du + \epsilon g); \qquad (3)$$

These are:
$$\frac{\partial H}{\partial u} = 0, \qquad \frac{\partial H}{\partial p} = \dot{z}, \qquad -\frac{\partial H}{\partial z} = \dot{p}$$

Two Point Boundary Value Problem

Pontryagin Necessary Conditions:

$$\dot{z} = Fz + Du + \,\cdot g \,, \qquad z(0) = z_o$$

$$\dot{p} = -Qz - F^T p - \,\cdot [\frac{\partial g}{\partial z}]^T, \quad p(t_f) = Sz(t_f), \text{ for } z(t_f) \text{ "free"}$$

$$0 = Ru + D^T p, \dots \text{ from which the optimal control is } u^* = -R^{-1}D^T p.$$

The state/co-state coupled system can be written as a 2n order system:

$$\dot{x} = A\,x + \,\cdot h(x,t)$$

where

$$x^T = [z^T \ \ p^T], \quad A = \begin{bmatrix} F & -DR^{-1}D^T \\ -Q & -F^T \end{bmatrix}, \quad h(x,t) = \begin{bmatrix} g \\ -\frac{\partial g}{\partial z}^T \end{bmatrix} \qquad (4)$$

Due to the nonlinear terms in $h(x,t)$, exact analytical solutions of Eq. (4) are most often impossible. A variety of iterative techniques are available; they are often expensive due to initial ignorance of a "good starting estimate"(of $p(t_o)$ or $p(t_f)$) required for reliable convergence. We seek to avoid iteration through use of a perturbation method & "quasi-analytical" integration. >>>

84

The Asymptotic Expansion of the Necessary Conditions

We seek a power series solution of the usual form

$$x(t) = x_0(t) + \epsilon x_1(t) + \epsilon^2 x_2(t) + \; \ldots \; + \epsilon^k x_k(t) + \; \ldots \tag{5}$$

Substitution of the power series into the state/co-state system of Eq. (4), and equating like powers of ϵ, leads to the <u>sequence</u> of linear systems:

$$\dot{x}_0 = A x_0 \longrightarrow x_0(t) \; ,$$

$$\dot{x}_1 = A x_1 + g_1(t, x_0(t)) \longrightarrow x_1(t)$$

$$\dot{x}_k = A x_k + g_k(t, x_0(t), x_1(t), \ldots, x_{k-1}(t)) \longrightarrow x_k(t)$$

with the boundary conditions

$$x_0(0) = \left\{ \begin{array}{c} z(0) \\ p_0(0) \end{array} \right\} \; , \; x_0(t_f) = \left\{ \begin{array}{c} z(t_f) \\ p_0(t_f) \end{array} \right\} \; ; \; \ldots \; ; \; x_k(0) = \left\{ \begin{array}{c} 0 \\ p_k(0) \end{array} \right\} \; , \; x_k(t_f) = \left\{ \begin{array}{c} 0 \\ p_k(t_f) \end{array} \right\}$$

where, at least formally, the sequence of solutions is given by

$$x_k(t) = e^{At} \left[x_k(0) + \int_0^t e^{-A\tau} g_k(\tau, x_0(\tau), x_1(\tau), \ldots, x_{k-1}(\tau)) \, d\tau \right] \; , \; k = 1, 2, 3, \ldots \tag{7}$$

But... how do we make efficient algorithms? Does convergence occur in the "real world"? Can the above be implemented in a way which automates the algebra usually associated with perturbation methods? What about secular terms? Does this approach apply to systems of non-trivial dimensions & "messy" nonlinear terms? We have made some progress in answering these questions.

85

Consider

$$\dot{x}_k = A x_k + g_k, \quad x_k(t) = e^{At} x_k(0) + e^{At}\int_0^t e^{-A\tau} g_k(\tau)\, d\tau, \quad k=1,2,\ldots \quad (8)$$

For the special case that u(t) can be represented as Fourier series, the Fourier series can be re-written as a matrix exponential

$$g_k(t) = b_{ok} + \sum_{r=1}^{N} b_{rk}\cos(\omega_r t) + a_{rk}\sin(\omega_r t) = G_k\, e^{\Omega t}\, c \quad (9)$$

where

b_{ok}, b_{rk}, a_{rk} are $2n \times 1$ vectors of Fourier coefficients

$G_k = [\, b_o, b_1, a_1, b_2, a_2, \ldots b_r, a_r, \ldots b_N, a_N\,]_k$, a $2n \times (2N+1)$ constant matrix

$c = \{\,1\ 1\ 0\ 1\ 0\ 1\ 0\ \ldots\ldots\ 1\ 0\,\}^T$, a $2N \times 1$ selection vector

$$\Omega_r = \begin{bmatrix} 0 & -\omega_r \\ \omega_r & 0 \end{bmatrix}, \quad \omega_r = r(2\Pi/(t_f - t_o))$$

$$\Omega = diag[\,0\,,\ \Omega_1\,,\ \Omega_2\,,\ \ldots\,,\ \Omega_r\,,\ \ldots\,,\ \Omega_N\,]$$

Substituting Eq. (9) into Eq. (8),

$$x_k(t) = e^{At} x_k(0) + \left[\int_0^t e^{-A\tau} G_k\, e^{\Omega\tau} d\tau\right]c = e^{At} x_k(0) + [\psi_k]c$$

Van Loan has established the interesting & useful identity which permits computation of the forced response using a matrix exponential (via, for example, Ward's Pade' algorithm):

$$e^{\begin{bmatrix} A & G_k \\ 0 & \Omega \end{bmatrix}t} = \begin{bmatrix} e^{At} & \psi_k \\ \hline 0 & e^{\Omega t} \end{bmatrix} \quad (10)$$

For large N, we can use superposition & keep the order of the matrix exponentials small .... thus the response to a relatively arbitrary $g_k(t)$ can be calculated via matrix exponentials.

Control Rate Smoothing & State Vector Augmentation

We choose to minimize.

$$J = 1/2\{z(t_f)^T S z(t_f) + u(t_f)^T S_0 u(t_f) + \dot{u}(t_f)^T S_1 \dot{u}(t_f)\}$$

$$+ 1/2 \int_0^{t_f} \{z^T Q z + u^T R_0 u + \dot{u}^T R_1 \dot{u} + \ddot{u}^T R_2 \ddot{u}\}\, dt$$

Subject to: $\dot{z} = Az + Du$. This can be converted to standard form via the definitions:

$$\tilde{z} = \begin{Bmatrix} z \\ u \\ \dot{u} \end{Bmatrix}, \quad \tilde{A} = \begin{bmatrix} A & D & 0 \\ 0 & 0 & I \\ 0 & 0 & 0 \end{bmatrix}, \quad \tilde{D} = \begin{bmatrix} 0 \\ 0 \\ I \end{bmatrix} \quad \begin{array}{l} \tilde{S} = block\ diag[S, S_0, S_1] \\ \tilde{Q} = block\ diag[Q, R_0, R_1] \\ \tilde{R} = R_2\ , \quad \tilde{u} = \ddot{u} \end{array}$$

So we can equivalently minimize

$$J = 1/2\ \tilde{z}(t_f)^T \tilde{S} \tilde{z}(t_f) + 1/2 \int_0^{t_f} \{\tilde{z}^T \tilde{Q} \tilde{z} + \tilde{u}^T \tilde{R} \tilde{u}\}\, dt$$

Subject to: $\dot{\tilde{z}} = \tilde{A}\tilde{z} + \tilde{D}\tilde{u}$. The necessary conditions have the identical form as those developed in the foregoing. Penalizing the control derivatives has been found most constructive in frequency-shaping the torque profiles to decrease excitation of the poorly modeled higher frequency modes.

Case 1 Optimal Detumble/Attitude Aquisition

STATE DYNAMICS

Euler (quaternion) parameters

$$\begin{Bmatrix} \dot{\beta}_0 \\ \dot{\beta}_1 \\ \dot{\beta}_2 \\ \dot{\beta}_3 \end{Bmatrix} = \frac{1}{2} \begin{bmatrix} 0 & -\omega_1 & -\omega_2 & -\omega_3 \\ \omega_1 & 0 & \omega_3 & -\omega_2 \\ \omega_2 & -\omega_3 & 0 & \omega_1 \\ \omega_3 & \omega_2 & -\omega_1 & 0 \end{bmatrix} \begin{Bmatrix} \beta_0 \\ \beta_1 \\ \beta_2 \\ \beta_3 \end{Bmatrix} \qquad \text{or} \quad \dot{\beta} = \frac{1}{2} (\omega) \beta$$

Euler's Equations

$$\begin{Bmatrix} \dot{\omega}_1 \\ \dot{\omega}_2 \\ \dot{\omega}_3 \end{Bmatrix} = \begin{Bmatrix} -I_1 \, \omega_2\omega_3 + u_1/I_1 \\ -I_2 \, \omega_3\omega_1 + u_2/I_2 \\ -I_3 \, \omega_1\omega_2 + u_3/I_3 \end{Bmatrix} \quad , \quad \begin{array}{l} I_1 = (I_3-I_2)/I_1 \\ I_2 = (I_1-I_3)/I_2 \\ I_3 = (I_2-I_1)/I_3 \end{array} \qquad \text{or} \quad \dot{\omega} = f(\omega, u)$$

BOUNDARY CONDITIONS $(t_f = 2 \text{ sec})$

$$\beta(0) = \begin{Bmatrix} .9699665 \\ .1318887 \\ .0238626 \\ .2029798 \end{Bmatrix} \quad , \quad \omega(0) = \begin{Bmatrix} .4 \\ .2 \\ 1.0 \end{Bmatrix} r/s \quad \beta(t_f) = \begin{Bmatrix} 1 \\ 0 \\ 0 \\ 0 \end{Bmatrix} \quad , \quad \omega(t_f) = \begin{Bmatrix} 0 \\ 0 \\ 0 \end{Bmatrix}$$

8

88

Case 1 Numerical Results for the TPBVP Solution

FINAL STATE ERRORS

	LINEAR SOLUTION	FIRST ORDER	SECOND ORDER
ΔB_0	$.01999$	$.00091$	7×10^{-7}
ΔB_1	$-.08232$	$-.00866$	$.00058$
ΔB_2	$.18033$	$-.00944$	$.00094$
ΔB_3	$.01734$	$-.00412$	$-.00034$
$\Delta \omega_1$	$.01914$	$-.01525$	$.00109$
$\Delta \omega_2$	$.43150$	$-.00292$	$.00295$
$\Delta \omega_3$	$.00461$	$-.00071$	$.00015$

$\approx 10°$ (Linear Solution, ΔB_0–ΔB_3)

$\approx .5°$ (First Order, ΔB_0–ΔB_3)

$\approx .05°$ (Second Order, ΔB_0–ΔB_3)

Case 1 Optimal Detumble/Attitude Acquisition Maneuver

torque history
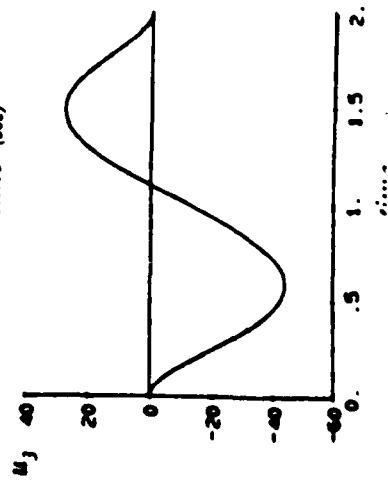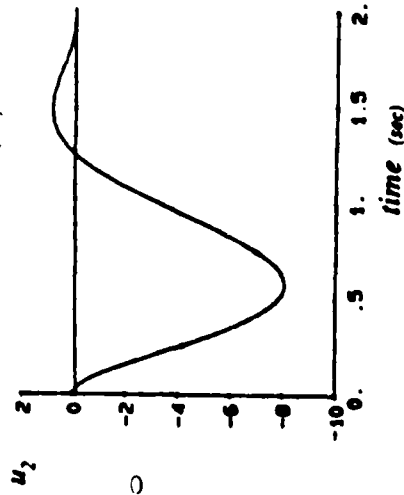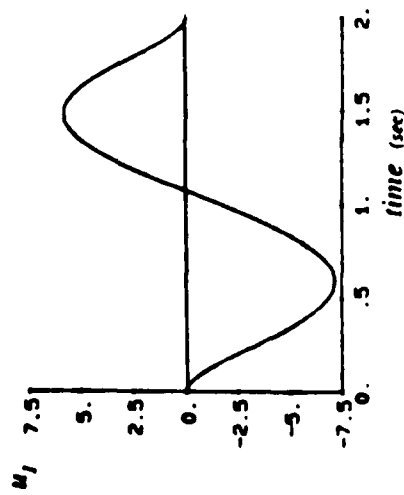
angular velocity
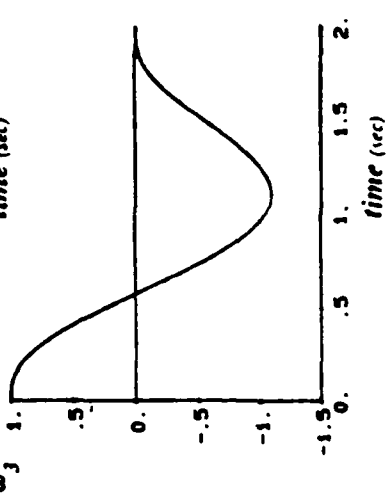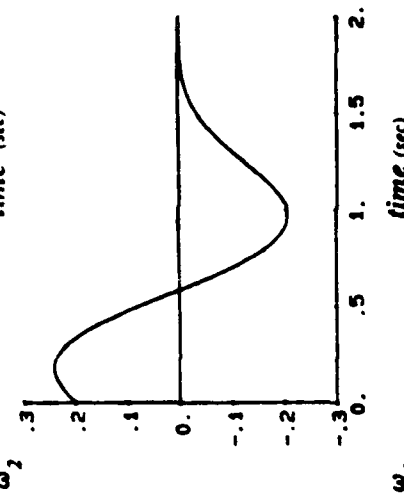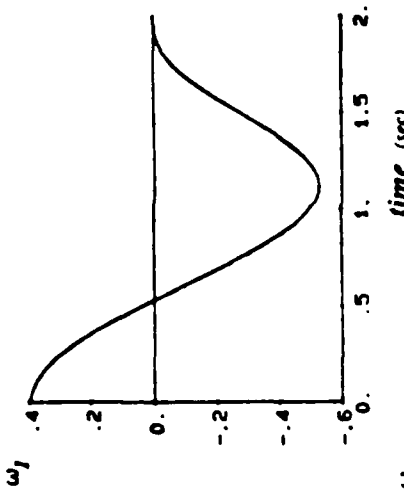
attitude
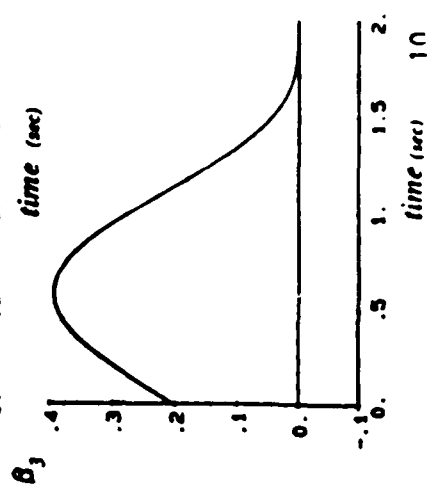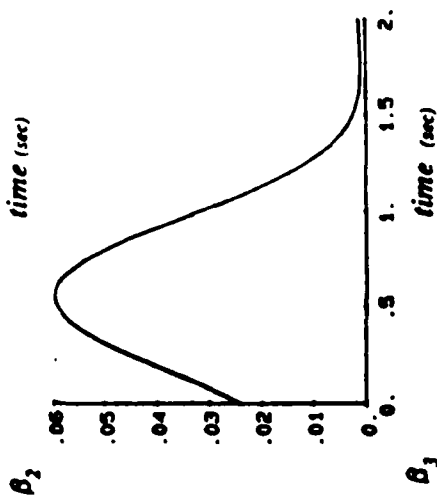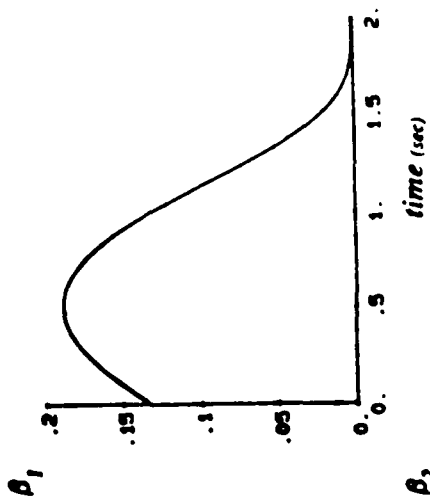
The Draper/RPL Slewing Experimental Configuration
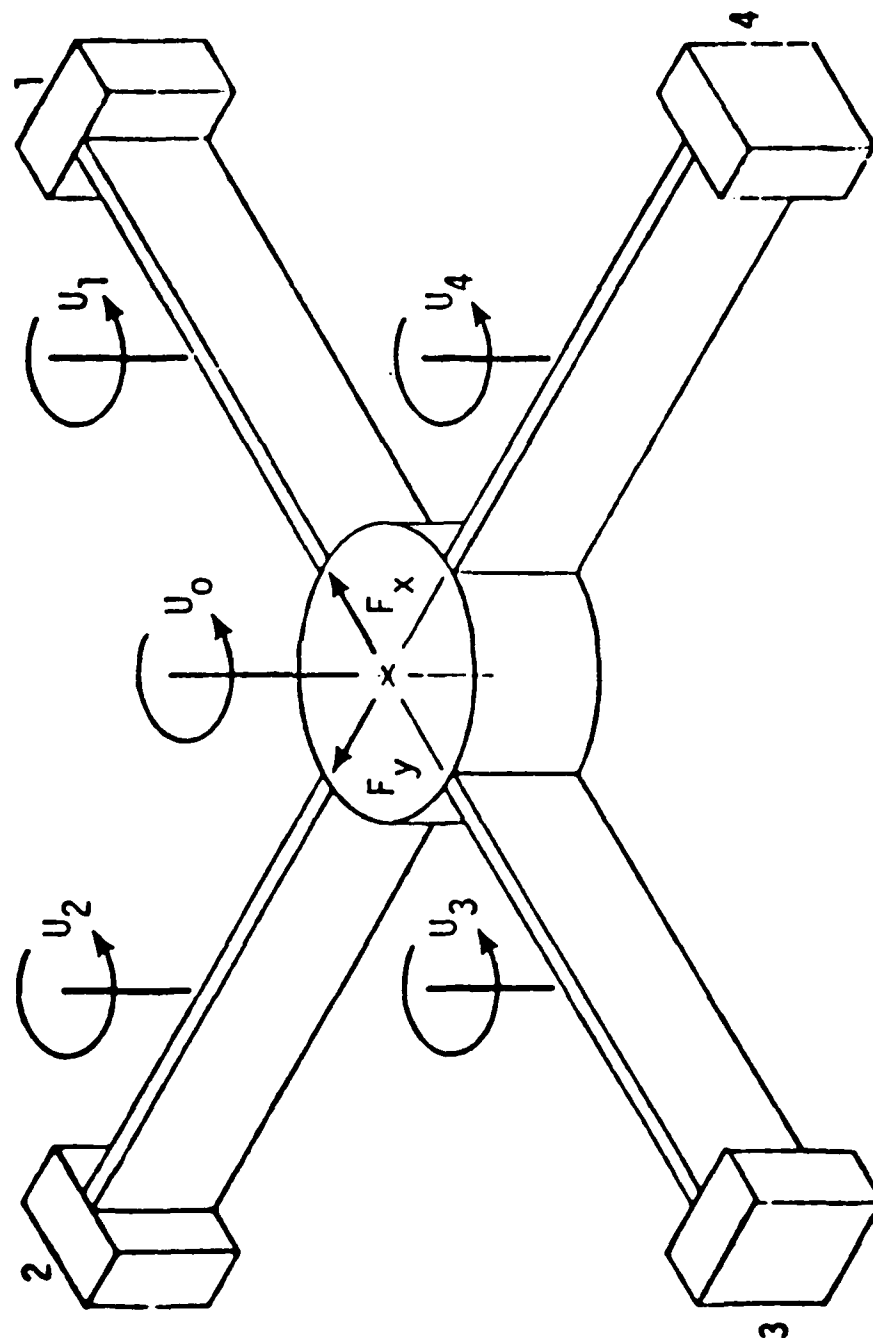
Draper/RPL Configuration: First Eleven in-plane Vibration Modes
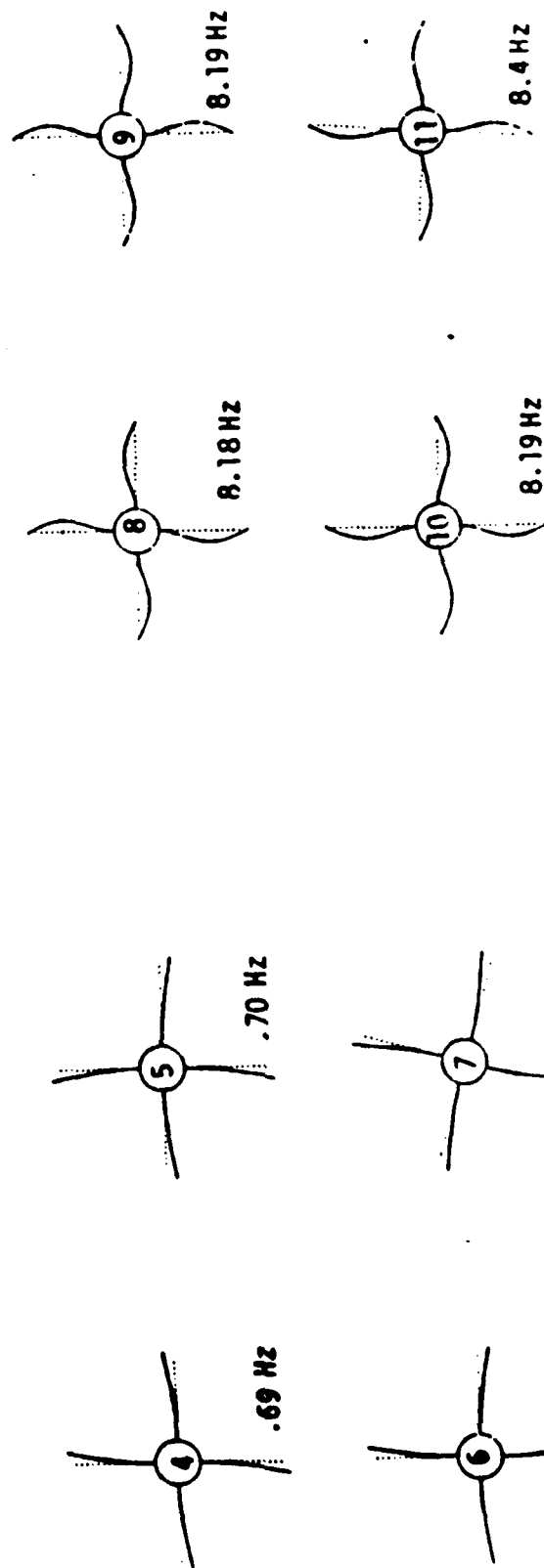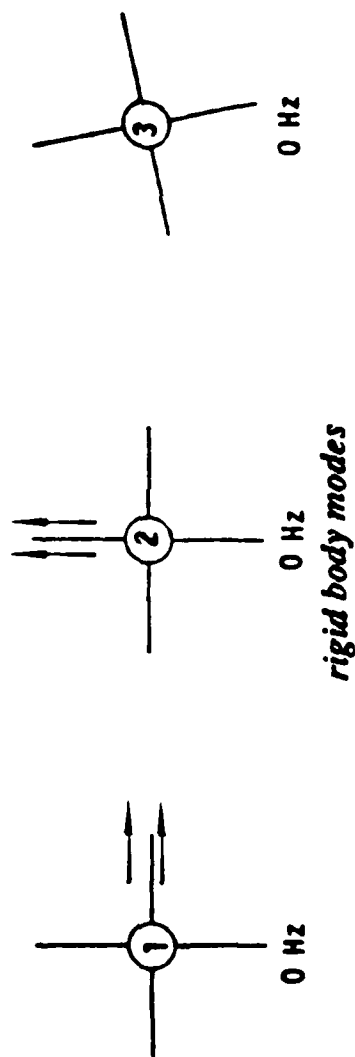
rigid body modes

first cantilever modes

second cantilever modes

1 — 0 Hz

2 — 0 Hz

3 — 0 Hz

4 — .69 Hz

5 — .70 Hz

6 — .70 Hz

7 — 1.2 Hz

8 — 8.18 Hz

9 — 8.19 Hz

10 — 8.19 Hz

11 — 8.4 Hz

12

Case 2 Numerical Results for the TPBVP Solution (small angle flexible body maneuver)

FINAL STATE ERRORS

	LINEAR SOLUTION	FIRST ORDER	SECOND ORDER
ϕ	-0.828E-5	0.276E-4	0.184E-5
θ	0.104E-2	0.667E-5	-0.878E-6
ψ	0.668E-3	-0.270E-4	0.130E-5
ω_1	-0.450E-3	0.150E-3	0.342E-5
ω_2	0.317E-2	0.293E-4	-0.474E-5
ω_3	0.597E-3	-0.396E-5	0.135E-6
η_1 (in plane)	-0.960E-3	-0.120E-5	-0.217E-8
σ_1 (out-of-plane)	0.317E-2	0.293E-4	-0.474E-5

Case 2 Optimal Maneuver with Vibration Suppression/Arrest
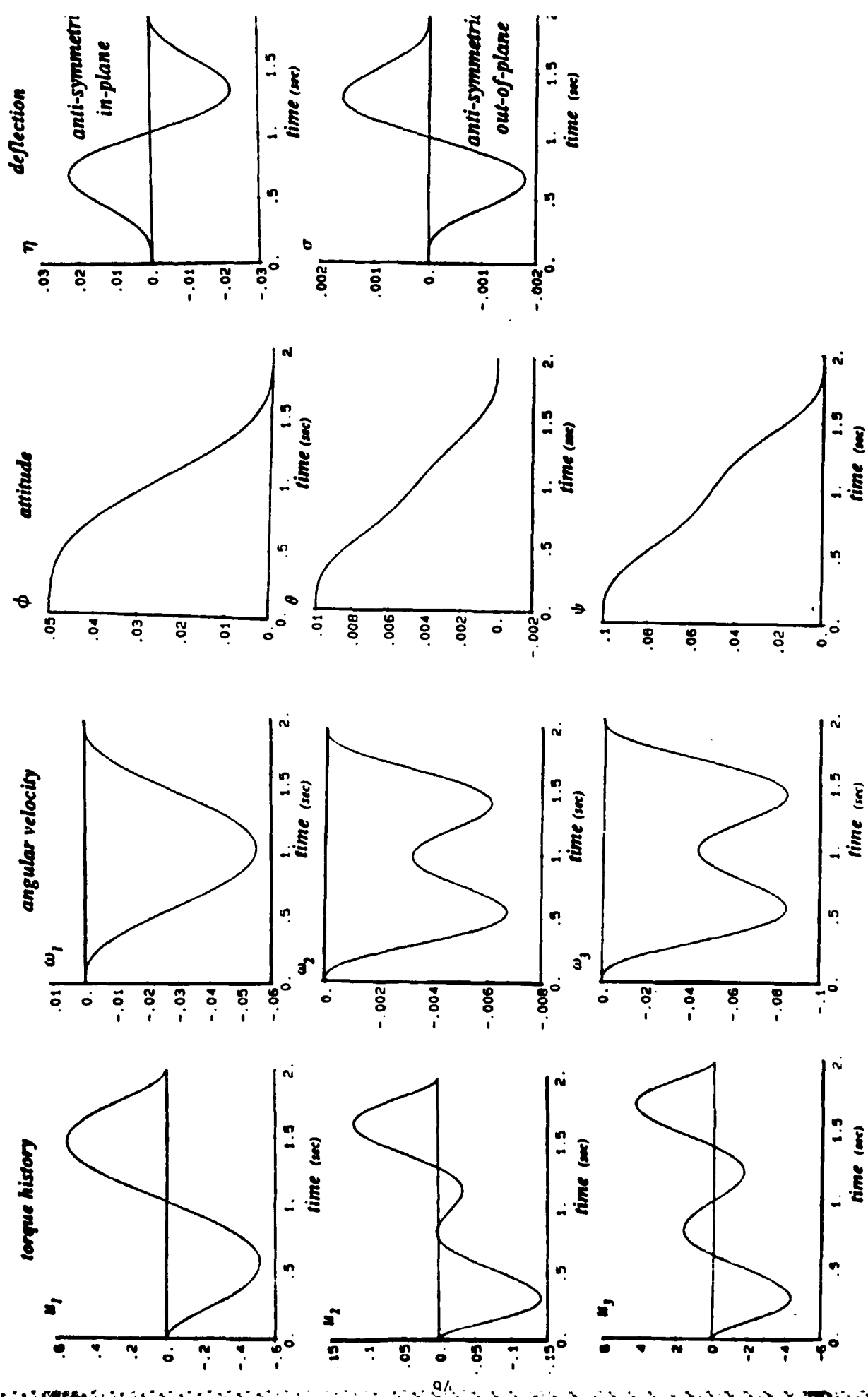
Concluding Remarks

A novel optimal control solution process has been developed for a general class of nonlinear dynamical systems

The method combines control theory, perturbation methods, and Van Loan's recent matrix exponential results

All controlled response integrations are accomplished via matrix exponentials (using Ward's Pade algorithm) and recursions developed herein

A variety of applications support the practical utility of this method; nonlinear rigid body optimal maneuvers are routinely solved; flexible body dynamical systems of order >40 have been solved

The method fails occasionally due to poor convergence of the perturbation expansion or numerical difficulties associated with computing the matrix exponential

The method is attractive because it appears to be a good candidate for semi-automation; no initial guess is required, and it usually
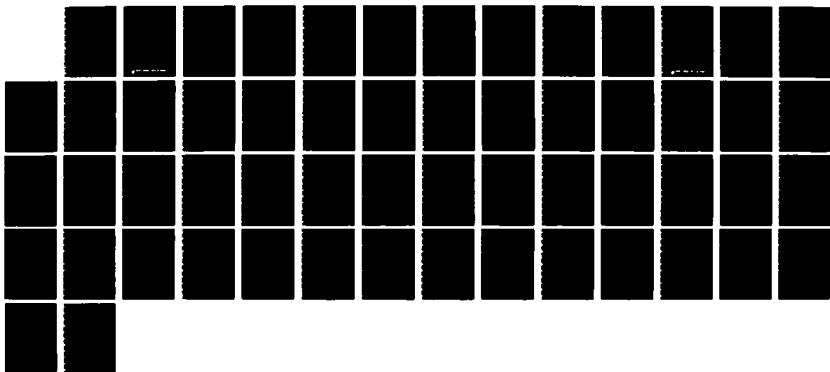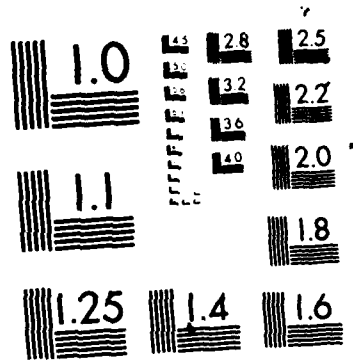
MICROCOPY RESOLUTION TEST CHART

NATIONAL BUREAU OF STANDARDS-1963-A

Identification of Vibrating Flexible Structures
S. Rajaram and J.L. Junkins

Identification of Vibrating Flexible Structures

S. Rajaram* and J.L. Junkins†

Virginia Polytechnic Institute and State University, Blacksburg, Virginia

This paper presents novel identification schemes to determine model parameters of vibrating structures. A time-domain identification method using transient response is discussed first. Next, a steady-state response method using nonresonant harmonic excitations is considered. An especially attractive method for uniquely identifying the parameters of a structure using both free and forced response is also discussed. Numerical results show that the methods are relatively immune to the presence of damping and many low-frequency modes with repeated or closely spaced frequencies.

Introduction

ACTIVE control of large space structures (LSS) necessitates a sufficiently accurate estimate of the parameters so that control laws can be tuned on-orbit to ensure stability and permit less control effort to be expended. Algorithms for design of insensitive or adaptive controls are not attractive due to the large number of degrees of freedom to be controlled. In fact, for most LSS application, the only feasible approach appears to be: 1) identify the structural parameters then 2) use this information to adjust the gains, and perhaps 3) use adaptive methods to change a small number of critical parameters in real time. This paper addresses issue 1 above.

Transient Response Identification Method

Many structural modal identification methods are available which extract modal characteristics, i.e., natural frequencies and mode shapes from a set of resonant steady-state responses due to a large number of harmonic excitations. These methods encounter analytical and numerical difficulties when the system frequencies are closely spaced and the "single mode resonant response" assumption is used. Also, the time required to achieve steady state may be prohibitively long for lightly damped, low-frequency structures. Time-domain techniques[1-4] for structural identification were first proposed by Ibrahim. Ibrahim's time-domain (ITD) method is a modal identification scheme. The ITD method has been successfully applied to reduce measurements from several laboratory experiments, however, this method has been found to lack reliable robustness. In some applications, rank deficient linear systems are encountered. Recently, Juang and Papa[5] have developed a more robust time-domain modal identification method; this method is based upon judicious use of singular value decomposition.

Identification in Configuration Space

Consider a vibrating structure governed by the following linear matrix differential equation:

$$M\ddot{x} + C\dot{x} + Kx = f \tag{1}$$

where x is the $n \times 1$ configuration vector of physical displacement, f the $n \times 1$ force vector, M the $n \times n$ symmetric positive

definite mass matrix, C the $n \times n$ symmetric positive semidefinite damping matrix, and K the $n \times n$ symmetric positive semidefinite stiffness matrix. Dots denote differentiation with respect to time.

It is assumed that a LSS can be satisfactorily modeled in the form given by Eq. (1). Our objective herein is to identify the poorly known coefficient matrices M, C, and K or some parameterication therefore, e.g., the system eigenvalues and eigenvectors. Equation (1) can be rewritten as

$$[\ddot{x}^T(t) \ \dot{x}^T(t) \ x^T(t)] \begin{vmatrix} M \\ C \\ K \end{vmatrix} = f^T(t) \tag{2}$$

T denotes the matrix transpose operation.

Now, consider an idealized measurement process wherein the position, velocity acceleration, and forces are measured at discrete instants, say $t_1, t_2, \ldots, t_m$. Upon writing m measurement equations ($m \geq 3n$) identical to Eq. (2), one for each measurement time, the resulting matrix equations can be written as

$$ZP = U \tag{3}$$

where Z is an $m \times 3n$ coefficient matrix, whose j row contains measurements of the system response at time t_j:

$$j\text{th row of } Z = [\ddot{x}^T(t_j)\dot{x}^T(t_j)x^T(t_j)] \tag{4}$$

U is a $m \times n$ matrix containing the following forcing functions:

$$j\text{th row of } U = f^T(t_j) \tag{5}$$

$$P = [M \ C \ K]^T \tag{6}$$

P is a $3n \times n$ matrix containing the unknown mass, damping, and stiffness parameters.

Since the number of elements in each column of P is $3n$ and $m > 3n$, Eq. (3) overdetermines the columns of P. The least-squares solution for P is given as

$$P = LU \tag{7}$$

where the least-squares operator is formally

$$L = (Z^T Z)^{-1} Z^T \tag{8}$$

For large systems, of course, the explicit inversion should be avoided in favor of the Q-R reduction, Cholesky decomposition, or a singular value decomposition approach for in-

creased efficiency and robustness.[6] The computations subsequently summarized in this paper were done using the Q-R algorithm. The only theoretical requirement is that the *least-squares coefficient matrix Z have full rank (3n)*. Physically, this rank condition can be achieved only if all degrees of freedom participate in the response. Hence, a fundamental requirement for identifying the structure is that the *excitation should have sufficient energy and frequency content to excite the higher modes of the system*. Qualitatively, it is also evident that the actuator locations and phase distribution of the actuator input are likely to be important. Thus, the mass, damping, and stiffness matrices of the structure can be identified, at least in principle. The method is obviously straightforward. However, it requires that the number of forces equal the order of the system. Also, acceleration, velocity, and displacement are to be measured at all of the degrees of freedom. These requirements pose obvious practical difficulties. It is shown in Ref. 7 that, in order to use a smaller number of forces than the number of degrees of freedom of the system, a priori knowledge of the mass matrix is required. It should be noted that the method, as presented above, does not require or exploit the symmetry of the system matrices and, hence, is applicable to a general dynamic system involving gyroscopic and circulatory forces.[7] It is also evident that the size of the linear systems which must be solved is 3n. Therefore, unless the matrices do, in fact, possess special properties, it is anticipated that practical computational restrictions will require $n < 50$ for this approach. Of course, the heavy redundancy implicit in *M*, *C*, and *K* as descriptions of distributed mass, damping, and stiffness often can be eliminated in terms of fewer physical parameters, but the estimation process then must be coupled with the structural modeling (e.g., finite element) process.

Identification in State Space

For control applications, the system dynamics is expressed in state equations. Introducing the "2n"-dimensional state vector

$$g(t) = [x^T(t) \ \dot{x}^T(t)]^T \tag{9}$$

Equation (1) can be written as

$$\dot{g} = Ag + Bf \tag{10}$$

where

$$A = \begin{bmatrix} 0 & I \\ -M^{-1}K & -M^{-1}C \end{bmatrix} \tag{11}$$

is the plant dynamic matrix and

$$B = \begin{bmatrix} 0 \\ D_i \end{bmatrix} \tag{12}$$

is the control distribution matrix. The structure of *B* is dependent upon type and location of the force inputs. When all degrees of freedom are not excited, the force vector contains zero entries and *B* will be a $(2n \times n_i)$ rectangular matrix, where n_i is the number of excitations. The unknown parameters to be identified are the elements of matrices *A* and *B*.

Consider the lower partition of Eq. (10)

$$\dot{x}(t) = -M^{-1}Kx(t) - M^{-1}Cx(t) + D_i f(t) \tag{13}$$

Equation (13) can be written as

$$x^T(t) = [x^T(t) \ \dot{x}^T(t) \ f^T(t)] \begin{bmatrix} (-M^{-1}K)^T \\ (-M^{-1}C)^T \\ D_i^T \end{bmatrix} \tag{14}$$

The matrices $M^{-1}K$, $M^{-1}C$, and B_i can be determined, following a procedure analogous to that outlined previously for configuration space identification. It is evident from Eq. (14) that the least-squares coefficient matrix includes the force vector. Immediately, it can be inferred that *the force vector should form an independent set for unique identification of the system parameters*. This statement holds true for configuration space identification also. It can be observed that $\dot{x}$ in the least-squares coefficient matrix, viz., Eq. (3), becomes independent of other variables only through the forcing functions.

Identification Using Orthogonal Polynominals

The measurement of acceleration, velocity, and displacement at all degrees of freedom, as required by the methods presented earlier, poses obvious practical difficulties. To obtain partial relief from this requirement, an orthogonal identification scheme is proposed. Orthogonal polynomials can be used to represent completely any function to a required degree of accuracy.[8]

Consider the lower portion of the state equations, viz., Eq. (13). Also, it is assumed that the accelerations and forces are measured at discrete instants of time. Then they can be expanded using orthogonal polynomials such as Chebyshev, Legendre, etc.

$$\ddot{x} = P_1 T(t) \tag{15}$$

where P_1 is a rectangular coefficient matrix and

$$T(t) = [T_0(t) T_1(t) .. T_{N-1}(t)]^T \tag{16}$$

is a column vector consisting of orthogonal polynomials. The intergral of $T_r(t)$ can be expressed via a recurrence relationship involving T_{r+1} and T_{r-1}. Integrating Eq. (15)

$$\dot{x} = P_2 T(t) + c' = y_1 + c' \tag{17}$$

Integrating further

$$x = P_3 T(t) + c't + c'' = y + c't + c'' \tag{18}$$

where P_1, P_2, and P_3 are $n \times N$ matrices containing the expansion coefficients. By substituting Eqs. (15), (17), and (18) into Eq. (13), the least-squares problem can be constructed as

$$[y^T(t) \ y^T(t) \ f^T(t) \ t \ I] \begin{bmatrix} -(M^{-1}K)^T \\ -(M^{-1}C)^T \\ B_i^T \\ D_i^T \\ d_2^T \end{bmatrix} = \dot{x}^T(t_i) \tag{19}$$

$$d_1 = -M^{-1}Kc' \tag{20}$$

$$d_2 = -M^{-1}Kc'' - M^{-1}Cc' \tag{21}$$

$M^{-1}K$, $M^{-1}C$, D_i, d_1, and d_2 can be estimated from Eq. (19). c' and c'' can be determined using Eqs. (20) and (21). Thus, the number of measurements are reduced by a factor of 3 and the initial displacement and velocity vectors, usually the equilibrium positions of the structure, are also estimated along with the parameters. It is also possible to use velocity or displacement measurements alone. Although several orthogonal polynomials exist, the use of Chebyshev polynomials have found a wide application[9] in solving linear and nonlinear differential equations. Since we are concerned

with the inverse problem (i.e., given the response, the best estimate of the system's parameters is to be determined), Chebyshev polynomials seem to be the natural choice.

Numerical Results for Identification from Transient Free Response

Four specific linear systems are considered as representative examples; a spring-mass damper system (Fig. 1), a plane truss (Fig. 2), a cantilever beam (Fig. 3), and a rectangular membrane (Fig. 4) are considered to study the effects of 1) repeated low frequencies and rigid-body modes, 2) damping, 3) choice of excitation and number of excitations vs degrees of freedom, 4) excitation frequency vs system natural frequency, 5) measurement errors, measurement duration, and sampling interval, and 6) model truncation errors. Synthetic measured data are generated for each case using known parameter values. Table 1 gives the undamped eigenvalues of the examples. The proposed identification schemes performed very well for all four examples. The results are summarized below.

The plane truss example, as can be seen from Table 1, has three repeated eigenvalues and three zero eigenvalues corresponding to the rigid-body modes. Arbitrary viscous damping is included in the first and second example problems. It is found that the identification algorithms recovered the system matrices without any difficulty. It is clear that restrictive assumptions such as proportional or negligible damping are unnecessary for the success of the identification algorithms. Three excitation types were considered: 1) harmonic, 2) bang-bang (rectangular wave), and 3) frequency swept harmonic (harmonic excitations with time-varying frequency). Harmonic excitations yield good results for the spring-mass damper and cantilever beam. For the plane truss, bang-bang and frequency swept harmonic excitations are useful. Orthogonal polynomial identification of the plane truss with bang-bang excitation did not recover the parameters very well. The orthogonal polynomials are unable to represent the accelerations satisfactorily. However, with frequency swept harmonic excitation, the orthogonal identifier recovered all parameters accurately. Thus, the orthogonal identification scheme apparently works best with smooth and continuous excitations. The number of excitations required for the identification of spring-mass damper and cantilever beam can be as few as one. For the plane truss, a minimum of five excitations are needed.

Upon varying the frequency of excitation over the range of the system natural frequencies, no significant degradation in the performance of the algorithm is observed. Measurement errors introduce estimate errors, of course. The effect of discrepancies between commanded and realized excitations is also studied by including noise in the excitations.

The cantilever beam and a simply supported membrane are chosen to illustrate the effect of model truncation. These are distributed systems; we are interested in obtaining a discrete representation. The response of the cantilever beam is obtained by using the eigenfunctions and assuming that six modes participate in the response. Hence, a sixth-order model is obtained first. The model identified using either a bang-bang or harmonic excitation is the same. A reduced-order model (fourth order) is identified next. Table 2 compares the exact eigenvalues with those obtained from identified models.
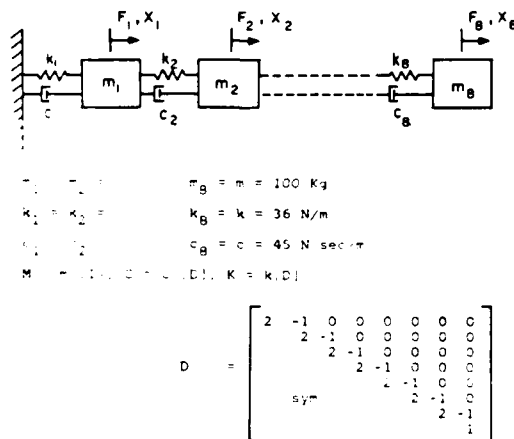
Fig. 1   Spring-mass damper.
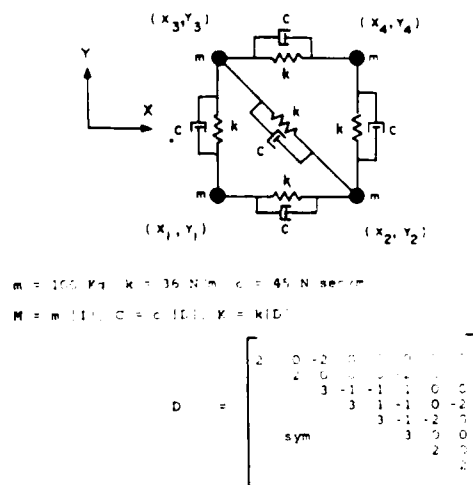
Fig. 2   Plane truss.
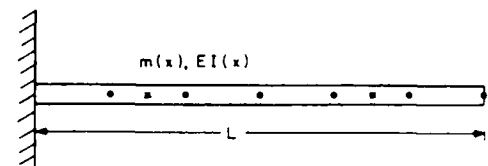
Fig. 3   Cantilever beam. $m(x)$ is the mass unit length, 2.4 kg m; $EI(x)$ the bending stiffness, 495 N/m²; L the length, 3.0 m; * the position of sensors; and ● position of actuators.
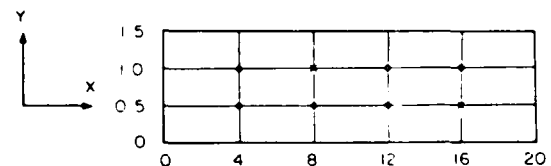
Fig. 4   Rectangular membrane. * is the position of sensors, and ● the position of actuators.

Table 1   Eigenvalues of example problems

Spring-mass damper	Plane truss[a]	Cantilever beam	Rectangular membrane
0.1107	0.0	5.6105	21.0028
0.3284	0.0	35.1607	41.9173
0.5349	0.0	98.4510	21.1783
0.7232	0.4592	192.9246	42.0055
0.8868	0.8485	318.9182	21.4676
1.0203	0.8485	476.4086	42.1521
1.1190	0.8485		
1.1796	1.1086		

[a] Undamped eigenvalues

It is also noted that the harmonic excitation resulted in a model that fits the measured acceleration fairly well. This is significant since accelerometers are the most commonly used sensors for vibration measurement. The bang-bang excitation, being rich in harmonic content, is able to excite the higher modes considerably and thus affects the identification of the reduced-order model. Table 3 gives the results for the membrane.

Identification Using Nonresonant Harmonic Excitations

The use of harmonic excitations for the identification of vibrating structures have received the attention of several investigators.[8][14] Raney[9] used such a scheme to successfully identify the effective masses, stiffnesses, and damping for a lightly damped structure having widely separated modes; the structures studied were 1/10- and 1/40-scale models of the Saturn launch vehicle. Several methods are suggested[9][14] to extract the normal modes from measured response. However, the use of normal modes is questionable when the damping in the system is not a proportional type. The methods using resonant harmonic excitations, as mentioned earlier, encounter both experimental and computational problems, when the system frequencies are closely spaced. A novel identification scheme using nonresonant harmonic excitations is presented in this section. The proposed scheme differs significantly from several of the existing methods which generally use resonant harmonic response to obtain the model parameters. The method requires that the structure be damped; the damping, however, can be arbitrary viscous damping.

Configuration Space Identification

Once again consider Eq. (1). Let the excitation $f(t)$ be given as

$$f_k(t) = \begin{Bmatrix} a_{1k}\sin(\omega_k t + \phi_{1k}) \\ a_{2k}\sin(\omega_k t + \phi_{2k}) \\ \vdots \\ \vdots \\ a_{nk}\sin(\omega_k t + \phi_{nk}) \end{Bmatrix}$$

Table 2 Comparison of eigenvalues for cantilever beam

Exact	Sixth-order model	Fourth-order model	
		Harmonic	Bang-bang
5.6105	5.6545	5.6282	11.2121
35.1607			
0[*]	35.1664	35.2092	36.0591
98.451	98.4524	98.3340	98.3429
192.9246	192.9292	192.9283	192.9373
318.9182	318.8330		
476.4086	475.9983		

Table 3 Comparison of eigenvalues for rectangular membrane

Exact	Sixth-order model	Fourth-order model	
		Harmonic	Bang-bang
21.0028	21.0008	20.4976	21.2253
41.9173	41.9201	42.0707	41.9604
21.1783	21.0860	21.4256[*]	31.0774
42.0055	41.9602		
21.4676	21.4405	21.4256[*]	34.5880
42.1521	42.1391		

[*]Imaginary part given by eigenvalue routine is neglected

---

or

$$f_k(t) = S_k\sin\omega_k t + C_k\cos\omega_k t \qquad k = 1,2,\ldots,m \qquad (22)$$

S_k and C_k are the amplitudes of the sine and cosine components of the excitation. The steady-state response of the structure then can be written as

$$x(t) = A\sin\omega_k t + B_k\cos\omega_k t \qquad k = 1,2,\ldots,m \qquad (23)$$

The structure is subjected to "m" harmonic excitations at frequencies $\omega_1,\omega_2,\ldots,\omega_m$. The excitation frequencies can be chosen arbitrarily and *need not* coincide with the system frequencies. For each excitation frequency "ω_k," the steady-state amplitudes A_k and B_k of the displacement are measured. Using Eqs. (22) and (23) in Eq. (2), we form the matrix equation

$$ZP = U \qquad (24)$$

where P is the same as in Eq. (6).

$$k\text{th row of } Z = [-\omega_k^2 A_k^T \quad -\omega_k B_k^T \quad A_k^T] \qquad (25)$$

$$(k+m)\text{th row of } Z = [-\omega_k^2 B_k^T \quad \omega_k A_k^T \quad B_k^T] \qquad (26)$$

$$k\text{th row of } U = S_k^T \qquad (27)$$

$$(k+m)\text{th row of } U = C_k^T \qquad (28)$$

For $m > 3n/2$, Eq. (24) represents an overdetermined system of equations. The least-squares solution for P is given formally as

$$P = (Z^T Z)^{-1} Z^T U \qquad (29)$$

Thus, system matrices M, C, and K can be identified directly from steady-state response. The same response data can be used to identify the system in state space. Also, the amplitudes of displacement must be measured at every degree of freedom. Alternatively, amplitudes of accelerations can be used. In that case, Eqs. (25) and (26) become

$$k\text{th row of } Z = [A_k^T \quad B_k^T/\omega_k \quad -A_k^T/\omega_k^2] \qquad (30)$$

$$(k+m)\text{th row of } Z = [B_k^T \quad -A_k^T/\omega_k \quad -B_k^T/\omega_k^2] \qquad (31)$$

A_k and B_k are the amplitudes of acceleration. It is assumed in the subsequent discussions that displacement amplitudes are measured and, hence, consider Eqs. (25) and (26) only.

State-Space Identification

Consider once again Eq. (13), which, using Eqs. (22) and (23), becomes

$$\begin{Bmatrix} -\omega_1^2 A_1^T \\ -\omega_m^2 A_m^T \\ -\omega_1^2 B_1^T \\ -\omega_m^2 B_m^T \end{Bmatrix} = \begin{bmatrix} A_1^T & -\omega_1 B_1^T & S_1^T \\ A_m^T & -\omega_m B_m^T & S_m^T \\ B_1^T & \omega_1 A_1^T & C_1^T \\ B_m^T & \omega_m A_m^T & C_m^T \end{bmatrix} \begin{bmatrix} (-M^{-1}K)^T \\ (-M^{-1}C)^T \\ D_1^T \end{bmatrix} \qquad (32)$$

Equation (32) can be solved via least squares to obtain $M^{-1}K$, $M^{-1}C$, and D_1. It should be noted that the amplitudes of the excitations directly enter into the least-squares coefficient matrix. Hence, they should form an independent set. This is achieved by varying the phase of the excitation, i.e., ϕ_{1k}, $\phi_{2k},\ldots,\phi_{nk}$ in Eq. (22) in a nonlinear fashion. This is precisely

the reason for choosing the excitation of the form given by Eq. (22). The same requirement holds true for the configuration space identification, since the amplitudes of A_{ik} and B_{ik} can be linearly independent only via the excitation amplitudes.

Numerical Results for a Steady-State Response Identification

Two numerical examples, viz., a spring-mass damper (Fig. 1) and a plane truss (Fig. 2), are considered to study the effects of several implementation issues such as 1) closely spaced/repeated frequencies and rigid-body modes, 2) number of excitations, and 3) choice of excitation frequency. The results are summarized under each of the items (1-3).

The plane truss example is used to study the effects of repeated frequencies and rigid-body modes. Thirty excitation frequencies were used ranging from 0.6 to 0.89 rad/s in steps of 0.1 rad/s. All of the parameters are identified exactly in the absence of measurement noise. Thus, the proposed scheme is capable of identifying systems with closely spaced frequencies. For state-space identification, the number of excitations can be as low as three for the spring-mass damper system. However, the plane truss requires a minimum of four excitations.

The excitation frequency was varied within the range of the system's undamped natural frequencies. The authors considered those cases where excitation frequencies were below the lowest frequency of the structure and above the highest frequency of the structure. No significant degradation of the identification scheme was observed, thus validating the fact that the excitation frequencies can be chosen fairly arbitrarily.

Identification Using Free- and Forced-Response Data

Identification of mass and stiffness matrices from model test results has been reported by several authors. The objective of these identification schemes is to modify an a priori mass or stiffness matrix so that measured eigenvalues and eigenvectors agree with those of the analytical model. Berman,[15][17] using a minimization procedure, developed a noniterative scheme based on the orthogonality relationships of eigenvectors for computing a "nearest neighbor" update of the mass matrix. Following Berman's approach, Wei[18] developed a related method for correcting the stiffness matrix. Chen and Wada[19] discuss an interactive system parameter refinement procedure, employing the Jacobian matrix (consisting of the derivatives of eigenvalues and eigenvectors with respect to system parameters). Recently, Chen et al.[20] applied a first-order matrix perturbation approach to identify the mass and stiffness matrices. Other related approaches can be found in Refs. 21 and 22.

Free-response data are used herein to estimate the eigenvalues and eigenvectors of the system. Using orthogonality conditions, the matrices equal to system matrices multiplied by unknown scale factors are determined initially. These scale factors are then uniquely estimated by subjecting the system to known forces and measuring the acceleration, velocity, and displacement at several locations. The approach presented herein embodies a fundamental advantage: *perfect measurements, lead, to within truncation errors and arithmetic errors, to the true system parameters.*

Berman's Method: A Summary

In the absence of damping Eq. (1) reduces to

$$Mx + Kx = 0 \qquad (33)$$

The orthogonality conditions of the system described by Eq. (33) are

$$E^T M E = I \qquad (34a)$$

$$E^T K E = \mathrm{diag}(\omega_1^2, \omega_2^2, \dots, \omega_n^2) = [\omega^2] \qquad (34b)$$

where

E: $(n \times n)$ modal matrix

I: $(n \times n)$ identity matrix

$\omega_1, \omega_2, \dots, \omega_n$ are the natural frequencies. Note that in Eqs. (34) the eigenvectors are normalized with respect to the mass matrix so that

$$e_i^T M e_i = 1 \qquad i = 1, 2, \dots, n \qquad (35)$$

e_i is the ith eigenvector (ith column of E). It will be assumed that the measured modal matrix is square.

Berman[16] assumes an analytical mass matrix M_1. The measured eigenvectors are normalized with respect to M_1 so that

$$e_i^T M_A e_i = 1 \qquad i = 1, 2, \dots, n \qquad (36)$$

Letting ΔM be the desired correction matrix, Berman minimizes the Euclidian norm

$$\epsilon = \| N^{-1} \Delta M N^{-1} \| \qquad (37)$$

subject to the constraint equation

$$E^T M E = I - m_a \qquad M = M_1 + \Delta M$$

where $m_a = E^T M_A E$ is a nondiagonal matrix having unity as diagonal elements. Choosing $N = M_1$ as the weight matrix, Berman obtains

$$\Delta M = M_A E m_a^{-1} (I - m_a) m_a^{-1} E^T M_1 \qquad (38)$$

It can be seen from Eq. (38) that ΔM is symmetrical and determined to satisfy the orthogonality relations. However, one can obtain different "ΔM"s depending upon the choice of M_1. *Also, the decision to minimize ϵ, while reasonable, is nevertheless arbitrary.*

It is evident that the resulting mass and stiffness matrices are not unique. Subsequently, this truth will be illustrated with a simple numerical example. Hence, it is concluded that in order to determine the system matrices uniquely, some more conditions in addition to the (necessary but *not* sufficient) orthogonality conditions must be satisfied. These additional conditions can be readily obtained from the equations of motion. The free-response data can be used to determine the eigenvalues and eigenvectors of the system. The estimated modal data then can be used in conjunction with the *forced-response* data to uniquely identify the system matrices.

Identification of Eigenvalues and Eigenvectors: Rajaram and Junkins' Approach

A system described by Eq. (33) will be considered. The modal coordinate transformation is introduced as

$$x(t) = E\eta(t) \qquad (39)$$

where $\eta(t)$ is the normal or modal coordinates of the system. Introducing Eq. (39) into the equations of motion, Eq. (33),

$$ME\ddot{\eta}(t) + KE\eta(t) = 0 \qquad (40)$$

Multiplying Eq. (40) by E^T, we get

$$E^T M E \ddot{\eta}(t) + E^T K E \eta(t) = 0 \qquad (41)$$

Due to the orthogonality properties of the eigenvectors, Eq. (41) represents a set of "n" uncoupled second-order equations. If the eigenvectors are normalized with respect to the

mass matrix as per Eqs. (34), Eq. (41) becomes

$$\ddot{\eta}(t) + [\omega^2]\eta(t) = 0, \qquad [\omega^2] = \text{diag}(\omega_1^2,\ldots,\omega_n^2) \qquad (42)$$

When the eigenvectors are not normalized, Eq. (41) can be written as

$$M_m\ddot{\eta}(t) + K_m\eta(t) = 0 \qquad (43)$$

M_m and K_m are diagonal matrices; the generalized "modal mass" and generalized "modal stiffness matrix," respectively. Also, K_m is related to M_m by the following relationship:

$$M_m = [\omega^2]K_m \qquad (44)$$

The solution of Eq. (42) can be written as

$$\eta_i(t) = c_i\cos\omega_i t + s_i\sin\omega_i t \qquad i = 1,2,\ldots,n \qquad (45)$$

c_i and s_i are constants depending upon $\eta_i(0)$ and $\dot{\eta}_i(0)$. Substituting Eq. (45) into the transformation Eq. (39), we obtain

$$x(t) = \sum_{i=1}^{n} (A_i\cos\omega_i t + B_i\sin\omega_i t) \qquad (46)$$

where it is evident

$$A_i = c_i e_i \quad \text{and} \quad B_i = s_i e_i$$

Identifying either A_i or B_i is equivalent to identifying a scaled version of the ith normalized eigenvector. A Gauss-Newton least-squares differential correction method or a direct method based on the Fourier transform[23] of $x(t)$ can be used to obtain the modal parameters (ω_i, A_i, B_i).

We now turn attention to estimating the properly scaled mass and stiffness matrices. Equation (43), in the presence of forces, becomes

$$M_m\ddot{\eta}(t) + K_m\eta(t) = E^T f(t) \qquad (47)$$

where the $(n \times 1)$ force vector $f(t)$ may contain zero entries, i.e., all of the degrees of freedom need not be forced. M_m and K_m are easily determined from the scalar components of Eq. (47), using the fact that $M_m(i,i) = \omega_i^2 K_m(i,i)$. It should be noted that, henceforth, the notation E will be used to represent the measured eigenvectors, normalized with respect to the a priori mass matrix. Since E is measured, transformation equation (39) can be used to transform measurements in physical space to modal space, i.e.,

$$\ddot{\eta}(t) = E^{-1}\ddot{x}(t) \qquad (48a)$$

$$\eta(t) = E^{-1}x(t) \qquad (48b)$$

Introducing Eqs. (48) into Eq. (47), for a known force vector, it is obviously possible to determine the diagonal elements of the modal stiffness matrix K_m and, using Eq. (44), M_m can be computed. The properly scaled, configuration space-mass matrix then can be obtained from

$$M = E^{-T}M_m E^{-1} \qquad (49)$$

Similarly the stiffness matrix is given as

$$K = E^{-T}K_m E^{-1} \qquad (50)$$

For high-dimensioned systems, of course, the inverses shown are replaced by appropriate matrix reduction algorithms.

Thus, the parameter matrices can be estimated uniquely. We need to estimate only "n" parameters, viz., the diagonal elements of M_m. The elements of K_m can be derived from those of M_m through Eq. (44). Also, the amount of forced-response data required to estimate the modal matrices is not large. We need only "$2n$" measurements ("n" accelerations and "n" displacements), in addition to the measurement of forces.

Identification of Damped Systems

We now turn our attention to the necessary modifications of the preceding approach for including viscous (or equivalent viscous) damping. The equations of motion for a damped system are given by Eq. (1).

The eigenvalues and eigenvectors of a damped system are complex quantities. In order to apply classical modal analysis techniques, it is a usual practice to assume that the damping is either small or of a proportional type. Since the measured modes are complex, methods have been proposed to extract the normal modes from the complex modes. However, it is possible to rigorously apply a generalized modal analysis technique by transforming Eq. (1) from configuration to state space and estimate the system matrices, analogous to the previous section.

Introducing the state vector

$$g(t) = [x^T(t)\dot{x}(t)]^T$$

Equation (1) can be written as

$$M^*\dot{g}(t) + K^*g(t) = f^*(t) \qquad (51)$$

where

$$M^* = \begin{bmatrix} -K & 0 \\ 0 & M \end{bmatrix} \qquad (52a)$$

$$K^* = \begin{bmatrix} 0 & K \\ K & C \end{bmatrix} \qquad (52b)$$

$$f^* = \begin{Bmatrix} 0 \\ f \end{Bmatrix} \qquad (52c)$$

The eigenvalues and eigenvectors of a system described by Eq. (51) occur in complex conjugate pairs, i.e., if λ_i is an eigenvalue, $\bar{\lambda}_i$ is also an eigenvalue. Similarly e_i and $\bar{e}_i$ are the eigenvectors of the system. The orthogonality relations are

$$E^T M^* E = I \qquad (53a)$$

$$E^T K^* E = -\Lambda \qquad (53b)$$

where Λ is a diagonal matrix of the eigenvalues. Note that the modal matrix is of order $(2n \times 2n)$. Also, the eigenvectors are normalized with respect to M^* to satisfy

$$e_i^T M^* e_i = 1 \qquad i = 1,2,\ldots,2n \qquad (54)$$

When the eigenvectors are not normalized, of course, Eqs. (53) become

$$E^T M^* E = M_n^* \qquad (55a)$$

$$E^T K^* E = K_n^* \qquad (55b)$$

where M_n^* and K_n^* are diagonal but complex matrices. The same notations as in the previous section are used. The

eigenvectors have the form

$$e_i = \begin{bmatrix} a_i \\ \lambda_i a_i \end{bmatrix} \tag{56}$$

The free response of the system can be written as

$$x(t) = \sum_{i-1}^{n} (a_i e^{\lambda_i t} + a_i e^{\lambda_i t}) \tag{57}$$

where $\lambda_i (= -\alpha_i + j\omega_i)$ and the ith eigenvalue, and α_i is the damping factor and ω_i the damped frequency of oscillation. Equation (57) also can be written as

$$x(t) = 2 \sum_{i-1}^{n} e^{-\alpha_i t}(C_i \cos\omega_i t - S_i \sin\omega_i t) \tag{58}$$

C_i and S_i are the real and imaginary components of a_i, respectively. A Gauss-Newton least-squares differential correction method[6] can be used to identify C_i, S_i, α_i, and ω_i ($i = 1,2,...,n$). Fast Fourier transform of $x(t)$ is quite useful in this case. The frequencies can be estimated from the power spectral density (psd) plot and used as a priori values in the Gauss-Newton algorithm. In this way, the convergence domain of the algorithm can be enhanced considerably. Using the orthogonality relations [Eqs. (56)] and the transformation

$$g(t) = \sum_{i-1}^{n} [e_i \eta_i(t) + \dot{e}_i \dot{\eta}_i(t)] = E\eta(t) \tag{59}$$

Eq. (52) reduces to

$$M_m^* \dot{\eta}(t) = K_m^* \eta(t) + E'f^*(t) \tag{60}$$

where

$$\eta(t) = [\eta_1(t)\dot{\eta}_1(t)...\eta_n(t)\dot{\eta}_n(t)]^T \tag{61}$$

is a complex modal coordinate vector. Equation (60) can be used to identify the M_m^* and K_m^* matrices from forced response, analogous to the previous section. After determining the modal matrices, M^* and K^* can be obtained from Eqs. (56). The method is similar to the one for the undamped system, except that the quantities involved are complex.

Numerical Examples Using Free and Forced Response

Example 1

Consider a two mass-spring system. The mass and stiffness are given as

$$M = \begin{bmatrix} 100 & 0 \\ 0 & 200 \end{bmatrix} \qquad K = \begin{bmatrix} 72 & -36 \\ -36 & 72 \end{bmatrix}$$

Choosing the a priori mass matrix M_A and stiffness matrix K_A for Berman's method[6,7] as

$$M_A = \begin{bmatrix} 90 & 0 \\ 0 & 220 \end{bmatrix} \qquad K_A = \begin{bmatrix} 65 & -32 \\ -32 & 79 \end{bmatrix}$$

The true system eigenvalues and eigenvectors are used as measurements. After carrying out algebra of Berman's method, the estimated mass matrix is found to be

$$M = \begin{bmatrix} 96.67 & 6.67 \\ 6.67 & 206.67 \end{bmatrix}$$

Although Berman's corrections to the diagonal elements are in the right direction, the off-diagonal elements' corrections are of comparable size and are no longer zero. A significantly *different* final mass matrix estimate would have been obtained, of course, if M_A were chosen differently. The estimated stiffness matrix for Berman's approach is found to be

$$K = \begin{bmatrix} 68.36 & -32.52 \\ -32.52 & 71.68 \end{bmatrix}$$

It can be noted that the diagonal terms are corrected fairly well while the corrections to off-diagonal terms are relatively small in this case.

Using the method developed above (with the eigenvalues and eigenvectors calculated using a finite Fourier transform), the mass matrix is determined from Eq. (49) to be

$$M = \begin{bmatrix} 100.00 & -0.8415E-04 \\ -0.8415E-04 & 200.0 \end{bmatrix}$$

and the estimated stiffness matrix, from Eq. (51), is calculated as

$$K = \begin{bmatrix} 71.995 & -35.997 \\ -35.997 & 71.9996 \end{bmatrix}$$

The small residual errors are the consequence of truncation of the Fourier transform of $x(t)$ to obtain eigenvalues or eigenvectors. If the Gauss-Newton iteration is used instead, the M and K matrix are recovered exactly (to eight digits). It is evident from this simple example that the proposed scheme correctly identifies the system matrices to within truncation errors in the finite Fourier transform. In essence, the scaling implicit within Berman's correction norm minimization is replaced by the requirement that the estimated M and K be consistent with a measured forced response.

Example 2

A two mass-spring damper system is considered. The various matrices are

$$M = \begin{bmatrix} 1 & 0 \\ 0 & 1 \end{bmatrix}, \quad K = \begin{bmatrix} 5 & -4 \\ -4 & 4 \end{bmatrix}, \quad C = \begin{bmatrix} 0.4 & -0.2 \\ -0.2 & 0.2 \end{bmatrix}$$

The eigenvalues are

$$\lambda_1, \bar{\lambda}_1 = -0.222593 \pm j2.578255$$

$$\lambda_2, \bar{\lambda}_2 = -0.027406 \pm j0.545796$$

Using the Gauss-Newton method, the eigenvalues and eigenvectors are estimated from free response. The free-response data are properly scaled by applying an impulsive force on the second mass. The system matrices are obtained using the excitation $f_2 = 0.1$ sign (sin 0.2t). The mass, stiffness, and damping matrices are identified exactly (eight digits). Thus the present method generalizes fully to include arbitrary viscous damping.

Conclusions

Three novel schemes are proposed to identify the parameters of vibrating structures. Numerical results on a variety of transparent examples support the validity of all three methods. The physical properties of mass, stiffness, and damping matrices are identified. All three proposed methods are applicable to damped structures. No assumptions regarding the nature of damping are made, other than it is of the viscous type. Systems with closely spaced frequencies present

no apparent computational difficulty. In fact, example structures with repeated frequencies and rigid-body modes are identified reliably without difficulty. It is also shown that multiple excitation vectors should be chosen to form an independent set. The methods have been illustrated, however, only for low-dimensioned examples; significant future effort should consider high-degree-of-freedom systems to evaluate the robustness and relative merits of these approaches. It is also important to reduce the dimensionality by coupling the estimation algorithms to the structural modeling process.

Acknowledgments

References

[1]Ibrahim, S.R. and Mikulcik, E.C., "A Time Domain Modal Vibration Test Technique," *Shock and Vibration Bulletin*, Bull. 43, Pt. 4, 1973, pp. 21-37.

[2]Ibrahim, S.R. and Mikulcik, E.C., "The Experimental Determination of Vibration Parameters from Time Responses," *Shock and Vibration Bulletin*, Bull. 46, Pt. 5, 197), pp. 187-196.

[3]Ibrahim, S.R. and Mikulcik, E.C., "A Method for the Direct Identification of Vibration Parameters from the Free Response," *Shock and Vibration Bulletin*, Bull. 47, Pt. 4, 1977, pp. 183-198.

[4]Ibrahim, S.R. and Mikulcik, E.C., "Limitations of Random Input Forces in Randomdec Computation for Modal Identification," *Shock and Vibration Bulletin*, Bull. 50, Pt. 3, 1980, pp. 99-112.

[5]Juang, J.N. and Papa, R.S., "An Eigensystem Realization Algorithm (ERA) for Modal Parameter Identification and Model Reduction," presented at the NASA/JPL Workshop on Identification and Control of Flexible Space Structures, San Diego, Calif., June 1984.

[6]Junkins, J.L., *Optimal Estimation of Dynamical Systems*, Sijthoff-Noordhoff, Leyden, the Netherlands, 1978.

[7]Hendricks, S.L. et al., "Identification of Mass, Damping and Stiffness Matrices for Large Linear Vibratory System," *AIAA Journal of Guidance, Control, and Dynamics*, Vol. 7, March-April 1984, pp. 244-245.

[8]Fox, L. and Parker, I.B., *Chebyshev Polynomials in Numerical Analysis*, Oxford University Press, London, 1968, Chap. 3.

[9]Raney, J.P., "Identification of Complex Structures Using Near Resonance Testing," *Shock and Vibration Bulletin*, Bull. 38, Pt. 2, 1968.

[10]Miramand, N., Billard, J.F., Le Leux, F., and Kernevez, J.P., "Identification of Structural Parameters by Dynamic Tests at a Single Point," *Shock and Vibration Bulletin*, Bull. 46, Pt. 5, 1976, pp. 197-212.

[11]Thoren, R.P., "Derivation of Mass and Stiffness Matrices from Dynamic Test Data," AIAA Paper 72-346, April 1972.

[12]Gravitz, S.I., "An Analytical Procedure for Orthogonalization of Experimentally Measured Modes," *Journal of the Aerospace Sciences*, Vol. 25, 1958, pp. 721-722.

[13]Rodden, W.P., "A Method for Deriving Structural Influence Coefficients from Ground Vibration Tests," *AIAA Journal*, Vol. 5, May 1967, pp. 991-1000.

[14]McGrew, J., "Orthogonalization of Measured Modes and Calculation of Influence Coefficients," *AIAA Journal*, Vol. 7, April 1969, pp. 774-776.

[15]Berman, A. and Flannely, W.G., "Theory of Incomplete Models of Dynamic Structures," *AIAA Journal*, Vol. 9, Aug. 1971, pp. 1481-1487.

[16]Berman, A., "Mass Matrix Correction Using an Incomplete Set of Measured Modes," *AIAA Journal*, Vol. 17, Oct. 1979, pp. 1147-1148.

[17]Berman, A. and Nagy, E.J., "Improvement of Large Analytical Model Using Test Data," *AIAA Journal*, Vol. 21, Aug. 1983, pp. 1168-1173.

[18]Wei, F.S., "Stiffness Matrix Corrections from Incomplete Test Data," *AIAA Journal*, Vol. 18, Oct. 1980, pp. 1274.

[19]Chen, J.C. and Wada, B.K., "Matrix Perturbation for Structural Dynamic Analysis," *AIAA Journal*, Vol. 15, Aug. 1977, pp. 1095-1100.

[20]Chen, J.C., Kuo, C.P., and Garba, J.A., "Direct Structural Parameter Identification by Modal Test Results," *24th AIAA/ASME/ASCE/AAS Structures, Structural Dynamics and Materials Conference*, Pt. 2, May 1983.

[21]Heylen, W. and Van Honacker, P., "An Automated Technique for Improving Modal Matrices by Means of Experimentally Obtained Dynamic Data," *24th AIAA/ASME/ASCE/AAS Structures, Structural Dynamics and Materials Conference*, Pt. 2, May 1983, pp.

[22]White, C.W. and Maytum, B.D., "Eigensolution Sensitivity to Parametric Model Perturbations," *Shock and Vibration Bulletin*, Bull. 46, Pt. 5, Aug. 1976, pp. 123-133.

[23]Rajaram, S., "Identification of Vibration Parameters of Flexible Structures," Doctoral Dissertation, Virginia Polytechnic Institute & State University, Blacksburg, Va., May 1984.

Eigenvalue Optimization Algorithms for Structure/Controller Design Iterations

D.S. Bodden and J.L. Junkins

Eigenvalue Optimization Algorithms
for Structure/Controller Design Iterations

D.S. Bodden*

Virginia Polytechnic Institute and State University, Blacksburg, Virginia

and

J.L. Junkins†

Texas A&M University, College Station, Texas

An eigenspace optimization approach is proposed and demonstrated for the design of feedback controllers for the maneuvers/vibration arrests of flexible structures. The algorithm developed is shown to be equally useful in sequential or simultaneous design iterations that modify the structural parameters, sensor/actuator locations, and control feedback gains. The approach is demonstrated using a differential equation model for the "Draper RPL configuration." This model corresponds to the hardware used for experimental verification of large flexible spacecraft maneuver controls. A number of sensor/actuator configurations are studied vis-a-vis the degree of controllability. Linear output feedback gains are determined using a novel optimization strategy. The feasibility of the approach is established, but more research and numerical studies are required to extend these ideas to truly high-dimensioned systems.

Parameterization of the Controlled System's Eigenvalues and Eigenvectors

CONSIDER a linear structure (modeled by a finite element or similar discretization scheme) in which the configuration vector x is governed by the system of differential equations

$$M\ddot{x} + C\dot{x} + Kx = Bu \tag{1}$$

where

$M = n \times n$ symmetric positive definite mass matrix
$C = n \times n$ symmetric positive semidefinite structural damping matrix
$K = n \times n$ symmetric positive semidefinite stiffness matrix
$B = n \times m$ control influence matrix
$x = n \times 1$ configuration vector
$u = m \times 1$ control vector $(\cdot) = d/dt(\ )$

Considering the case of linear output feedback control, let the local position, velocity, and acceleration measurements be denoted by

$$y_1 = H_1 x, \quad y_2 = H_2 \dot{x}, \quad y_3 = H_3 \ddot{x} \tag{2}$$

which represent the linear relationship of the locally measured position y_1, velocity y_2, and acceleration y_3, where

$y_1 = m_1 \times 1$ vector $H_1 = m_1 \times n$ matrix

$y_2 = m_2 \times 1$ vector $H_2 = m_2 \times n$ matrix

$y_3 = m_3 \times 1$ vector $H_3 = m_3 \times n$ matrix

For linear output feedback, we seek the constant gain matrices G_1, G_2, and G_3 so that

$$u = -[G_1 y_1 + G_2 y_2 + G_3 y_3]$$

$$= -G_1 H_1 x - G_2 H_2 \dot{x} - G_3 H_3 \ddot{x} \tag{3}$$

Substitution of Eq. (3) into Eq. (1) gives the closed-loop system

$$\tilde{M}\ddot{x} + \tilde{C}\dot{x} = \tilde{K}x = 0 \tag{4}$$

where the closed-loop system's matrices are

$$\tilde{M} = M + BG_3 H_3, \quad \tilde{C} = C + BG_2 H_2, \quad \tilde{K} = K + BG_1 H_1 \tag{5}$$

Introduce the notations

$$M = M(a), \quad C = C(a), \quad K = K(a)$$

$$B = B(c), \quad H_i = H_i(b), \quad G_i = G_i(g) \tag{6}$$

where a is a vector of the structural and geometric model parameters (defining mass, stiffness, damping, configuration lengths, cross-sectional areas, etc.), b a vector of the sensor-type and location parameters, c a vector of the actuator-type and location parameters, and g a vector of the control gains.

Defining the $N \times 1$ global structural and control parameter vector as

$$p^T = \{a^T b^T c^T g^T\} \tag{7}$$

it is apparent from Eqs. (5-7) that

$$\tilde{M} = \tilde{M}(p), \quad \tilde{C} = \tilde{C}(p), \quad \tilde{K} = \tilde{K}(p) \tag{8}$$

The details of the parameterizations of Eqs. (8) are dependent upon the particular modeling approach. Often, these are simple algebraic expressions (the elements of p appear explicitly in $\tilde{M}, \tilde{C}, \tilde{K}$).

Considering the first-order state-space differential equation, which is the equivalent to the second-order closed-loop

system of Eq. (4),

$$A\dot{z} = Bz \tag{9}$$

where

$$z = \left\{ \begin{array}{c} x \\ \dot{x} \end{array} \right\}, \quad A = \begin{bmatrix} M & 0 \\ 0 & \tilde{M} \end{bmatrix}, \quad B = \begin{bmatrix} 0 & M \\ -\tilde{K} & -\tilde{C} \end{bmatrix} \tag{10}$$

it is evident that

$$A = A(p), \qquad B = B(p) \tag{11}$$

The right and left eigenvalue problems [associated with the $z = \phi e^{\lambda t}$ solutions of Eq. (9)] are

right: $\lambda_i A \phi_i = B \phi_i$, left: $\lambda_i A^T \psi_i = B^T \psi_i$,

$$i = 1, 2, \ldots, 2n \tag{12}$$

where the conventional normalizations for the eigenvectors are adopted as

$$\psi_j^T A \phi_i = \delta_{ij}, \qquad \psi_j^T B \phi_i = \delta_{ij} \lambda_i \tag{13}$$

Since $A = A(p)$ and $B = B(p)$, it seems natural to consider the eigenvalues $\{\lambda_1, \ldots, \lambda_{2n}\}$ and eigenvectors $\{\phi_1, \psi_1, \ldots, \phi_{2n}, \psi_{2n}\}$ to be functions of the parameter vector p, viz.,

$$\lambda_i = \lambda_i(p), \quad \phi_i = \phi_i(p), \quad \psi_i = \psi_i(p) \tag{14}$$

Except for occasional singular events (e.g., multiple eigenvalues or near-multiple eigenvalues), the nonlinear functional dependence of Eqs. (14) can be assumed to be continuous.

Qualitative Approach to Eigenspace Optimization

Most structural and control optimality criteria can be stated explicitly in terms of λ_i and ϕ_i or directly as functions of p. It is obvious that an algorithm that can effectively optimize p (over some admissible set to minimize some optimality criteria and satisfy the constraints stated as functions of p and λ_i) provides a *direct* method for controller/structure optimization problems. Unfortunately, there are several formidable difficulties, the two most prominent being:

1) The $N \times 1$ p vector is of high dimension, even for structural and control system models of moderate complexity. The dimension N of p can be several hundred.

2) The functional relationship implied by Eq. (14) is the solution fo the large eigenvalue problem of Eqs. (12) and (13). It is typically a highly nonlinear function of p and is occasionally characterized by singular local behavior (bifurcation points at repeated roots, for example).

Practical optimization algorithms that can deal with these two sources of difficulty in a rigorous and globally convergent way do not exist. However, we have developed a strategy for carrying out optimizations and suboptimizations, in spite of these two sources of difficulty. There are two heuristic ideas underlying our approach:

1) Regions of extremely high sensitivity (to the p vector) are generally undesirable. Therefore, if the performance index or constraints include a measure of eigenvalue solution sensitivity, successful suboptimizations are obviously less likely to encounter the singular events.[2]

2) Exact eigenvalue placement (or "pole placement"), for a high-order system, is not a reasonable design approach. Rather than attempting to prescribe an exact point location for every eigenvalue, it is more reasonable (and leads to better algorithms) to move all of the eigenvalues into an *acceptable region* of the complex plane. From the viewpoint of pole placement, this allows attention to be locally concentrated upon just the "problem children" eigenvalues that are the farthest outside the acceptable region or those that locally

dominate a measure of optimality or sensitivity. This allows judicious and lower-dimensional suboptimizations to be made and is a key to attacking truly high-order systems.

These two qualitative ideas serve as the main motivation of our approach. Of course, an initial design point (values for the elements of p) is required. Typically, the initial design point will be the output of some (arbitrary) structural design process and, probably, a constant-gain optimal regulator design for the given structure. Thus, the present family of algorithms are designed to *begin* with the typical output of a conventional *sequential* structure—controller design process. However, for moderate-dimensional applications, we have been able to initiate control gain optimizations with a free-vibration (zero control gains) case and still achieve reliable convergence.

Central to the application of the optimization algorithms developed below lies the necessity to compute efficiently the partial derivatives of the generalized eigenvalues and eigenvectors of Eqs. (12-14). Attractive algebraic equations have been derived that explicitly determine these derivatives as "side calculations" at much less computational expense than the solution of the eigenvalue problem itself. The development of these equations is briefly summarized below for the first and second partial derivatives of the eigenvalues.

Partial Derivatives of the Closed-Loop Eigenvalues with Respect to Structural Model and Control System Parameters

Differentiating Eqs. (12) with respect to a typical element p_ℓ of p, upon premultiplying the resulting two equations by ψ_j^T and ϕ_j^T and making use of Eqs. (13), gives

$$\frac{\partial \lambda_i}{\partial p_\ell} \delta_{ij} + (\lambda_i - \lambda_j) \psi_j^T A \frac{\partial \phi_i}{\partial p_\ell} = \psi_j^T \left[\frac{\partial B}{\partial p_\ell} - \lambda_i \frac{\partial A}{\partial p_\ell} \right] \phi_i \tag{15}$$

$$\frac{\partial \lambda_i}{\partial p_\ell} \delta_{ij} + (\lambda_i - \lambda_j) \phi_j^T A^T \frac{\partial \psi_i}{\partial p_\ell} = \phi_j^T \left[\frac{\partial B^T}{\partial p_\ell} - \lambda_i \frac{\partial A^T}{\partial p_\ell} \right] \psi_i \tag{16}$$

Equations (15) and (16) hold for $i = 1, 2, \ldots, 2n$; $j = 1, 2, \ldots, 2n$; and $\ell = 1, 2, \ldots, N$. For $i = j$, both Eqs. (15) and (16) reduce to the following well-known result[1] for the gradients of the $2n$ eigenvalues

$$\frac{\partial \lambda_i}{\partial p_\ell} = \psi_i^T \left[\frac{\partial B}{\partial p_\ell} - \lambda_i \frac{\partial A}{\partial p_\ell} \right] \phi_i \tag{17}$$

Thus, having solved for eigenvalues and eigenvectors, a moderate side calculation produces the first-order eigenvalue sensitivities. Differentiating Eq. (17), with respect to p_m, we obtain the following equation for the second partial derivatives:

$$\frac{\partial^2 \lambda_i}{\partial p_\ell \partial p_m} = \psi_i^T \left[\frac{\partial^2 B}{\partial p_\ell \partial p_m} - \frac{\partial \lambda_i}{\partial p_m} \frac{\partial A}{\partial p_\ell} - \lambda_i \frac{\partial^2 A}{\partial p_\ell \partial p_m} \right] \phi_i$$

$$+ \frac{\partial \psi_i^T}{\partial p_m} \left[\frac{\partial B}{\partial p_\ell} - \lambda_i \frac{\partial A}{\partial p_\ell} \right] \phi_i + \psi_i^T \left[\frac{\partial B}{\partial p_\ell} - \lambda_i \frac{\partial A}{\partial p_\ell} \right] \frac{\partial \phi_i}{\partial p_m} \tag{18}$$

Since Eq. (18) involves $\partial \phi_i / \partial p_m$ and $\partial \psi_i / \partial p_m$, we must either evaluate or eliminate them. We choose the latter method. Following Plaut,[1] we project $\partial \psi_i / \partial p_m$ and $\partial \phi_i / \partial p_m$ onto the eigenvectors themselves as

$$\frac{\partial \phi_i}{\partial p_\ell} = \sum_{k=1}^{2n} a_{ki} \phi_k, \qquad \frac{\partial \psi_i}{\partial p_\ell} = \sum_{k=1}^{2n} b_{ki} \psi_k \tag{19}$$

where a_{ki} and b_{ki} are scalar constants. For $i \neq j$, substituting Eqs. (19) into Eqs. (15) and (16) yields

$$(\lambda_i - \lambda_j)a_{ji} = \psi_j^T \left[\frac{\partial B}{\partial p_i} - \lambda_i \frac{\partial A}{\partial p_i} \right] \phi_i \qquad (20)$$

$$(\lambda_i - \lambda_j)b_{ji} = \phi_j^T \left[\frac{\partial B^T}{\partial p_i} - \lambda_i \frac{\partial A^T}{\partial p_i} \right] \psi_i \qquad (21)$$

For the case of distinct eigenvalues, Eqs. (20) and (21) provide the a_{ji} and b_{ji} values, except for a_{ii} and b_{ii} (which remain undetermined). The normalization of Eq. (13), upon setting $j = i$ and differentiating with respect to p_i and substituting Eq. (19), yields

$$a_{ii} + b_{ii} = -\psi_i^T \frac{\partial A}{\partial p_i} \phi_i \qquad (22)$$

Substitution of Eq. (17) into Eq. (18) gives

$$\frac{\partial^2 \lambda_i}{\partial p_i \partial p_m} = \psi_i^T \left[\frac{\partial^2 B}{\partial p_i \partial p_m} - \lambda_i \frac{\partial^2 A}{\partial p_i \partial p_m} \right] \phi_i$$

$$- \psi_i^T G_{im} \phi_i \psi_i^T \frac{\partial A}{\partial p_i} \phi_i + \left\{ \frac{\partial \psi_i}{\partial p_m} \right\}^T G_{ii} \phi_i + \psi_i^T G_{ii} \frac{\partial \phi_i}{\partial p_m} \qquad (23)$$

with $G_{ik} \equiv \partial B / \partial p_k - \lambda_i (\partial A / \partial p_k)$. Substitution of Eqs. (19) into Eq. (23) gives

$$\frac{\partial^2 \lambda_i}{\partial p_i \partial p_m} = \psi_i^T \left[\frac{\partial^2 B}{\partial p_i \partial p_m} - \lambda_i \frac{\partial^2 A}{\partial p_i \partial p_m} \right] \phi_i - \psi_i G_{im} \phi_i^T \frac{\partial A}{\partial p_i} \phi_i$$

$$+ (a_{ii} + b_{ii})\psi_i^T G_{ii} \phi_i + \sum_{k=1, k \neq i}^{2n} \{ b_{ki}\psi_k^T G_{ii} \phi_i + a_{ki}\psi_i^T G_{ii} \phi_k \} \qquad (24)$$

Finally, eliminating $a_{ii} + b_{ii}$ using Eq. (22) and a_{ji} and b_{ji} for $j \neq i$ using Eqs. (20) and (21) gives the final expressions for the second partial derivatives,

$$\frac{\partial^2 \lambda_i}{\partial p_i \partial p_m} = \psi_i^T \left[\frac{\partial^2 B}{\partial p_i \partial p_m} - \lambda_i \frac{\partial^2 A}{\partial p_i \partial p_m} \right] \phi_i$$

$$- \psi_i^T G_{im} \phi_i \psi_i^T \frac{\partial A}{\partial p_i} \phi_i - \psi_i^T \frac{\partial A}{\partial p_m} \phi_i \psi_i^T G_{ii} \phi_i$$

$$+ \sum_{k=1, k \neq i}^{2n} \left[\frac{\psi_i^T G_{im} \phi_k \psi_k^T G_{ii} \phi_i + \psi_k^T G_{im} \phi_i \psi_i^T G_{ii} \phi_k}{(\lambda_i - \lambda_k)} \right] \qquad (25)$$

which, of course, are singular for repeated eigenvalues.

Closed-Loop Response

The response of the controlled configuation to initial disturbances is determined using a modal approach. The modal coordinates η are mapped into the state space by

$$z = [\phi]\eta, \qquad \dot{z} = [\phi]\dot{\eta} \qquad (26)$$

where $[\phi]$ is the right modal matrix. Substituting Eqs. (26) into Eq. (9), premultiplying by $[\psi]^T$ (the left modal matrix) and utilizing Eqs. (13), the equations of motion are uncoupled and given by

$$\dot{\eta}_i = \lambda_i \eta_i, \qquad i = 1, 2, \dots, 2n \qquad (27)$$

The solution to Eq. (27) is

$$\eta_i = e^{\lambda_i (t - t_0)} \eta_i(t_0), \qquad i = 1, 2, \dots 2n \qquad (28)$$

The initial conditions are mapped into modal space by premultiplying Eqs. (26) by $[\phi]^{-1} = [\psi]^T A$ and utilizing Eq. (13) to give

$$\eta(t_0) = [\psi]^T A z(t_0) \qquad (29)$$

The system response in normal coordinates is then given by Eqs. (28) and (29). However, the eigenvalues and eigenvectors are in the general complex consisting of n eigenvalues and n eigenvectors plus their associated n complex conjugates. We seek a solution that will eliminate the complex conjugates and thus allow us to truncate the number of modes used in the solution.

The modal matrices are partitioned as follows:

$$[\psi] = \begin{bmatrix} \psi_1 & \bar{\psi}_1 \\ \psi_2 & \bar{\psi}_2 \end{bmatrix}, \qquad [\phi] = \begin{bmatrix} \phi_1 & \bar{\phi}_1 \\ \phi_2 & \bar{\phi}_2 \end{bmatrix} \qquad (30)$$

where ψ_1, ψ_2, ϕ_1, and ϕ_2 are $n \times k$ matrices normalized by Eqs. (13). It follows that $\bar{\psi}_1$, $\bar{\psi}_2$, $\bar{\phi}_1$, and $\bar{\phi}_2$ are also $n \times k$ matrices and are thus the complex conjugates of ψ_1, ψ_2, ϕ_2, respectively. The vector of normal coordinates η can also be partitioned as

$$\eta = \left\{ \begin{array}{c} \zeta \\ \bar{\zeta} \end{array} \right\} \qquad (31)$$

where ζ is a $k \times 1$ vector. It can be shown that $\bar{\zeta}$ is also $k \times 1$ and is the complex conjugate of ζ. Substituting Eqs. (30) and (31) into Eq. (26), the response in configuration coordinates is

$$z = \left\{ \begin{array}{c} x \\ \dot{x} \end{array} \right\} = \left\{ \begin{array}{c} \phi_1 \zeta + \bar{\phi}_1 \bar{\zeta} \\ \phi_2 \zeta + \bar{\phi}_2 \bar{\zeta} \end{array} \right\}$$

$$= 2 \left\{ \begin{array}{c} [Re\phi_1][Re\zeta] - [Im\phi_1][Im\zeta] \\ [Re\phi_2][Re\zeta] - [Im\phi_2][Im\zeta] \end{array} \right\} \qquad (32)$$

From Eq. (32), it is evident that the complex conjugates of the n eigenvalues and eigenvectors are not needed and that the k modes can be used to determine the response. The measured beam deflections and deflection rates follow from Eq. (2) and the controlled response from Eq. (3).

A Model of Draper/RPL Configuration

Referring to Figs. 1 and 2, we consider the planar rotational/vibrational dynamics of the demonstration experimental model sponsored by the U.S. Air Force Rocket Propulsion Laboratory for testing the control laws for maneuvering flexible spacecraft; this experimental work is presently being conducted at the C.S. Draper Laboratory.[2] The central hub is supported by an air bearing table with four appendages cantilevered from the hub. Table 1 summarizes the Draper/RPL configuration parameters. Following Turner and Chun,[2] we form a discretized model for the system by assuming that the elastic deformations of each of the arms (relative to a body-fixed undeformed state) can be represented as linear combination of the comparison functions.

$$\phi_k(z) = 1 - \cos\left(\frac{k\pi z}{L}\right) + \frac{1}{2}(-1)^{k+1}\left(\frac{k\pi z}{L}\right)^2 \qquad (33)$$

so that the transverse body-fixed deformation of the jth arm is modeled as

$$y_j(t,z) = \sum_{k=1}^{N} q_{kj}(t)\phi_k(z), \qquad j = 1, 2, 3, 4, \quad 0 \leq z \leq L \qquad (34)$$

Radial elongation of the arms is neglected, as are out-of-plane deformations. For the numerical results presented below, we took $\bar{N} = 10$. Using Eq. (34) to evaluate the potential and kinetic energy[3] leads to equations of the form of Eq. (1), with the configuration vector

$$x = [\theta \vdots q_{11}q_{21}\cdots \vdots q_{N1} \vdots q_{12}q_{22}\cdots q_{N2} \vdots \cdots q_{14}q_{24}\cdots q_{N4}]^T$$

We restrict attention to the class of antisymmetric deformations whereby $y_1(t,z) = y_2(t,z)$ and $y_3(t,z) = y_4(t,z)$; thus, $q_{i1}(t) = q_{i2}(t)$ and $q_{i3}(t) = q_{i4}(t)$. For this class of antisymmetric motions, the configuration vector can be collapsed to

$$x = [\theta \vdots q_{11}q_{21}\cdots q_{N1} \vdots q_{13}q_{23}\cdots q_{N3}]^T \tag{35}$$

For $\bar{N} = 10$, the order of the system of Eq. (1) is thus 21. The explicit expressions for the elements of the M and K matrices are developed in Ref. 3. We take $C = \mu K$, where μ is a constant. For the numerical examples presented, $\mu = 1 \cdot E - 5$; the controlled response of the first seven modes is insensitive to an order of magnitude variation of μ. In Fig. 3, we show the first nine normal modes.

The eigenvalues and eigenvectors for the first seven modes have converged in the numerical sense that increasing $\bar{N}$ does not change the first four or five digits, whereas modes eight and nine have converged to about three digits. (However, the last ten higher-frequency computed eigenvalues and eigenvec-

tors, as expected, are not as accurately calculated.) Thus, we restrict our optimization discussions to the first nine modes. After the first (rigid-body) mode, the remaining modes occur in near pairs. The antisymmetric, "opposition" modes are simple cantilever beam modes characterized by the adjacent beams moving in opposition (the constraint torques between the hub and the beam clamp cancel in equal and opposite pairs, resulting in a zero rotation of the hub). The antisymmetric "unison" modes are perturbed cantilever modes (with varied frequencies) characterized by all four beams moving in unison; the hub has nonzero rotation for these modes. As is evident, the corresponding pair of unison and opposition frequencies are closely spaced; this spacing decreases with increasing mode number.

Table 1 Draper/RPL configuration parameters

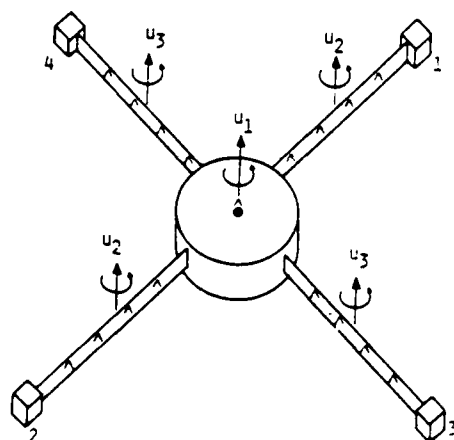|	
Hub radius	1 ft
Rotary inertia of hub, r	8 slug-ft^2
Mass density of beams, ρ	5.22 slug ft^3
Elastic modulus of the arms, E	1.1×10^7 lb/in.^{2}
Arm thickness, t_a	0.125 in.
Arm height, h_a	6 in.
Arm length, L	4 ft
Tip mass	0.156941 slug
Rotary inertia of tip masses	0.0018 slug-ft^2

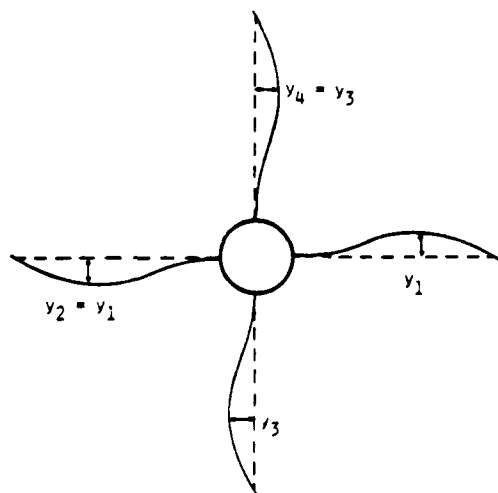Fig. 1 The Draper/RPL configuration.

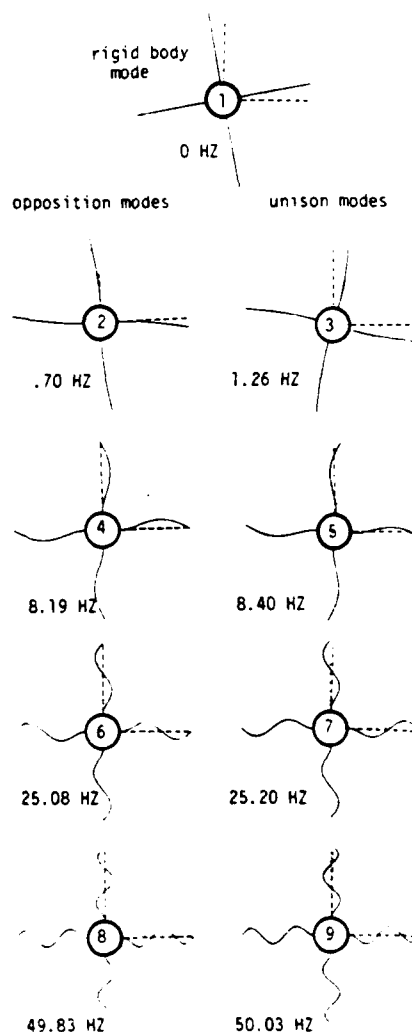Fig. 2 Anti-symmetric deformation.

Fig. 3 First nine normal modes.

Actuator/Sensor Configuration

We admit torque actuators on the central hub and at some station z on each appendage. We also admit rotational position and velocity sensors on the hub and deflection and deflection rate sensors at some stations on each appendage. For the case in which the actuators consist of a torque u_1 applied to the hub, a torque u_2 applied at station z_1 on appendages 1 and 2, and a torque u_3 applied at station z_2 on appendages 3 and 4, the right-hand side of Eq. (1) is

$$Bu = \begin{bmatrix} 1 & 2 & 2 \\ 0 & 2\phi'(z_1) & 0 \\ 0 & 0 & 2\phi'(z_2) \end{bmatrix} \begin{Bmatrix} u_1 \\ u_2 \\ u_3 \end{Bmatrix} \quad (36)$$

where

$$\phi'(z) = \frac{d}{dz}[\phi(z)], \quad \phi(z) = [\phi_1(z)...\phi_{10}(z)]^T$$

and, if rotational position and velocity sensors are located on the hub, while colocated deflectional position and velocity sensors are located at stations $x_1,...,x_8$ on each appendage then the sensor influence matrices H_1, H_2 are both the same 9×21 matrix,

$$H_i = \begin{bmatrix} 1 & 0^T & 0^T \\ 0 & \phi^T(x_1) & 0^T \\ \vdots & \vdots & \vdots \\ 0 & \phi^T(x_4) & 0^T \\ 0 & 0^T & \phi^T(x_5) \\ \vdots & \vdots & \vdots \\ 0 & 0^T & \phi^T(x_8) \end{bmatrix}, \quad i = 1,2 \quad (37)$$

and

$$y_i^T = [\theta y_1(t,x_1)...y_1(t,x_4)y_3(t,x_5)...y_3(t,x_8)], \quad y_2 = \frac{d}{dt}(y_1)$$

$$(38)$$

and the gains G_1 and G_2 are both 3×9 matrcies. For the numerical examples below, we initially set $z_1 = z_2 = L/2$, $x_1 = x_5 = L/4$, $x_2 = x_6 = L/2$, $x_3 = x_7 = 0.7L$, $x_4 = x_8 = 0.9L$, and selectively admit structural parameters, actuator locations, and sensor locations along with the control gain vector in p.

Minimum Modification Strategy for Structural/Controller Design Iterations

Consider a constrained optimization problem wherein we seek the optimal value of the parameter vector p that extremizes some performance measure

$$J = J[\lambda_1(p),...,\lambda_{2n}(p), \quad \phi_1(p),...,\phi_2(p),p] \quad (39)$$

subject to the satisfaction of the N_α equality constraints

$$\alpha_j[\lambda_1(p),...,\lambda_{2n}(p), \quad \phi_1(p),...,\phi_{2n}(p),p] = 0$$

$$j = 1,2,...,N_\alpha \quad (40)$$

and N_β inequality constraints

$$\beta_{jL} \leq \beta_j[\lambda_1(p),...,\lambda_{2n}(p), \quad \phi_1(p)...,\phi_{2n}(p),p] \leq \beta_{jt}$$

$$j = 1,2,...,N_\beta \quad (41)$$

Thus, the performance measure and constraints are defined in terms of the eigensolution, but we also admit explicit dependence upon p to include, for example, structure and control system criteria. Equations (39-41) define a nonlinear programming problem for which a number of algorithms have been developed and applied during the past two decades.[4-6] One iteration stategy confines local attention to only the locally violated inequality constraints and all of the functions of Eqs. (39) and (40). Specifically, one can seek the smallest correction vector Δp that achieves specified increments of ΔJ, $\Delta\alpha_j$, and $\Delta\beta_j$ for a subset of the functions of Eqs. (39-41). Linearizing these equations about p_i results in

$$\Delta\gamma = \left[\frac{\partial\gamma}{\partial p}\bigg|_{p_i}\right]\Delta p \quad (42)$$

where $\gamma = [J,\alpha_j,\beta_j]^T$. Since Eqs. (42) constitute, typically, a small number of equations in a large number of unknowns, we expect an infinity of exact Δp solutions; some criterion must be introduced to select a particular solution. Motivated by the desire to satisfy, as nearly as possible, the implicit local linearity assumption, we seek a "small Δp" solution. Minimizing the correction norm $\Delta p^T W \Delta p$ (for W a suitable weight matrix) subject to Eq. (42) gives

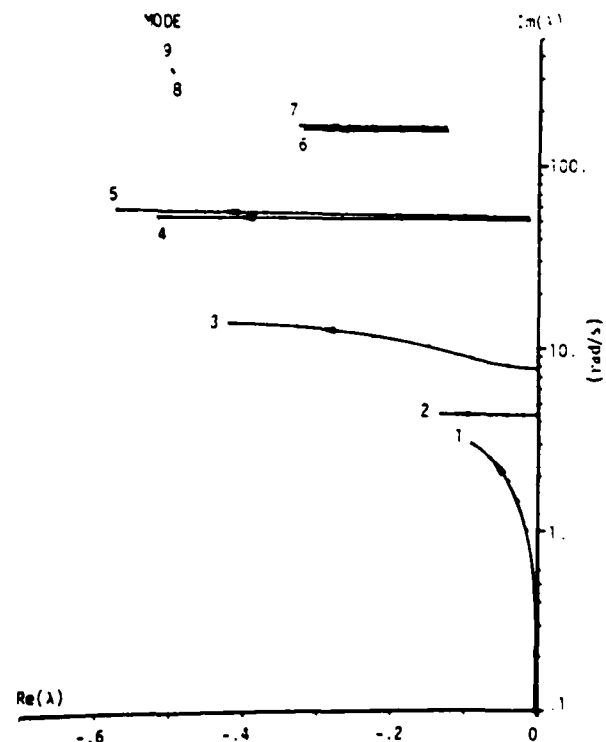$$\Delta p = W^{-1}\left[\frac{\partial\gamma}{\partial p}\bigg|_{p_i}\right]^T \Lambda \quad (43a)$$

Fig. 4 Eigenvalue placement locus of first nine modes: case 1 (continuation parameter α varys from zero to one in six increments from right to left along each eigenvalue trajectory).

where Λ is a Lagrange multiplier vector obtained by solving

$$\left[\frac{\partial\gamma}{\partial p}\Big|_{p_i}\right]W^{-1}\left[\frac{\partial\gamma}{\partial p}\Big|_{p_i}\right]^T\Lambda = \Delta\gamma \qquad (43b)$$

Thus, the size of the linear system we must solve is equal to the number of functions [from Eqs. (39-41)] that we seek to change by the increment vector $\Delta\gamma$, regardless of the number of elements in the Δp vector. The partial derivatives needed in Eq. (42) can be evaluated by the chain rule partial differentiation of Eqs. (38-40), making use of the eigenvalue gradients of Eq. (17). Of course, second-order optimization algorithms can also be used,[5] in which case one will need the second partial derivatives of Eqs. (25).

As a nonlinear programming strategy, we first seek a nearest *feasible p*, which satisfies all of the constraints [Eqs. (40) and (41)] and then include J increments in $\Delta\gamma$ to seek a constrained optimal solution. This strategy can be formalized[4]; it is fully equivalent to the gradient projection constrained optimization algorithms.

For example, we can apply the above developments to place the Draper/RPL system's closed-loop eigenvalues in a desired region and, subject to this condition, minimize a robustness measure (e.g., the sensitivity of the eigenvalues with respect to variation of uncertain system parameters).

Numerical Examples: Eigenvalue Placement for the Draper/RPL Configuration

Case 1

This first example is a modification of a result presented in Ref. 2. We consider the problem of finding a minimum norm gain vector $g \equiv p$ (42 elements of G_1 and G_2) that results in the eigenvalues of the closed-loop system [Eq. (9)] satisfying the prescribed constraints of

$$\gamma_{objective} - \gamma(g) = 0 \qquad (44)$$

where, in particular, we consider the constraint vector

$$\gamma(g) = [\omega_1(g)\ \zeta_1(g)\ \zeta_2(g)...\zeta_v(g)]^T \qquad (45)$$

The damping factors $\zeta_i(g)$ and damped frequencies $\omega_i(g)$ are related to the eigenvalues $\lambda_i(g)$ as

$$\zeta_i = -Re[\lambda_i(g)]/\{[(Re\lambda_i(g)]^2 + [Im\lambda_i(g)]^2\}^{1/2}$$

$$\omega_i = Im[\lambda_i(g)], \qquad i = 1,2,... \qquad (46)$$

The eigenvalues are labeled according to the ordering

$$|Im\lambda_1(g)| \le |Im\lambda_2(g)| \le ... \le |Im\lambda_v(g)| \qquad (47)$$

The objective values of the damping factors and the first natural frequency (the elements of $\gamma_{objective}$), for the specific

numerical example here, are prescribed as

$$\gamma_{objective} = [3.0\ 0.03\ 0.03\ 0.03\ 0.01\ 0.01\ 0.002$$
$$0.002\ 0.0015\ 0.0015] \qquad (48)$$

In order to enhance the convergence, a continuation procedure is used: Eq. (44) is replaced by the one-parameter (α) family

$$\alpha\gamma_{objective} - \gamma[g(\alpha)] = 0, \qquad 0 \le \alpha \le 1 \qquad (49)$$

Obviously, $\alpha = 0$ results in the trivial solution $g(0) = 0$ (corresponding to free, uncontrolled vibration), whereas $g(1)$ is the desired solution [since Eq. (49) becomes identical to Eq. (44)]. Sweeping α from 0 to 1 allows us to define "stepping-stone" problems that are arbitrarily near the converged neighboring solutions; thus, the generalized Newton algorithms using Eq. (43), with $W = I$ and $p \equiv g$, can be initiated with an arbitrarily close starting estimate and very nearly guarantee satisfaction of the implicit linearity assumption. For the particular calculations herein, we found rather large α increments of 1/6 led to reliable convergence. Thus, six intermediate α solutions were required to achieve final convergence; for each α value, two or three iterations [Eq. (43)] were required to find the $g(\alpha)$ satisfying Eq. (49).

As a specific example, we used the initial g vector (displayed as the elements of G_1 and G_2),

$$G_1 = G_2 = \begin{bmatrix} 0.001 & 0 & 0 & 0 & 0 & 0 & 0 & 0 & 0 \\ 0 & 0 & 0 & 0 & 0 & 0 & 0 & 0 & 0 \\ 0 & 0 & 0 & 0 & 0 & 0 & 0 & 0 & 0 \end{bmatrix}$$

The (1,1) elements were set slightly nonzero, since exactly zero causes the "rigid-body" eigenvalue to be zero with a resulting
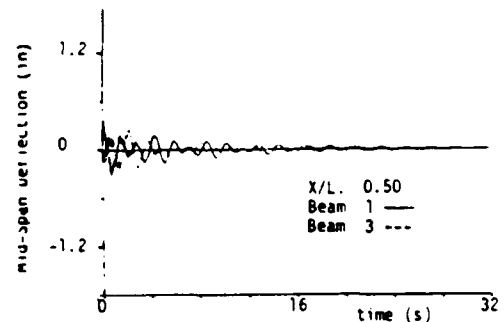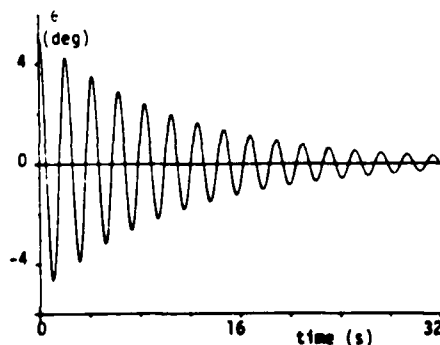

Fig. 6   Beam deflection response (midspan stations): case 1.

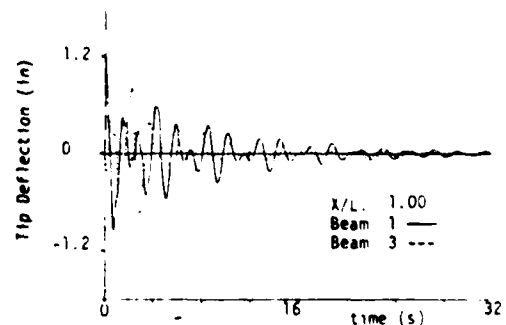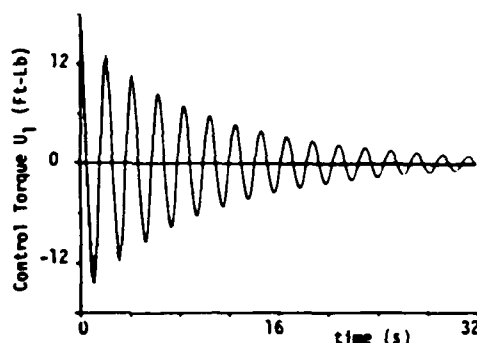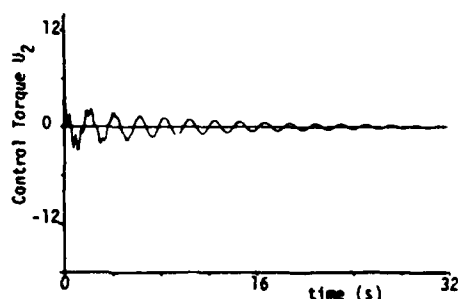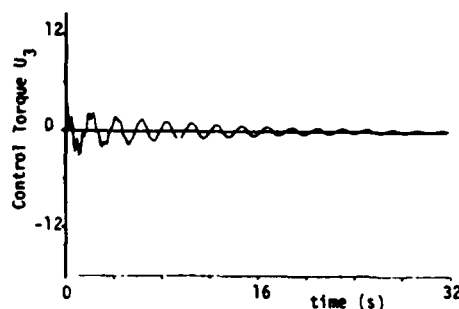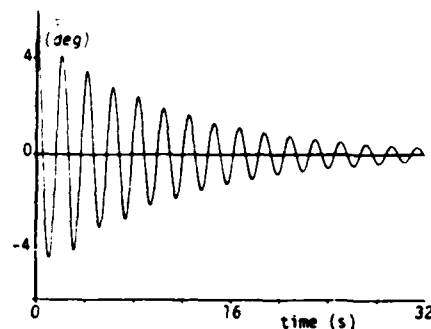Fig. 5   Closed-loop response of $\theta(t)$: case 1.

Fig. 7   Beam deflection response (tip stations): case 1.

Fig. 8   Control torque $U_1(t)$: case 1.

Fig. 10   Control torque $U_3(t)$: case 1.

Fig. 9   Control torque $U_2(t)$: case 1.

Fig. 11   Closed-loop response of $\theta(t)$: case 2.

rank-deficient linear system (because the damping ratio sensitivity vanishes if $\lambda_i \rightarrow 0$).
The final converged gain matrices were found to be (only three digits are shown)

$$G_1 = \begin{bmatrix} 153 & 4.38 & .0 & 21.5 & .0 & 4.38 & 0.0 & 21.5 & 0.0 \\ 0.0 & 2.66 & 7.89 & 13.9 & 22.5 & 2.65 & 7.89 & 13.9 & 22.5 \\ 0.0 & 2.66 & 7.89 & 13.9 & 22.5 & 2.65 & 7.89 & 13.9 & 22.5 \end{bmatrix} \tag{50a}$$

$$G_2 = \begin{bmatrix} 4.06 & -0.389 & 0.0 & -1.73 & 0.0 & -0.389 & 0.0 & -1.73 & 0.0 \\ 0.0 & 0.094 & -0.036 & 0.188 & -0.100 & 0.061 & -0.170 & 0.135 & -0.211 \\ 0.0 & 0.061 & 0.170 & 0.135 & -0.211 & 0.094 & -0.036 & 0.188 & -0.100 \end{bmatrix} \tag{50b}$$

where the 12 zeros indicate elements of G_1 and G_2 not used in p. The locii of the first nine closed-loop eigenvalues are plotted in Fig. 4 for $0 \le \alpha \le 1$, with $\alpha = 0$ the point nearest the imaginary axis in all cases. Note that, for eigenvalues 8 and 9, the structural damping produced damping factors exceeding the objective damping factors and thus these eigenvalues experienced little movement. All other higher calculated eigenvalues [Eqs. (10-12)] remained in the left half-plane, although this does not occur if the structural damping is assumed negligible.

The closed-loop response for the controlled configuration was calculated for initial disturbances of $\theta(t_0) = 5$ deg rigid-body rotation and $q_{11}(t_0) = 0.02$, which corresponds to a tip deflection of 1.66 in. for arms 1 and 2. The hub angle time history and beam deflection time histories for $z/L = \frac{1}{2}$ and 1 are illustrated in Figs. 5-7, respectively. The torque actuator responses are shown in Figs. 8-10 for actuators u_1, u_2, and u_3, respectively. In Fig. 8, it can be seen that there are high-frequency oscillations superimposed on the first few cycles of the low-frequency response. This is due to the high-frequency vibration of modes 8 and 9, but these are quickly damped out due to the structural and controller damping. Also, note that u_1 is doing most of the work compared to u_2 and u_3, a desired

result, even though we have not forced this condition by weighting.

Case 2

This case is the same as case 1 except that we modified the parameter vector to include the sensor and actuator locations, in addition to the 42 control gains of case 1, as

$p =$ actuator location vector c

$=$ sensor location vector b

$=$ gain vector g (51)

Thus, the two appendage actuator stations (z_1, z_2) plus the eight actuator sensor $(x_1,...,x_8)$ stations brings the total dimension of p to 52. Upon applying the minimum norm correction of Eq. (43) to satisfy the constraint of Eq. (44), with $W = I$, we found the sensor and actuator stations were moving undesirably large amounts, so we introduced weights of 10^2 on the actuator positions and the two inboard sensor stations, while a weight of 10^3 was applied to the two outboard sensors. With this modest artwork on the weight selection, the minimum norm algorithm was applied (with six continuation

steps as in case 1) and reliable covergence ensued to place the eigenvalues to satisfy Eqs. (44) and (48).

The resulting converged gain matrices were found to be

$$G_1 = \begin{bmatrix} 92.1 & 1.71 & 0.0 & 10.5 & 0.0 & 1.75 & 0.0 & 10.7 & 0.0 \\ 0.0 & 1.55 & 4.93 & 9.36 & 15.2 & 1.57 & 5.06 & 9.56 & 15.5 \\ 0.0 & 1.57 & 4.85 & 9.15 & 14.9 & 1.59 & 4.98 & 9.38 & 15.2 \end{bmatrix}$$ (52a)

$$G_2 = \begin{bmatrix} -4.14 & -0.165 & 0.0 & -2.43 & 0.0 & -0.305 & 0.0 & -2.80 & 0.0 \\ 0.0 & -1.09 & 2.07 & -2.80 & 4.54 & -1.13 & 1.43 & -2.76 & 3.87 \\ 0.0 & -1.10 & 1.85 & -2.60 & 4.28 & -1.21 & 1.72 & -3.04 & 4.46 \end{bmatrix}$$ (52b)

and the converged (initial values in parenthesis) appendage actuator stations were

$$z_1 = 0.1959 L \quad (0.5 L), \text{ on appendages 1 and 2}$$

$$z_2 = 0.1841 L \quad (0.5 L), \text{ on appendages 3 and 4} \quad (53)$$

whereas the converged (initial) sensor stations were, on appendages 1 and 2,

$$x_1 = 0.2546 \ (0.25 L) \qquad x_3 = 0.7155 \ (0.7 L)$$

$$x_2 = 0.5414 \ (0.5 L) \qquad x_4 = 0.9317 \ (0.9 L) \quad (54a)$$

and on appendages 3 and 4,

$$x_5 = 0.2564 \ (0.25 L)$$

$$x_6 = 0.5443 \ (0.5 L)$$

$$x_7 = 0.7167 \ (0.7 L)$$

$$x_8 = 0.9321 \ (0.9 L) \quad (54b)$$

The continuation/root locus of the eigenvalues is essentially identical to Fig. 4. However, the freedom to move the sensor and actuator locations has proved constructive; by comparison of Eqs. (50) and (52), it is obvious that the gains have been substantially reduced. Note in Eq. (53) that the appendage torquers hae been moved much closer to the hub, whereas the sensors have been moded significantly away from the hub. The net effect is that, even though the closed-loop eigenvalues have the same position, smaller control torques are required. This is evident in comparing the controlled response of case 2 to the same initial conditions as case 1 (Figs. 11-16), with the corresponding figures of case 1 (Figs. 5-10). Note that the peak torque is 17 ft-lb for case 1, whereas it is only 13 ft-lb for case 2. The controlled response is virtually unchanged (as might be expected, since the two sets of eigenvalues are the same).

Case 3

This case is the same as case 2 with two new ingredients: 1) two structural parameters the appendage length L and the tip mass m_{tip} are varied to provide some structural design control over the free-vibration frequency spectrum of the structure; and 2) in comparison to case 2, the case 3 controlled "rigid-body mode" eigenvalue is constrained to be the lower
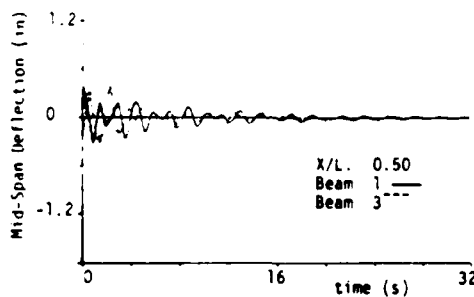

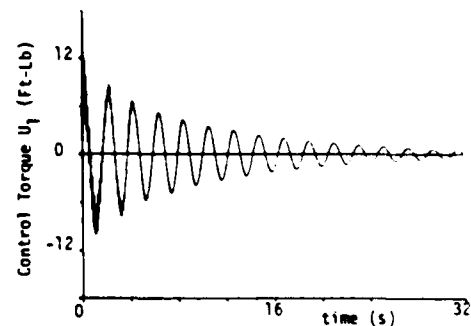Fig. 12 Beam deflection response (midspan stations): case 2.

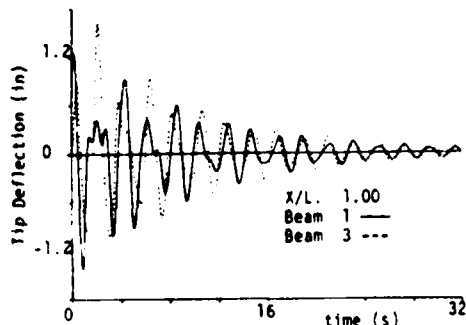Fig. 14 Control torque $U_1(t)$: case 2.

Fig. 13 Beam deflection response (tip stations): case 2.
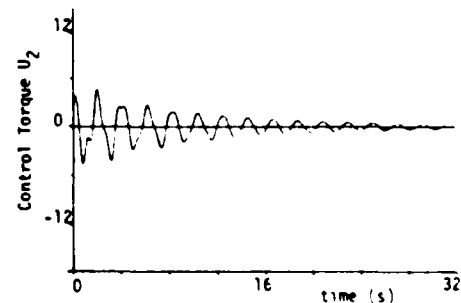
Fig. 15 Control torque $U_2(t)$: case 2.
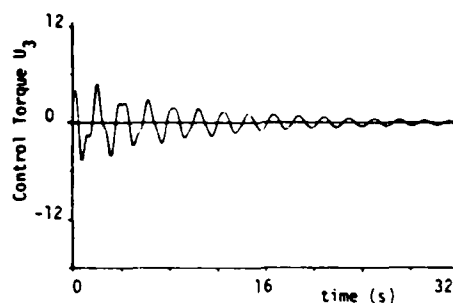
Fig. 16   Control torque $U_3(t)$: case 2.

Fig. 18   Beam deflection response (midspan stations): case 3.

Fig. 17   Closed-loop response of $\theta(t)$: case 3.

Fig. 19   Beam deflection response (tip stations): case 3.

frequency and is much more heavily damped, to be consistent with a "slewing" attitude maneuver/vibration arrest control law.

Thus, we adopt the following 12 objective constraints for the closed-loop eigenvalues (where the nonzero numbers in parentheses indicate initial natural frequencies of original uncontrolled configuration):

$\gamma_{objective} =$

$$\left\{ \begin{array}{llll} \omega_1 = 0.3 \, r/s & (0) & \text{rigid body mode frequency} \\ \omega_2 = 4.5 \, r/s & (4.37) & \text{first flexural mode frequency} \\ \omega_3 = 8.3 \, r/s & (7.91) & \text{second flexural mode frequency} \\ \zeta_1 = 0.7 & (0) & \text{rigid body mode damping factor} \\ \zeta_2 = 0.03 & (0) & \text{first flexible mode damping factor} \\ \zeta_3 = 0.03 & (0) & \text{second flexible mode damping factor} \\ \zeta_4 = 0.01 & (0) & \text{third flexible mode damping factor} \\ \zeta_5 = 0.01 & (0) & \text{fourth flexible mode damping factor} \\ \zeta_6 = 0.002 & (0) & \text{fifth flexible mode damping factor} \\ \zeta_7 = 0.002 & (0) & \text{sixth flexible mode damping factor} \\ \zeta_8 = 0.0015 & (0) & \text{seventh flexible mode damping factor} \\ \zeta_9 = 0.0015 & (0) & \text{eighth flexible mode damping factor} \end{array} \right.$$

(55)

These constraints were imposed in two stages. First, the structural parameters (L, M_{tip}) were adjusted to drive ω_2 and ω_3 to their objective values. In the second stage, the 52 control gains and sensor/actuator stations are modified (in 6 continuation steps as in case 2) to drive γ to the above objective values. Convergence was reliably obtained and the resulting control were found to be

The converged (initial) appendage actuator positions were

$z_1 = 0.4102 \, L \ (0.5 \, L)$, on appendages 1 and 2

$z_2 = 0.4102 \, L \ (0.5 \, L)$, on appendages 3 and 4   (57)

whereas the converged (initial) appendage sensor positions were, on appendages 1 and 2,

$x_1 = 0.2539 \, L \ (0.25 \, L)$

$x_2 = 0.5010 \, L \ (0.5 \, L)$

$x_3 = 0.7608 \, L \ (0.7 \, L)$

$x_4 = 0.9653 \, L \ (0.9 \, L)$ (58a)

and on appendages 3 and 4,

$x_5 = 0.2539 \, L \, (0.25 \, L)$

$x_6 = 0.5010 \, L \ (0.5 \, L)$

$x_7 = 0.7608 \, L \ (0.7 \, L)$

$x_8 = 0.9653 \, L \ (0.9 \, L)$ (58b)

$$G_1 = \begin{bmatrix} 4.84 & 0.148 & 0.0 & 1.01 & 0.0 & 0.148 & 0.0 & 0.101 & 0.0 \\ 0.0 & 0.034 & 0.116 & 0.214 & 0.315 & 0.037 & 0.125 & 0.231 & 0.341 \\ 0.0 & 0.036 & 0.125 & 0.231 & 0.341 & 0.034 & 0.116 & 0.214 & 0.315 \end{bmatrix}$$ (56a)

$$G_2 = \begin{bmatrix} 16.3 & -0.026 & 0.0 & -0.148 & 0.0 & -0.026 & 0.0 & -0.148 & 0.0 \\ 0.0 & 0.065 & 0.011 & 0.138 & -0.256 & -0.066 & -0.068 & 0.111 & -0.068 \\ 0.0 & 0.066 & -0.448 & -0.111 & -0.448 & 0.065 & 0.011 & 0.137 & -0.256 \end{bmatrix}$$ (56b)
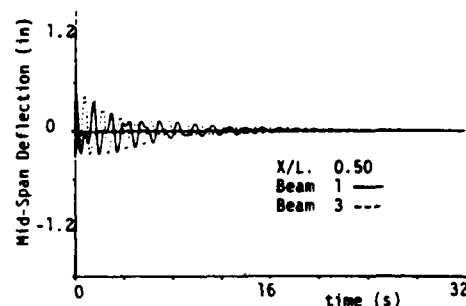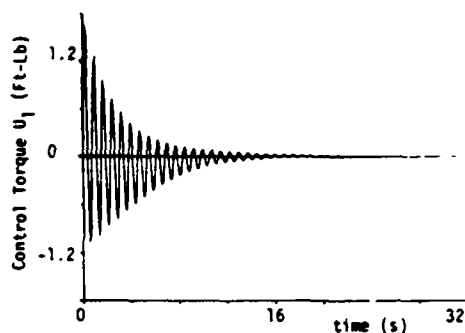
Fig. 20   Control torque $U_1(t)$: case 3.
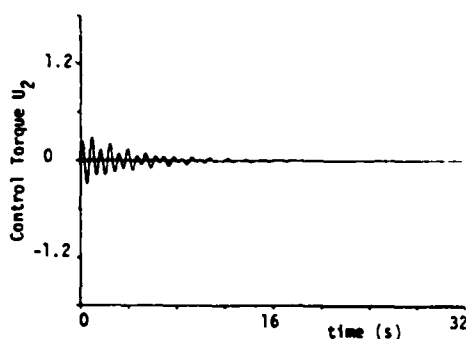
Fig. 21   Control torque $U_2(t)$: case 3.
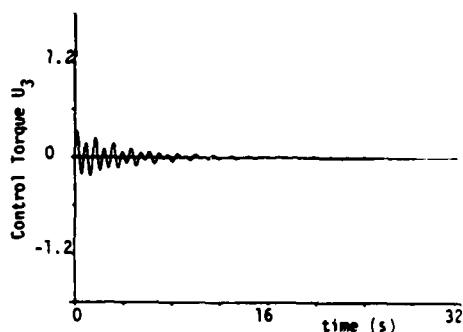
Fig. 22   Control torque $U_3(t)$: case 3.

The converged (initial) values for L and M_{up} were found to be

$L = 3.67$ ft   (4 ft)

$M_{up} = 0.19871$ slugs   (0.156941 slugs)

The controlled response for case 3 is given in Figs. 17-22 for comparison with cases 1 and 2. Note the following features: 1) the rigid-body maneuver and complete vibration arrest is accomplished in approximately 15 s (about half the time required for cases 1 and 2); 2) the peak control torque is reduced by about an order of magnitude; and 3) the location of sensors is not significantly different from case 2, but the actuator posi-

tions are different (closer to midspan). It is also evident that the present maneuver controls are much more attractive than cases 1 and 2. We have done a variety of parameter variations further establishing that the rigid-body eigenvalue placement is the most important feature of case 3. For any reasonable variation of the sensor/actuator stations and/or structural parameters, we can optimize the control gains to place the eigenvalues in the same position and achieve analogous results.

Conclusions

We have developed and demonstrated a minimum modification strategy for structural and control parameter optimization. Numerical experience indicates occasional difficulties with the uncontrolled modes being destabilized, but since all of the eigenvalues (up through a conservative number) are calculated on each iteration, these problems can be circumvented by introducing appropriate constraints to stabilize these modes. The method has worked well on the problems studied to date and appears to be an attractive approach to follow in the development of an interactive software system for structure/controller design iterations. Extension of the ideas of this paper to determine the weight matrices for imposing eigenvalue placement upon optimal quadratic regulators is presented in Ref. 8. The algorithms presented herein have been found relatively immune to the high dimensionality and nonlinearity of the eigenvalue placement problem.

References

[1] Plaut, R.H. and Huseyin, K., "Derivatives of Eigenvalues and Eigenvectors in Non-Self-Adjoint Systems," *AIAA Journal*, Vol. 11, Feb. 1973, pp. 250-251.

[2] Turner, J.D. and Chun, H.M., "Optimal Feedback Control of a Flexible Spacecraft During a Large Angle Rotational Maneuver," AIAA Paper 82-1589, Aug. 1982.

[3] Chun, H.M., "Optimal Distributed Control of a Flexible Spacecraft During a Large Angle Rotational Maneuver," MS Thesis, Massachusetts Institute of Technology, Cambridge, June 1982.

[4] Junkins, J.L., "Equivalence of the Minimum Norm and Gradient Projection Constrained Optimization Techniques," *AIAA Journal*, Vol. 10, July 1972, pp. 927-929.

[5] Fiacco, A.V. and McCormick, G.P., *Nonlinear Programming: Sequential Unconstrained Minimization Techniques*, John Wiley & Sons, New York, 1968.

[6] Anderson, L., "Direct Design of Multivariable Control Systems Through Singular Value Decomposition," AAS/AIAA Astrodynamics Conference, Aug. 1983.

[7] Junkins, J.L., Bodden, D.S., and Kamat, M.P., "An Eigenvalue Optimization Approach for Feedback Control of Flexible Structures," presented at SECTAM XII, Calloway Gardens, GA., May 1984.

[8] Junkins, J.L., Bodden, D.S., and Turner, J.C., "A Unified Approach to Structure and Control System Design Iterations," *Proceedings of 4th International Conference on Applied Numerical Modeling*, Society of Theoretical and Applied Mechanics, Republic of China, Dec. 1984, pp. 483-490.

OPTIMAL REDESIGN OF DYNAMIC STRUCTURES VIA SEQUENTIAL LINEAR PROGRAMMING

K. B. Lim

J. L. Junkins

Texas A&M University

OPTIMAL REDESIGN OF DYNAMIC STRUCTURES
VIA SEQUENTIAL LINEAR PROGRAMMING

Kyong B. Lim
Graduate Research Assistant
Department of Engineering Science & Mechanics
Virginia Polytechnic Institute and State University
Blacksburg, Virginia 24061

John L. Junkins
Professor
Department of Aerospace Engineering
Texas A&M University
College Station, Texas 77843

ABSTRACT

A sequential linear programming approach for optimal placement/constrained optimization of eigenvalues and eigenvectors of linear dynamical systems is presented. As an example, the total mass of a structure is minimized while the natural frequencies for selected modes are gradually driven to desired values. This highly nonlinear constrained optimization problem is locally linearized and linear assumptions enforced by specifying maximum allowable local parameter changes. However, the above constraints on the magnitude of local parameter change restricts the magnitude of changes in the system characteristics, and in particular, eigenvalue constraint objectives which may differ significantly from nominal starting values. The above difficulty is overcome by a well tested continuation technique which replaces the original, possibly rigid, constraints by an adjustable sequence of neighboring constraints. The above approach appears computationally suitable for redesign of high-dimensioned, complex dynamical systems. Numerical examples are included to demonstrate the practical merit of this approach.

NOMENCLATURE

J	cost function
p_s	design vector
p^s	starting design vector
Δp	design vector change
f_o	constraint vector
f^o	constraint objective vector
F	current constraint objective vector
Y	continuation parameter
ϵ	maximum allowable local parameter change vector
y	transformed design vector change
x	generalized displacement vector
M	global mass matrix
K	global stiffness matrix
M_j	mass matrix for j-th element
K_j	stiffness matrix for j-th element
h_j	beam element length
θ	mass/length distribution
η	bending stiffness distribution
E	Young's modulus
ρ	mass density
ψ	element shape function
ξ_ℓ	nondimensionalized element coordinates
p^ℓ	lower bound vector on nodal thickness
p^u	upper bound vector on nodal thickness
λ_o	eigenvalue vector
λ^o	objective eigenvalue vector
ω	natural frequency
v	eigenvector

INTRODUCTION

The practical need for optimal redesign of existing dynamic structures is clearly evident. A good example is aeroelastic tailoring where stiffness, mass and geometrical characteristics of an aircraft structure are optimally distributed using composite materials, for the improvement of aeroelastic properties. For dynamic structures in general, modifications are usually focused on modal characteristics. However, since modal characteristics and design vectors are related by eigenvalue problems, the relationship is naturally complex in addition to being numerically formidable for high dimensioned systems. The optimization problem is further complicated if the designer wishes to consider a large number of constraints, mostly inequalities, on the minimum and/or maximum allowable design vector.

In this paper, the optimal redesign problem is treated as a general nonlinear programming problem. The cost function and constraint equations are linearized about a nominal design to obtain a sequential set of linear optimization problems. The above linearization assumes a good initial guess of the design vector. Unfortunately, for problems which includes eigenvalue constraints and are structurally complex, good initial guess of the design vector may be impossible to obtain, or at best depends heavily on the designer's experience and the type and amount of redesign desired. The above need for good initial guess can be overcome; at least to a very significant degree, by introducing the continuation method of handling constraint equations. This amounts to replacing the original constraint equations by a sequential neighboring set of constraint equations. Earlier applications of continuation techniques are given in [1,2] where closed-loop eigenvalue constraints are considered in the context of control system design. The present work was motivated by the introduction in [3] of sequential linear programming algorithm to optimize damper locations for vibration suppression. In [3,4], the sequential linear programming approach combined with the continuation method is used for the design of control systems. The development in this paper closely parallels the work in [4] and differs primarily in the optimization/design objectives, i.e., structural redesign instead of controls design.

To demonstrate the proposed approach of optimal structural redesign, a Finite Element (FE) model of a cantilever beam is considered. The thickness at the nodes are chosen as design parameters for a constant width, rectangular cross section beam. The cost function to be minimized is chosen as the total mass of the beam while selected natural frequencies are gradually driven to desired values subjected to

geometrical inequality constraints on the maximum and minimum thickness along the beam.

TRANSFORMATION OF A GENERAL NONLINEAR PROGRAMMING PROBLEM TO A SEQUENTIAL LINEAR PROGRAM

Let us consider the general nonlinear programming problem,

$$\text{maximize} \quad J(p)$$
$$p$$
$$\text{subject to} \quad f(p) \ \{<, \ =, \ >\} \ f^O \qquad (1)$$

where p is the design vector and f^O is the constraint objective. By linearizing Eq. (1) about a nominal design, i.e. at i-th step, we get,

$$\text{maximize} \quad J(p_{i-1}) + \frac{\partial J}{\partial p}\Big|_{p_{i-1}} \Delta p + \dots$$
$$\Delta p$$

subject to

$$f(p_{i-1}) + \frac{\partial f}{\partial p}\Big|_{p_{i-1}} \Delta p + \dots \ \{\leq, =, \geq\} \ f^O \qquad (2)$$
where
$$p_i = p_{i-1} + \Delta p$$

The formulation in Eq. (2) suffers two major problems; a feasible solution to the original problem may not exist, and a sufficiently good initial guess to validate linear expansion maybe impossible to obtain. The continuation method resolves the above problems by (i) seeking at least a feasible solution to a neighbor of the original problem if indeed a feasible solution to the original problem does not exist and, (ii) eliminating the need for a good initial guess by starting the iteration with a neighboring converged solution. The continuation method does the above by replacing the original constraint objectives, f^O, by a sequential neighboring set of constraint objectives, $F(\gamma)$, where

$$F(\gamma_i) = (1 - \gamma_i) \ f(p^S) + \gamma_i \ f^O \qquad (3)$$

where p^S is an arbitrarily chosen starting design vector (more appropriately, p^S is associated with the unmodified existing structure) and γ_i is a scalar parameter satisfying

$$0 = \gamma_0 \leq \gamma_1 \leq \gamma_2 \dots \leq \gamma_N = 1$$

The convex combination of starting constraint and final constraint shown in Eq. (3) reveals the following facts:

at $\gamma = \gamma_0 = 0$, $F(0) = f(p^S)$

at $\gamma = \gamma_N = 1$, $F(1) = f(p^O)$

i.e. if convergence is achieved at $\gamma = 1$, we recover the original objective constraint condition. It is also obvious but nevertheless important to note that if the problem has a feasible solution at $\gamma = 1$, the problem will be solved in N steps.

Applying the continuation technique of Eq. (3) to the right hand side of Eq. (2), we obtain

$$\text{maximize} \quad J(p_{i-1}) + \frac{\partial J}{\partial p}\Big|_{p_{i-1}} \Delta p + \dots \qquad (4)$$
$$\Delta p$$

subject to

$$f(p_{i-1}) + \frac{\partial f}{\partial p}\Big|_{p_{i-1}} \Delta p + \dots \ \{\leq, =, \geq\} \ (1-\gamma_i) f(p^S) + \gamma_i \ f^O$$
where
$$p_i = p_{i-1} + \Delta p$$

The optimization problem of Eq. (4) must be transformed to a non-negative variable so that the Simplex algorithm [5] may be used directly. In addition, the output of a Simplex algorithm may still predict large corrections for some elements of Δp. For the above reasons, we introduce bounds on the maximum allowable local parameter change,

$$-\epsilon \leq \Delta p \leq \epsilon \qquad (5)$$

which enhances local linearizations. The transformation to non-negative variables and the bounding of local change can be easily done by introducing a linear transformation.

$$y = \Delta p + \epsilon \qquad (6)$$

Using Eq. (5) and (6) in (4), we obtain the standard linear program at step "i",

$$\text{maximize} \quad \frac{\partial J}{\partial p}\Big|_{p_{i-1}} y + \dots \qquad (7)$$
$$y$$

subject to

$$\frac{\partial f}{\partial p}\Big|_{p_{i-1}} y \{\leq, =, \geq\} (1-\gamma_i) f(p^S) + \gamma_i f^O - f(p_{i-1}) + \frac{\partial f}{\partial p}\Big|_{p_{i-1}} \epsilon$$

$$y \leq 2\epsilon$$
$$y \geq 0$$

where

$$\Delta p = y - \epsilon$$
$$p_i = p_{i-1} + \Delta p$$

MINIMUM WEIGHT DESIGN OF A BEAM FINITE ELEMENT MODEL

To demonstrate the approach outlined earlier, we consider here the problem of minimum weight design of a cantilever beam structure modeled by finite elements. A nominal uniform beam is assumed given and its corresponding natural frequencies known. The problem is to find the minimum weight configuration among all those which satisfies desired natural frequency equality constraints and thickness inequality constraints. We note here that the above constraints may arise form physical factors such as material property limitations, desired natural frequency locations or static buckling design limitations.

Consider the linear free vibration equations

$$M\,x(t) + K\,x(t) = 0 \qquad (8)$$

where

$$M = \sum_{j=1}^{ne} M_j \qquad K = \sum_{j=1}^{ne} K_j \qquad (9a)$$

represents the global mass and stiffness matrices. For thin beams in transverse vibration, the j-th element mass and stiffness matrices takes the form,

$$M_j = \frac{h}{2} \int_{-1}^{1} \theta_j\,(\xi)[\psi][\psi]^T d\xi \qquad (9b)$$

$$K_j = \frac{8}{h^3} \int_{-1}^{1} \eta_j\,(\xi) \left[\frac{d^2\psi}{d\xi^2}\right] \left[\frac{d^2\psi}{d\xi^2}\right]^T d\xi \qquad (9c)$$

where ψ is the element shape function, θ_j and η_j are the mass and stiffness distributions over j-th element and h represents the element length.

To form the design vector, we let the thickness values at some judicious choice of FE nodes be the unknowns and linearly interpolate the nodal values whenever we need internal values. The design vector can then be written as

$$p = (P_1, \ldots, P_{NP})^T$$

where P_i represents the beam thickness at i-th node and NP is the total number of design parameters.

We now formulate the minimum weight eigenvalue placement problem as,

minimize $J(p)$
  p

where

$$J(p) = \rho a h [1/2, 1, 1, \ldots, 1, 1, 1/2] p \qquad (10a)$$

subject to

$$\lambda_j = \lambda^o_j \qquad j = 1, \ldots, NM \qquad (10b)$$

$$p^{\ell}_j \le p_j \le p^u_j \qquad j = 1, \ldots, NP \qquad (10c)$$

where λ^o is the objective (desired) eigenvalue and p^{ℓ}, p^u are the lower and upper bounds on nodal thicknesses.

Following earlier derivations, the problem posed in Eq. (10) can be transformed to the form of Eq. (7) to obtain the linear program at step i,

maximize $-hc^T y$ \qquad (11a)
  y

subject to

$$Ey \le g + E\epsilon \qquad (11b)$$

$$y \le 2\epsilon \qquad (11c)$$

$$\frac{\partial \lambda}{\partial p}\Big|_{p_{i-1}} y = (1-\gamma_i)\lambda(p^s) + \gamma_i \lambda^o - \lambda(p_{i-1}) + \frac{\partial \lambda}{\partial p}\Big|_{p_{i-1}} \epsilon \qquad (11d)$$

$$y \ge 0 \qquad (11e)$$

where

$$\Delta p = y - \epsilon$$
$$p_i = p_{i-1} + \Delta p$$

and

$$E = \left[\begin{array}{c} I \\ \hline -I \end{array}\right]$$

$$g = \left[\begin{array}{c} p^u - p_{i-1} \\ \hline -p^{\ell} + p_{i-1} \end{array}\right]$$

The major computational effort required in the problem as posed in Eq. (11) involves solving the generalized symmetric eigenvalue problem

$$\lambda M v = K v$$

for the selected NM modes and the solution of the linear program itself using the Simplex Method. The eigenvalue sensitivities required in Eq. (11d) is derived in [6] and given as,

$$\frac{\partial \lambda_i}{\partial p_j} = v_i^T \left(\frac{\partial K}{\partial p_j} - \lambda_i \frac{\partial M}{\partial p_j}\right) v_i \qquad (12)$$

The stiffness and mass sensitivity matrices required above can be computed and assembled in same fashion as stiffness and mass matrices themselves in Eq. (9), and is given by,

$$\frac{\partial M}{\partial p_j} = \sum_{r=1}^{ne} \frac{\partial M_r}{\partial p_j} \qquad , \qquad \frac{\partial K}{\partial p_j} = \sum_{r=1}^{ne} \frac{\partial K_r}{\partial p_j} \qquad (13a)$$

where

$$\frac{\partial M_j}{\partial p_k} = \frac{h}{2} \int_{-1}^{1} \frac{\partial \theta_j}{\partial p_k}\,(\xi)[\psi][\psi]^T d\xi \qquad (13b)$$

$$\frac{\partial K_j}{\partial p_k} = \frac{8}{h^3} \int_{-1}^{1} \frac{\partial \eta_j}{\partial p_k}\,(\xi) \left[\frac{d^2\psi}{d\xi^2}\right] \left[\frac{d^2\psi}{d\xi^2}\right]^T d\xi \qquad (13c)$$

We emphasize here that in the above problem, the continuation family of constraint objectives, as given by Eq. (3), was applied only to the eigenvalue constraints of Eq. (10b) since it was deemed the only compromisable and nontrivial constraint.

NUMERICAL EXAMPLE

Table 1 gives the data for the particular cantilever beam FE model considered. Two cases were computed to illustrate the main features of the design approach, specifically, the effect of relaxing constraints and the effect of different starting beam configuration on the final converged configurations.

The effects of relaxing stiffness constraints are given in Table 2. The starting frequencies and objective natural frequencies are given in Table 2a. The total mass design history is given in Table 2b. It is noted that all three cases reached the final objectives. In addition, the total mass decreases as the lower bounds on thickness decreases, thus verifying the fact that more design flexibility leads to better performance. Table 2c shows the uniform initial design vector, the imposed lower and upper bounds and the final design configurations, which is highly non-uniform. Incidentally, several elements of the design vector have reached their lower and upper limits and clearly this is useful information to the designer.

The effects of different starting beam configurations are give in Table 3. Obviously, different nominal beams corresponds to different initial natural frequencies. However, all three completely different starting beams converged to essentially the same total weight and similar configuration beam as seen in Tables 3b and 3c. The results above are consistent with a conclusion reached in [3] that the continuation procedure with sequential linear optimization more often converges and yields the same solutions for different initial conditions than does conventional nonlinear optimization routines.

In the previous examples, the thickness constraints and the objective frequencies were not too demanding. The above relaxed circumstance were the main reasons for the success of all previous runs. Additional results, not shown here, indicates that imposing more restrictive bounds on the thickness made the realization of frequency objectives more difficult and in some cases its convergence to desired conditions impossible.

CONCLUSIONS

A sequential linear programming approach combined with a continuation method of handling constraints has been derived for attacking a class of nonlinear programming problems and in particular, optimal structural redesign problems. The numerical robustness of the proposed algorithm has been demonstrated by a minimum weight redesign problem with eigenvalue constraints consisting of 20 degrees of freedom and 38 constraints with 11 design parameter.

A major advantage of the linear optimization approach presented here is that at each continuation step, an optimal solution, if it exists, can be found very efficiently using the well founded Simplex method. The reason is that only a finite number of feasible possibilities exists and the he Simplex algorithm efficiently computes the optimal solution. A second major advantage is the flexibility to handle equality and inequality constraints on both the design variables and functions thereof.

Finally, and perhaps most importantly, failures to reach the final ($\gamma = 1$) solution is usually softened by convergence to an intermediate ($0 < \gamma < 1$) neighbor. The active constraint set and gradient information of the final convergence provides a basis for intelligent revisions of the problem statement.

REFERENCES

1. Bodden, D.S. and Junkins, J.L., "Eigenvalue Optimization Algorithms for Structural/Control Design Iterations," ACC, San Diego, CA, June 6-8, 1984

2. Junkins, J.L., Bodden, D.S. and Turner, J.D., "A Unified Approach to Structure and control System Design Iterations," Fourth International Conference on Applied Numerical Modelling, Tainan, Taiwan, Dec. 27-29, 1984

3. Horta, L.G., Juang, J-N, and Junkins, J.L., "A Sequential Linear Optimizatio. Approach for Controller Design," AIAA Paper 85-1971-CP, AIAA Guidance, Navigation & Control Conference, Snowmass, CO, Aug. 19-21, 1985

4. Lim, K.B. and Junkins, J.L. "Minimum Sensitivity Eigenvalue Placement via Sequential Linear Programming," Proceedings of the Mountain Lake Dynamics and Control Institute, Mountain Lake, VA, June 9-11, 1985, pp. 122-144

5. Hadley, G., Linear Programming, Addison-Wesley Publishing Co., Inc., Reading, MA, 1962

6. Fox, R.L. and Kapoor, M.P., "Rates of Change of Eigenvalues and Eigenvectors," AIAA Journal, Vol. 6, No. 12, Dec. 1968, pp. 2426-29

Young's Modulus	21.5×10^6 psi
mass density	.065 lb/in^3
beam width	1 in
beam length	100 in
number of elements (uniform length)	10
number of degrees of freedom	20
dimension of design vector	11
number of equality constraints on frequencies	5
number of lower bound inequality constraints on thickness	11
number of upper bound inequality constraints on thickness	11
number of inequality constraints on maximum allowable local parameter change	11

Table 1. Data for graphite epoxy cantilever beam finite element model

ω^s (rad/sec)	ω^o (rad/sec)
1.84	2.82
11.5	10.9
32.3	30.8
63.5	67.0
105.1	104.8

Table 2a. Effect of relaxing constraints-starting and objective frequencies.

$$p^s = (1,\ldots,1)^T$$
$$p^u = (2,\ldots,2)^T$$

γ	$p^\ell = .5$	$p^\ell = .3$	$p^\ell = .1$
0	6.5	6.5	6.5
.1	6.1	6.1	6.1
.2	5.8	5.8	5.8
.3	5.7	5.6	5.6
.4	5.5	5.2	5.1
.5	5.6	5.1	4.5
.6	5.7	5.1	4.3
.7	5.8	5.2	4.4
.8	5.9	5.3	4.5
.9	6.0	5.4	4.6
1.0	6.1	5.6	4.7

Table 2b. Effect of relaxing constraints-total mass histories for different stiffness constraints

Node No.	Nodal Coord. (in.)	Starting Thickness (in.)	$p^{\ell} = .5$ Final Thickness (in.)	$p^{\ell} = .3$ Final Thickness (in.)	$p^{\ell} = .1$ Final Thickness (in.)
1	0	1.0	1.791	1.753	1.620
2	10	1.0	.531	.300	.100
3	20	1.0	1.811	2.000	1.916
4	30	1.0	1.407	.482	.100
5	40	1.0	.668	1.139	1.083
6	50	1.0	1.116	1.252	1.148
7	60	1.0	.589	.657	.666
8	70	1.0	.500	.300	.100
9	80	1.0	1.092	1.157	.990
10	90	1.0	.500	.434	.371
11	100	1.0	.500	.300	.100

Table 2c. Effort of relaxing Constraints - converged design vector ($\gamma = 1$)

$$p^{u} = (2,\ldots,2)^{T}$$

Mode No.	$\omega^{s}(1)$	$\omega^{s}(2)$	$\omega^{s}(3)$	$\omega^{s}(4)$	ω^{f}
1	1.84	1.70	1.75	3.14	3.00
2	11.5	11.4	9.67	10.8	11.5
3	32.4	31.7	23.7	29.3	30.8
4	63.5	61.1	49.7	59.2	67.0
5	105.2	105.7	89.9	91.2	105.2

Table 3a. Effect on different starting beam configurations - starting and final frequencies for four beams.

$$p^{L} = (.5,\ldots,.5)^{T}$$

$$p^{u} = (2,\ldots,2)^{T}$$

Y	Starting beam (1)	Starting beam (2)	Starting beam (3)	Starting beam (4)
0	6.5	6.4	5.7	6.5
.1	6.1	6.0	5.7	6.1
.2	5.9	5.7	5.6	6.1
.3	5.7	5.5	5.4	6.1
.4	5.6	5.5	5.3	6.1
.5	5.7	5.6	5.4	6.0
.6	5.8	5.7	5.5	6.0
.7	5.9	5.9	5.7	6.0
.8	6.0	6.0	5.8	6.1
.9	6.0	6.0	5.9	6.1
1.0	6.1	6.1	6.0	6.1

Table 3b. Effect of different starting beam configurations-total mass histories

Node No.	Beam (1) p^s	Beam (1) p^f	Beam (2) p^s	Beam (2) p^f	Beam (3) p^s	Beam (3) p^f	Beam (4) p^s	Beam (4) p^f
1	1.00	1.91	.95	1.90	.80	2.00	1.50	2.00
2	1.00	.50	.85	.50	.90	.50	1.50	.50
3	1.00	1.77	1.00	1.79	1.30	1.62	1.50	1.67
4	1.00	1.71	.95	1.69	.70	.50	1.50	1.26
5	1.00	.59	1.10	.59	.90	1.71	1.50	1.32
6	1.00	1.04	.91	1.04	.90	.50	.60	.50
7	1.00	.71	1.20	.71	1.00	1.51	.60	1.06
8	1.00	.50	1.00	.50	1.00	.50	.60	.50
9	1.00	.96	.88	.97	.50	.50	.60	.69
10	1.00	.50	1.00	.50	.60	.70	.60	.72
11	1.00	.50	.98	.50	1.40	.52	.60	.50

Table 3c. Effect of different starting beam configurations - starting and final thickness

A SIMULTANEOUS STRUCTURE/CONTROLLER DESIGN ITERATION METHOD

J. L. Junkins

D. W. Rew

A SIMULTANEOUS STRUCTURE/CONTROLLER
DESIGN ITERATION METHOD

John L. Junkins and Dong Won Rew
Department of Engineering Science and Mechanics
Virginia Polytechnic Institute and State University
Blacksburg, VA 24061

Abstract

Several methods are presented for placement/constrained optimization of the closed loop eigenvalues and eigenvectors of linear dynamical systems. A unified approach is taken to (i) iterate the design parameters in the plant being controlled, (ii) the location of sensor and actuators, (iii) the elements of a direct output feedback gain matrix, and (iv) the weight matrices in a time-domain LQG performance index, or (v) a combination of the foregoing, to accomplish a constrained, simultaneous optimization of the system's closed loop eigenvalues, eigenvectors, and their sensitivities. A low dimensioned discrete system and an order 42 model of a flexible structure controlled via direct output feedback are used to illustrate the approach.

1. INTRODUCTION

We show below that several different methods to design high order linear feedback control laws can be unified in the sense that a single approach can be taken to "optimally tune" these methods vis-a-vis the placement and sensitivity of the closed-loop eigenvalues and eigenvectors. In Sections 2 and 3, we formulate a generalized closed loop eigenvalue sensitivity and constrained optimization approach. In Sections 4, 5, 6, we show how three different approaches to design of linear feedback controllers lead naturally to the problem formulated in Sections 2 and 3. In Section 7, we summarize numerical solutions of two examples, finally in Section 8, we offer concluding remarks.

2. CLOSED LOOP EIGENVALUE PROBLEM

We are concerned with linear dynamical systems in the generalized state-space form

$$Z\dot{x} = Ax + Bu + d \tag{1}$$

with linear output

$$y = Hx \tag{2}$$

and linear feedback control

$$u = Gy \tag{3}$$

Thus the closed loop system is governed by

$$Z\dot{x} = \bar{A}x + d \tag{4}$$

where

Z, A are n x n real matrices
x   is an n x 1 real state vector
u   is an m x 1 real control vector
d   is an n x 1 real disturbance vector
y   is an r x 1 real measured output vector
B   is an n x m real matrix

H   is an r x n real matrix
G   is an m x r real control gain matrix

and the closed loop system matrix is

$$\bar{A} = A + BGH \tag{5}$$

In the absence of disturbances (d = 0), the closed loop performance can be obtained by assuming an exponential solution of the form $x = \alpha \exp(\lambda t)$; this leads to the generalized eigenvalue problems:

$$\text{right: } \lambda_i Z\alpha_i = \bar{A}\alpha_i; \quad \text{left: } \lambda_i Z^T\beta_i = \bar{A}^T\beta_i \tag{6}$$

where $i = 1,2,\ldots,n$ and α_i, β_i are the right and left eigenvectors corresponding to the assumed distinct eigenvalues $(\lambda_1, \ldots, \lambda_n)$. The eigenvalues and eigenvectors are generally complex. We adopt the conventional normalizations:

$$[\beta]^T Z[\alpha] = [I] \quad , \quad [\beta]^T \bar{A}[\alpha] = \text{diag}[\lambda_i] \tag{7}$$

where $[\alpha] = [\alpha_1 \ldots \alpha_n]$ and $[\beta] = [\beta_1 \ldots \beta_n]$ are the right and left "modal" matrices.

Let us now address the situation in which all, or at least, some of the matrices A, Z, B, H, G, and therefore $\bar{A} = A + BGH$, are functions of a q x 1 system design vector p. The elements p_l of p can be, for example, (i) the control gains (elements of G), (ii) an indirect parameterization of G (e.g., the weights in an LQG performance measure), (iii) sensor/actuator locations (parameterization of the elements of B, H), or (iv) plant model parameters (parameterization of the elements of A, Z). Since $\bar{A} = \bar{A}(p)$ and $Z = Z(p)$, it is evident that $\lambda_i = \lambda_i(p)$ and $\alpha_i = \alpha_i(p)$; except for isolated events (e.g. bifurcation points, near-multiple eigenvalues, etc.), we can consider $\lambda_i(p)$ and $\alpha_i(p)$ to be continuous and differentiable. It is therefore reasonable to question whether or not it is feasible to "tune" p to solve a constrained optimization of $\lambda_i(p)$ and $\alpha_i(p)$.

The first and second order sensitivities of the eigenvalues are derived in references [1] and [2], these are as follows:

$$\frac{\partial \lambda_i}{\partial p_l} = \beta_i^T \left[\frac{\partial \bar{A}}{\partial p_l} - \lambda_i \frac{\partial Z}{\partial p_l} \right] \alpha_i \tag{8}$$

$$\frac{\partial^2 \lambda_i}{\partial p_l \partial p_m} = \beta_i^T \left[\frac{\partial^2 \bar{A}}{\partial p_l \partial p_m} - \lambda_i \frac{\partial^2 Z}{\partial p_l \partial p_m} \right] \alpha_i$$
$$- \beta_i^T [P_{im}\alpha_i \beta_i^T \frac{\partial Z}{\partial p_l}] \alpha_i - \beta_i^T [\frac{\partial Z}{\partial p_m} \alpha_i \beta_i^T P_{il}] \alpha_i$$

$$+ \sum_{k=1, k \neq i}^{n} [\frac{a_i^T P_{im} a_k a_k^T P_{i\ell} a_i + a_k^T P_{im} a_i a_i^T P_{i\ell} a_k}{(\lambda_i - \lambda_k)}]$$

$$(9)$$

where

$$P_{im} \equiv \frac{\partial \bar{A}}{\partial p_m} - \lambda_i \frac{\partial Z}{\partial p_m} \qquad (10)$$

and

$$\frac{\partial \bar{A}}{\partial p_\ell} \quad , \quad \frac{\partial Z}{\partial p_\ell} \quad , \quad \frac{\partial^2 \bar{A}}{\partial p_\ell \partial p_m} \quad , \quad \frac{\partial^2 Z}{\partial p_\ell \partial p_m}$$

are determined from direct differentiation of the parametric system model (which obviously must be a continuous parameterization). Analogous development lead to the sensitivity of the eigenvectors, and the above simplify considerably for the most usual case that Z = the identity matrix. Clearly the above formulations suffer singularities near multiple eigenvalues. It should be noted that having completed the solution of the eigenvalue problem, the evaluation of the eigenvalue partial derivatives represent a rather modest additional computational expense.

3. EIGENVALUE/EIGENVECTOR PLACEMENT/OPTIMIZATION

One popular course (in attempting to place eigenvalues for multiple-input, multiple-output systems, MIMO) is to make use of various decoupling devices to map the problem into a family of "pseudo-equivalent" single-input, single-output systems and thereby render the eigenvalue placement problem trivial. The problem with this entire class of approaches lies in the fact that artificial, physically meaningless constraints are invariably introduced which often lead to poor controller designs as well as numerical difficulties; see Ref. [3] for a discussion of these issues and the recent literature. In lieu of attempting to eliminate the redundancy in an ad hoc fashion (more parameters to specify than the typical number of eigenvalue constraints), we elect to follow the pattern of Refs. 1, 4-7 and exploit the redundancy to optimize a performance measure.

Consider the following optimization problem: We wish to minimize a criterion function

$$C = \text{function} (\lambda_1(p),...,\lambda_n(p), a_1(p),...,a_n(p), p)$$

$$= f(p) \qquad (11)$$

subject to a vector function of m_e equality constraints

$$g_0 - g(p) = 0 \qquad (12)$$

and a vector function of m_{ie} inequality constraints

$$h_\ell \leq h(p) \leq h_u \qquad (13)$$

where g_0, h_ℓ, h_u are given constant vectors de-

fining the family of admissible designs.

First, consider only the equality constraints of Eq. (12). The starting iterative p_{start} may result in large violations of Eq. 12 and is often too far from a zero of Eq. (12) to permit reliable convergence using a generalized Newton algorithm. Let us first find a feasible p which satisfies Eqs. (12) and then Eqs. (13), before we consider the issue of optimization. In lieu of g_0, we introduce the "portable" objective constraint vector g_p such that

$$g_p = \gamma g_0 + (1 - \gamma) g(p_{start}) \qquad (14)$$

with a homotopy or continuation parameter γ satisfying $0 \leq \gamma \leq 1$. Replacing g_0 in Eq. (12) by g_p of Eq. (14), and considering $p = p(\gamma)$, gives a homotopy family of equality constraints

$$H(p(\gamma)) = \gamma g_0 + (1 - \gamma) g(p_{start}) - g(p(\gamma)) = 0$$

$$(15)$$

Notice the boundary conditions on Eq. (15)

at $\gamma = 0$: $H(p(0)) = g(p_{start}) - g(p(0)) = 0$ (16)

at $\gamma = 1$: $H(p(1)) = g_0 - g(p(1)) = 0$ (17)

from which we conclude that $p(0) = p_{start}$ satisfies Eq. (15) for $\gamma = 0$, and $p(1)$, if it can be determined, is a feasible solution of Eq. (12), since Eq. (15) $\rightarrow$ Eq. (12) for the special case $\gamma = 1$. By sweeping γ slowly and iterating on $p(\gamma)$ to satisfy Eq. (15), we can always initiate each iteration with a nearby converged solution and thereby very nearly guarantee convergence (failure will occur only in the event of locally singular events such as bifurcations, turning points, etc., in which other remedial action, Ref. 8, can be taken).

Preparing to develop an iterative process for $p(\gamma)$, we expand Eq. (15) about some estimate for $p(\gamma_i)^*$; we seek a correction Δp such that Eq. (15) will be satisfied to first order as

$$H(p(\gamma_i) + \Delta p) = H(p(\gamma_i)) + [\frac{\partial H}{\partial p}|_i] \Delta p = 0 \qquad (18)$$

where

$$H(p(\gamma_i)) = \gamma_i g_0 + (1-\gamma_i) g(p_{start}) - g(p(\gamma_i)) \quad (19)$$

$$[\partial H/\partial p|_i] = -[\partial g(p(\gamma_i))/\partial p(\gamma_i)] \qquad (20)$$

Since the dimension m_e of H is typically much less than the dimension of p, Eqs. (18) are usually underdetermined. Thus a criterion must be introduced to select a particular solution for Δp. We choose to minimize the correction norm $\Delta p^T \Delta p$; this serves to be as consistent as possible with the small correction assumption implicit in retaining linear terms and also is an appropriate design philosophy (large design changes are qualitatively less attractive than small ones!). Minimizing

---

$^*p(\gamma_i)$ is estimated from a converged solution for a neighboring $p(\gamma_{i-1})$.

126

$\Delta p^T W \Delta p$ subject to Eq. (18) gives

$$\Delta p = -W^{-1}\left[\tfrac{\partial H}{\partial p}\Big|_1\right]^T \left[\tfrac{\partial H}{\partial p}\Big|_1\right]W^{-1}\left[\tfrac{\partial H}{\partial p}\Big|_1\right]^{T\;-1} H(p(\gamma_1)) \quad (21)$$

where W is a positive definite weight matrix. We use Eq. (21) to iterate for $p(\gamma_1)$ in a Newton-like manner by recursively computing

$$p(\gamma_1)_{new} = p(\gamma_1)_{old} + \Delta p_1$$

until convergence is achieved, for each of a sequence of γ's

$$\{0 = \gamma_0 < \gamma_1 < \dots \gamma_N = 1\} \quad (22)$$

Since $p(\gamma_1)$ is initiated from a nearby converged solution, we can insure (by choosing $\Delta\gamma$ sufficiently small in $\gamma_i = \gamma_{i-1} + \Delta\gamma$) that the elements of $H(p(\gamma_1))$ are arbitrarily small; failure of the correction in Eq. (21) will occur only if the Jacobian $[\partial H/\partial p|_1]$ becomes locally rank deficient.

In Ref. 1, we show how to generalize the above continuation method for equality constraints in a fashion which locally includes the active (violated) subset of inequality constraints and a gradient projection decrement of the performance criterion J of Eq. (11).

The resulting algorithm has been used successfully as a nonlinear constrained minimization algorithm and is superior to conventional constrained minimization (nonlinear programming) algorithms, owing to the use of continuation to enhance convergence. As is shown in Ref. 8, the domain of reliable convergence is vastly larger than conventional Newton and quasi-Newton algorithms. Alternatively, we show in Ref. 7 a method to make the local corrections via a linear or quadratic programming algorithm imbedded in a similar homotopy family. In any event, the use of adaptive continuation and homotopy algorithms to enhance convergence is a very important device; it insures that failure of the optimization algorithm will not be due to a failed local linearity assumption.

4. DIRECT OUTPUT FEEDBACK CONTROL

An easy to state MIMO control design approach is to seek the m x r elements of the gain matrix G in the closed loop system matrix of Eq. (5) such that the eigenvalues and eigenvectors of $\bar{A} = A + BGH$ solve a constrained optimization problem of the form of Eqs. (11)-(13). The design vector can easily be expanded to admit sensor/actuator locations and plant model parameters. Reference 1 treats this problem in detail and includes numerical solutions for more than 50 design variables. References 4-6 present other, lower dimensioned applications of this generic type, although the numerical methods do not make use of the minimum correction norm and continuation methods of the foregoing section. However, the minimization, in Refs. 5 and 6 of eigenvalue placement sensitivity, represent significant applications of this approach to design of robust control laws.

5. OPTIMAL TUNING OF LQG REGULATOR WEIGHTS

Consider the minimization of the classic linear quadratic Gaussian performance index

$$J = \tfrac{1}{2}\int_0^\infty (x^T Q x + u^T R u)dt \quad (23)$$

subject to

$$\dot{x} = Ax + Bu \; , \quad (24)$$

The necessary conditions for minimizing Eq. (23) subject to Eq. (24) are, in addition to Eq. (24), as follows (Ref. 9)

$$\dot{\lambda} = -Qx - A^T\lambda \quad (25)$$

$$u = -R^{-1}B^T\lambda \quad (26)$$

where $\lambda(t)$ is an n x 1 co-state (Lagrange multiplier vector). If we seek a feedback control, then we assume

$$\lambda(t) = Kx \quad (27)$$

and Eqs. (24-(26) give the matrix Riccati equation for K(t)

$$\dot{K} + KA + A^T K - K[BR^{-1}B^T]K + Q = 0 \quad (28)$$

for the infinite upper limit of integration in Eqs. (24), $\dot{K} \to 0$, and Eq. (28) becomes the algebraic matrix Riccati equation which, if the system (24) is controllable, can be solved for the symmetric positive matrix K using Potter's method of Ref. 10. Since K is constant, using (27) in (26) gives a constant gain feedback and results in a closed loop system of the form of Eq. (4) with Z = I and closed loop system matrix

$$\bar{A} = A - BR^{-1}B^T K \quad (29)$$

The dependence of J upon the initial state x(0) can be eliminated by considering x(0) to be uniformly distributed on the unit sphere. Then in lieu of minimizing J, we minimize the expectation $\varepsilon(J)$; this leads (Ref. 4) to

$$\varepsilon(J) = \tfrac{1}{2}\,\text{trace }[K\varepsilon(x(0)x^T(0))] \quad (30)$$

If we assume x(0) to be taken independently and be scaled appropriately, $\varepsilon(x(0), x^T(0))$ is an identity matrix, so we can replace the functional minimization of Eq. (23) by the algebraic requirement of minimizing the trace of K. Since K is dependent upon the choice of weight matrices Q and R, through the algebraic solution of Eq. (28), we see that both the quadratic performance index of Eq. (30), and any constraints we choose to impose upon the closed loop eigenvalues and eigenvectors (of $\bar{A} = A - BR^{-1}B^T K$) depend implicitely upon Q and R. The question of choosing Q and R to achieve eigenvalue and eigenvector optimization arises quite naturally, and the problem has exactly the form adressed in Section 3.

Two issues require special attention, first note that the sensitivities of K follow from differentiation of Eq. (28), for $\dot{K} = 0$, as the fol

lowing Liapunov equation

$$\frac{\partial K}{\partial p_{\ell}} \bar{A} + \bar{A}^T \frac{\partial K}{\partial p_{\ell}} = -\frac{\partial Q}{\partial p_{\ell}} + K \frac{\partial}{\partial p_{\ell}} [BR^{-1}B^T]K$$

$$- K \frac{\partial A}{\partial p_{\ell}} - \frac{\partial A^T}{\partial p_{\ell}} K \qquad (31)$$

For the special case that the p_{ℓ} are a parameterization of Q and R, the above simplifies to

$$\frac{\partial K}{\partial p_{\ell}} \bar{A} + \bar{A}^T \frac{\partial K}{\partial p_{\ell}} = -\frac{\partial Q}{\partial p_{\ell}} - K[BR^{-1} \frac{\partial R}{\partial p_{\ell}} R^{-1}B^T]K \quad (32)$$

Secondly, we consider the fact that if we iterate arbitrarily upon the elements of Q and R, they may become indefinite or negative; this can be avoided by using Cholesky decompositions

$$Q = [Q^{1/2}][Q^{1/2}]^T \quad , \quad R = [R^{1/2}][R^{1/2}]^T \quad (33)$$

with

$$Q^{1/2} = \begin{bmatrix} q_{11}^2 & 0 & \cdots & 0 \\ q_{12} & q_{22}^2 & & 0 \\ \vdots & \vdots & \ddots & \\ q_{1n} & q_{2n} & \cdots & q_{nn}^2 \end{bmatrix} \qquad (34)$$

$$R^{1/2} = \begin{bmatrix} r_{11}^2 & 0 & \cdots & 0 \\ r_{12} & r_{22}^2 & & 0 \\ \vdots & \vdots & \ddots & \\ r_{1m} & r_{2m} & \cdots & r_{mm}^2 \end{bmatrix} \qquad (35)$$

Thus $p = [q_{11} \ \cdots \ q_{nn} : r_{11} \ \cdots \ r_{mm}]^T$, and using any real numbers for q_{11} and r_{11} will guarantee Q and R remain positive semi-definite.

We can easily augment p by sensor/actuator locations, etc., to consider more general eigenvalue/eigenvector optimization problems.

In Ref. 11, we consider the more general quadratic index

$$J = \frac{1}{2} \int_0^\infty \begin{Bmatrix} x \\ u \end{Bmatrix}^T \begin{bmatrix} Q & N \\ N^T & R \end{bmatrix} \begin{Bmatrix} x \\ u \end{Bmatrix} dt \qquad (36)$$

In which case the optimal control is given by

$$u = -R^{-1}(B^T K + N^T)x \qquad (37)$$

and K satisfies the modified Riccati equation

$$\bar{Q} + K\bar{A} + \bar{A}^T K - K[BR^{-1}B^T]K = 0 \qquad (38)$$

$$\bar{Q} = Q - NR^{-1}N^T \qquad (39)$$

$$\bar{A} = A - BR^{-1}N^T \qquad (40)$$

The closed loop system matrix becomes

$$\bar{A} = A - BR^{-1}B^T K - BR^{-1}N^T \qquad (41)$$

The presence of the cross-coupling weight N ≠ 0 in

Eq. (41) obviously affects the eigen-solution; in Ref. 11, we establish conclusively that including N allows constructive optimization of the system eigenvalues and eigenvectors.

6. THE GENERALIZED PROBLEM OF MOERDER AND CALISE

Reference 4 considers the problem of minimizing $\epsilon(J)$, where

$$J = \frac{1}{2} \int_0^\infty [x^T Q x + u^T R u]dt + f(G) \qquad (42)$$

subject to

$$\dot{x} = Ax + Bu \qquad (43)$$

$$y = Hx \qquad (44)$$

$$u = Gy \qquad (45)$$

Analogous to the preceeding section, $\epsilon(J)$ can be written algebraically as

$$\epsilon(J) = \text{trace } [K] + f(G) \quad , \quad \epsilon\{x(0)x^T(0)\} = I, \quad (46)$$

where K satisfies the Riccati-like equation

$$S(Q,R,A,B,G,K) = \bar{A}^T K + K\bar{A} + H^T G^T RGH\bar{Q} = 0 \qquad (47)$$

where $\bar{A}$ is given by Eq. (5). Reference 4 gives an attractive algorithm for iterating for K, G, given Q, R, A, B, H. Obviously, the design vector for this approach can also admit parameterizations of Q, R, A, B, H, and algorithms can be developed analogous to Sections 2-5 above using continuation methods, as necessary, to enhance convergence.

7. NUMERICAL EXAMPLES

As a simple, low-dimensioned example, consider tuning the weights for an LQG controller of the type in Section 5, with

$$A = \begin{bmatrix} 0 & 0 & 0 & 1 & 0 & 0 \\ 0 & 0 & 0 & 0 & 1 & 0 \\ 0 & 0 & 0 & 0 & 0 & 1 \\ -2 & 1 & 0 & 0 & 0 & 0 \\ 1 & -3 & 2 & 0 & 0 & 0 \\ 0 & 1 & -1 & 0 & 0 & 0 \end{bmatrix}, \quad B = \begin{bmatrix} 0 & 0 \\ 0 & 0 \\ 0 & 0 \\ 1 & 0 \\ 0 & 0 \\ 0 & 1/2 \end{bmatrix} \qquad (48)$$

$$\begin{bmatrix} Q & N \\ N^T & R \end{bmatrix} = LL^T \qquad (49)$$

$$L = \begin{bmatrix} p_1^2 & & & 0 \\ p_9 & p_2^2 & & \\ \vdots & & \ddots & \\ p_{30} & \cdots & p_{36} & p_8^2 \end{bmatrix} = \begin{bmatrix} .25^2 & & & \\ 1 & & & \\ 1 & & & \\ .1^2 & & & \\ & .1^2 & & \\ & & 1 & \\ & & & 1 \end{bmatrix} \text{(starting estimate)} \quad (50)$$

We adopted the following performance measure (eigenvalue placement penalty)

$$J(p) = \frac{1}{2} \sum_{k=1}^{3} \phi_i^2 \ h(\phi_i) \qquad (51)$$

128

where

$$\phi_1 = \phi_1(p) = 1 - \zeta_1(p) \quad , \quad 1 = 1,2,3 \qquad (52)$$

$h(\cdot)$ is the heavyside unit step function

$$\zeta_1 = \text{damping factor} = \frac{-Re(\lambda_1)}{|\lambda_1|} = \zeta_1(p) \qquad (53)$$

$$\omega_1 = Im(\lambda_1) = \omega_1(p)$$

(note, the eigenvalues occur in three complex conjugate pairs $\lambda_1 = Re(\lambda_1) \pm j\, Im(\lambda_1)$, $1 = 1,2,3$). We also adopted the three equality constraints

$$g_1 = \omega_{1o} - \omega_1(p) = 0, \quad 1 = 1,2,3 \qquad (54)$$

and of course, we require for stability that $\zeta_1 > 0$. The objective values of ω_{1o} were simply taken as the corresponding zero gain values. Observe that the performance measure of Eq. (51) simply seeks to "herd" the eigenvalues to the left, subject to Eq. (54), which attempts to maintain the imaginary components constant (this is simply an illustration). In Table 1, the progress of a continuation process is summarized. The homotopy was designed such that $\gamma = 1$ corresponds to $J(p(1)) = 0$; we did not expect to be able to achieve $\zeta_1 = 1$, (i.e., drive J to zero) while holding the ω_1 constant!

Observe in Table 1 and Figure 1 (the corresponding locus of the eigenvalues during the continuation iterations) that as γ was swept from zero to .90, in variable steps, the eigenvalues marched steadily to the left until it was impossible to maintain the imaginary parts constant. Notice the dramatic increase achieved in damping; not all weight matrices are created equal! The initial diagonal guess (Eq. (50)) on the weight matrix square root converged to

$$L = \begin{bmatrix} .592^2 & & & & & & & \\ -.058 & 1.29^2 & & & & & & \\ .067 & -.039 & 1.47^2 & & & & & \\ 0 & 0 & 0 & 1.08^2 & & & & \\ 0 & 0 & 0 & -0.001 & .101^2 & & & \\ 0 & 0 & 0 & 0 & -.001 & .101^2 & & \\ .043 & -.202 & -0.041 & 0 & 0 & 0 & .174^2 & \\ -.177 & .198 & -0.026 & 0 & 0 & 0 & -.013 & .340^2 \end{bmatrix}$$

$$(55)$$

where zero's mean the converged entries were smaller than 10^{-5}. Notice that the lower left corner is non-zero, thus $N \neq 0$ to achieve the solution of Table 1 and Fig. 1. Notice in Table 2 and Fig. 2 that constraining $N = 0$ for this case results in a much less attractive eigenvalue placement; especially for the third mode. Thus the cross coupling terms are significant.

As a second example, we refer to Ref. 1 wherein a spatially discretized scheme leads to the linear second order system

$$Mz + C\dot{z} + Kz = Du \qquad (56)$$

to model a flexible structure with a central rigid hub and four cantilevered flexible beams. The dimensions of M, C, K were 21 x 21; the first 10 modes were considered accurately modeled. A

torque actuator acts on the central hub and two pairs of appendage torquers (nominally acting at the mid span of opposing beams); the two torquer pairs are constrained to impart identical torques to the structure, so effectively u is a 3 x 1 vector and x of Eq. (1) is a 42 x 1 vector. Twenty sensors (ten pairs of position and velocity sensors) are located at various points on the structure. The above can be cast in the from of the problem discussed in Section 2, and the algorithms of Section 3 immediately apply. In Ref. 1, we solve several eigenvalue optimization problems using this structure. In one, we simultaneously optimize 42 control gains, 8 sensor locations, and 2 plant design parameters to impose 12 eigenvalue constraints and, subject to these constraints, minimize the sum square of the control gains. The continuation process of Section 3 converged reliably, even starting with zero feedback gains. The eigenvalue trajectories during the continuation iterations are shown in Fig. 3.

8. DISCUSSION

The present paper establishes important connections between various approaches for designing constant gain linear feedback controllers, and presents a unified numerical optimization strategy for simultaneous or sequential tuning of control gains, sensor/actuator locations, plant design parameters, and various weight matrices, vis-a-vis constraints and optimality criteria specified in terms of the closed loop eigenvalues and eigenvectors. The methods presented have been found rather robust with respect to computational problems one usually expects for high dimensioned nonlinear optimization applications.

9. REFERENCES

1. Bodden, D. S., and Junkins, J. L., "Eigenvalue Optimization Algorithms for Structure/Controller Design Iterations," 1984 American Controls Conference, June 1984, San Diego, CA, to appear, AIAA J. of Guidance, Control, and Dynamics.

2. Plaut, R. H., and Huseyin, K., "Derivatives of Eigenvalues and Eigenvectors in Non-Self-Adjoint Systems," AIAA Journal, Vol. 11, No. 2, pp. 250-251, Feb. 1973.

3. Laub, A. J., Kinnemann, and Wette, M., "Algorithms and Software for Pole Assignment by State Feedback," IEEE Symposium of Computer Aided Control System Design, Santa Barbara, CA, March 1985.

4. Moerder, D. D., and Calise, A. J., "Convergence of a Numerical Algorithm for Calculating Optimal Output Feedback Gains," to appear, IEEE Trans on Automatic Control, 1985.

5. Raman, R. V., Modal Insensitivity with Optimality, Ph.D. Dissertation, Mech. Engr., Drexel Univ., June 1984.

6. Cavin, R. K., and Howse, J. W., "Regulator Design with Modal Insensitivity," IEEE Trans. on Automatic Control, Vol. AC-24, No. 3, pp. 466-469, June 1979.

7. Horta, L. G., Juang, J. N., and Junkins, J. L., "A Linear Optimization Approach for Flexible Structure Controller Design," AIAA Guidance and Control Conference, Snowmass, Colorado, August 1985.

8. Dunyak, J. P., Watson, L. T., and Junkins, J. L., "Robust Nonlinear Least Square Estimation Using the Chow-Yorke Homotopy Method," AIAA J. of Guidance, Control, and Dynamics, Vol. 7, No. 6, pp. 752-754, Nov.-Dec., 1984.

9. Lee, E. B., and Markus, L., FOUNDATIONS OF OPTIMAL CONTROL THEORY, John Wiley and Sons, Inc., New York, 1967.

10. Potter, J. E., "Matrix Quadratic Solutions," SIAM J. of Applied Math., Vol. 14, No. 3, May, 1966, pp. 496-501.

11. Rew, D. W., and Junkins, J. L., "Tuning Optimal Quadratic Regulator Weight Matrices to Satisfy Closed Loop Eigenvalue Constraints and Optimality Criteria," Presented to the AIAA/VPI&SU Symposium on Dynamics and Control of Large Structures, Blacksburg, VA, June 1985.

Figure 3 DRAPER/RPL Eigenvalue Continuation Locus

TABLE 1 Eigenvalues for LQG Weight Matrix Iterations with $N \neq 0$

γ	ω_1	ζ_1	ω_2	ζ_2	ω_3	ζ_3
0	.38	.14	1.37	.24	2.03	.06
.2	.38	.34	1.37	.33	2.02	.07
:	:	:	:	:	:	:
.90	.37	.92	1.40	.64	2.00	.72

no convergence for $\gamma > .9...$

TABLE 2 Eigenvalues for LQG Weight Matrix Iterations with $N = 0$

γ	ω_1	ζ_1	ω_2	ζ_2	ω_3	ζ_3
0	.38	.14	1.37	.24	2.03	.06
.2	.28	.52	1.37	.11	2.02	.14
:	:	:	:	:	:	:
.57	.37	.78	1.38	.85	2.01	.06

...no convergence for $\gamma > .57...$
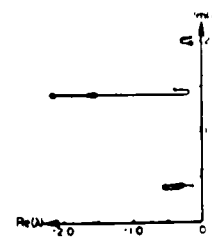

Figure 1 Example 1 $N \neq 0$

Figure 2 Example 1 $N = 0$

AN ALGORITHM FOR ITERATIVE MODIFICATION
LQR WEIGHT MATRICES TO IMPOSE EIGENVALUE CONSTRAINTS

D. W. Rew

J. L. Junkins

Mountain Lake Dynamics and Control Institute
Virginia Polytechnic Institute and State University
Mountain Lake, Virginia
June 9-11, 1985

ABSTRACT

A mathematical formulation and associated algorithm is presented which can be used to tune the weight matrices in an optimal quadratic regulator to impose constraints and eigenspace optimality criteria upon closed loop systems eigenvalues. The algorithm is found to be efficiently applicable to moderately high dimensioned problems; reliable convergence has been routinely demonstrated with over one hundred and fifty weight matrix elements being optimized to place eigenvalues in a dynamical system of order fourteen. These results provide a basis for optimism that the approach is applicable to a significant family of problems.

I. Introduction

The design of practical structural control systems requires reliable methods to determine the feedback gain matrix. With some approaches, the gain matrix is directly iterated to satisfy design constraints, while with some others, it is selected by solving the Linear Quadratic Gaussian (LQG) regulator problem.

The former type may require a large number of design constraints, since an arbitrary direct feedback gain matrix does not guarantee the stability of closed loop system. However, the latter (LQG) type of design may encounter other difficulties, as examples, the resulting closed loop system may become physically meaningless due to arbitrary weights in the criterion, or numerical difficulties may be encountered in solving the Riccati equation.

In recent papers by Junkins, et al., [1,2], structure and control design techniques to satisfy eigenvalue constraints have been

introduced. We have shown that the direct feedback gain parameters along with plant parameters can be iterated via a nonlinear programming method based upon using continuous minimum norm correction strategy and homotopy methods to enhance consequence. We also introduced a scheme for tuning the weight matrices in a LQG performance criterion to achieve eigenvalue placement constraints. This paper aims at developing an algorithm for optimally adjusting LQG weight matrices and assessing its effectiveness.

In Sections 2 and 3, we formulate an eigenvalue sensitivity and parameterization scheme considering the LQG weight matrices as design variables. In Section 4, we show how LQG eigenvalue placement optimization can be formulated as a nonlinear programming process. In Section 5 and 6, we discuss numerical results and offer concluding remarks.

II. Closed-Loop Eigenvalue Problem

Consider the linear dynamical system in the state-space form:

$$\dot{x} = Ax + Bu \tag{1}$$

with linear feedback control

$$u = -Kx \tag{2}$$

where x is nx1 state vector

u is mx1 control vector

and A, B and K are plant, controller influence, and control gain matrices with proper dimensions. We assume, for initial simplicity, that the full state is measurable.

Substituting the control law of Eq. (2) in Eq. (1), we obtain the closed-loop system

133

$$\dot{x} = \overline{A}x \tag{3}$$

where $\overline{A} = A - BK$

Assuming exponential solutions of the form $x = \alpha \text{Exp}(\lambda t)$, we are led to the eigenvalue problems:

$$\begin{aligned} \lambda_i \alpha_i &= \overline{A}\alpha_i \\ \lambda_i \beta_i &= \overline{A}^T \beta_i \end{aligned} \quad i = 1,2,\ldots,n \tag{4}$$

where α_i and β_i are the right and left eigenvectors corresponding to the eigenvalue λ_i with the usual normalizations:

$$\beta_i^T \alpha_j = \delta_{ij} \quad , \quad \beta_i^T \overline{A}\alpha_j = \lambda_i \delta_{ij} \tag{5}$$

Suppose that the gain matrix K in Eq. (2) is parameterized by the vector p. In addition, we consider $\lambda(p)$ and $\alpha(p)$ to be continuous and differentiable with respect to p. The continuous and differentiable assumptions are usually satisfied except at isolated bifurcation points. The first and second partial derivatives of eigenvalues with respect to the ℓth and m^{th} elements of p are given by

$$\frac{\partial \lambda_i}{\partial p_\ell} = \beta_i^T \frac{\partial \overline{A}}{\partial p_\ell} \alpha_i \tag{6}$$

$$\begin{aligned} \frac{\partial^2 \lambda_i}{\partial p_\ell \partial p_m} &= \beta_i^T \frac{\partial^2 \overline{A}}{\partial p_\ell p_m} \alpha_i \\ &+ \sum_{k=1,k\neq i}^{n} (\beta_i^T P_m \alpha_k \beta_k^T P_\ell \alpha_i + \beta_k^T P_m \alpha_i \beta_i^T P_\ell \alpha_k)/(\lambda_i - \lambda_k) \end{aligned} \tag{7}$$

where

$$P_m \equiv \frac{\partial \overline{A}}{\partial p_m}$$

The detail derivations of Eqs. (6) and (7) can be found in [1,4].

134

From Eq. (3), we have for the present case

$$\frac{\partial \overline{A}}{\partial p_{\ell}} = - \beta \frac{\partial K}{\partial p_{\ell}} \tag{8}$$

The evaluation of Eq. (8) depends on the parameterization scheme chosen for the K matrix, which will be discussed in the following section.

III. Regulator Control Problem

In this section, we derive optimality conditions for three controllers: direct feedback, LQG, and modified LQG types. The closed-loop stability of these controllers and their respective parameterization schemes are discussed.

The derivatives of the closed-loop system materix ($\overline{A}$) required for eigenvalue sensitivity calculation are derived. Consider the classical LQG problem:

$$\text{minimize } J = \int_0^\infty (x^T Q x + u^T R u) dt \tag{9}$$

subject to Eq. (1) where the weight matrices Q and R are assumed to be positive definite.

By introducing a symmetric positive definite matrix P_{ss}, the optimal solution can be derived. First, we rewrite Eq. (9) as

$$J = \int_0^\infty [x^T Q x + u^T R u + \frac{d}{dt}(x^T P_{ss} x)] dt - x_\infty^T P_{ss} x_\infty + x_0^T P_{ss} x_0 \tag{10}$$

where x_0 and x_∞ are the state values evaluated at $t = 0$ and $t = \infty$, respectively. Assuming that our closed-loop system is asymptotically stable, we can let x_∞ vanish.

135

Substituting Eq. (1) into Eq. (10), we then obtain

$$J = \int_0^\infty [x^T(Q + P_{ss}A + A^TP_{ss})x + u^TRu + 2x^TP_{ss}Bu]dt + x_0^TP_{ss}x_0$$

(11)

In this equation, we substitute the direct feedback control law of Eq. (2) to get

$$J = \int_0^\infty x^T[Q + P_{ss}\bar{A} + \bar{A}^TP_{ss} + K^TRK]x\,dt + x_0^TP_{ss}x_0$$

(12)

where $\bar{A}$ is the stability matrix in Eq. (3). Given Q, R and K matrices, the stability of the system (3) is guaranteed when there exists soltuion P_{ss} to the Liapunov equation [7]

$$Q + P_{ss}\bar{A} + \bar{A}^TP_{ss} + K^TRK = 0$$

(13)

With this, we can formulate a parameter optimization problem in the form:

$$\underset{K}{\text{minimize}}\ J = x_0^TP_{ss}x_0$$

(14)

Subject to Eq. (13). If we consider x_0 to be uniformly distributed over the unit sphere, then minimizing the expected value of Eq. (14) is equivalent to minimizing the trace of P_{ss}.

It should be noted that stable feedback controls requires that all the eigenvalues of $\bar{A}$ be in the left half plane of the eigenspace. Therefore, if we attempt to impose additional constraints that all the closed-loop eigenvalues have negative real parts, Eq. (13) embodies redundant constraints.

In References [1] and [2], we developed an algorithm which simply modifies K elements without the constraints (13) to enforce all eigenvalues being in the left half plane. Also, we can consider

136

generalized performance index of Eq. (14) with an extra penalty function of the gains. An attractive algorithm of iterating P_{ss} and K to minimize such a generalized criterion can be found in Ref. [5].

Next, minimizing the integrand of Eq. (11) with respect to K and assuming that the minimum value is zero, we obtain the classical LQG optimal control law

$$u = - R^{-1}B^T P_{ss} x \tag{15}$$

where P_{ss} is the solution of the algebraic Riccati equation

$$Q + P_{ss}A + A^T P_{ss} - P_{ss}BR^{-1}B^T P_{ss} = 0 \tag{16}$$

Thus, the minimum performance index becomes

$$J^* = x_0^T P_{ss} x_0 \tag{17}$$

Note that if the open loop system is either completely controllable or exponentially stable, then the solution to Eq. (16) exists [7]. This condition is somewhat less restrictive compared to the case of direct feedback. However, we have to solve matrix quadratic equation (16) instead of linear equation (13) for P_{ss}. Then, as long as either the controllability or exponential stability of open loop system is maintained, then the solution can be found by using Shur method [6]. Since the equation (17) is a Liapunov stability function, the resulting closed loop system is always asymptotically stable [7].

Now we consider more general quadratic index

$$J = \int_0^\infty \begin{Bmatrix} x \\ u \end{Bmatrix}^T \begin{bmatrix} Q & N \\ N^T & R \end{bmatrix} \begin{Bmatrix} x \\ u \end{Bmatrix} dt \tag{18}$$

For this performance index, the modified optimal control law and algebraic Riccati equation are given by

137

$$u = -R^{-1}(N^T + B^T P_{ss})x \qquad (19)$$

$$\tilde{Q} + P_{ss}\tilde{A} + \tilde{A}^T P_{ss} - P_{ss}BR^{-1}B^T P_{ss} = 0 \qquad (20)$$

where

$$\tilde{A} = A - BR^{-1}N^T \qquad (21)$$

$$\tilde{Q} = Q - NR^{-1}N^T \qquad (22)$$

Then, the corresponding closed loop stability matrix becomes

$$\bar{A} = A - BR^{-1}(N^T + B^T P_{ss}) \qquad (23)$$

It should be noted that cases in which $\tilde{Q}$ is not positive definite or the pair $(\tilde{A},B)$ is not controllable, there may be no solution to Eq. (20). But if a positive definite solution of the corresponding algebraic Riccati equation can be found, this solution can be useful in the design of particular control system. Allowing the "cross coupling weight matrix" N to be chosen non-zero is shown below to permit constructive optimization of the closed loop eigenvalues.

Let's assume that there exists a positive definite solution P_{ss} although the theoretical conditions for the existence of P_{ss} (under these generalized circumstances) have not been clearly defined. Then, the minimum of the performance index can be found and becomes Eq. (17). Here we elect to parametrize the weight matrix in Eq. (18), which must be symmetric positive definite. Introducing weight matrix parameter vectors q, r and n, and using Cholesky decomposition, we rewrite the weight matrix in the form.

$$\begin{bmatrix} Q & N \\ N^T & R \end{bmatrix} = LL^T \qquad (24)$$

with

138

$$
L = \begin{bmatrix}
q_{11}^2 & & & & & \\
q_{21} & q_{22}^2 & \ddots & & & 0 \\
\vdots & & & & & \\
q_{n1} & \cdots \cdots & q_{nn}^2 & & & \\
n_{11} & n_{12} & \cdots & n_{1n} & r_{11}^2 & \\
\vdots & \vdots & \ddots & \vdots & \vdots & \ddots \\
n_{m1} & n_{m2} & \cdots & n_{mn} & r_{m1} & \cdots & r_{mm}^2
\end{bmatrix}
\tag{25}
$$

Therefore, the global weight parameter vector p becomes

$$
p = [q_{11}, q_{21}, \ldots, q_{nn}, r_{11}, r_{21}, \ldots r_{mm}, n_{11}, n_{21}, \ldots, n_{mn}]^T
\tag{26}
$$

For the calculation of closed loop eigenvalue sensitivity in the previous section, we need to differentiate Q, R and N matrices with respect to the elements of p.

The partial derivatives of Eq. (24) with respect to the ℓth element of the parameter vector p leads to

$$
\frac{\partial}{\partial p_\ell}
\begin{bmatrix}
Q & N \\
N^T & R
\end{bmatrix}
= \frac{\partial L}{\partial p_\ell} L^T + L \frac{\partial L^T}{\partial p_\ell}
\tag{27}
$$

where the partial derivative of L can be obtained by direct differentiation (as simple arrays of all zeroes except a unit value in the element corresponding to p_ℓ).

Using Eq. (27), we write the partial derivative of the closed loop stability matrix

$$
\frac{\partial \overline{A}}{\partial p_\ell} = - B \frac{\partial R^{-1}}{\partial p_\ell} (N^T + B^T P_{ss}) - BR^{-1} (\frac{\partial N^T}{\partial p_\ell} + B^T \frac{\partial P_{ss}}{\partial p_\ell})
\tag{28}
$$

It can be shown that the partial derivatives of P_{ss} are obtained by solving the algebraic Liapunov equation

139

$$\frac{\partial P_{ss}}{\partial p_\ell} \tilde{A} + \bar{A}^T \frac{\partial P_{ss}}{\partial p_\ell} = -\frac{\partial \tilde{Q}}{\partial p_\ell} - P_{ss} \frac{\partial \tilde{A}}{\partial p_\ell} - \frac{\partial \tilde{A}^T}{\partial p_\ell} P_{ss} + P_{ss} B R^{-1} B^T P_{ss} \qquad (29)$$

where $\tilde{A}$, $\tilde{Q}$ and $\bar{A}$ are given in Eqs. (21), (22) and (23), respectively. The solution of Eq. (29) are derived in Ref. [1] and is given below.

$$\frac{\partial P_{ss}}{\partial p_\ell} = [\beta]^T [T_\ell][\beta] \qquad (30)$$

where

$$[T_\ell]_{ij} = \frac{1}{\lambda_i + \lambda_j} \left[[\alpha]^T [RHS_\ell][\alpha] \right]_{ij}, \qquad (31)$$

$[\alpha]$, $[\beta]$ are $n \times n$ modal matrices whose columns are α_i, β_i, respectively and $[RHS_\ell]$ is the right-hand side of Eq. (29). Therefore, using Eq. (28), the first and second derivatives of eigenvalues in Eq. (6) and (7) can be efficiently calculated.

For the classical LQG case of $N = 0$, the Q and R matrices may be parameterized separately by using the same scheme presented here with q and r vectors.

IV.   Optimization Approach for Eigenvalue Placement

The problem of eigenvalue placement can be formulated by an optimization approach in which we seek to impose specified eigenspace constraints and minimize an eigenvalue placement, sensitivity or other closed loop eigenvalue/eigenvector performance criterion.

Utilizing the parameterization scheme described in the previous section, we consider the following sets of equality and inequality constraints:

$$g_{oi} - g_i(p) = 0 \qquad\qquad i = 1,2,\ldots m_e \qquad (32)$$

140

$$f_{oj} - f_j(p) > 0 \qquad\qquad j = 1,2,\ldots m_{ie} \qquad\qquad (33)$$

where g_{oi} and f_{oi} are objective constraint function values or
constraint boundaries corresponding to the ith closed loop eigenvalue,
and $g_i(p)$ and $f_i(p)$ are current values of these constraint
functions. The feasible solution to Eqs. (32), (33) can be obtained
by either considering the locally active inequality constraints as
equality type, or by minimizing a bounded quadratic penalty function
subject to the equality constraints. We choose the latter approach,
which leads to an optimization (nonlinear programming) problem of the
form:

$$\text{minimize } \frac{1}{2} \sum_i K_i \phi_i^2 h(-\phi_i) \qquad\qquad (34)$$

subject to Eq. (32) where

$$\phi_i = f_{oi} - f_i(p).$$

$K_i > 0$ is a weighting factor and $h(\cdot)$ is the heaviside unit step
function. This nonlinear programming problem can be solved by using
continuous minimum norm correction algorithm of Ref. [3]. The
essential feature of this algorithm is to solve a set of nonlinear
equations for variable continuation steps. Its first step is to
generate a homotopy family of problems by introducing "portable"
objective function values defined by the linear map

$$g_p(\gamma) = \gamma g_0 + (1 - \gamma)g(p_{start}) \qquad\qquad (35)$$

with a homotopy or continuation parameter γ satisfying $0 \le \gamma \le 1$. If
we replace the original objective g_0 in Eq. (32) by the portable
objective $g_p(\gamma)$, we obtain a homotopy family of constraint functions:

$$H(p(\gamma)) = \gamma g_0 + (1 - \gamma)g(p_{start}) - g(p(\gamma)) = 0 \qquad\qquad (36)$$

141

Thus, at $\gamma = 0$, the above has the solution p_{start}, and at $\gamma = 1$, it becomes the original equations, so $p(1)$ is the desired solution. Since Eq. (36) is usually underdetermined, a unique correction vector Δp can be obtained by a minimum norm solution of the truncated Taylor series expansion of Eq. (36): that is, we minimize $\Delta p^T \Delta p$ subject to the equality constraint

$$H(p(\gamma) + \Delta p) = H(p(\gamma)) + [\frac{\partial H}{\partial p}]\Delta p = 0 \tag{37}$$

Then, the minimum norm correction vector, Δp takes the standard form

$$\Delta p = [\frac{\partial H}{\partial p}]^T [[\frac{\partial H}{\partial p}][\frac{\partial H}{\partial p}]^T]^{-1} \Delta H \tag{38}$$

where

$$\Delta H = -H(p(\gamma))$$

and

$$[\frac{\partial H}{\partial p}] = - [\frac{\partial g(p)}{\partial p}]$$

Using Eq. (38) and starting with a neighboring solution at step $\gamma = \gamma_{i-1}$, we refine $p(\gamma_i)$ recursively by computing

$$p(\gamma_i)_{new} = p(\gamma_i)_{old} + \Delta p \tag{39}$$

until local convergence for each γ_i; final convergence is achieved by incrementing γ_i after each local convergence until γ approaches 1 (or, if $\gamma = 1$ cannot be achieved, continue the process until γ is as large as possible, i.e., we accept the final local convergence). Along with the iterations to satisfy the equality constraints, the performance index can be reduced by introducing the performance index as an extra equality constraint with zero objective value. Incidentally, this procedure has been shown theoretically equivalent to the gradient

142

projection algorithm for constrained optimization problems [9], if an equivalent homotopy imbedding is introduced to control step size in the classical gradient projection method.

V. Computational Study

As a test example to demonstrate optimal tuning of the weights for an LQG controller, we selected the DRAPER/RPL model [1]. It consists of a central rigid hub and four arms (identical cantilever beams) with tip masses; in addition, it is assumed that torque actuators are located at the center of the hub and at the middle span of each appendage. The model is described by Eq. (1) in which the order of the system is $n = 14$ and and the number of actuators is $m = 3$. The number of controller inputs is three (instead of five) since the actuators or opposing appendages are constrained to apply identical control torques. The detailed configuration and the nominal structural parameter values may be found in [1].

For this example, we adopted three equality and five inequality constraints on the dominant closed loop eigenvalues, i.e.

$$\omega_{oi} - \omega_i(p) = 0 \qquad i = 1,2,3 \qquad (40)$$
$$1 - \varsigma_j(p) > 0 \qquad j = 1,2,...,5 \qquad (41)$$

where ω_i and ς_i are undamped frequency and damping factor corresponding to the ith eigenvalue, respectively. We implicitly require that all remaining eigenvalues remain in the stable left-half plane. The objective frequency values were taken as

$$\omega_{o1} = .53 \quad , \quad \omega_{o2} = 4.38 \quad , \quad \omega_{o3} = 7.91.$$

The equality constraints of Eq. (40) were employed, for simplicity and to avoid possible bifurcations leading to unnecessary numerical

143

complications, so that the desired eigenvalue locus will remain horizontal. The objective damping factors were taken as the critical damping condition ($\zeta_{oi} = 1$); these were chosen to move the eigenvalues as far as possible to the left-hand side (these critical damping factors obviously cannot be achieved while holding the frequencies constant!). However, progress toward this objective will tend to increase the damping factors as much as possible and will be constructive vis-a-vis eigenvalue placement; we implicitly expect final local convergence for some $\gamma < 1$. The quadratic penalty terms for each mode in Eq. (34) were equally weighted, i.e., $K_i = 1$, $i = 1,2,\ldots,5$. The total set of 8 constraints of Eqs. (40) and (41) were imposed, by iterating 153 parameters representing Q, R and N matrices with the starting diagonal matrix

$$L = \text{diag } \{1^2,1^2,1^2,1^2,1^2,1^2,1^2,.3^2,.3^2,.3^2,.3^2,.3^2,.3^2,.3^2,1^2,1^2,1^2\}$$

At each continuation step starting with $\gamma_0 = 0$, $\gamma_1 = .1$ and $\Delta\gamma = .1$, the convergence to the intermediate solutions was reliable for small values of γ, but it became necessary to make $\Delta\gamma$ adaptive for larger γ values. If the local iterations at γ_{i+1} did not converge, then the step size $\Delta\gamma$ was reduced by half until it became less than .005 without achieving local convergence.

In Tables 1 and 2, the results of two cases 1) with $N \neq 0$ and 2) with $N = 0$ are reported for variable continuation steps. For both cases, the damping factors for all modes including the <u>unconstrained modes</u> increased dramatically and similar eigenvalue locus were obtained as can be seen in Fig. 1.

At each iteration, the norm of both control gain vector (K matrix) and eigenvalue sensitivities with respect to gain elements

144

were calculated. Figure 2 and Fig. 3 show that the gain and sensitivity norms for both cases increased exponentially. However, the gain norm for Case 1 was much less than that for Case 2, and similar result for eigenvalue sensitivity norm was obtained. The number of gradient calculations for the optimization were counted 133 and 99 for Cases 1 and 2, respectively. Most of computation time was spent in solving the algebraic Riccati equation by Shur method.

Instead of Shur method, a Newton type of algorithm [8] can be used to solve the Riccati equation and to (possibly) save computation time (after the first nonzero γ continuation step is made by the Shur method). The convergence of a Newton algorithm will likely be quadratic since the iteration can be initiated with "arbitrarily close" estimates of the solution vector at each continuation step. However, the modest increase in storage requirments should be considered.

For both cases, the starting diagonal matrices resulted in convergence to fully populated weight matrices at the end of the continuation iterations. Obviously the eigensolution and gain matrix are constructively affected by properly chosen off-diagonal elements (N) of the weight matrix.

VI. Conclusions

This study presents numerical results obtained by an algorithm for sequential tuning of LQG weight matrices. It is obvious that physical performance measures usually does not dictate unique choices for the LQG weight matrices. We have shown that the fully populated weight matrices, especially including the cross-coupling terms in LQG

145

performance criterion, affect both the control gain and closed loop eigensolution. Since these matrices are often selected as simple diagonal or block diagonal matrices, the desirability of systematic methods to optimize these weights is evident. The results of the present study are a basis for optimism that for systematic eigenvalue placement can be achieved; the present method has been found reliable and numerically stable for the test examples considered in this study.

VII. References

[1] Bodden, D. S. and Junkins, J. L., "Eigenvalue Optimization Algorithms for Structural/Controller Design Iterations," Presented at the 1984 American Control Conference, June 6-8, 1984, San Diego, California.

[2] Junkins, J. L., Bodden, D. S., and Turner, J. D., "A Unified Approach to Structure and Control System Design Iterations," Fourth International Conference on Applied Numerical Modeling, Tainan, Taiwan, Dec. 1984.

[3] Junkins, J. L. and Dunyak, J. P., "Continuation Methods for Enhancement of Optimization Algorithms," Presented to 19th Annual Meeting, Society of Engineering Science, University of Missouri, Rolla, Oct. 1982.

[4] Plaut, R. H. and Huseyin, K., "Derivatives of Eigenvalues and Eigenvectors in Non-Self-Adjoint Systems," AIAA Journal, Vol. 11, No. 2, pp. 250-251, Feb. 1973.

[5] Moerder, D. D. and Calise, A. J., "Convergence of Numerical Algorithm for Calculating Optimal Output Feedback Gains," To appear IEEE Trans. on Automatic Control, 1985.

[6] Laub, A. J., "A Shur Method for Solving Algebraic Riccati Equations," IEEE Trans. on Automatic Control, Vol. AC-24, No. 6, Dec. 1979, pp. 913-921.

[7] Kwakernaak, H. and Sivan, R., Linear Optimal Control Systems, New York, Wiley-Interscience, 1972.

[8] Kleinman, D. L., "On an Iterative Technique for Riccati Equation Computations," IEEE Trans. on Automatic Control, Vol. AC-13, No. 1, Feb. 1968, pp. 114-115.

[9] Junkins, J. L., "Equivalence of the Minimum Norm and Gradient Projection Constrained Optimization Techniques," AIAA Journal, Vol. 10, No. 7, July 1972, pp. 927-929.
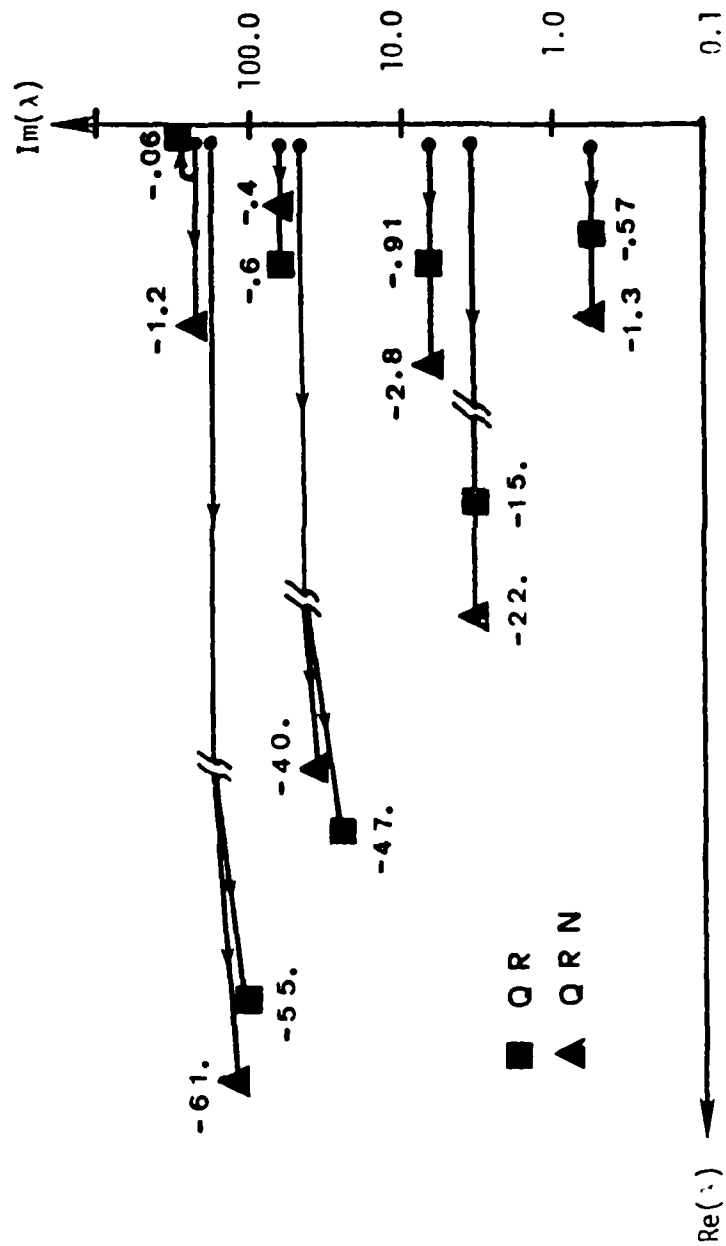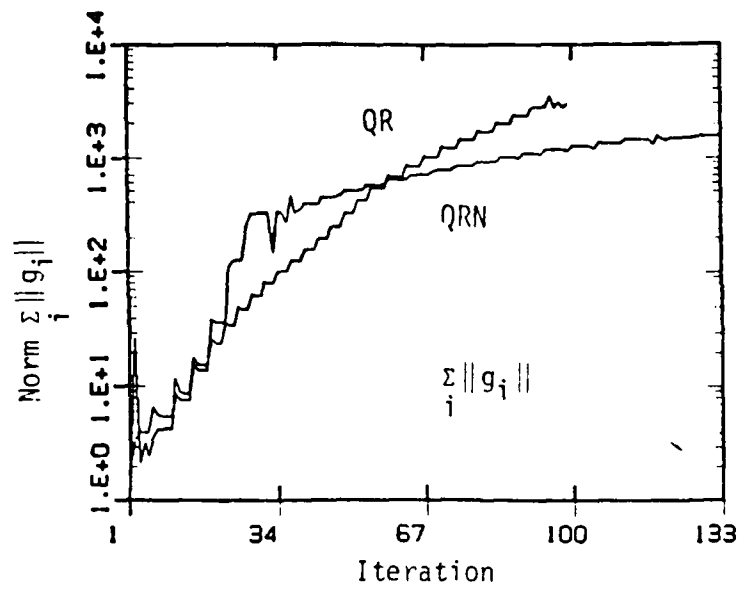
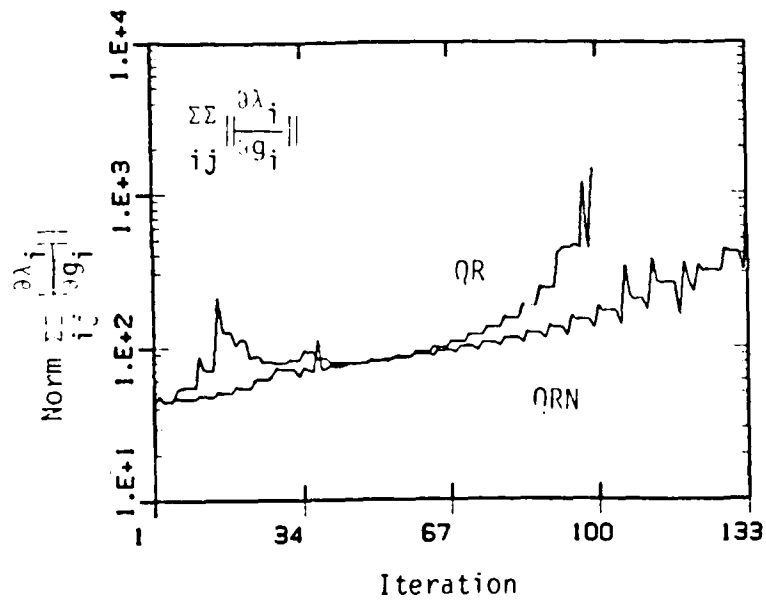Figure 1 Eigenvalue Locus

Figure 2   Norm of Gain Vector

Figure 3   Norm of Eigenvalue Sensitivity
with Respect to Gain Element

149

TABLE 1

Eigenvalues for LQG Weight Matrix Iterations with N ≠ 0

γ	ω_1	ζ_1	ω_2	ζ_2	ω_3	ζ_3	ω_4	ζ_4	ω_5	ζ_5	ω_6	ζ_6	ω_7	ζ_7	|G|
0	.53	.708	4.38	.026	7.91	.009	52.6	.001	53.9	.001	166.2	.003	167.1	.003	2.17
.1	.53	.894	4.38	.176	7.91	.030	52.6	.007	53.9	.004	166.3	.009	167.1	.005	5.45
.2	.54	.915	4.38	.428	7.91	.042	52.6	.017	53.9	.005	166.2	.022	167.1	.007	13.8
.55	.56	.919	4.37	.981	7.91	.114	26.8	.832	53.9	.007	128.9	.431	167.0	.007	1554

no convergence for γ > .55

TABLE 2

Eigenvalues for LQG Weight Matrix Iteration with N = 0

γ	ω_1	ζ_1	ω_2	ζ_2	ω_3	ζ_3	ω_4	ζ_4	ω_5	ζ_5	ω_6	ζ_6	ω_7	ζ_7	|G|
0	.53	.708	4.38	.026	7.91	.009	52.6	.001	53.9	.001	166.2	.003	167.1	.003	2.17
.1	.53	.709	4.38	.158	7.91	.073	52.6	.009	53.9	.011	166.6	.009	166.7	.005	24.4
.2	.54	.710	4.37	.334	7.91	.129	52.8	.020	53.7	.019	166.5	.019	166.8	.004	79.1
.63	.56	.710	4.37	.961	7.91	.342	23.31	.900	53.5	.013	139.1	.369	166.8	.004	2773

no convergence for γ > .63

END

11-86

DTIC